INSTITUTE OF SEISMOLOGY
UNIVERSITY OF HELSINKI

REPORT S-46

LITHOSPHERE 2006

FOURTH SYMPOSIUM ON THE STRUCTURE, COMPOSITION AND EVOLUTION OF THE LITHOSPHERE IN FINLAND

PROGRAMME AND EXTENDED ABSTRACTS

edited by

Ilmo T. Kukkonen, Olav Eklund, Annakaisa Korja, Toivo Korja, Lauri J. Pesonen and Markku Poutanen

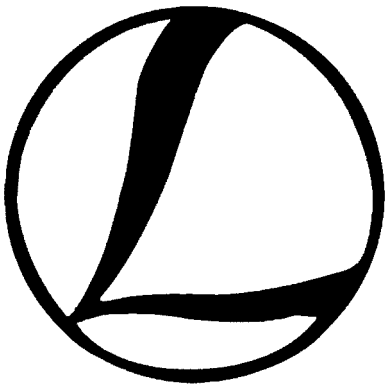

Geological Survey of Finland
Espoo, November 9-10, 2006

Helsinki 2006

Editor-in-Chief: Pekka Heikkinen
Guest Editors: Ilmo T. Kukkonen, Olav Eklund, Annakaisa Korja, Toivo Korja, Lauri J. Pesonen, Markku Poutanen

Publisher: Institute of Seismology
P.O. Box 68
FIN-00014 University of Helsinki
Finland
Phone: +358-9-1911 (switchboard)
Fax: +358-9-191 51626
http://www.seismo.helsinki.fi

ISBN 952-10-2167-5
ISSN 0357-3060

Helsinki 2006
Helsinki University Press

LITHOSPHERE 2006

FOURTH SYMPOSIUM ON THE STRUCTURE, COMPOSITION AND EVOLUTION OF THE LITHOSPHERE IN FINLAND

PROGRAMME AND EXTENDED ABSTRACTS

Geological Survey of Finland,
Espoo,
November 9-10, 2006

CONTRIBUTORS

Finnish National Committee of the International Lithosphere Programme (ILP)
Finnish Geodetic Institute
Geological Survey of Finland
Institute of Seismology, University of Helsinki
Division of Geophysics, University of Helsinki
Geophysics, Department of Physical Sciences, & Department of Geology, University of Oulu
Sodankylä Geophysical Observatory, University of Oulu
Department of Geology and Mineralogy, Åbo Akademi University
Department of Geology, University of Turku

ORGANIZING COMMITTEE AND EDITORS

Olav Eklund	Department of Geology 20014 University of Turku, Finland E-mail: olav.eklund@utu.fi
Annakaisa Korja	Institute of Seismology P.O. Box 68, 00014 University of Helsinki, Finland E-mail:annakaisa.korja@helsinki.fi
Toivo Korja	University of Oulu, Department of Physical Sciences, Geophysics, POB 3000, FIN-90014, University of Oulu
Ilmo T. Kukkonen	Geological Survey of Finland P.O. Box 96, 02151 Espoo, Finland E-mail: ilmo.kukkonen@gtk.fi
Lauri J. Pesonen	Division of Geophysics P.O. Box 64, 00014 University of Helsinki E-mail: lauri.pesonen@helsinki.fi
Markku Poutanen	Finnish Geodetic Institute Geodeetinrinne 2, 02430 Masala, Finland E-mail: markku.poutanen@fgi.fi

References of Lithosphere Symposia Publications

Pesonen, L.J., Korja, A. and Hjelt, S.-E., 2000 (Eds.). Lithosphere 2000 - A Symposium on the Structure, Composition and Evolution of the Lithosphere in Finland. Programme and Extended Abstracts, Espoo, Finland, October 4-5, 2000. Institute of Seismology, University of Helsinki, Report S-41, 192 pages.

Lahtinen, R., Korja, A., Arhe, K., Eklund, O., Hjelt, S.-E. and Pesonen, L.J., 2002 (Eds.). Lithosphere 2002 – Second Symposium on the Structure, Composition and Evolution of the Lithosphere in Finland. Programme and Extended Abstracts, Espoo, Finland, November 12-13, 2002. Institute of Seismology, University of Helsinki, Report S-42, 146 pages.

Ehlers, C., Korja A., Kruuna, A., Lahtinen, R., Pesonen, L.J. (Eds.), 2004. Lithosphere 2004 – Third Symposium on the Structure, Composition and Evolution of the Lithosphere in Finland. Programme and Extended Abstracts, Turku, Finland, November 10-11, 2004. Institute of Seismology, University of Helsinki, Report S-45, 131 pages.

Kukkonen, I.T., Eklund, O., Korja, A., Korja, T., Pesonen, L.J. and Poutanen, M. (Eds.), 2006. Lithosphere 2006 – Fourth Symposium on the Structure, Composition and Evolution of the Lithosphere in Finland. Programme and Extended Abstracts, Espoo, Finland, November 9-10, 2006. Institute of Seismology, University of Helsinki, Report S-46, 233 pages.

Keywords (GeoRef Thesaurus, AGI): lithosphere, crust, upper mantle, Fennoscandia, Finland, Precambrian, Baltic Shield, symposia

TABLE OF CONTENTS

PREFACE

The biannual LITHOSPHERE symposium has become a tradition after the very successful first meeting of this kind in 2000. The aim of the LITHOSPHERE symposia is to provide a forum for both geologists and geophysicists for interdiscliplinary discussions, and presentation of reviews and new results. Once again, the meeting invitation and the call for papers have been well-received, and as a result there are 46 titles included in this extended abstract volume representing a wide range of geological and geophysical subjects. The symposium has been designed around the following themes:

Theme 1: Continents Through Time
Theme 2: The Structure, Composition and Evolution of the Crust and Upper Mantle
Theme 3: Plate Movement of Fennoscandia, Post-glacial Uplift and Quaternary Climate
Theme 6: Open Forum
Theme 7: General Discussion and Poster Awards

The two-day symposium will take place in Otaniemi, Espoo, at the Geological Survey of Finland, November 9-10, 2006, with participation from the Universities in Helsinki, Turku, Åbo and Oulu, the Geological Survey of Finland and the Finnish Geodetic Institute. The Symposium will be hosted by the ILP and the Geological Survey of Finland. Posters prepared by graduate- or postgraduate students will be evaluated and the best will be awarded.

This special volume ***"LITHOSPHERE 2006"*** contains the programme and extended abstracts of the symposium in alphabetical order.

Espoo, October 24, 2006

Ilmo T. Kukkonen, Olav Eklund, Annakaisa Korja, Toivo Korja,
Lauri J. Pesonen and Markku Poutanen

Lithosphere 2006 Organizing Committee

LITHOSPHERE 2006 Symposium
Programme

Thursday, November 9

9.30 - 10.00	Registration at the Geological Survey of Finland, J.J. Sederholm Auditorium, Betonimiehenkuja 4, Espoo
10.00-10.05	Opening of the symposium (Organising Committee)
10.05-11.00	**Session 1: Continents through time (part I)** (Chair I.T. Kukkonen)
10.05-10.50	**D.A.D. Evans**. Evidence for pre-Pangea supercontinents, and the search for accurate reconstructions (invited talk)
Break	
11.00-11.20	**J. Vuollo and S. Mertanen**. Dyke swarms and plate movements
11.20-12.00	**M. Bilker-Koivula**. Global gravity field models from satellite measurements
12.00-12.20	**R. Lahtinen, A. Korja and M. Nironen**. Continent formation: the Fennoscandian perspective
12.20-12.40	**J. Korhonen**: World Digital Magnetic Anomaly Map: Global sources of anomalies
Lunch	
13.30-14.50	**Session 2: Structure, Composition and Evolution of the Crust (part I)** (Chair O. Eklund)
13.30-13.50	**M. Nironen and A. Korja.** FIRE 2 & 2A profile: interpretation and correlation to surface geology
13.50-14.10	**T. Stålfors, C. Ehlers and A. Johnson.** The granite-migmatite zone of southern Finland – A history of structural control and intrusions
14.10-14.30	**I.T. Kukkonen and L.S. Lauri**. Modelling the thermal evolution of a Precambrian orogen: high heat production migmatitic granites of southern Finland
14.30-14.50	**L.S. Lauri, M. Cuney, O.T. Rämö, M. Brouand and R. Lahtinen.** Petrology of the Svecofennian late orogenic granites with emphasis on the distribution of uranium
Coffee	
15.10-15.30	**P. Tuisku, H. Huhma , P. Mikkola and M. Whitehouse**. Geology and correlation of the Lapland Granulite Belt
15.30-15.50	**Session 3: Plate Movement of Fennoscandia, Post-glacial Uplift and Quaternary Climate** (Chair T. Korja)
15.50-16.10	**H. Koivula, M.Tervo and M. Poutanen**. Contemporary crustal motion in Fennoscandia observed with continuous GPS networks
16.10-16.30	**P.-L. Forsström**. Modelling the Eurasian Ice Sheet: focus on basal temperatures and isostacy

16.30-16.50 **K. Moisio and J. Mäkinen.** Rheology of the lithosphere and models of postglacial rebound

16.50-17.10 **M. Poutanen and the National ILP Committee of Finland**. Upper mantle dynamics and Quaternary climate in cratonic areas; a proposal for an ILP Project

17.10-18.30 **Poster session**

T. Elbra, I. Lassila, E. Hæggström, L.J. Pesonen, I.T. Kukkonen and P. Heikkinen. Ultrasonic seismic P- and S- velocities – the case of the Outokumpu deep drill core and FIRE profile samples.

K. Hagelberg, P. Peltonen and T. Jokinen. Tyrisevä – an ultramafic intrusion in Vammala Ni-belt: petrography, structure and ore potential

M.J. Holma, V.J. Keinänen and I.M. Lahti. Structurally controlled gold mineralisation in the lower part of the Kumpu Group, Lake Immeljärvi, Kittilä: Implications for late-orogenic crustal-scale deformation in Central Lapland

T. Hyvönen, T. Tiira, A. Korja and K. Komminaho. Crustal tomography in central Fennoscandian Shield

T. Janik, E. Kozlovskaya, J. Yliniemi and FIRE Working Group. Crust-mantle boundary in the central Fennoscandian shield: constraints from wide-angle P- and S-wave velocity models and results of FIRE reflection profiles

F. Karell. Magnetic fabric investigation on rapakivi granites in Finland

T. Kivisaari and P. Hölttä. Metamorphism of the Archean Tuntsa-Savukoski area, NE-Finland: preliminary results

E. Kozlovskaya, M. Poutanen and POLENET/FI colleagues. POLENET/FI - a multidisciplinary geophysical experiment in Northern Fennoscandia and Antarctica during the International Polar Year 2007-2008

E. Kozlovskaya, G. Kosarev, I. Aleshin, J. Yliniemi, O. Riznichenko and I. Sanina. Composition of the crust and upper mantle derived from joint inversion of receiver function and surface wave phase velocity of SVEKALAPKO teleseismic records

Y. Kähkönen. Geochemistry of coherent andesites at Palvajärvi, Paleoproterozoic Tampere Belt, southern Finland: evidence for alteration, petrogenesis and tectonic setting

L.S. Lauri, T. Andersen, P. Hölttä, H. Huhma and S. Graham. Neoarchean growth of the Karelian craton: New evidence from U–Pb and Lu–Hf isotopes in zircons

T. Ruotoistenmäki. Classification of Finnish bedrock sub-areas using lithogeochemical analysis of Finnish plutonites

H. E. Ruotsalainen, S. Hietala, S. Dayioglu, J. Moilanen, L. J. Pesonen and M. Poutanen. Keurusselkä impact structure – preliminary geophysical investigations

J. Salminen and L.J. Pesonen. Paleomagnetic and petrophysical investigation of the Mesoproterozoic monzodioritic sill, Valaam, Russian Karelia

H. Silvennoinen and E. Kozlovskaya. 3-D structure and physical properties of the Kuhmo Greenstone Belt (eastern Finland): constraints from gravity modelling and seismic data and implications for the tectonic setting

T. Siren and I.T. Kukkonen. Three-dimensional visualization of FIRE seismic reflection sections (computer demo)

P. Sorjonen-Ward, A. Ord, Y. Zhang, P. Alt-Epping, T. Cudahy, A. Kontinen and U. Kuronen. Numerical simulations of geological processes relating to the Outokumpu mineral system

T. Torvela. Deformation history of a ductile, crustal-scale shear zone in SW Finland – reactivation and deformation partitioning

M. Tuusjärvi and L.S. Lauri. Modeling the source of the Svecofennian late orogenic granites: a case study from West Uusimaa, Finland

K. Vaittinen, I. Lahti, T. Korja and P. Kaikkonen. Crustal conductivity of the central Fennoscandian Shield revealed by 2D inversion of GGT/SVEKA and MT-FIRE datasets

J. Woodard and C. J. Hetherington. The composition of fluorapatite and monazite from the Naantali Carbonatite, southwest Finland: implications for timing and conditions of carbonatite emplacement

18.30-20.00 Networking, snacks & wine at the GTK lobby

Friday, November 10

9.00-10.00 **Session 4: Structure, Composition and Evolution of the Crust and Upper Mantle (part II)** (Chair A. Korja)

9.00-9.20 **P. Heikkinen, I.T. Kukkonen and FIRE Working Group**. FIRE transects: reflectivity of the crust in the Fennoscandian Shield

9.20-9.40 **K. Sundblad, M. Beckholmen, O. Nilsen and T. Andersen**. Palaeozoic metallogeny of Røros (Norway); a tool for improving Palaeoproterozoic crustal models in Karelia

9.40-10.00 **N. L. Patison, V.J. Ojala, A. Korja, V. Nykänen & the FIRE Working Group**. Gold exploration and the crustal structure of northern Finland as interpreted from FIRE seismic reflection profiles 4, 4A & 4B

Coffee

10.20-11.00 **Session 5: Continents through time (part II) (Chair M. Poutanen)**

10.20-10.40 **A. Deutsch, L.J. Pesonen, S. Dayioglu**. Impact cratering: its geological, biological and economical Role

10.40-12.00 **Session 6: Structure, Composition and Evolution of the Crust (part III)** (Chair M. Poutanen)

10.20-10.40	**P. Sorjonen-Ward**. Orogenic processes and mineralization through time – some general concepts and comparisons with FIRE 3 and 3A reflection seismic interpretation
10.40-11.00	**J. Karhu and A. Torppa**, Evidence for organic carbon subduction from Paloeproterozoic carbonatites
11.00-11.20	**M. Pajunen, M.-L.Airo, T. Elminen, I. Mänttäri, M.Vaarma, P. Wasenius and M. Wennerström**. Tectonic and magmatic evolution of the Svecofennian crust in southern Finland
11.20-11.40	**A.V. Luttinen, V.Lobaev, O.T. Rämö, M. Cuney, B.G.J. Upton, V. Lindqvist**. Geochemistry of basalt dykes and lavas from Inkoo and Lake Ladoga: Widespread 1.53–1.46 Ga high-Ti and-Zr magmatism in southern Fennoscandian Shield?
11.40-12.00	Discussion
Lunch	
12.50-13.50	**Session 7: Structure, Composition and Evolution of the Crust and Upper Mantle (part IV)** (Chair P. Heikkinen)
12.50-13.10	**O. Eklund**. The magmatic end of the Svecofennian orogeny
13.10-13.30	**P. Kosunen, A. Korja, M. Nironen and FIRE Working Group**. Post-collisional extension in central Svecofennian, Central Finland
13.30-13.50	**E. Kozlovskaya**. Seismic studies of the upper mantle in the Fennoscandian Shield: main results and perspectives for future research
Coffee	
14.10-14.30	**H. O´Brien, P. Peltonen, M. Lehtonen and D. Zozulya** . Mantle stratigraphy of the Karelian craton: a 620 km long 3-D cross section revealed by mantle-derived xenocryst chemistry
14.30-14.50	**T. Korja , P. Kaikkonen, I. Lahti, L. B. Pedersen, M. Smirnov, K. Vaittinen, BEAR WG and EMTESZ WG**. Electrical conductivity of upper mantle in Fennoscandia
14.50-16.30	Open forum/Short presentations/Discussion IGCP projects ICDP IODP IPY 2007-2008
16.30-17.00	Final Discussion and Poster Awards Concluding Remarks

EXTENDED ABSTRACTS

Global gravity field models from satellite measurements

M. Bilker-Koivula

Finnish Geodetic Institute, P.O. Box 15, FIN-02431 MASALA
E-mail: Mirjam.Bilker@fgi.fi

Since the launch of the dedicated gravity satellites CHAMP and GRACE, many new global gravity field models have become available. An overview of the models is given in this paper. Static global models derived from CHAMP and GRACE data show a significant improvement in the long-wavelength components of the models compared with pre-CHAMP models. Monthly global gravity models derived from GRACE are available for nearly all months starting from August 2002 up till present. The models have been corrected for solid earth, ocean and pole tides and non-tidal atmospheric and ocean variability. The resulting gravity variations are mainly due to continental water storage and good agreements can be found between mass variations derived from GRACE and variations predicted by hydrological models.

Keywords: gravity field, gravity satellite, CHAMP, GRACE

1. Introduction

Recently, our knowledge of the Earth's gravity field has improved due to the dedicated gravity satellite missions CHAMP and GRACE.

Traditionally, a model of the global gravity field is obtained combining many different measurement techniques. High-resolution point data, obtained using absolute and relative gravimeters, and more regional results from aerial gravimetry and altimetry are combined with gravity field information obtained from satellite orbits. Due to the different qualities and inhomogeneous distributions of the data sets, models derived in this way have an inhomogeneous quality distribution and long-wavelength errors.

The dedicated satellite missions CHAMP and GRACE have improved the situation by providing homogeneous high accurate gravity field information.

2. Gravity information obtained using satellites

As soon as the first satellites were put into space, their information has been used to improve the knowledge on the Earth's gravity field. By satellite laser ranging, the orbit of a satellite could be determined. The difference between the actual measured orbit and the orbit predicted by a gravity field model can be used to improve the model. As the satellites are followed from fixed stations on earth, the information obtained by satellite laser ranging is not homogeneously distributed over the Earth. This situation changed when GPS receivers were put on board satellites. Now, orbits can be tracked continuously with high accuracy.

However, most satellites fly high in space at more than thousand kilometres above the Earth's surface. As the Earth's gravity field attenuates when moving away from the earth, the gravity field information obtained from these orbits has a low resolution and terrestrial data is needed to determine high-resolution gravity field models.

The gravity missions CHAMP, GRACE and GOCE were designed to change this. Through their low-flying orbits and the homogeneous distribution of the satellite observations, the low-wavelength information of gravity models is strengthened and a homogeneous accuracy of the models is achieved over the whole Earth.

Besides satellite orbits, another important contribution to pre-CHAMP global gravity field models came from satellite altimetry. Averaging sea-surface heights of the oceans

measured with altimetry, geoid heights were obtained which were used in global gravity field determination. Then, these same global gravity field models were used in oceanography to calculate geoid heights needed to calculate sea-surface topography from altimetry!

Now, CHAMP and GRACE made it possible to calculate accurate global gravity field models without using satellite altimetry. Thus, providing accurate independent global models for use in oceanography.

The first mission CHAMP has been in orbit since 2000. CHAMP started at an altitude of about 450 km and is coming slowly down to about 300 km altitude by the end of its lifetime. The satellite's orbit is determined with GPS and an accelerometer on board provides observations to correct for non-gravitational forces. CHAMP has contributed to the improvement of the long-wavelength part of the gravity field.

The second mission, the satellite-pair GRACE, became operational in 2002. The two satellites will during their lifetime slowly come down from the starting altitude of about 500 km to 300 km. In addition to orbit determination by GPS, the distance between the satellites is accurately measured. Both satellites are also equipped with an accelerometer to correct for non-gravitational forces. GRACE has improved the knowledge of the medium wavelength part of the gravity field. Additionally, it has become possible to calculate monthly global gravity field models, enabling studies of the temporal variations in the gravity field.

The GOCE satellite, to be launched in 2007, will carry a gradiometer on board. It will further improve knowledge on the short-wavelength part of the gravity field.

3. Static global gravity field models

Table 1 gives an overview of the static global gravity field models that have been published by the CHAMP and GRACE science teams. The EIGEN-models are developed at the GeoForschungsZentrum Potsdam (GFZ) and the TEG and GGM models at the Center for Space Research of the University of Texas (UTCSR). Several other groups have also produced models, but they are not considered here. All models are produced as coefficients of spherical harmonic expansions up to a maximum degree and order.

The satellite-only models go up to degree an order 120 in the case of CHAMP and up to degree and order 150 in case of the later GRACE models. However, the highest orders of these models have weak solutions and should be treated with care. The later CHAMP and GRACE models include more observations and perform therefore better than the earlier models when comparisons are made with altimeter data and geoid heights obtained from GPS and levelling (e.g. *Reigber et al., 2005b*, *Tapley et al., 2005*, and *Bilker, 2005*). Comparisons of the new models with the widely used pre-CHAMP model EGM96 show that CHAMP and GRACE have improved the accuracy of the long- and mid-wavelength (up to degree 70) components of the Earth's gravity field model (e.g. *Reigber et al., 2005b*, *Tapley et al., 2004b*, *Tapley et al. 2005*, and *Bilker, 2005*).

The models that combine CHAMP and GRACE data with surface data also benefit from the improvement of the long-wavelength components. An overall improvement can be seen when comparing for example geoid heights with heights from GPS and levelling (*Tapley et al., 2005*, *Förste et al., 2005*, and *Förste and Flechtner, 2006b*).

It can be concluded that the new static models are an improvement over EGM96, which means that independent high-accuracy models are now available for oceanography and orbit determination.

4. Monthly global gravity field models

In addition to new static global gravity field models, the GRACE mission produces also monthly global gravity field models, making it possible to study temporal changes in the gravity field. The monthly models are produced by three processing centers: UTCSR, GFZ and the Jet Propulsion Laboratory (JPL).

The UTCSR models are available for most months starting from August 2002 till present. The GFZ has produced models covering most months from February 2003 till present. The JPL solutions cover most months in 2003, 2004 and 2005 (situation mid-October 2006).

Although the monthly models go up to degree and order 120, errors increase rapidly with increasing degree. Therefore, higher order coefficients should not be used (see e.g. *Neumeyer et al., 2006*) or a smoothing technique should be applied (see e.g. *Wahr et al., 1998*).

The provided monthly models have been corrected for solid earth, ocean and pole tides and non-tidal atmospheric and ocean variability. The remaining gravity variations are mainly due to changes in continental water storage and other non-modelled gravity changes such as post-glacial rebound. Many groups are studying these gravity changes using GRACE monthly models. Good agreements are found between mass variations determined with GRACE and variations predicted by global hydrology models (e.g. *Tapley et al., 2004a*, *Schmidt et al., 2006,* and *Neumeyer et al., 2006*). Other examples are the detection of gravity changes related to the 2004 Sumatra-Andaman earthquake (*Han et al., 2006*) and the detection of a decrease in the Antarctic ice-sheet mass (*Velicogna and Wahr, 2006*).

References

Bilker, M., 2005. Evaluation of the new gravity field models from CHAMP and GRACE with GPS-levelling data in Fennoscandia. In: Viljanen, A., Mäntyniemi, P. (Eds.), *XXII Geofysiikan Päivät*, Helsinki 19.-20.5.2005, Geofysiikan Seura, Helsinki, 2005, pp. 21-26. ISBN 951-97663-3-2/ISSN 0358-2981.

Förste, Ch. and Flechtner, F., 2006a. Satellite-only Gravity Field Model EIGEN-GL04S1, http://www.gfz-potsdam.de/pb1/op/grace/results/grav/g006_eigen-gl04s1.html [24.05.2006].

Förste, Ch. and Flechtner, F., 2006b. Combined Gravity Field Model EIGEN-GL04C, http://www.gfz-potsdam.de/pb1/op/grace/results/grav/g005_eigen-gl04c.html [31.05.2006].

Förste, C., Flechtner, F., Schmidt, R., Meyer, U., Stubenvoll, R., Barthelmes, F., König, R., Neumayer, K.H., Rothacher, M., Reigber, Ch., Biancale, R., Bruinsma, S., Lemoine, J.-M., Raimondo, J.C., 2005. A New High Resolution Global Gravity Field Model Derived From Combination of GRACE and CHAMP Mission and Altimetry/Gravimetry Surface Gravity Data, Geophysical Research Abstracts, Vol. 7, 2005, EGU General Assembly, Vienna, Austria, 24-29, April 2005 [http://www.gfz-potsdam.de/pb1/op/grace/results/grav/g004_EGU05-A-04561.pdf]

Han, S.-C., Shum, C.K., Bevis, M., Ji, C., Kuo, C.-Y., 2006, Crustal Dilitation Observed by GRACE After the 2004 Sumatra-Andaman Earthquake, Science, Vol. 313, 4 August 2006.

Neymeyer, J., Barthelemes, F., Dierks, O., Flechtner, F., Harnisch, M., Hinderer, J., Imanishi, Y., Kroner, C., Meurers, B., Petrovic, S., Reigber, Ch., Schmidt, R., Schwintzer, P., Sun, H.-P., Virtanen, H., 2006, Combination of temporal gravity variations resulting from superconducting gravimeter (SG) recordings, GRACE satellite observations and global hydrology models, Journal of Geodesy, Vol. 79, No. 10-11, February, 2006, pp. 573-585.

Reigber, Ch., 2004. First GFZ GRACE Gravity Field Model EIGEN-GRACE01S, http://www.gfz-potsdam.de/pb1/op/grace/results/grav/g001_eigen-grace01s.html [20.01.2004].

Reigber, Ch., Balmino, G., Schwintzer, P., Biancale, R., Bode, A., Lemoine, J.-M., Koenig, R., Loyer, S., Neumayer, H., Marty, J.-C., Barthelmes, F., Perosanz, F., Zhu, S. Y., 2002. A high quality global gravity field model from CHAMP GPS tracking data and Accelerometry (EIGEN-1S). Geophysical Research Letters, 29(14), 10.1029/2002GL015064, 2002.

Reigber, Ch., Schwintzer, P., Neumayer, K.-H., Barthelmes, F., König, R., Förste, Ch., Balmino, G., Biancale, R., Lemoine, J.-M., Loyer, S., Bruinsma, S., Perosanz, F., Fayard, T., 2003. The CHAMP-only Earth Gravity Field Model EIGEN-2. Advances in Space Research 31(8), 1883-1888, 2003 (DOI: 10.1016/S0273--1177(03)00162-5)

Reigber, Ch., Jochmann, H., Wünsch, J., Petrovic, S., Schwintzer, P.,Barthelmes, F., Neumayer, K.-H., König, R., Förste, Ch., Balmino, G., Biancale, R., Lemoine, J.-M., Loyer, S., Perosanz, F., 2005a. Earth Gravity Field and Seasonal Variability from CHAMP. In: Reigber, Ch., Lühr, H., Schwintzer, P., Wickert, J. (eds.), Earth Observation with CHAMP - Results from Three Years in Orbit, Springer, Berlin, 25-30, 2005.

Reigber, Ch., Schmidt, R., Flechtner, F., König, R., Meyer, U., Neumayer, K.-H., Schwintzer, P., Zhu, S.Y., 2005b. An Earth gravity field model complete to degree and order 150 from GRACE: EIGEN-GRACE02S, Journal of Geodynamics 39(1),1-10

Reigber, Ch., Schwintzer, P., Stubenvoll, R., Schmidt, R., Flechtner, F., Meyer, U., König, R., Neumayer, H., Förste, Ch., Barthelmes, F., Zhu, S.Y., Balmino, G., Biancale, R., Lemoine, J.-M., Meixner, H., Raimondo, J.C., 2005c: A High Resolution Global Gravity Field Model Combining CHAMP and GRACE Satellite Mission and Surface Gravity Data, Joint CHAMP/GRACE Science Meeting, GFZ, July 5-7, 2004.

Schmidt, R., Schwintzer, P., Flechtner, F., Reigber, Ch., Günter, A., Döll, P., Ramillien, G., Cazenave, A., Petrovic, S., Jochmann, H., Wünsch, J., 2006, GRACE observations of changes in continental water storage, Global and Planetary Change 50 (2006), pp. 112-126.

Tapley, B., Bettadpur, S., Chambers, D., Cheng, M., Gunter, B., Kang, Z., Kim, J., Nagel, P., Ries, J., Rim, H., Roesset, P., Roundhill, I., 2001. Gravity Field Determination from CHAMP using GPS Tracking and accelerometer Data: Initial Results, EOS Trans. AGU, 82(47), Fall Meet. Suppl., Abstract G41C-02, 2001.

Tapley, B., Bettadpur, S., Ries, J., Thompson, P., Watkins, M., 2004a, GRACE Measurements of Mass Variability in the Earth System, Science, Vol. 305, 23 July 2004.

Tapley, B., Bettadpur, S., Watkins, M., Reigber, Ch., 2004b. The Gravity Recovery and Climate Experiment: Mission Overview and Early Results, Geophys. Res. Lett., 31(9), L09607, DOI:10.1029/2004GL019920, 2004.

Tapley, B., Ries, J., Bettadpur, S., Chambers, D., Cheng, M., Condi, F., Gunter, B., Kang, Z., Nagel, P., Pastor, R., Pekker, T., Poole, S., Wang, F., 2005. GGM02 - An improved Earth gravity field model from GRACE, Journal of Geodesy (2005), DOI 10.1007/s00190-005-0480-z

Velicogna, I. and Wahr, J., 2006, Measurements of Time-Variable Gravity Show Maa Loss in Antarctica, Science, Vol. 311, no. 5768, 24 March 2006, DOI: 10.1126/science.1123785.

Wahr, J., Molenaar, M., Bryan, F., 1998. Time variability of the Earth's gravity field: Hydrological and oceanic effects and their possible detection using GRACE, Journal of Geophysical Research, Vol. 103, No. B12, 1998, pp. 30205-30229.

Table 1. Static global gravity field models from the CHAMP and GRACE missions.

Model	**Description**	**Maximum degree**	**Reference**
Satellite-only			
EIGEN-1S	88 days CHAMP + multi-satellite data	100	*Reigber et al. (2002)*
EIGEN-2	6 months CHAMP	120	*Reigber et al. (2003)*
EIGEN-3p	3 years CHAMP	120	*Reigber et al. (2005a)*
EIGEN-CHAMP03S	33 months CHAMP	120	*Reigber et al. (2005a)*
EIGEN-GRACE01S	39 days GRACE	120	*Reigber (2004)*
EIGEN-GRACE02S	110 days GRACE	150	*Reigber et al. (2005b)*
EIGEN-GL04S1	GRACE + LAGEOS	150	*Förste and Flechtner (2006a)*
GGM01S	111 days GRACE	120	*Tapley et al. (2004b)*
GGM02S	363 days GRACE	160	*Tapley et al. (2005)*
Combinations			
TEG-4	80 days CHAMP + multi-satellite and surface data	200	*Tapley et al. (2001)*
GGM01C	GGM01S + multi-satellite and surface data	200	*Tapley et al. (2004b)*
GGM02C	GGM02S + multi-satellite and surface data	200	*Tapley et al. (2005)*
EIGEN-CG01C	860 days CHAMP + 200 days GRACE + surface data	360	*Reigber et al. (2005c)*
EIGEN-CG03C	860 days CHAMP + 376 days GRACE + surface data	360	*Förste et al. (2005)*
EIGEN-GL04C	EIGEN-GL04S1+ surface data	360	*Förste and Flechtner (2006b)*

Impact cratering: its geological, biological and economical role

Alex Deutsch[1], Lauri J. Pesonen[2], Selen Dayioglu[2]

[1]Institute for Planetology, University of Muenster, D-48149 Muenster , Germany
[2]Laboratory for Solid Earth Geophysics, U of Helsinki, P.O. Box 64, 00014 Helsinki, Finland

Keywords: impact structures, cratering, evolution

The study of the impact crater populations on planetary bodies with a variety of remote sensing techniques in combination with age dating on lunar and meteoritic samples have verified unambiguously that hypervelocity collision was the dominant geological process throughout the early solar system. It not only created heavily cratered surfaces, as documented e.g., for the lunar highlands, Mercury, or some of the satellites of the large gas planets, yet was the basic process in accretion too. Those parts of the lunar surfaces saturated with impact craters allowed estimate the impact rate produced by intense bombardment in the period from 4.6 to about 3.75 Ga which is by orders of magnitude higher than the current rate. Planet Earth, as part of the solar system, experienced the same bombardment as the other bodies in the inner solar system, yet subsequent geological processes have removed totally the Hadean record of cratering. Spherule beds forming wide-spread traceable horizons in Archean - Proterozoic terranes may form the oldest witness for impact processes – if they indeed represent ejecta material. By comparison with other planetary bodies it is evident that large-scale impact cratering was a very effective process for forming, deforming, and recycling crust on Earth up to Palaeoproterozoic times.

On the Earth-Moon system, a variety of possible effects have been ascribed to impact. Currently, the best working hypothesis for the origin of the Moon is the impact of a Mars–sized object with proto-Earth. This resulted in the insertion into Earth orbit of vaporized material from the projectile and the Earth, which condensed to form the Moon. Heat, generated by the early impacts, may have amplified outgassing of Earth´s initial crust and upper mantle (lithosphere), thus, contributing to the formation of the primordial atmosphere and hydrosphere. Some impacting bodies in turn, may have contributed to the Earth´s budget of volatiles and early oceans. This bombardment would also have resulted in development and destruction of early life, with the largest impacts having capacity to effectively sterilize the whole surface of the Earth. In more recent geological times, at least one mass extinction event notably that one at the Cretaceous - Tertiary (Paleogene) boundary 65 m.yrs. ago, which killed the dinosaurs and many other species, is linked to a global environmental catastrophe caused by a major impact. This event created the Chicxulub impact structure, Yucatan peninsula, Mexico, now covered by up to 1 km post-impact sediments (Fig. 1b). Impact still is one of the most important geological processes in our solar system as documented, for example, by the spectacular impact of comet Shoemaker-Levi 9 on Jupiter in 1994. On Earth, plate tectonics, metamorphic overprint, sedimentation, and erosion have removed a large part of the impact record. However, we should be aware that the recently drilled about 10-km-sized Lake Bosumtwi structure, Ghana, West Africa, was created by an impact just 1 m.yrs. ago. Only about 700 000 yrs. ago, 1/3 of the Earth's surface was covered glassy ejecta material, the Australasian tektites.

Repeated notices in the press of close fly-by of small astroidal bodies remind us that hypervelocity collisions represent a constant danger for civilization. To assess impact probabilities and create strategies of diverting cosmic projectiles is in the focus of NEO (near-Earth objects) research.

In this presentation we will review the effects of impacts on planetary evolution including development and erosion of an atmosphere, on the biosphere and the lithosphere. We will present some highlights of recent impact research topics (deep drilling, experimental research), and want to summarize the enormous economic value of terrestrial impact structures. Finally, we will discuss the role of impact processes in modern geoscience education taking place in high schools, universities, museums and science centers.

Fig. 1a.

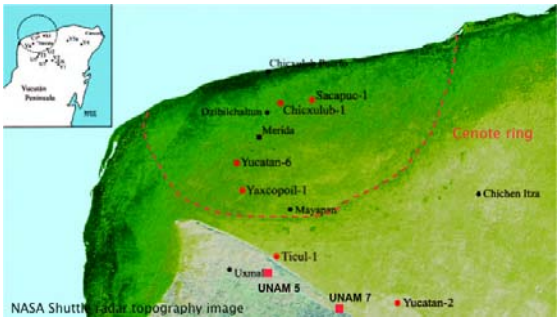

Fig 1b.

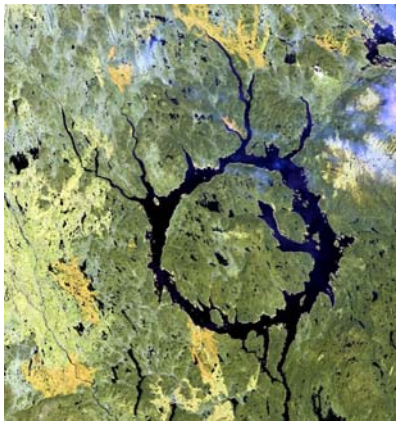

Fig. 1c.

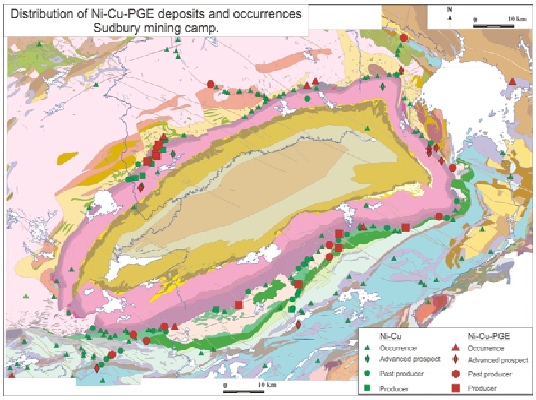

Fig 1d.

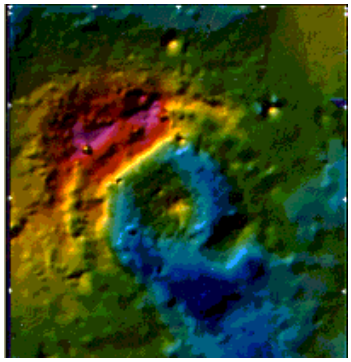

Fig 1e

Fig. 1f

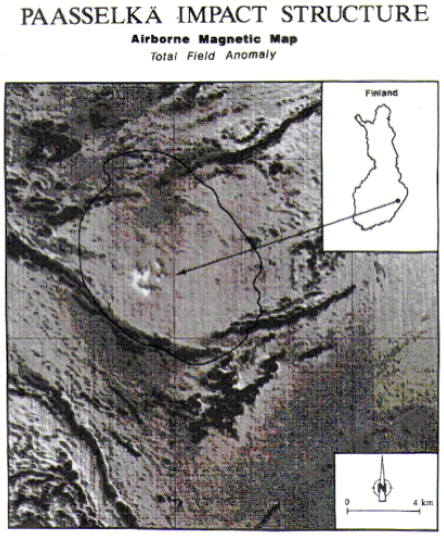

Fig. 1g

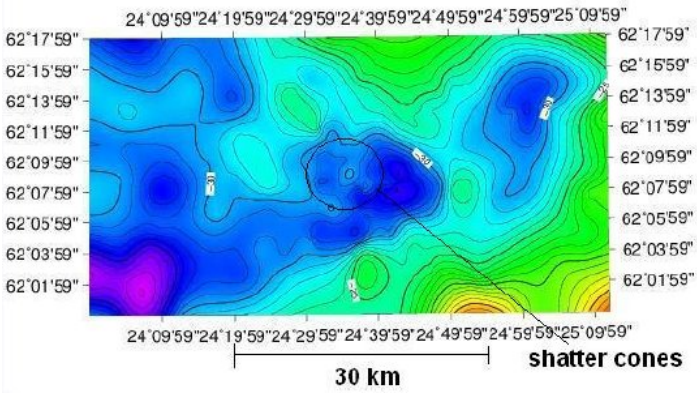

Fig. 1h

Figure 1. Examples of the various effects of meteorite impacts on planetary evolution. (a) A possible scenario of the evolution of the Moon from a gigantic collision of a Mars-sized body with pro-Earth. (b) Chicxulub structure (D 180 km), Yucatan (Mexico), the candidate crater for the 65 Ma mass-extinction. (c) Gravity anomalies of the Vredefort structure, South Africa, erasing from deep seated crustal structures caused by a large impact at ca. 2.023 Ga ago (Prof. Roger Gibson, University of Witwatersrand), (d) Sudbury, Canada, a deformed and eroded huge impact structure (ca. 1. 85 Ga) providing the world largest nickel occurrences and an excellent educational facility to understand impact cratering as a catastrophic process (Geoscience North Museum, Sudbury). (e) A satellite image of the Manicouagan impact structure (D 100 km, age 212 Ma), Canada. Note the ring-shaped lake and radial pattern of rivers and fractures. The water system has a hydropower energy station. (f) Gigantic (tens of meters) impact breccia blocks within the breccia layer, part of the Popigai impact structure (100 km, 35 Ma), N. Siberia. (g) Airborne high-resolution magnetic map of the Paasselkä impact structure (D 10 km, age ?), E. Finland, with its central anomalies (white spots). Drilling through these anomalies lead to discovery of shock features and also a 25 m thick sulphide ore layer (Pesonen et al., 1998). (h) Gravity map of the most recent (No. 11) impact structure discovery, the Keurusselkä structure (D 20-30 km, age ?; Hietala and Moilanen, 2004). The solid ring is the area where shatter cones have been found, the middle ring denotes the gravity anomaly (Ruotsalainen et al., 2005).

Reference

French, B.M., 1998. *Traces of Catastrophe-A handbook of Shock-Metamorphic Effects in Terrestrial Meteorite Impact Structures*. LPI Distribution No. 954, Lunar and Planetary Institute, Houston. 120 pp.

The magmatic end of the Svecofennian orogeny

Olav Eklund

Department of Geology, University of Turku, FIN-20014, Turku, Finland

In the search for the end of the Svecofennian orogeny, more and more age determinations cluster in the time frame 1800 Ma – 1760 Ma. Age data from shoshonitic lamprophyres and carbonatites, occuring in extensional tectonic settings, indicate that shield scale extension took place between 1790 and 1765 Ma. The lack of magmatic rocks with more depleted mantle signature from this age in Finland and associated areas indicate that delamination of an enriched lihospheric mantle by a hot convective asthenosphere may have caused the specific magmatism for this time frame.

Keywords: Svecofennian, uplift, lamprophyre, shoshonite

1. Introduction

Over a long period, ages between 1800 and 1765 Ma have been reported sporadically around the Fennoscandian shield from several different rock types. In Lapland, age determinations from the Central Lapland Granite Complex are slightly younger than 1800 Ma, such as the 1773±8 Ma Maunun Matti granite (Rovaniemi) (Hölttä et al., 2003) and the 1796±3 Ma Jääskö appinite (Hölttä, pers. com.). Several other age determinations near the CLGC reveal the same ages (see Corfu and Evins 2001 and references therein). The Nattanen-type postorogenic granite intrusions in Finnish Lapland and Kola peninsula reveal ages between 1.80 Ga to 1.77 Ga (Lauerma 1982, Huhma 1986, Rastas et al. 2001). Corfu and Evins (2001) investigated Archaean gneisses from the Suomojärvi complex in northern Finland. Titanite and monazite metamorphic ages of these Archaean rocks are between 1780 and 1765 Ma. These ages are also common in the Belomorian belt. Lower crustal and mantle xenoliths found in kimberlites cutting Archaean rocks in east-central Finland contain 1.80 Ga zircons (Hölttä et al., 2000; Peltonen and Mänttäri 2001).

In southern Finland, rocks within this age frame usually belong to the shoshonitic rock series extending in a 600 km belt from lake Ladoga to the Åland archipelago (Eklund et al 1998; Andersson et al 2006). Characteristic of this magmatic event are shoshonitic lamprophyres and their plutonic equivalenets. Diagnostic are high contents of Ba, Sr and LREE and hydrous mafic silicates with high Mg#. Granites of this age are shoshonitic high Ba-Sr granites associated with shoshonitic lamprophyres. However, peraluminous granites are found in this age frame such as the Vuoksi intrusion in Russian Karelia (Eklund et al 1998). Pegmatites in southern Finland also usually fall into this age frame.

New age data from lamprophyres in Ladoga region reveal ages around 1800 Ma for their emplacement. The same ages and compositions are found in lamprophyres in Savo (Lake Syväri, Nilsiä). These lamprophyres appear as filling between blocks in half graben structures. Preliminary results of age determinations of carbonatites in southern Finland indicate a monazite microprobe age on 1776 Ma for the Naantali carbonatite (Woodard, pers. com.) and a zircon age of 1792 Ma for the Halpanen cabonatite (Alexei Rukhlov et al., in prep.).

Andersson et al., (2006) suggest that the protolith for the shoshonitic rocks are enriched pockets in the lithospheric mantle due to carbonate metasomatism that took place during the subduction stage of the Svecofennian orogeny.

2. Late-orogenic granite and metamorphic ages in southern Finland and W Ladoga.
The shoshonitic-carbonatitic magmatism in southern Finland post date the extensive post-collisional intra crustal melting that started around 1.85 Ga and ended around 1.79 Ga (Kurhila et al 2006). In the Turku area,Väisänen et al. (2002) revealed the age 1824±5 Ma for the high temperature – low pressure metamorphism. They suggest that the anatectic melts in the area were formed between 1.83 Ga to 1.81 Ga, perhaps down to 1.80 Ga.

In West Uusimaa, Mouri et al. (2005) recorded metamorphic ages by analysing monazite from the mesosome and leucosome and Sm-Nd garnet – whole rock isochrons. The monazite ages are between 1832 and 1816 Ma while the Sm-Nd ages are 1.81 – 1.79 Ga. They concluded that the monazite ages refer to the peak metamorphism (750 – 800 ºC) while the Sm-Nd ages refer to a closure temperature of the system, when the temperature of the crust must have been less than 700 °C.

From the Sulkava thermal dome Korsman (1984) reported U-Pb ages (zi) of 1833 ±16 Ma from the leucosome and 1810 ±7 Ma from the mesosome. Monazite ages gave 1817± 4 Ma for the leucosome and 1840 Ma for the mesosome. Vaasjoki and Sakko (1988) reported an $Pb^{207/206}$ age of 1796 Ma determined from a molybdenite.

New metamorphic ages from Sulkava (Baltybaev et al., 2006) obtained from monazites in the sillimanite-K-feldspar zone idicate an age of 1795±5 Ma. Metamorphic ages obtained by partial leaching of sillimanites give an age of 1779±19 Ma.

From the western shore of Ladoga, Baltybaev et al. (2006) report metamorphic ages from the Ladoga granulite area north of Käkisalmi. Metamorphic ages obtained by partial leaching of sillimanites give an age of 1877± 6.6 Ma and monazite ages of 1860 ±4.4 Ma. No younger metamorphic ages were found in that area.

3. Post-collisional uplift
The 1795±5 Ma Ruokolahti granite is situated in the southern part of the Sulkava thermal dome (Nykänen 1988). Niiranen (2000) compared the regional metamorphism with the contact metamorphism of the dyke and concluded that there was an exhumation of about 9 km between the regional metamorphism and the intrusion of the granite. With respect to the new age determinations from Sulkava, it seems that the exhumation of the crust was very rapid compared to western Ladoga, where there is a time gap on 60 Ma between the regional metamorphism and the intrusion of the shoshonites. In east-central Finland, there are no data for the young regional metamorphism, but still the intrusive age for the shoshonites is the same as those in southern Finland and W Ladoga. In Southern Lapland there are metamorphic ages resembling the shoshonitic ages. In the Central Lapland Granite Complex, there are mafic rocks similar to the shoshonites that intruded coevally with some granite phases 1795 Ma.

4. Discussion
We may conclude that there was a shield scale thermal event 1800-1765 Ma ago that affected the enriched lithospheric mantle as well as the crust. In southern Finland this event was associated with a rapid uplift, while this uplift has not been documented yet elsewhere.

To generate the multitude of magmas observed during this thermal event, we need to create a model that is able to melt different sources situated at different levels of the lithosphere over an extensive area. Until now, all mafic rocks analysed seem to stem from an enriched lithospheric mantle. The lamprophyres and carbonatites may stem from metasomatized pockets with low solidus temperatures. The granites appearing at this time

differ in composition. Some of them are high-Ba-Sr granites that may have been differentiated from a lamprophyric magma, other are peraluminous S-type granites with clear crustal affinities. It is difficult to produce intracratonal post-collisional granites without influx of hot mafic magma into the crust. Beneath the Central Lapland Granite Batolith, there is a positive Bouguer anomaly. The same with the crust west Ladoga. These anomalies may represent mafic rocks in the crust, the rocks that generated crustal melting.

The most likely way to produce the multitude of compositions for the rocks formed during this time frame is the erosion of the enriched litospheric mantle by the hot asthenosperic mantle after the compressional stage of the newly formed shield. The lithosphere responded to the hot asthenosphere in different ways. In the accretionary arc complex of southern Finland, it seems that extensive mantle delamination took place because of the rapid uplift. This delamination is not registered in W-Ladoga. In east-central Finland, it seems that the asthenosphere melted enriched pockets in the lithosphere causing the lamprophyre magmatism. This magmatism was related to extensional tectonics. In Lapland the melting takes place also in the crust over extensive areas. This may be explained by mafic intraplating with subsequent melting of the crust.

The tectonic postion and the new age determinations from lamprophyres in east-central Finland give the impression that the magmatism was triggered by extensional tectonics, probably due to the orogenic collapse. However, the consequences how the lithospheric asthenospheric interface reacted to this collapse differ in different parts of the shield. Mantle delamination with rapid uplift in south, small melt generation in the central part and extensive melt production in the northern part of the shield.

References

Andersson U.B., Eklund, O., Fröjdö, S., Konopelko, D., 2006. 1.8 Ga Magmatism across the Fennoscandian shield; spatial variations in subcontinental mantle enrichment *Lithos* 86, 110 – 136.

Baltybaev, Sh. K., Levchenkov, O.A., Levsky, L.K., Eklund, O., Kilpeläinen, T., 2006. Two metamorphic stages in the Svecofennian belt: Evidence from isotopic geochronological study of the Ladoga and Sulkava metamorphic complexes. Petrologya 14, No 3, 268-283. (in Russian)

Corfu, F., Evins, P. M., 2001. Late Paleoproterozoic minazite and titanite U-Pb ages in the Archaean Suomujärvi Complex, N-Finland. Prec. Res., 116, 171 – 182.

Eklund, O., Konopelko, D., Rutanen, H., Fröjdö, S. And Shebanov, A.D.,1998. 1.8 Ga Svecofennian Postorogenic Shoshonitic Magmatism in the Fennoscandian Shield. Lithos 45, 87-108.

Hölttä, P.,Huhma, H., Mänttäri, I., Peltonen, P., Juhanoja, J., 2000. Petrology and geochemistry of mafic granulite xenoliths from the Lahtijoki kimberlite pipe, eastern Finland. Lithos 51, 109 – 133.

Hölttä, P., Huhma, H,m Lahtinen, R., Nironen, M., Perttunen, V., Vaasjoki, M., Väänänen, J., 2003. Modelling of orogeny in northern Finland. In: O. Eklund. Lapland-2003. Excursion guide to Finnish and Swedish Lapland 1-7.9.2003. Geocenter report nr. 20. Turku University – Åbo Akademi University, 59 pp.

Huhma, H., 1986. Sm-Nd, U-Pb, and Pb-Pb isotopic evidence for the origin of the Early Proterozoic Svecocarelian crust in Finalnd. Geol. Surv. Finland. Bulletin 337. 48 p.

Korsman, K., Hölttä, P., Hautala, T., Wasenius, P., 1984. Metamorphism as an indicator of evolution and structure of crust in eastern Finland. Geol. Surv. Finland Bull. 328, 40 pp.

Kurhila, M., Mänttäri, I., Rämö, O.T., Nironen, M., 2006. The lateorogenic granites of southern Finland – A belt of igneous activity over a period of at least 60 Ma. Bull. Geol. Soc. Finland. Special issue 1, the 27th Nordic Geological Winter Meeting, Abstract Volume p. 80.

Lauerma, R., 1982. On the ages of some granitoid and schist complexes in Northern Finland. Bull. Com. Geol. Soc. Finland 54, 1-2. 85-100.

Niiranen, T., 2000. Svecofennisen orogenian jälkeinen ekshumaatio ja isostaattinen tasapainottuminen Kaakkois-Suomessa. M.Sci. thesis, University of Turku, department of geology, 70 pp.

Nykänen, O., 1988. Virmutjoen kartta-alueen kallioperä. Geological map of Finland 1:100 000, Explanation to the map sheet 4121 Virmutjoki. 64 pp.

Peltonen, P., Mänttäri, I., 2001., An ion microprobe U-Pb-Th study on zircon xenocrysts from the Lahtijoki kimberlite pipe, eastern Finland. Bull. Geol. Soc. Finland 73, 47-58.

Rastas, P., Huhma, H., Hanski, E., Lehtonen, M.I., Härkönen, I., Kortelainen, V., Mänttäri, I., Paakkola, J., 2001. U-Pb isotopic studies on the Kittilä greenstone area, Central Lapland, Finland. Geol. Surv. Finland, Spec. Pap. 33, 95-141.

Vaasjoki, M., Sakko, M., 1988. The evolution of the Raahe-Ladoga zone in Finland: isotopic constraints. Geol. Surv. Finland Bull. 343, 7-32.

Väisänen, M., Mänttäri, I., Hölttä, P., 2002. Svecofennian magmatic and metamorphic evolution of the Turku Migmatite complex, southwestern Finland as revealed by U-Pb zircon SIMS geochronology. Prec. Res. 116, 111-127.

Ultrasonic seismic P- and S- velocities – the case of the Outokumpu deep drill core and FIRE profile samples

T. Elbra[1], I. Lassila[2], E. Hæggström[2,3], L. J. Pesonen[1], I.T. Kukkonen[4] and P. Heikkinen[5]

[1] Division of Geophysics, PO Box 64, FIN-00014, University of Helsinki, Finland
[2] Electronics Research Unit, PO Box 64, FIN-00014, University of Helsinki, Finland
[3] Helsinki Institute of Physics, PO Box 64, FIN-00014 University of Helsinki, Finland
[4] Geological Survey of Finland, PO Box 96, FIN-02151 Espoo, Finland
[5] Institute of Seismology, P.O. Box 68, FIN-00014 University of Helsinki, Finland

The geological evolution of the Archean to Proterozoic Outokumpu area is poorly known due to lack of seismic velocity data of the rocks as a function of depth. Measurements of the seismic P- and S- velocities of the Outokumpu deep drill core samples under crustal pressures and temperatures are therefore required. For this purpose a novel ultrasonic instrument to estimate the seismic velocities (Vp and Vs) down the drill core under crustal temperatures and pressures has recently been constructed at the University of Helsinki. The instrument will be also used in high resolution FIRE (and subsequent) seismic reflection studies. Moreover, the new instrument provides a facility to start to compile seismic P- and S-wave velocity data of crustal units of the Fennoscandia to improve the seismic interpretations of the lithosphere under Finland. In the future the instrument will be also used to map the petrophysical P- and S-wave velocities of other deep drill cores of several impact structures like Bosumtwi (Ghana), Chicxulub (Mexico) and Chesapeake Bay (Virginia).

Keywords: Outokumpu, FIRE-profile, P- and S-wave velocities, ultrasonic method

1. Introduction

The Outokumpu formation, economically the most important geological terrain in Finland, is well-known for its polymetallic massive sulphide ore deposits and is also one of the oldest ophiolitic formations in the world. The Outokumpu formation is part of the Palaeoproterozoic overthrusted nape, and has suffered multiple tectonic events and metamorphisms since 1.97 Ga. The geology of Outokumpu area is complex and the formation consists of various rock types like granite bodies, gneisses, schists, skarn formations and ultramafic units forming the so-called Outokumpu association. Geophysically the Outokumpu area is located in a complex network of geophysical anomaly patches and distinct gravity anomalies.

The Geological Survey of Finland (GTK) has lately carried out wide-angle seismic profiles in the framework of the FIRE seismic reflection project and the Outokumpu Deep Drilling Project (ODDP; Fig. 1). The data from FIRE reveal complex seismic reflectors whose origin is, however, poorly understood. Hence a wider knowledge of physical properties (e.g. seismic velocities of rocks) is therefore required. In order to understand recent seismic reflection data and to gain more information about the Outokumpu formation a new ultrasonic device was constructed in Kumpula in collaboration between the Division of Geophysics and the Electronics Research Unit of the Physics Department. Currently the instrument is ready and in test use. Hereby we report first Vp/Vs results of Outokumpu deep drill core samples and seismic reflection (FIRE) samples.

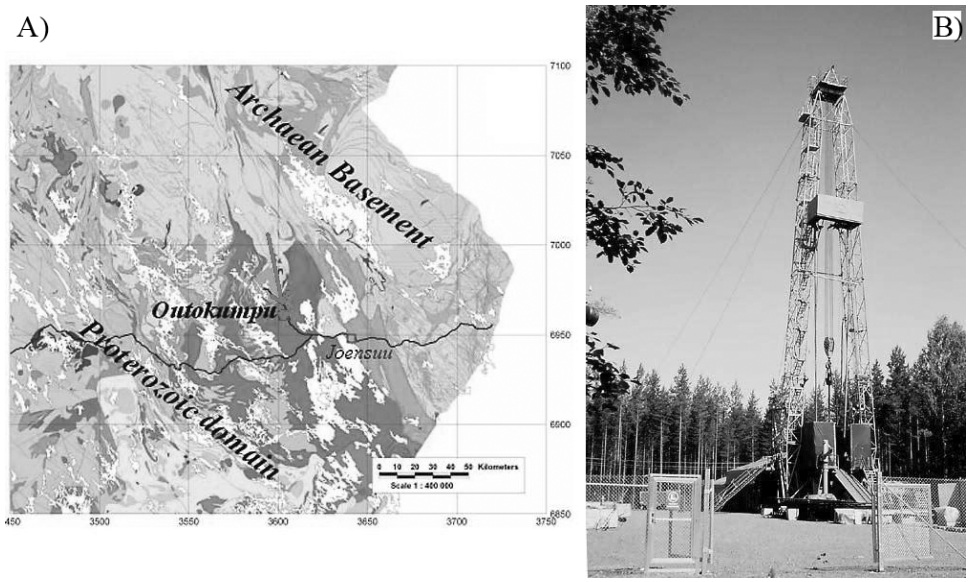

Figure 1. (a) Location of the Outokumpu Deep Drill Core in NE Finland (arrow) and (b) the on-site drilling platform (after Kukkonen *et al* 2004).

2. Instrumentation

A semiautomatic instrument (Fig. 2; Lassila *et al.* 2006), which is capable of measuring longitudinal and shear wave phase velocities (Vp and Vs) under varying temperature (20-300 ºC) and uni-axial pressure (0-300 MPa), was built in order to improve the Outokumpu data as well as the Outokumpu part of the ongoing seismic FIRE-reflection project. The time-of-flight (TOF) measurements were done using the ultrasonic pitch-catch method in desired temperature and pressure conditions, and repeated in same conditions using the ultrasonic pulse-echo method. The TOF signal passing through the delay line and reflecting back from the sample surface was recorded. By subtracting the TOF through the delay lines from the TOF trough the delay lines and the sample, the effect of temperature and pressure on the delay lines was eliminated. The received ultrasonic signal, temperature and pressure values were recorded with a PC. The Vp and Vs were then calculated.

3. Results

The ultrasonic Vp and Vs measurements were carried out on several ODDP and FIRE samples in order to test the situation in the upper crust by changing P and T simultaneously (Fig. 3), and to determine the effect of T and P separately on Vp and Vs (Fig 4). Preliminary results showed a clear pressure dependence of Vp and Vs. Vs also shows a clear trend of lower values at higher temperatures. The dependence of Vp on temperature, however, was not clear. Good correlation with Vp data from previous laboratory measurements (unpublished data by Elbra) was also observed. The results obtained with the device will be used to understand recent seismic reflection (FIRE) data from the Outokumpu area in Finland.

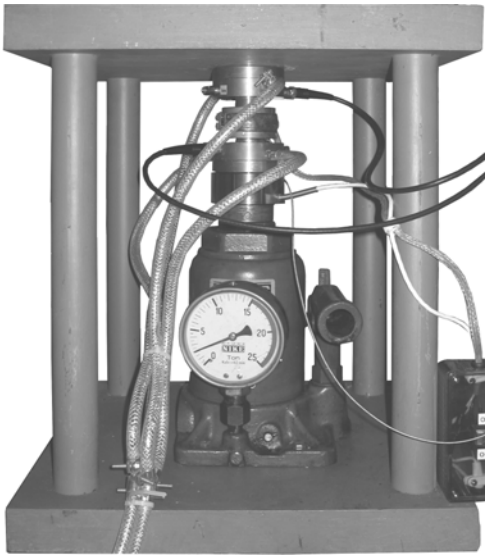

Figure 2. New ultrasonic seismic velocity (Vp and Vs under crustal P-T conditions) apparatus.

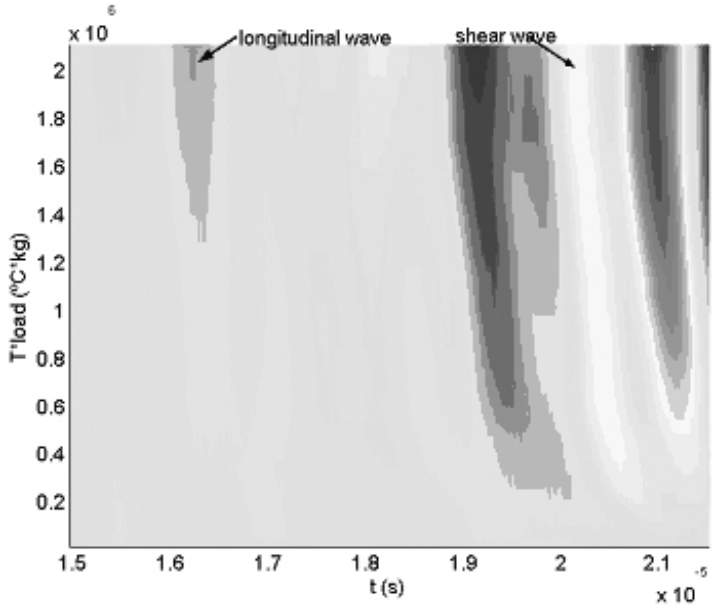

Figure 3. Example of the signal through two delay lines and the sample. The temperature and the load were changing at the same time to simulate the situation in the crust. From the time of arrival determined from this picture, we must still subtract the time of flight through the delay lines. As no contact gel was used the signal to noise ratio was reduced at lower pressures.

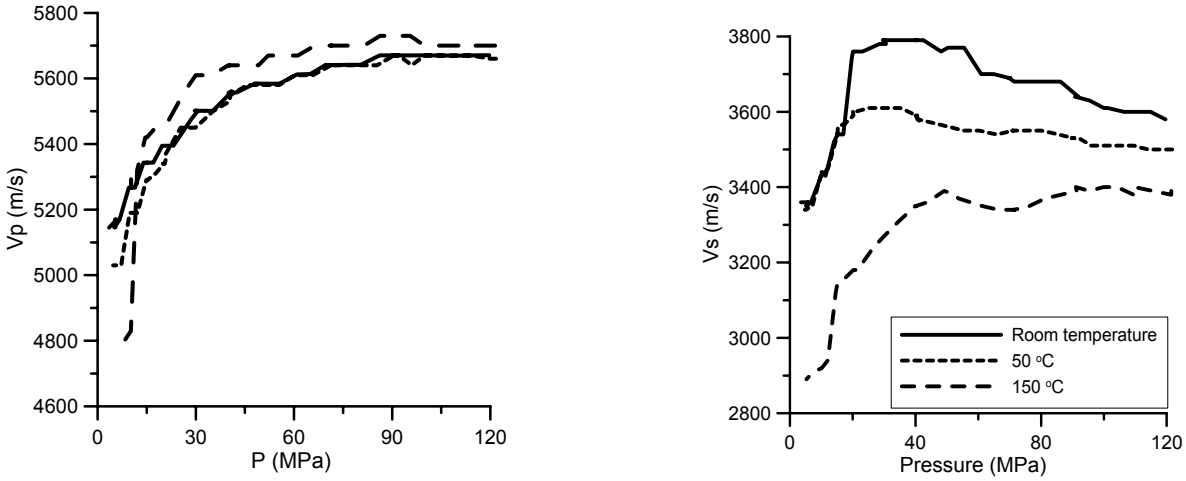

Figure 4. Vp (left) and Vs (right) versus pressure at various temperatures. The sample presented in this plot comes from the Outokumpu deep drill core from the unit called Outokumpu association and consists of mafic rocks.

4. Acknowledgments

This research was supported by the Outokumpu Oyj Foundation.

References

Kukkonen, I.T. (editor), 2004. Outokumpu Deep Drilling Project, International Workshop, October 25-26, 2004, Espoo, Finland. Program and Extended Abstracts. Geological Survey of Finland, Espoo Unit, *Geophysical Research Report Q10.2/2004/1*, 49 p.

Lassila, I. Elbra, T., Lehtiniemi, R., Seppänen, H. Haapalainen, J., Karppinen, T., Hæggström, E., Pesonen, L.J. and Kukkonen, I., 2006. "Device for measuring P- and S-wave velocities in rock samples under crustal conditions", Quantitative Nondestructive Evaluation 2006, Oregon, USA, 30.7-4.8, 2006

Evidence for pre-Pangean supercontinents, and the search for accurate reconstructions

David A.D. Evans

Department of Geology & Geophysics, Yale University
210 Whitney Avenue, New Haven CT 06520-8109 USA
E-mail: dai.evans@yale.edu

Keywords: supercontinents, Rodinia, Nuna, paleomagnetism

Pangea is the youngest supercontinent in Earth history, and the only one for which we have ample evidence of its existence through numerous independent methods. Reconstruction of Pangea shows an interlocking network of 0.6–0.3 Ga orogens surrounding older cratons, suggesting that Pangea assembled through plate convergence at the expense of now-vanished Neoproterozoic–Paleozoic oceans. The stratigraphic record and Neoproterozoic ages of rift-to-passive-margin successions on many of those pre-Pangean cratons suggest fragmentation of an earlier supercontinent, named Rodinia (McMenamin and McMenamin, 1990). Widespread fragments of 1.3–1.0 Ga orogenic belts within those same cratons appear to record aggregation of Rodinia in the same manner as its successor landmass Pangea. Fifteen years ago, a conceptual paradigm for Rodinia reconstructions (Moores, 1991; Dalziel, 1991; Hoffman, 1991) charted the course for all subsequent tests using the methods of tectonostratigraphy, geochronology, and paleomagnetism. This paradigm juxtaposes elements of "East Gondwanaland" (including northern Australia, Mawsonland, and possibly South China) against western Laurentia; elements of "West Gondwanaland" (including Amazon, Rio de la Plata, and possibly Congo or Kalahari) against eastern Laurentia; and northern cratons (Baltica, Siberia, North China) around the various marginal segments of northern Laurentia. A well known variant is the placement of Siberia adjacent to western Laurentia (Sears and Price, 1978, 2000, 2003). One recent summary reconstruction, from Pisarevsky et al. (2003a), is shown in Figure 1. Some of the proposed juxtapositions unify Archean and Paleoproterozoic terrains that imply connections for more than a billion years prior to Rodinia's breakup. The variations of reconstructions within the Rodinia paradigm show an anastomosing network of Archean cratonic nuclei, Paleoproterozoic foldbelts, and early Mesoproterozoic rift-to-passive-margin cover successions, suggesting that Rodinia asembled via amalgamation of fragments from an earlier supercontinent, which has been named Hudsonland (Williams et al., 1991), Nuna (Hoffman, 1996), Capricornia (Krapez, 1999), or Columbia (Rogers and Santosh, 2002; Zhao et al., 2002, 2004). Most speculations on reconstructions of this late Paleoproterozoic supercontinent refer heavily to aspects of the Rodinia paradigm, implying only minor shuffling of cratons between 1.8 and 1.0 Ga.

Figure 1. Rodinia reconstruction after Pisarevsky et al. (2003a). Cratons are restored to the present Laurentian reference frame.

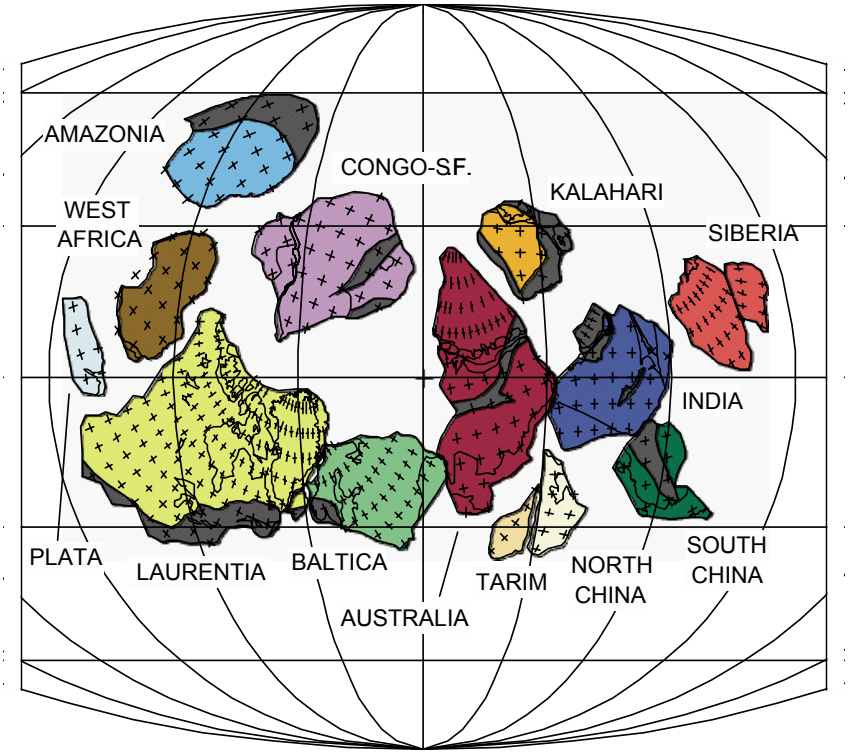

Figure 2. Radically revised Rodinia, according to this paper. Cratons have been restored to their paleogeographic latitudes at 780 Ma.

Recent paleomagnetic data, however, have strained the Rodinia paradigm to the limit of imminent rupture. Led by scientists from the Tectonics Special Research Centre in Perth, (established by the late Chris Powell), paleomagnetic results from Western Australia at three ages successively negated the SWEAT reconstruction at 755 Ma (Wingate and Giddings, 2000), both the SWEAT and AUSWUS configurations at 1070 Ma (Wingate et al., 2002), and all three of the SWEAT, AUSWUS, and AUSMEX juxtapositions at 1200 Ma (Pisarevsky et al., 2003b). A direct Rodinian connection between western Laurentia and Australia can only be accommodated by the AUSMEX reconstruction with collision after 1200 Ma and breakup prior to 755 Ma. If so, then collision as late as 1200 Ma would render as irrelevant all Paleoproterozoic tectonic comparisons between the two blocks, "Grenvillian" collision would need to be invoked along the western Laurentian margin which by current knowledge contains no record of such an event, and complete breakup earlier than 750 Ma would conflict with younger ages of ca.700 Ma from rift successions in the North American Cordillera (Lund et al., 2003; Fanning and Link, 2004). In the case of Siberia, the western Laurentian connection appears to be invalidated by the spread of Riphean paleomagnetic poles from Turukhansk uplift and the Sette-Daban foldbelt (Pisarevsky and Natapov, 2003), and only an indirect connection—that is, with an intervening gap—is permitted between Siberia and northern Laurentia. Incorporation of geomagnetic polarity from precisely dated igneous rocks in the Keweenawan of Laurentia, and the Umkondo large igneous province of Kalahari, refutes all proposed direct juxtapositions of those two cratons at 1108 Ma (Hanson et al., 2004). Among recent paleomagnetically-based models of Rodinia, the high-latitude positions of Congo-São Francisco and India at various ages within the 1100–800 Ma interval appear to conflict with low-latitude positions of other cratons (Pisarevsky et al., 2003a), suggesting that those blocks be excluded from Rodinia. Amazon may have been connected to southern Laurentia at 1200 Ma (Tohver et al., 2002), but not at ca.960 Ma (D'Agrella-Filho et al., 2003). In summary, the recent paleomagnetic data would seem to require that Rodinia was rather small and short-lived: a substantially more diminutive entity than the great and enduring early Neoproterozoic supercontinent as originally conceived. The only successful paleomagnetic confirmation of a tectonically-based reconstruction is that of northeast Laurentia and Baltica (Gower et al., 1990; Pesonen et al., 2003; Pisarevsky et al., 2003a).

One could question the veracity of Proterozoic paleomagnetic data, even on general terms. What do we know about the Precambrian geomagnetic field? How impervious are the rocks to remagnetization? What guarantees that the paleomagnetic results are primary? On broader geodynamic issues, are the age comparisons precise enough to rule out rapid continental motions (with or without true polar wander, TPW) as the cause of paleomagnetic discrepancies with the standard Rodinia models? All of these are valid concerns, yet all have been addressed with initial success by empirical studies. First, at a fine scale, the magnetostratigraphic record of stratabound polarity reversals in correlatable horizons across sedimentary basins (e.g., Kirschvink, 1978; Idnurm et al., 1995; Gallet et al., 2000) suggests a sporadically reversing geodynamo similar to that of today. Second, paleomagnetism of large Proterozoic evaporite basins has yielded a concentration of deposits in subtropical latitudes similar to that of the last 250 Myr, consistent with a geocentric-axial-dipolar magnetic field for most of the last two billion years (Evans, in press). Third, the rocks studied to generate the new paleomagnetic poles are essentially unmetamorphosed and have been demonstrated through field stability tests (e.g., baked-contact, fold, conglomerate) to retain primary magnetic remanences. Fourth, although

some intervals of Neoproterozoic-Paleozoic time appear to be characterized by rapid continental motions and/or true polar wander (see Evans, 2003; Maloof et al., 2006), the ages of poles discussed above are precise enough to distinguish all but the fastest allowable TPW, or the broader distribution of pole comparisons may suffice for the argument at hand (e.g., the Laurentian and Siberian APW swaths, despite poor age constraints for the latter curve).

If the paleomagnetic data are robust and appear to discredit the original Rodinia paradigm, then perhaps the original paradigm should be reconsidered. During the past three years, I have been developing a radically different Rodinia model that incorporates the most reliable paleomagnetic poles and integrates these with global tectonostratigraphy. I claim that according to existing paleomagnetic data under the assumption of a geocentric-axial-dipole magnetic field on an Earth of constant radius, this new Rodinia reconstruction is the *only* possible model allowable for inclusion of all the largest 10-12 cratons spanning the entire time interval of ca.1100–750 Ma, i.e., in accordance with the original concept of a supercontinent assembled via "Grenvillian" collisions and disaggregated by mid-Neoproterozoic rifts.

My proposed Rodinia (Figure 2) includes few traditional cratonic connections, but these include a Greenland-Baltica link that includes rotation at ca.1100 Ma about an Euler pole near the conjoined Scoresby Sund and Finnmark regions (Piper, 1980; Gower et al., 1990), and Australia-India-South China connections similar to those hypothesized by Powell and Pisarevsky (2002) and one option presented by Li et al. (2004). The radical Rodinia revisions include: western Laurentia connected to elements of "West" Gondwanaland such as West Africa, Rio de la Plata, and Amazon; northern Laurentia connected to Congo-São Francisco, Australia connected to Baltica but not directly with Laurentia, Kalahari next to Mawsonland, and Siberia on the outer edge of the supercontinent beyond India. One potential shortcoming of the model is that no large craton remains in the world to collide with the Grenville Province of Laurentia; instead, this orogen must be considered in terms of circum-Pacific orogens involving only accretionary tectonism—a topic currently being explored (Evans, 2005, 2006). The same would be required of the Sveconorwegian and Namaqua-Natal orogens, also facing outward the Mirovian ocean in my proposed Rodinia. There are many intriguing possible intercratonic correlations that can be drawn in the framework of an entirely different global context, and I hope that the revised Rodinia inspires more attention on previously neglected cratons such as West Africa and Rio de la Plata.

The present paper will focus on Baltica, within the contexts of classical versus revised Rodinia models. Depending on the reconstructions, various margins of Baltica are predicted to have billion-year-long or substantially shorter durations of juxtaposition with other cratons. The longer-lived connections are predicted to have assembled with Rodinia's predecessor Nuna during the Svecofennian and globally related orogenies at ca.1900–1800 Ma. Older cratonic connections have been postulated between Karelia and the Superior craton, based on matching ages from 2500–2100 Ma dyke swarms in both regions. A diminutive area of Archean preservation hampers our ability to construct global paleogeography from that time interval, and we may only be able to test specific hypothesized cratonic connections.

References

D'Agrella-Filho, M.S., Pacca, I.G., Elming, S.-A., Trindade, R.I., Geraldes, M.C., and Teixeira, W., 2003. Paleomagnetic and rock magnetic studies of Proterozoic mafic rocks from western Mato Grosso State, Amazonian craton. Geophysical Research Abstracts (European Geophysical Society), v.5, no.05619.

Dalziel, I.W.D., 1991. Pacific margins of Laurentia and East Antarctica-Australia as a conjugate rift pair: Evidence and implications for an Eocambrian supercontinent. Geology, v.19, p.598-601.

Evans, D.A.D., 2003. True polar wander and supercontinents. Tectonophysics, v.362, p.303-320.

Evans, D.A.D., 2005. Do Avalonian terranes contain the lost Grenvillian hinterland? Geological Association of Canada Abstracts, v.30, p.54-55.

Evans, D.A.D., 2006. Grenville collision without another continent? Geological Association of Canada Abstracts, v.31, p.46-47.

Evans, D.A.D., in press. Proterozoic low orbital obliquity and axial-dipolar geomagnetic field from evaporite palaeolatitudes. Nature.

Fanning, C.M., and Link, P.K., 2004. U-Pb SHRIMP ages of Neoproterozoic (Sturtian) glaciogenic Pocatello Formation, southeastern Idaho. Geology, v.32, p.881-884.

Gallet, Y., Pavlov, V.E., Semikhatov, M.A., and Petrov, P.Yu., 2000. Late Mesoproterozoic magnetostratigraphic results from Siberia: Paleogeographic implications and magnetic field behavior. Journal of Geophysical Research, v.105 (B7), p.16481-16499.

Gower, C.F., Ryan, A.B., and Rivers, T., 1990. Mid-Proterozoic Laurentia-Baltica: an overview of its geological evolution and a summary of the contributions made by this volume. In: Gower, C.F., Rivers, T., and Ryan, B., eds., Mid-Proterozoic Laurentia-Baltica. Geological Association of Canada Special Paper 38, p.1-20.

Hanson, R.E., Crowley, J.L., Bowring, S.A., Ramezani, J., Gose, W.A., Dalziel, I.W.D., Pancake, J.A., Seidel, E.K., Blenkinsop, T.G., and Mukwakwami, J., 2004. Coeval large-scale magmatism in the Kalahari and Laurentian cratons during Rodinia assembly. Science, v.304, p.1126-1129.

Hoffman P.F., 1991, Did the breakout of Laurentia turn Gondwanaland inside-out?: Science, v.252, p.1409-1412.

Hoffman P.F., 1996, Tectonic genealogy of North America, in Van der Pluijm B.A. & Marshak S., eds, Earth Structure: An Introduction to Structural Geology and Tectonics, McGraw-Hill, p.459-464.

Idnurm, M., Giddings, J. W. & Plumb, K. A., 1995. Apparent polar wander and reversal stratigraphy of the Palaeo-Mesoproterozoic southeastern McArthur Basin, Australia. Precambrian Research, p.72, p.1-41.

Kirschvink, J.L., 1978. The Precambrian-Cambrian boundary problem: Paleomagnetic directions from the Amadeus Basin, central Australia. Earth and Planetary Science Letters, v.40, p.91-100.

Li, Z.X., Evans, D.A.D., and Zhang, S., 2004. A 90° spin on Rodinia: possible causal links between the Neoproterozoic supercontinent, superplume, true polar wander and low-latitude glaciation. Earth and Planetary Science Letters, v.220, p.409-421.

Lund, K., Aleinikoff, J.N.,Evans, K.V., and Fanning, C.M., 2003. SHRIMP U-Pb geochronology of Neoproterozoic Windermere Supergroup, central Idaho: Implications for rifting of western Laurentia and synchroneity of Sturtian glacial deposits. Geological Society of America Bulletin, v.115, p.349-372.

Maloof, A.C., Halverson, G.P., Kirschvink, J.L., Schrag, D.P., Weiss, B.P., and Hoffman, P.F., 2006. Combined paleomagnetic, isotopic, and stratigraphic evidence for true polar wander from the Neoproterozoic Akademikerbreen Group, Svalbard. Geological Society of America Bulletin, v.118, p.1099-1124.

McMenamin, M.A.S., and McMenamin, D.L.S., 1990, The Emergence of Animals: The Cambrian Breakthrough: New York, Columbia University Press, 217 p.

Moores, E.M., 1991. Southwest US – East Antarctic (SWEAT) connection: A hypothesis. Geology, v.19, p.425-428.

Pesonen, L.J., Elming, S.-Å., Mertanen, S., Pisarevsky, S., D'Agrella-Filho, M.S., Meert, J.G., Schmidt, P.W., Abrahamsen, N., and Bylund, G., 2003. Palaeomagnetic configuration of continents during the Proterozoic. Tectonophysics, v.375, p.289-324.

Piper, J.D.A., 1980. Analogous Upper Proterozoic apparent polar wander loops. Nature, p.283, v.845-847.

Pisarevsky, S.A. and Natapov, L.M., 2003. Siberia and Rodinia. Tectonophysics, v.375, p.221-245.

Pisarevsky S.A., Wingate M.T.D., Powell C.McA., Johnson S. & Evans D.A.D., 2003a, Models of Rodinia assembly and fragmentation. In: Yoshida, M., Windley, B.F., and Dasgupta, S., eds., Proterozoic East Gondwana: Supercontinent Assembly and Breakup. Geological Society of London Special Publication 206, p.35-55.

Pisarevsky, S.A., Wingate, M.T.D., and Harris, L.B., 2003b. Late Mesoproterozoic (ca 1.2 Ga) palaeomagnetism of the Albany-Fraser orogen: No pre-Rodinia Australia-Laurentia connection. Geophysical Journal International, v.155, p.F6-F11.

Powell, C.McA., and Pisarevsky, S.A., 2002. Late Neoproterozoic assembly of East Gondwana. Geology, v.30, p.3-6.

Rogers J.J.W. & Santosh M., 2002, Configuration of Columbia, a Mesoproterozoic supercontinent, Gondwana Research, v.5, p.5-22.

Sears, J.W., and Price, R.A., 1978. The Siberian connection: a case for the Precambrian separation of the North American and Siberian cratons. Geology, v.6, p.267-270.

Sears J.W. & Price R.A., 2000, New look at the Siberian connection: No SWEAT, Geology, v.28, p.423-426.

Sears, J.W. and Price, R.A., 2003. Tightening the Siberian connection to western Laurentia. Geological Society of America Bulletin, v.115, p.943-953.

Tohver, E., van der Pluijm, B.A., Van der Voo, R., Rizzotto, G., and Scandolara, J.E., 2002. Paleogeography of the Amazon craton at 1.2 Ga: Early Grenvillian collision with the Llano segment of Laurentia. Earth and Planetary Science Letters, v.199, p.185-200.

Williams, H., Hoffman, P.F., Lewry, J.F., Monger, J.W.H., and Rivers, T., 1991. Anatomy of North America: thematic portrayals of the continent. Tectonophysics, v.187, p.117-134.

Wingate, M.T.D., and Giddings, J.W., 2000. Age and palaeomagnetism of the Mundine Well dyke swarm, Western Australia: Implications for an Australia-Laurentia connection at 755 Ma. Precambrian Research, v.100, p.335-357.

Wingate, M.T.D., Pisarevsky, S.A., and Evans, D.A.D., 2002. Rodinia connections between Australia and Laurentia: No SWEAT, no AUSWUS? Terra Nova, v.14, p.121-128.

Zhao, G., Cawood, P.A., Wilde, S.A., and Sun, M., 2002. Review of global 2.1-1.8 Ga orogens: implications for a pre-Rodinia supercontinent. Earth-Science Reviews, v.59, p.125-162.

Zhao, G., Sun, M., Wilde, S.A., and Li, S., 2004. A Paleo-Mesoproterozoic supercontinent: assembly, growth and breakup. Earth-Science Reviews, v.67, p.91-123.

Modelling the Eurasian ice sheet: focus on basal temperatures and isostacy

Pirjo-Leena Forsström

Center for Scientific Computing
Keilaranta 14
FIN-02100 Espoo, Finland
E-mail: Pirjo-leena.forsstrom@csc.fi

Simulation of the Eurasian ice sheet dynamics during the Weichselian glaciationis realised with SICOPOLIS ice sheet model. The simulations produce topographic changes and basal temperatures that are not controversial with observations.

Keywords: Eurasian Ice Sheet, Weichselian glaciation, ice sheet model, topographic depression and rebound, basal temperatures.

Ice sheets have a profound influence on climate and global sea level by affecting atmospheric and oceanic circulation patterns and planetary albedo through changes in ice sheet extent, height and stability *(Hughes, 1987, 1992, 1998)*. Circulation effects depend on the height of the ice sheet and on temperature effects on the ice sheet area *(Rind, 1987)*. Isostatic depression and rebound of the lithosphere due to changing ice loads has a strong influence on local climatology. An important feedback factor for ice sheets and climate is the effect of proglacial ice-dammed lakes, forming in topographic lows on ice-sheet margins. To study these complex climate-related processes, numerical models are invaluable. An ideal tool to study the Northern Hemisphere Ice Sheets, would be an integrated climate-ocean-ice sheet-land processes model. The land system includes components like isostatic effects, hydrology and permafrost. Combined models for these systems form the Earth System Models. These models have fundamentally insatiable computational requirements, and are still very much under development.

During cold climatic spells, ice-free areas were subjected to low surface temperatures. During these times, the ground temperatures underneath ice sheets can be notably warmer and more stable than outside the ice sheet *(Paterson, 1994)*. If an ice sheet is thick and has long, stable occupation time, the temperature variations underneath the ice sheet are probably smaller compared to values outside the ice sheet. Conditions at the ice sheet base are controlled by ice sheet pressure, temperature, hydrology and properties of the underlying substrate.

To investigate the Eurasian ice sheet mass balance and geographic extent, a thermodynamic ice sheet model is applied, with a particular interest in calving margin discharge. This is realised by the ice-sheet model SICOPOLIS (SImulation COde for POLythermal Ice Sheets; *Greve, 1997a,b*), run in combination with data manipulation and analysis programs. SICOPOLIS was one of the ice sheet model codes compared in the European Ice Sheet Modelling INiTiative (EISMINT) *(Huybrechts and Payne, 1996; Payne et al., 2000)*. The EISMINT benchmarks and intercomparisions provide valuable results of the accuracy and consistency of ice sheet model codes. SICOPOLIS is based on the continuum-mechanical balance equations and jump conditions of mass, momentum and energy. The model treats ice as an incompressible, heat-conducting, isotropic power-law fluid with thermo-mechanical coupling due to the strong temperature dependence of the

flow law. SICOPOLIS is based on the shallow-ice approximation (SIA), that is, normal stress deviators and shear stresses in vertical planes are neglected. The large-scale behaviour of ice sheets is simulated well with the SIA; however, it is not valid locally in the vicinity of ice domes and close to the margin.

Isostatic depression and rebound of the lithosphere due to changing ice loads is described by a local-lithosphere-relaxing-asthenosphere (LLRA) model with an isostatic time lag τ_{iso} *(LeMeur and Huybrechts, 1996; Greve, 2001)*. In the LLRA model, an ice load at a given position causes a steady-state displacement of the lithosphere in the vertical direction. The value of the displacement is determined by the balance between ice load and the boyance force which the lithosphere experiences. As the astenosphere is viscous, the lithosphere assumes the displacement after a time lag. The time lag used here is 3000 years. A more detailed description of the model is given by *Greve (1997a,b, 2001)*. The geothermal heat flux is prescribed at the lower boundary of the lithosphere layer.

The model computes the three-dimensional evolution of ice extent, thickness, velocity, temperature and water content in the temperate ice region and age in response to external forcing. The forcing due to climate and heat from Earth's interior, are (i) the mean annual air temperature at the ice surface, (ii) the surface mass balance, which is ice accumulation (here assumed to be snowfall) minus ablation (here assumed to be melting), (iii) the global sea level and (iv) the geothermal heat flux entering the ice mass from below. Surface processes like refreezing are accounted for. Sea level changes were derived from the SPECMAP record *(Imbrie et al., 1984)*. The seasonal temperature and precipitation distributions are interpolated linearly between the present *(Legates and Wilmott, 1990)* and Last Glacial Maximum (LGM) anomaly values with a glaciation index $g(t)$. This index scales the GRIP $\delta^{18}O$ record *(Dansgaard and others, 1993)* to represent LGM ($g=1$) and present ($g=0$) conditions. The model is initialised in an arbitrarily chosen ice-free state, 250 ka ago. The model needs approximately 50 ka to clear the effect of the initial state. Climate conditions are tied to the Greenland ice core record. Thus, the simulation runs through one complete glaciation and deglaciation before the time period of interest, the Weichselian, which started 115 000 ka BP and ended 10 000 ka BP.

The topographic lithosphere evolution during the Weichselian glaciations is dominated by ice dome loading, resulting in lithosphere depression. From the rebound rates that aim towards an isostatic balance, the previous load can be deduced. This can be seen in the simulation results: the evolving ice sheet depressed southern parts of Sweden and Finland below sea level as we approach the LGM. Also, marine Baltic areas are thus depressed. The central Barents Sea area is depressed to a depth of around 1 km. At the LGM, these areas get deeper. Southern Sweden and Finland have warped to a depth of -300 meters. This depression is greatest at 18 ka ago, with a bathymetric depth of -800 m at the Gulf of Bothnia. This depression helps the ice sheet to deglaciate quickly as sea level rises. The Younger Dryas cooling affects a heavily reduced Fennoscandian ice sheet, clearly not correctly simulated. Central and eastern Barents Sea areas stay heavily glaciated until the end of Weichselian. The Danish Straits, Skagerrak and Kattegat, the NCIS onset areas, are approximately 600 meters deep duringglaciation. The Norwegian Channel is depressed to -900 meters at the LGM. The Norwegian Channel is at its widest at around 18 ka ago, with a central depth of 1 km. The central Barents Sea area is heavily depressed from the LGM to the Holocene. The Bear Island Trough and Franz Victoria Trough are the causeways to marine depths, as is the St. Anna Trough but not to such an extent as it is shallower. As the deglaciation starts with the onset of marine transgression, the southern Scandinavian Ice

Sheets (SIS) margin becomes marine 17.7 ka ago. At 17.1 ka ago, the SIS margin is marine up to Lake Ladoga. The marine area expands until 15,5 ka ago, when the Danish straits are closed by rebound. An ice lake exists in the Baltic Sea area until 14,3 ka ago, when the marine connection opens again, this time through southern Sweden. The simulated topography change is not controversial with observations.

The simulated basal temperatures in the western ice sheet marginal areas are above –1 °C. Similar basal conditions prevail in the Barents Sea area at Storfjorden and at the deepening of Storbanken, leading to the Bear Island Trough. The ice sheet at Franz Josef Land remains cold throughout the LGM and warms only in the Holocene. In the southwest sector of the SIS and also on the Norwegian coast, there was a large temperate base and temperate ice area. As a fast flow in the Nordic Channel area sets on, for example at 22 ka ago, the temperate base area expands to the Kattegat area on the Swedish coast, around 23 ka ago. Under the main ice dome, the highest temperatures prevail around the LGM, 21,8 ka ago. The basal temperature is then -1,5 °C in areas surrounding the Gulf of Bothnia. In Figure 1., the ratio of the area covered by temperate ice can be compared to the total ice-covered area (A_{temp}/A_{total}) to contrast the onset of fast flow with the spatial extent and basal temperature conditions.

The ground areas below thick ice sheets experience warmer temperatures than the areas subjected to the chilly LGM aerial temperatures. The atmospheric temperature anomaly is approximately -20 °C. In the results, this area is situated on the southern margin of the modelled ice sheet. The ice sheet occupies the area for a short time period around the LGM, with a thin ice cover of a few hundred meters. This is in accordance with *Šafanda et al., (2004)*, who reported a mean ground temperature anomaly of -18 °C in the glacial period. In Siljan, western Sweden, *Balling et al., (1990)* reported a lack of significant vertical variation in the ground temperature gradient. This area is in close proximity to the SIS ice divide. In the simulations, the Siljan area is either cold-based or maintains a maximum basal ice sheet temperature of -2 to -4 °C. In a study of the Outokumpu area, eastern Finland, *Kukkonen and Šafanda (1996)* concluded from heat transfer modelling, ground surface temperature values of -1 to -2 °C during the Weichselian. In the simulation results, this area is covered by an ice sheet in glacial times, with basal ice sheet temperatures in the range of -3,5 to -1,5 °C. In coclusion, the simulated temperatures are in broad agreement with the observations mentioned above. The lithosphere surface temperatures, and thus also deeper ground temperatures, vary more in areas with sporadic ice cover.

References

Balling, N. 1980. The land uplift in Fennoscandia, gravity field anomalies and isostacy. In: Mörner, N.-A. (ed.) *Earth Rheology, Isostacy and Eustacy*, 297-321. John Wiley and Sons, New York. 599 pp.

Dansgaard, W., S.J. Johnsen, H.B. Clausen, D. Dahl-Jensen, N.S. Gundestrup, C.U. Hammer, C.S. Hvidberg, J.P. Steffensen, A.E. Sveinbjörnsdottir, J. Jouzel and G. Bond. 1993. Evidence for general instability of past climate from a 250-kyr ice-core record. Nature, 364, 218-220.

Greve, R. 1997a. A continuum-mechanical formulation for shallow polythermal ice sheets. Phil. Trans. Roy. Soc. London, A355, 921-974.

Greve, R. 1997b. Application of a polythermal three-dimensional ice sheet model to the Greenland ice sheet: Response to steady-state and transient climate scenarios. J. Climate, 10 (5), 901-918.

Greve, R. 2001. Glacial isostasy: Models for the response of the Earth to varying ice loads. In: Straughan, B., R. Greve, H. Ehrentraut and Y. Wang (Eds.), Continuum Mechanics and Applications in Geophysics and the Environment, Springer, Berlin etc., 307-325.

Hughes, T.J. 1987. The marine ice transgression hypothesis. Geografiska Annaler. 69, 237-250.

Hughes, T.J. 1992. Abrupt climate change related to unstable ice-sheet dynamics: toward a new paradigm. Palaeoceanography, Palaeoclimatology, Palaecology (Global and Planetary Change Section, 97, 203-234.

Hughes, T.J. 1998. Ice Sheets. Oxford University Press, pp. 343.

Huybrechts, Ph., A.J. Payne and EISMINT Intercomparison Group.1996. The EISMINT benchmarks for testing ice-sheet models. Ann. Glaciol., 23, 1-12.

Imbrie, J., J.D. Hays, D.G. Martinson, A. McIntyre, A.C. Mix, J.J.M orley, N.G. Pisias, W.L. Prell and N.J. Shackleton. 1984. The orbital theory of Pleistocene climate: Support from a revised chronology of the marine delta18O record. Milankovitch and climate, part I, A.Berger and others (Eds.), D.Reidel Publishing Company, Dordrecht, Holland, 269-305 (NATO ASI Series C: Mathematical and Physical Sciences 126)

Kukkonen, I.T. and J. Šafanda. 1996. Palaeoclimate and structure: The most important factors controlling subsurface temperatures in chrystalline rocks. A case history from Outokumpu, eastern Finland. Geophys. J. Int., 126, 101-112.

Legates, D. R. and C. J. Wilmott, 1990. Mean seasonal and spatial variability in global surface air temperature. Theor. Appl. Climatol., 41, 11-21.

LeMeur, E. and P. Huybrechts. 1996. A comparison of different ways of dealing with isostasy: examples from modelling the Antarctic ice sheet during the last glacial cycle. Ann. Glaciol., 23, 309-317.

Paterson, W.S.B. 1994. The Physics of Glaciers. (3rd Edition). Pergamon, Oxford.

Payne, A.J. and D.T. Baldwin. 1999. Thermomechanical modelling of the Scandinavian Ice Sheet: implications for ice stream formation. Ann. Glaciol., 28, 83-89.

Payne, A.J. , Ph. Huybrechts, A. Abe-Ouchi, R. Calov, J.L. Fastook, R. Greve, S.J. Marshall, I. Marsiat, C. Ritz, L. Tarasov, and M.P.A. Thomassen. 2000. Results from the EISMINT model intercomparison: the effects of thermomechanical coupling. J. of Glaciol., 46 (153), 227-238.

Rind, D. 1987. Components of the ice age circulation. J.Geophys. Res., 92 (D4), 4241-4281.

Šafanda, J., J. Szewczyk and J. Majorowicz. 2004. Geothermal evidence of very low glacial temperatures on a rim of the Fennoscandian ice sheet. Geophys. Res. Lett., L07211, doi:10.1029/2004GL019547.

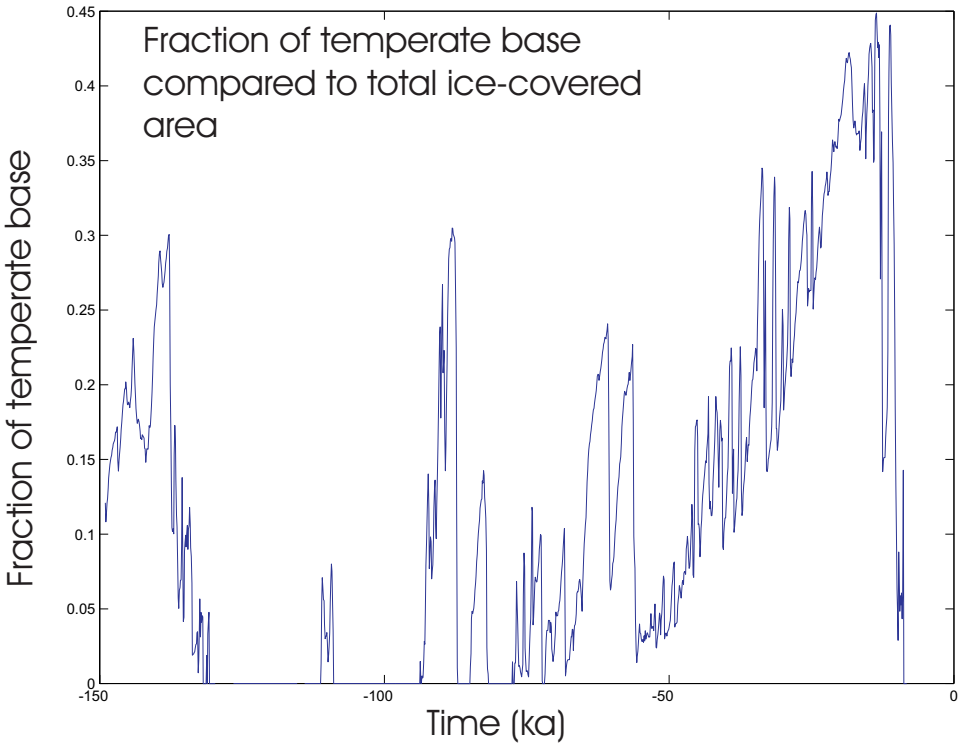

Figure 1: The fraction of temperate base compared to the total ice-covered area in the simulation results. The horizontal axis is time in ka, and the vertaical axis is the ratio.

Tyrisevä – an ultramafic intrusion in Vammala Ni-belt: petrography, structure and ore potential

K. Hagelberg[1], P. Peltonen[2] and T. Jokinen[2]

[1]Department of Geology, P. O. Box 64, 00014 University of Helsinki
[2]Geological Survey of Finland, P. O. Box 96, FI-02151 Espoo
Email: kerstin.hagelberg@helsinki.fi

The Tyrisevä intrusion in south-western Finland has been studied by means of petrography, mineral chemistry and geophysical surveys in order to constrain its internal structure and potential for Ni-sulphide deposits. No distinct layered series has developed in the intrusion, and the intrusion like many others in the Vammala area is interpreted to represent a remnant of synorogenic feeder dyke or sill. The intrusion is cumulate textured with olivine and clinopyroxene as the main cumulus minerals. The forsterite and nickel content of the olivines are fairly low, and on a Ni vs. Fo diagram Tyrisevä plots for the most part within the field of unmineralised intrusions.

Keywords: Svecofennian, Vammala Nickel Belt, Ni-Cu-sulfide deposit, olivine

1. Introduction

The Svecofennian mafic and ultramafic nickel deposits are the economically most important group of nickel deposits within the Fennoscandian Shield *(Häkli et al. 1979, Häkli and Vormisto 1985)*. The Tyrisevä ultramafic intrusion is located 20 km west of the former Vammala Ni-Cu mine. It belongs to the Vammala nickel belt between the Tampere and Hämeenlinna schist belts *(Häkli et al. 1979)*. Three mineralized nickel-copper deposits have been mined in the area (Stormi in Vammala, Kylmäkoski and Kovero-oja).

The Vammala area consists of sedimentary rocks that have been intensely metamorphosed into veined mica gneisses *(Matisto 1971)*. These metasediments are cut by synkinematic granodiorites and quartzdiorites *(Kilpeläinen and Rastas 1992)*. Black schists and graphite gneisses have been found in the area, and are interpreted to have caused sulphide saturation and triggered ore formation in the mafic and ultramafic intrusions in the Vammala area *(Lamberg 2005, Peltonen 1995a)*. The Ni-Cu deposits within the Vammala nickel belt are hosted by relatively small, lensoidal ultramafic-mafic intrusions *(Häkli et al. 1979, Mancini et al. 1996)*. *Peltonen (1995)* interpret the lenses as remnants of synorogenic feeder dykes and/or sills.

The Tyrisevä intrusion outcrops in only one location. Geophysical measurements and diamond drilling has been conducted in the area, and interpretations concerning petrography, structure and geochemistry are based on further study of this data. Only one diamond drill-core has penetrated the intrusion, but the base of the intrusion has not been located. The aim of the study is to determine in which direction the fractionation has proceeded and thereby locate the most favorable part for ore deposition.

2. Structure, petrography and geochemistry of the intrusion

No distinct layered series has been recognized in the Tyrisevä intrusion. The layers grade into one another and the direction of crystallization cannot with certainty be determined. Rhythmic layering is locally present.

The intrusion is cumulate textured. The main silicates are olivine, clinopyroxene, orthopyroxene and various amphiboles. Olivine, clinopyroxene, chromite and infrequently

orthopyroxene appear in the cumulus phase. Olivine occurs as cumulus grains of various sizes. The cumulus grains form networks with pyroxene and amphibole in the interstices. At places the cumulus grains are slightly elongated. Tremolite, hornblende and various sulphides are the main intercumulus minerals along with minor clinopyroxene. The intercumulus amphibole commonly encloses the cumulus phase in a poikilitic manner. The predominance of clinopyroxene over orthopyroxene is a typical feature for the ultramafic intrusions in the Vammala area *(Mäkinen 1987)*. The sulfide phase consists in order of abundance of pyrrhotite, pentlandite, chalcopyrite, pyrite, cubanite and sphalerite. The sulfides are mainly present in the intercumulus space, but also appear as rounded inclusions in pyroxene. The main oxides are magnetite, chromite and ilmenite. All the silicates have undergone various degrees of alteration, but in most cases the cumulus-texture is still preserved. Olivine has altered mainly into serpentine, iddingsite and magnetite. Pyroxene has altered into a pale brown uralite.

The Tyrisevä intrusion has similar geochemical features as the other ultramafic intrusions in the area. In his study on the Vammala, Ekojoki, Murto and Posionlahti intrusions, *Peltonen (1995b)* recognized some common features in the geochemistry of the intrusions, which apply for the Tyrisevä intrusion as well; whole rock MgO decrease towards the margins of the intrusion while Al_2O_3, CaO and SiO_2 increase in the same direction. *Peltonen (1995b)* concluded that these characteristics suggest concentration of Fe-Mg cumulus minerals in the central parts of the intrusions, and that the post-cumulus material becomes more abundant towards the margins.

3. Composition of olivine

The Fo content of the olivines varies between 67 and 79,5 mol%. The forsterite content of the mineralized intrusions in the area are slightly higher (79.0-82.4 mol% in Vammala and Ekojoki) *(Peltonen 1995b)*. The Ni content of the Tyrisevä olivines is rather low and shows a positive correlation with the Fo content. Plotted on a diagram with mineralized and barren reference intrusions in the Vammala area, Tyrisevä plots for the most part in the unmineralized field (Fig. 1). According to *Naldrett (2004)* and *Naldrett et al. (1984)* the low Ni content of olivines in barren intrusions in comparison to mineralized intrusions indicates that they have been equilibrated with a larger amount of sulphides than the mineralized intrusions or with magmas depleted in Ni prior to emplacement.

4. Geophysical results

The Tyrisevä intrusion is clearly visible on magnetic maps, and is situated in a positive Bouguer-anomaly domain. The size of the intrusion has been further investigated using ground surveys according to which the horizontal dimensions of the intrusion are approximately 1200 by 300 m with a depth of 300-400 m. The contact in the north is rather incoherent possibly due to later deformation *(Peltonen and Jokinen 2002)*. Based on ground geophysics the southern part of the intrusion is quite strongly magnetized (susceptibility 0.05 SI) and has low density (2.80 g/cm^3). The northern part of the intrusion shows weaker magnetism (0.01 SI) and higher density (3.05 g/cm^3). In the central part there is a section where both magnetism and density are high. This section is related to a moderately good (~50Ωm) SAMPO conductive body at a depth of 150-200 m. The low density of the intrusion can be explained by the strong serpentinization of the ultramafic rocks, and the magnetism by disseminated magnetite.

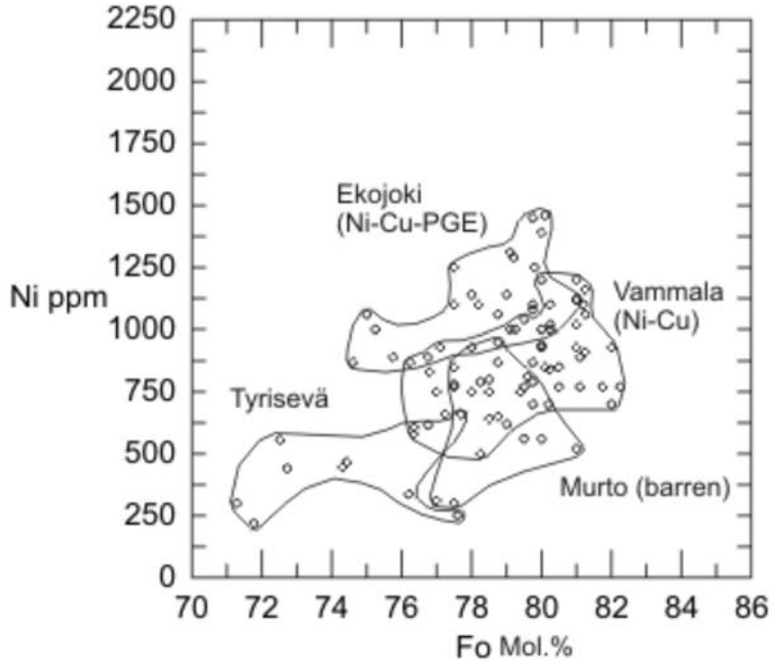

Figure 1. Compositions of olivines from mineralized Ekojoki and Vammala intrusions compared with Tyrisevä and barren Murto intrusions. Ekojoki, Vammala and Murto analyses after *Peltonen (1995a)*, Tyrisevä analyses from this study.

References

Häkli, T. A., Vormisto K. and Hänninen, E., 1979. Vammala, a nickel deposit in layered ultramafite, southwest Finland. Economic geology 74, 1166-1182.

Häkli, T., A. and Vormisto, K., 1985. The Vammala nickel deposit. In: Papunen H., Gorbunov, G. I. (Eds.), Nickel-copper deposits of the Baltic Shield and Scandinavian Caledonides. Geological survey of Finland Bulletin 333, 273-286.

Kilpeläinen, T. and Rastas, J., 1992. Vammalan Stormin Ni-malmin ympäristön metamorfisista ja rakennegeologisista tutkimuksista. Institution of geology and mineralogy, University of Turku, Publication No. 30, 1-18.

Lamberg, P., 2005. From genetic concepts to practice- lithogeochemical identification of Ni-Cu mineralised intrusions and localisation of the ore. Geological survey of Finland Bulletin 402, 264 pp.

Mäkinen, J., 1987. Geochemical characteristics of Svecokarelidic mafic-ultramafic intrusions associated with Ni-Cu occurrences in Finland. Geological Survey of Finland Bulletin 342, 109 pp.

Mancini, F., Papunen, H. and Marshall B. 1996. Petrogenetic and tectonic interpretations of ultramafic bodies in the Vammala Nickel Belt, southwestern Finland, from the study of the Sääksjärvi ultramafic complex. International Geology Review 38, 268-283.

Matisto, A., 1971. Explanation to the map of rocks, sheet 2121 Vammala. Geological Survey of Finland, 44 pp.

Naldrett, A. J., 2004. Magmatic sulfide deposits; geology, geochemistry and exploration. Springer Verlag, Berlin, 727 pp.

Naldrett, A. J., Duke, J. M., Lightfoot, P. C. and Thompson J. F. H., 1984. Quantitative modelling of the segregation of magmatic sulfides: an exploration guide. Canadian Mining Metal Bulletin, 1-11.

Peltonen, P., 1995a. Magma-country rock interaction and the genesis of Ni-Cu deposits in the Vammala Nickel Belt, SW Finland. Mineralogy and Petrology 52, 1-24.

Peltonen, P., 1995b. Petrogenesis of ultramafic rocks in the Vammala Nickel Belt: Implications for crustal evolution of the early Proterozoic Svecofennian arc terrane. Lithos 34, 253-274.

Peltonen, P. and Jokinen, T., 2002. Tutkimustyöselostus Äetsän kunnassa Tyrisevän alueella suoritetuista malminetsintätukimuksista vuosina 1998-2001. Geological Survey of Finland, M19/2121/2002/2

FIRE transects: reflectivity of the crust in the Fennoscandian Shield

P. Heikkinen[1*], I.T. Kukkonen[2] and FIRE Working Group

[1]Institute of Seismology, University of Helsinki, P.O. Box 26, FIN-00014 Helsinki, Finland
[2]Geological Survey of Finland, P.O. Box 96, FIN-02151 Espoo, Finland
*E-mail: pekka.heikkinen@seismo.helsinki.fi

The FIRE (Finnish Reflection Experiment) consortium carried out Vibroseis measurements in the Fennoscandian Shield in 2001-2003 on four lines transecting the major geological units in the Shield. The seismic reflection data, with a total processed profile length of 2104 km, give new information on the crustal structure of the Fennoscandian Shield, providing important and very useful data source for the studies of the tectonic evolution of the Shield.

Keywords: reflection seismics, crustal structure, Fennoscandian Shield

1. Introduction

The FIRE (Finnish Reflection Experiment) consortium – consisting of the Geological Survey of Finland, and Universities of Helsinki and Oulu, with Russian company Spetsgeofizika S.G.E. as a contractor, carried out Vibroseis measurements in the central part of the Fennoscandian Shield in 2001-2003. The four FIRE transects (Figure 1) run over the most important geological units of the Fennoscandian Shield. The location of the survey lines was based on decided on three main lines of argument: geological relevance, available roads and existence of previous wide-angle reflection/refraction data. Seismic reflection profiling has turned out to be the most efficient tool in studying the deep structure of the earth's crust. The large scale reflection surveys conducted during the last 10-15 years in Canada in the Lithoprobe project (Clowes et al., 1996), in Australia (Korsch, 1998) and also in the Fennoscandian Shield (BABEL Working Group, 1993a,b, Korja and Heikkinen, 2005) have provided new insights on the structure and evolution of the Precambrian crust. The recently published results (Kukkonen and Lahtinen, 2006) show that the seismic images from the FIRE profiles will also significantly improve our understanding of the tectonic process which formed the Fennoscandian Shield.

2. Data

The FIRE project has resulted in an extensive data set consisting of 2104 km of processed seismic CMP-sections in the Fennoscandian Shield. The analysis of the signal attenuation shows that the amplitude of the recorded seismic signal is above the background noise to at least 20 s TWT (two-way-travel time) corresponding to 60-70 km depth. At some locations the signal stayed well above the noise level during the complete recording time of 30 s (about 100-110 km). As this analysis was done using unprocessed shot gathers, it is expected that stacking and processing furthermore has improved the signal-to-noise ratio of the data. It can be thus assumed that reliable seismic images can be obtained throughout the whole crust.

The frequency range of the Vibroseis sources used was 12-80 Hz, which corresponds to wavelengths of about 500-75 metres. The analysis of the frequency content of the processed NMO stacked sections showed that in the upper crust (above 3.5-5.0 s TWT) the complete source signal bandwidth is present. Frequencies of up to 60 Hz are present in the

depth range of the crust (from 0 s to about 15-17 s TWT). Theoretically, this bandwidth allows reflective layers with thickness as small as 20 m in the upper crust and 30 m in the lower crust to be observed.

The basic data processing was done by Spetsgeofyzika producing two data sets which were later migrated at the Institute of Seismology. The normal CMP-stacks have record length of 30 s which corresponds about 100 km depth. The DMO-stacks with 16 s long trace length image better steeply dipping structures. In the DMO-sections in the upper part of the crust boundaries with dips up to 70 degrees can be seen.

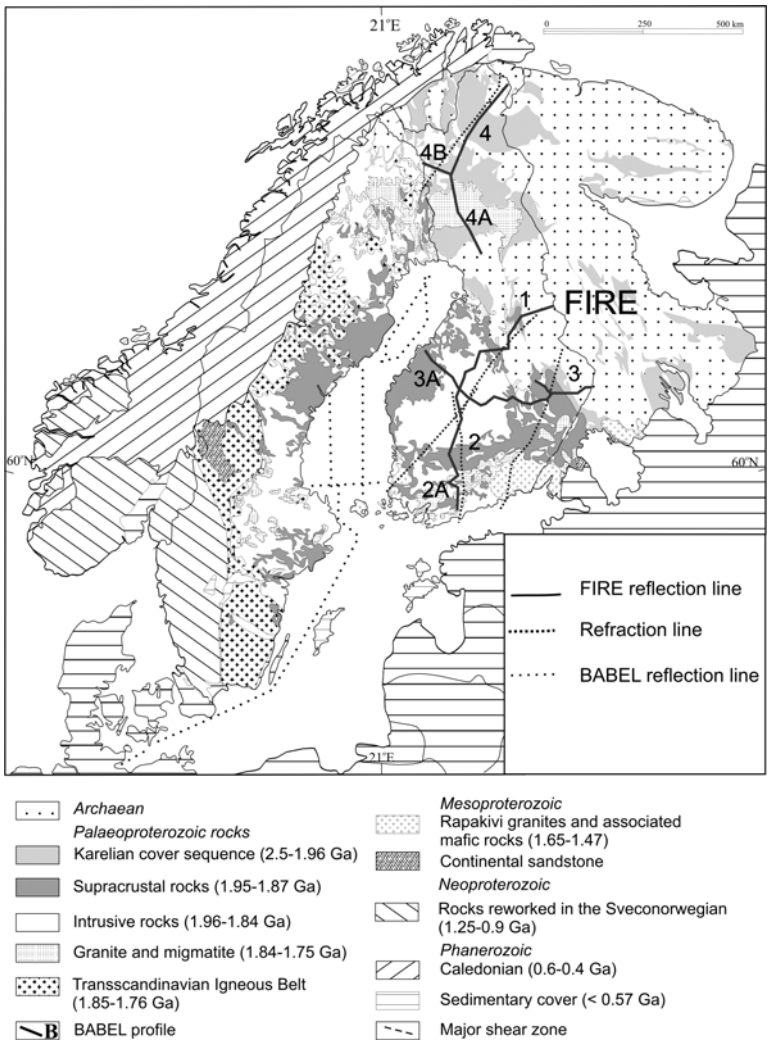

Figure 1. Seismic profiles in Finland. The FIRE transects are marked with solid lines, BABEL profiles with dotted lines and refraction profiles with thin dotted lines (modified from Korja and Heikkinen, 2005).

3. Reflectivity

In general, the crust along FIRE transects is seismically very reflective, particularly in the upper and middle crust. Where correlation with surface geology is possible, most of the strong reflectors can be correlated with basic or intermediate rocks in a felsic environment or faults and shear zones. The reflecting zones in the upper crust can be followed in many

places from the surface down to the middle crust. Such structures were imaged particularly in central Finland, where E-dipping reflectors can be followed for 100-200 km in the uppermost 40 km under the Central Finland Granitoid Complex (Figure 2). These structures probably represent thrust faults developed during the collisional stages of the Svecofennian orogen.

There is a general vertical change in the character of reflectivity at about 10-15 km depth in all FIRE transects. In the uppermost crust, sharp reflectors are observed, whereas in the deeper layers the reflectors become more diffuse and ill defined as the reflected signals contain less high frequencies than in the upper crust. The analysis of frequency content of data suggests that this effect should not be attributed to the acquisition method or later processing, but is a genuine property of the crust. The analysis also indicates the frequency content is not caused only by normal attenuation of the seismic signals. Although the factors behind this vertical variation in the character of reflectivity are not fully known, we tentatively attribute the 'softening' of reflectors below 10-15 km to rheological properties of the crust.

Lower crustal reflectivity is more diffuse, due to the nature of the lower crust, especially in central and southern Finland in the Proterozoic areas of the anomalous high-velocity lower crust. In these areas, the reflection Moho is diffuse and recognized from gradual disappearance of lower crustal reflectivity over a depth interval of about 3-5 km. In areas where wide-angle refraction data is available, depths of the refraction and reflection Moho are in a good agreement (*Luosto*, 1996 *and references therein, Fennia Working Group, 1998*).

There is a distinct difference particularly between the lower crustal reflectivity in the BABEL data in the Gulf of Bothnia (reflective lower crust) and the FIRE data in central Finland (weakly reflective, diffuse lower crust). The difference cannot be attributed to differences in acquisition methods, since both types of lower crust were recorded on the NW end of the FIRE 3A transect on the Bothnian Bay Coast (Fig. 2). Reflective, laminated lower crust was also recorded beneath the Lapland Granulite Belt.

Strong upper mantle reflectors were not detected in the FIRE data. Where sharp reflectors cutting the lower crust and extending into the mantle have been observed in Shield areas, these structures have been attributed to subduction processes (Cook at al., 1999). In such cases the lower crust is usually very reflective and the reflection Moho is sharp. Such lower crust is observed on the FIRE transects only along line 4A and on the western end of line 3A.

The FIRE data show that the central and northern parts of the Fennoscandian Shield have more or less similar reflective properties as the Canadian and Australian Shields. An apparent difference between the FIRE and Canadian and Australian data sets is the high proportion of anomalously thick high-velocity lower crust and deep Moho areas imaged in the FIRE transects. However, areas with comparable lower crustal properties and areal extent have been described in Wyoming, North America, and Mount Isa, North Australia (Clowes at al., 2002, Drummond et al., 1998).

References

BABEL Working Group, 1993a. Integrated seismic studies of the Baltic Shield using data in the Gulf of Bothnia region. Geophysical Journal International, 112: 305-324.

BABEL Working Group, 1993b. Deep seismic reflection/refraction interpretation of crustal structure along BABEL profiles A and B in the southern Baltic Sea. Geophysical Journal International, 112: 325-343.

Clowes, R.M., Calvert, A.J., Eaton, D.W., Hajnal, Z., Hall, J. and Ross, G.M.,1996. LITHOPROBE reflection studies of Archaean and Proterozoic crust in Canada. Tectonophysics 264: 65-88.

Clowes, R.M., Burianyk, M.J.A., Gorman, A.R. and Kanasevich, E.R., 2002. Crustal velocity structure from SAREX, the Southern Alberta Refraction Experiment. Canadian Journal of Earth Sciences, 39, 351-373.

Cook, F.A., van der Velden, A.J., Hall, K.W., Roberts, B.J., 1999. Frozen subduction in Canada's Northwest Territories: Lithoprobe deep lithospheric reflection profiling of the western Canadian Shield. Tectonics, 18, 1-24.

Drummond, B.J., Goleby, B.R., Goncharov, A.G., Wyborn, L.A.I., Collins, C.D.N. and MacCready, T., 1998. Crustal-scale structures in the Proterozoic Mount Isa Inlier of North Australia: their seismic response and influence on mineralization. Tectonophysics, 288, 43-56.

Fennia Working Group, 1998. P- and S-velocity structure of the Baltic Shield beneath the FENNIA profile in southern Finland. Institute of Seismology, University of Helsinki, Finland, Report S-38, 14 p.

Korja, A. and Heikkinen, P., 2005. The accretionary Svecofennian orogen – Insights from the BABEL profiles. Precambrian Research, 136: 241-268.

Korsch, R.J., Goleby, B.R., Leven, J.H., Drummond, B.J., 1998. Crustal architecture of central Australia based on deep seismic reflection profiling. Tectonophysics 288: 57-69.

Kukkonen, I.T. and Lahtinen, R. (eds) 2006. Finnish Reflection Experiment FIRE 2001-2005, Geological Survey of Finland, Special Paper 43, 247 pp.

Luosto, U., 1997. Structure of the Earth's Crust in Fennoscandia as Revealed from Refraction and Wide-Angle Reflection Studies, Geophysica, 33(1), 3-16.

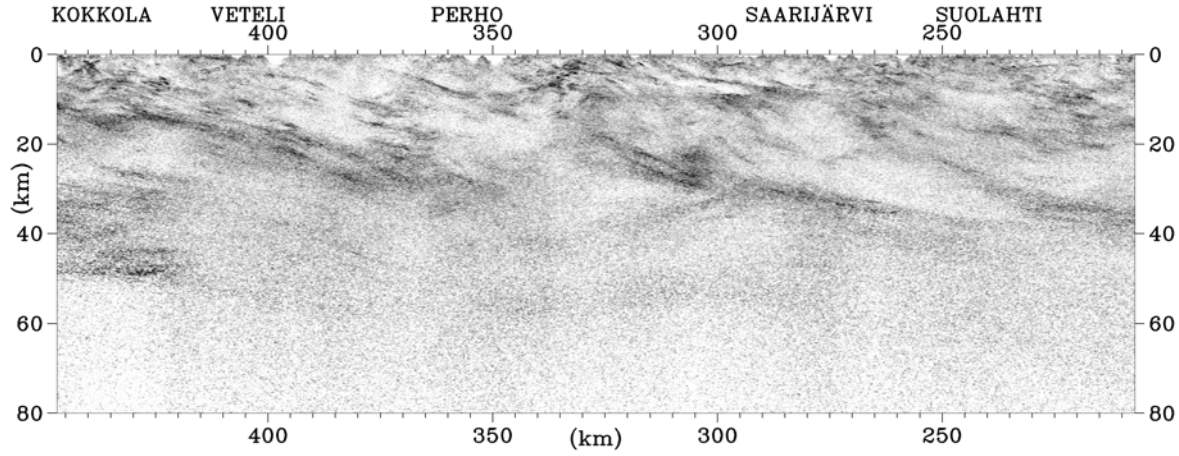

Figure 2. Western end of FIRE 3A showing sharp upper crustal reflectivity and more diffuse middle and lower crust. Listric-type strong reflectors dipping at low angles to E-ESE can be followed for over 100-200 km to depths of about 40 km. Two different types of lower crust are seen in the section: At ca. 430 km near Kokkola, the lower crustal reflecticvity changes abruptly from a diffuse reflectivity in central Finland to strongly reflective (BABEL-type) lower crust on the Bothnian Bay coast. Location of line 3A: see Fig. 1.

Structurally controlled gold mineralisation in the lower part of the Kumpu Group, Lake Immeljärvi, Kittilä: Implications for late-orogenic crustal-scale deformation in Central Lapland

Marko J. Holma[1]*, Veikko J. Keinänen[2] and Ilkka M. Lahti[2]

[1]Department of Geosciences, P.O. Box 3000, FI-90014 University of Oulu, Finland
[2]Geological Survey of Finland, P.O. Box 77, FI-96101 Rovaniemi, Finland
*Email: marko.holma@oulu.fi

Laboratory, microscopy and field studies on the metasedimentary Kumpu Group rocks in the Lake Immeljärvi area, Kittilä, have revealed that the NNE-striking Immeljärvi fault that cuts through the local lithostratigraphy is associated with at least two types of hydrothermal veins: quartz-haematite and auriferous calcite-quartz-sulphide. There are also conglomerate and quartzite boulders cut by quartz-carbonate-pyrite veins. Rocks along the fault are locally albitised and carbonated. The discovered veins strengthen mineralisation potential of the Immeljärvi fault and other similarly oriented structures south from the Sirkka Shear Zone. In addition, this supports the hypothesis that also the post-1.88 Ga Kumpu Group is cut by the late-orogenic gold mineralisation.

Keywords: Sirkka, Levi, Levitunturi, Kätkätunturi, Immeljärvi fault, Sirkka conglomerate, Levi Formation, Vielmajoki, veins, bornite, clausthalite, naumannite, hessite, gold

1. Introduction

This work reports preliminary results obtained from studies of the Kumpu Group rocks in the Lake Immeljärvi area, Kittilä (Fig. 1). The objectives of the present study were:

1. To investigate the abundance and character of quartz-carbonate veins in the Kumpu Group rocks in the area of interest.
2. To make some observations in what extent and style(s) the *lower* part of the Kumpu Group is altered.

Hydrothermal veins and their related alterations were chosen for a study as such features are not only classic markers of notable deformation, but also important indicators for gold mineralisation. In the Kittilä greenstone area, most orogenic gold vein deposits have spatial correlation with structures that penetrate into the Sodankylä, Savukoski or Kittilä Groups (Table 1). In contrast, especially the Kumpu Group rocks have long been held to be uninteresting targets for structurally controlled ore deposits. In fact, even veins in general – whether hydrothermal or intrusive – are only seldom observed in the Kumpu Group (or perhaps they are not just mentioned?).

The main investigation methods were geological mapping and sampling. In addition, 11 thin sections were studied under ordinary polarising microscope and some also with the electron probe microanalyser (EPMA) JEOL JXA-8200 at the Institute of Electron Optics of the University of Oulu.

2. Previous investigations

This study is a continuation of the work by *Holma & Keinänen (2006a, 2006b)* who studied a single exposure in the Lake Immeljärvi area (no. 1 in Fig. 1B). The current study, in contrast, is more regional in scale. Its field works were guided by *Mikkola (1941)*, *Mäkelä (1968)* and *Kortelainen (1983)*, the three publications of which all give short

descriptions about veins cutting the Kumpu Group rocks in the current study area. However, since the nature and mineralogical composition of these veins has remained poorly constrained, it was found that a more detailed study was needed to resolve whether those veins are somehow related to the mineralised calcite-quartz-sulphide veins reported by *Holma & Keinänen (2006a, 2006b)*. This vein style was not documented before from Central Lapland.

3. The study area

The Lake Immeljärvi area (Fig. 1B) is favourable for a study of this kind, because here one can make observations on the Kumpu Group rocks more easily than perhaps anywhere else. This is not only due to the excellent road network, but also the fact that here the local Kumpu Group lithostratigraphy is cut by a fault (the Immeljärvi fault) that gives an exceptional opportunity to make remarks and collect samples from the lower part of the stratigraphy. This part of the Kumpu stratigraphy is generally poorly exposed[1].

One of the most prominent features of the study area is the Lake Immeljärvi, about 20–30 m deep elongated lake of which waters flow from S to N via several narrow waterways. One of the brooks is the River Vielmajoki (Fig. 1B).

4. Regional setting

From the seven lithostratigraphic groups of the CLGB, four must be mentioned here. They are, in the order of decreasing age: Sodankylä, Savukoski, Kittilä and Kumpu (Table 1).

The Sodankylä Group comprises clastic metasedimentary rocks with strong terrigeneous signature (e.g. quartzite). After these epiclastic sediments were deposited, the intracratonic basin grew deeper and wider and consequently more fine-grained sediments accumulated on the older and coarser sediments. Basin subsidence led to the formation of the Savukoski and Kittilä Groups, the former comprising phyllite, tuffite and graphitic phyllite and mafic to ultramafic metavolcanic rocks, and the latter, which is a true oceanic basin sequence, mafic metavolcanic rocks with intercalating metasedimentary rocks.

The youngest lithostratigraphic group in the Kittilä greenstone area is the Kumpu Group. All the highest landscape forms in Central Lapland are composed of the molasse-like metasedimentary rocks of this group, comprising conglomerate, siltstone and quartzite (Table 1, Fig. 1). These rocks, being <1.88 Ga in age (*Hanski et al., 2001*), record the youngest preserved Precambrian depositional event in the region. The most prominent fells composed of these rocks are Levitunturi (531 m amsl), Kätkätunturi–Pyhätunturi (505 m and 450 m, respectively) and Aakenusvaara (~330 m), all three that are tectonically dismembered from each other by a set of NNE-striking deformation zones (Fig. 1A). These fault zones are quite straight and thus are though to be formed in the last significant tectonic event affecting throughout the entire Central Lapland. *Väisänen et al. (2000)* and *Väisänen (2002)* have proposed that the conjugate pattern these faults form was probably generated in an E–W oriented compression less than 1.77 Ga ago[2].

On the basis of aerogeophysical maps, these late straight faults are part of a much larger fault system (as Fig. 2 shows only a small fraction of these, see the Appendix map of

[1] From a stratigraphic point of view, the local Kumpu stratigraphy cannot be directly correlated with that of the Kumputunturi fell itself, as their sedimentary successions are actually quite different (*Lehtonen et al., 1998*).

[2] According to *Väisänen et al. (2000)* and *Väisänen (2002),* this maximum age of faulting is based on the fact that some of these faults affect the 1.77 Ga old Nattanen-type granites.

Lehtonen et al., 1998). Several of these faults have been named, including the faults of Immeljärvi and Muusanlammit (Fig. 1A). Both fault zones are deeply eroded and form lakes and valleys with relatively steep slopes on both sides (Fig. 3).

5. Results

Our results confirm the earlier observations of *Holma & Keinänen (2006a, 2006b)* that hydrothermal veins locally cut the Kumpu Group rocks, at least in the Immeljärvi valley (Fig. 3A). Hydrothermal veins cutting the Kumpu Group have now been recognised from three different locations in our study area (Fig. 1). *Holma & Keinänen (2006a, 2006b)* give a detailed description of the vein occurrence marked with no. 1 in the Fig. 1B (from now on, Site 1). The other two vein locations (Sites 2 and 3) were found during this study. All these three areas are described below.

Host rocks

Site 1: Road cut composed of dark-grey to greenish conglomerate typical to the lower part of the Kumpu Group (the Sirkka conglomerate of the Levi Formation). Except the couple of metres high road cut, the area is relatively flat and unexposed.
Site 2: Light-grey, well-sorted clastic quartzite with rare conglomeratic interbeds. The pebbles in such interbeds are generally well-rounded quartzite or barren vein quartz, but there are also platy shale/schist fragments. As this site occurs in a pretty steep slope of the Kätkätunturi fell, many outcrops can be found from the area.
Site 3: This site differs from the other two in that there are no outcrops, but only several rather angular boulders in where quartz-carbonate-pyrite veins occur. The boulders are composed of clastic quartzite and a quartzite containing conglomeratic interbeds, both undoubtedly representing the Kumpu Group. These rocks are of the same type as quartzite at the Site 2. Angularity and the big size (up to a few cubic metres) of some of the boulders suggest a very short transport distance.

Hydrothermal veins

Site 1: The veins are mainly composed of calcite and minor quartz. There are also Cu-sulphides in these veins: bornite, chalcopyrite and chalcocite. Additional ore minerals include accessory clausthalite (PbSe), naumannite (Ag_2Se), hessite (Ag_2Te) and electrum (Au,Ag). As similar veins have not been documented elsewhere from the region, *Holma & Keinänen (2006a, 2006c)* suggested they were emplaced during tectonic activity along the Immeljärvi fault. Typical veins are up to 1.5 cm in wide and they are separated from the other veins by non-fractured wall rock. In the most intensively veined parts of the conglomerate, however, the host rock is nearly brecciated by veins. Some veins show shapes reminiscent of tension gash veins. Some others are clearly formed as fibrous pressure fringe overgrowths for some of the clasts in the conglomerate. Vein calcite is fibrous or elongate-blocky in character.
Site 2: The main minerals in the veins are quartz and haematite[3]. Accessory minerals include monazite and apatite. The dominating vein microstructure is elongate-blocky. The host rock is mainly composed of quartz, but contains also minor tourmaline, haematite, rutile, apatite, monazite, zircon and sericite. The veins are generally narrow, in the range of 1–5 mm. Some veins are broader though, perhaps up to a few centimetres. In places, the

[3] An interesting anecdote: according to *Mikkola (1941, p.117)*, the haematite content in these veins is locally so high that there has been, during 1850s, even an attempt to mine the Fe out of the rock.

veins form breccia-like networks. Most vein boundaries are sharp. It appears that the veins are more common closer to the Lake Immeljärvi and hence the fault (cf. numbers 2 and 3 in Fig. 2).
Site 3: The veins in the studied boulders were all composed of quartz and carbonate[4]. However, they are completely different from those quartz-carbonate veins occurring at the Site 1. In this location the veins are not fibrous nor elongate-blocky or fine-grained; instead, vein minerals are blocky-textured, rather coarse and more euhedral in shape. The veins are also different by their mineralogical content as here quartz dominates over (or at least equals) the carbonate, and the carbonate species is not a calcite, but a Fe-rich carbonate (probably siderite). Lastly, there are no Cu- or Pb-minerals, but pyrite, which is lacking from the veins at the Site 1.

Hydrothermal alteration
The results reported here are valid only for the *lower* part of the Kumpu Group, because most of our field studies were conducted on the lowest level slopes of the Kätkätunturi fell and in the vicinity of the Lake Immeljärvi where topography is nearly flat (e.g. in the River Vielmajoki area; no. 3, Fig. 1B).
Site 1: The calcite-quartz-sulphide veins contain minor albite against fracture walls. There is albite in the host rocks as well, but its amount is insignificant. However, the matrix of the conglomerate is, locally at least, rich in carbonate. This is indicated by the craggy surface of the rock as it contains dark brown patches of weathered carbonates. The green hue the fresh surface of the rock has is derived from the abundantly occurring chlorite, which is probably metamorphic in origin. There is chlorite also in the veins themselves, but only against the wall rock.
Site 2: The majority of veins occur without any marks of macroscopically visible alteration, but in thin section scale minor haematite, rutile, apatite and monazite can be observed in the wall rock, the minerals that could be related to alteration. However, some veins are bordered by reddish brown halo, which is either real alteration, or due to more recent weathering.
Site 3: Rather strong albitisation and carbonation.

6. Conclusions
Gold mineralisation related to quartz-haematite and calcite-quartz-sulphide veins in the Immeljärvi valley in the lower Kumpu Group rocks have been recognised. A third vein style (quartz-carbonate-pyrite) has been observed in boulders. The results indicate that 1) gold mineralisation is later than 1.88 Ga (the maximum age for the Kumpu Group), 2) the southern side of the SSZ is prospective, 3) the Immeljärvi fault was active at the time of mineralisation, and 4) the Kumpu Group rocks have potential for structurally controlled ore deposits.

[4] The past tense is used here purposely, because only two days after we found these boulders, most of them were buried under a pile of gravel (the area was an active construction site). Nevertheless, despite the fact that the boulders could have been removed slightly, we are convinced that their origin is not far: we did not find these boulders by accident as we were directed to the Vielmajoki River area by a discovery made by E. Mikkola more than 60 years earlier (*Mikkola, 1941, p. 118-119*). So, amazingly, the boulders we were looking for were there to last only for those two days after we studied them. Serendipity at its best?

Acknowledgements
We would like to thank Dr. Juhani Ojala for his contribution to the final outcome of this progress report. The first author also acknowledges the financial support of the Finnish Graduate School in Geology.

References

Hanski, E., Huhma, H. & Vaasjoki, M., 2001. Geochronology of northern Finland: a summary and discussion. In: Vaasjoki, M. (ed.) Radiometric age determinations from Finnish Lapland and their bearing on the timing of Precambrian volcano-sedimentary sequences. Geol. Surv. of Finland, Spec. Pap. 33, 255–279.

Holma, M.J. & Keinänen, V.J., 2006a. A new discovery of calcite-quartz-sulphide veins in the Kumpu Group conglomerate, Lake Immeljärvi, Kittilä (Part 1: Macroscopic studies). Bull. Geo. Soc. Finland, Special Issue 1, p. 50.

Holma, M.J. & Keinänen, V.J., 2006b. A new discovery of calcite-quartz-sulphide veins in the Kumpu Group conglomerate, Lake Immeljärvi, Kittilä (Part 2: Microscopic studies). Bull. Geo. Soc. Finland, Special Issue 1, p. 50.

Holma, M.J. & Keinänen, V.J., 2006c. The NNE-striking Immeljärvi tectonic structure in Kittilä – a potential host for mineralisation? Available from: <http://en.gtk.fi/Research/meetings/nordic>

Kortelainen, V., 1983. Sirkka-konglomeraatin ja Levitunturin kvartsiitin sedimentologia Kittilässä. Pro gradu -tutkielma, Helsingin yliopiston geologian laitos, 101 s. (in Finnish)

Lehtonen, M., Airo, M.-L., Eilu, P., Hanski, E., Kortelainen, V., Lanne, E., Manninen, T., Rastas, P., Räsänen, J. & Virransalo, P., 1998. Kittilän vihreäkivialueen geologia. Lapin vulkaniittiprojektin raportti. Summary: The stratigraphy, petrology and geochemistry of the Kittilä greenstone area, northern Finland. A report of the Lapland Volcanite Project. Geol. Surv. of Finland, Rep. of Inv. 140, 144 p.

Mäkelä, K., 1968. Sirkka-muodostumasta ja stratigrafian yleispiirteistä Keski-Lapin liuskealueella. Filosofian lisensiaatti -tutkimus. Oulun Yliopisto, Geologian laitos, 88 s. (in Finnish)

Mikkola, E., 1941. Suomen geologinen yleiskartta. Lehdet B7-C7-D7, Muonio, Sodankylä ja Tuntsajoki. Kivilajikartan selitys. English summary: The general geological map of Finland. Sheets B7-C7-D7, Muonio, Sodankylä and Tuntsajoki. Explanation to the map of rocks. Suomen geologinen toimikunta, 286 s.

Väisänen, M., 2002. Structural features in the central Lapland greenstone belt, northern Finland. Geol. Surv. of Finland, unpub. report K21.42/2002/3, 20 p.

Väisänen, M., Airo, M.-L. & Hölttä, P., 2000. Field investigations in the Central Lapland Greenstone Belt, northern Finland, 1998–1999. Geol. Surv. of Finland, unpub. report K21.43/2000/1, 19 p.

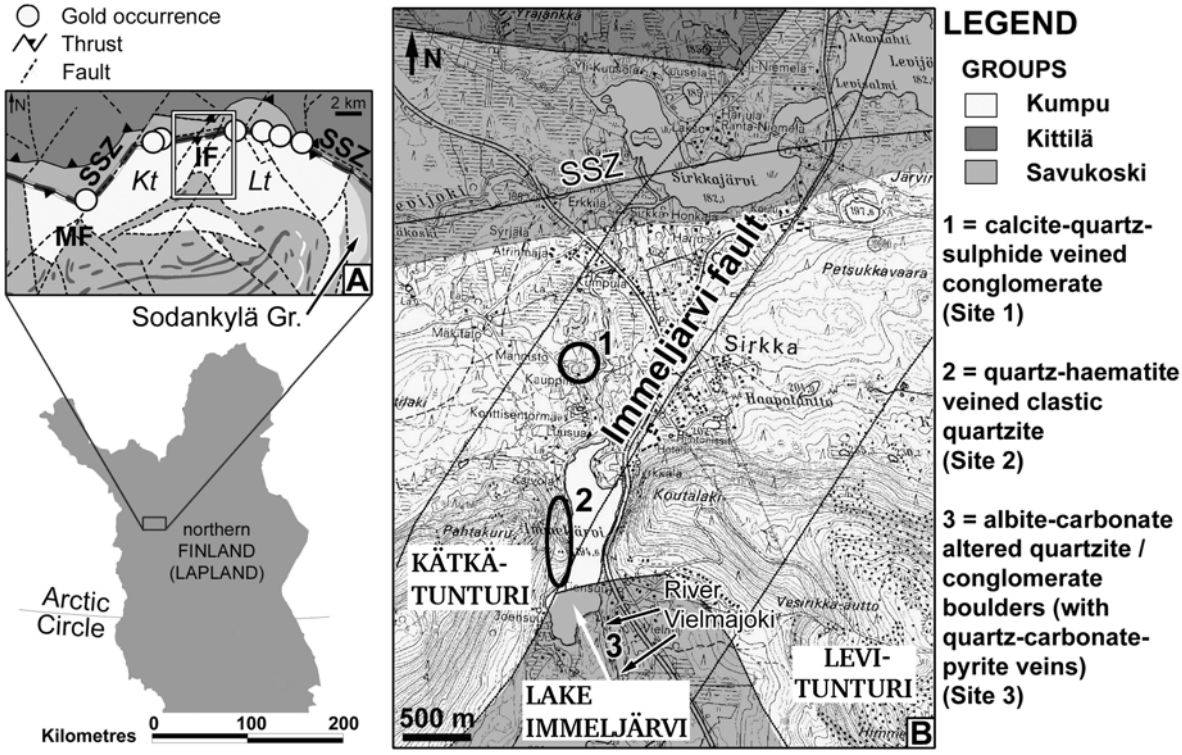

Figure 1. A) Sketch map of regional structural elements and main geological domains in the study area. The light-coloured areas are mainly topographic highs composed of the Kumpu Group metasedimentary rocks. The box indicates the area of main interest depicted in the Fig. 1B in more detail. SSZ = Sirkka Shear Zone, IF = Immeljärvi fault, MF = Muusanlammit fault, Kt = Kätkätunturi fell, Lt = Levitunturi fell. B) The lines delineating the SSZ and Immeljärvi fault are from 1:250 000 scale maps and should be taken as approximations. Veins in the "Site 1" have been described by *Holma & Keinänen (2006a, 2006b)*, whereas this study depicts the vein characteristics in the other two locations. Geology after *Lehtonen et al. (1998)*. Topographic map@National Land Survey of Finland. Licence 13/MYY/06.

Table 1. Lithostratigraphy of the Kittilä greenstone area (*Lehtonen et al., 1998)*. Those groups marked with a star are present in the area shown by the Fig. 1A. The studied veins occur in the bottom part of the Kumpu Group.

Group	Main lithology	Age (Ga)
★ Kumpu	Quartzite, siltstone, conglomerate	1.88-1.80
Lainio	Quartzite, conglomerate, intermed. to felsic metavolcanic rocks	
★ Kittilä	Fe- and Mg-metatholeiite, BIF, mica schist	~2.02-1.99
★ Savukoski	Phyllite, graphitic phyllite, tuffite, Fe-metatholeiite, metakomatiite	>2.05
★ Sodankylä	Quartzite, mica schist, mica gneiss	>2.2
Onkamo	Tholeiitic and komatiitic metavolcanic rocks	
Salla	Intermed. to felsic metavolcanic rocks	

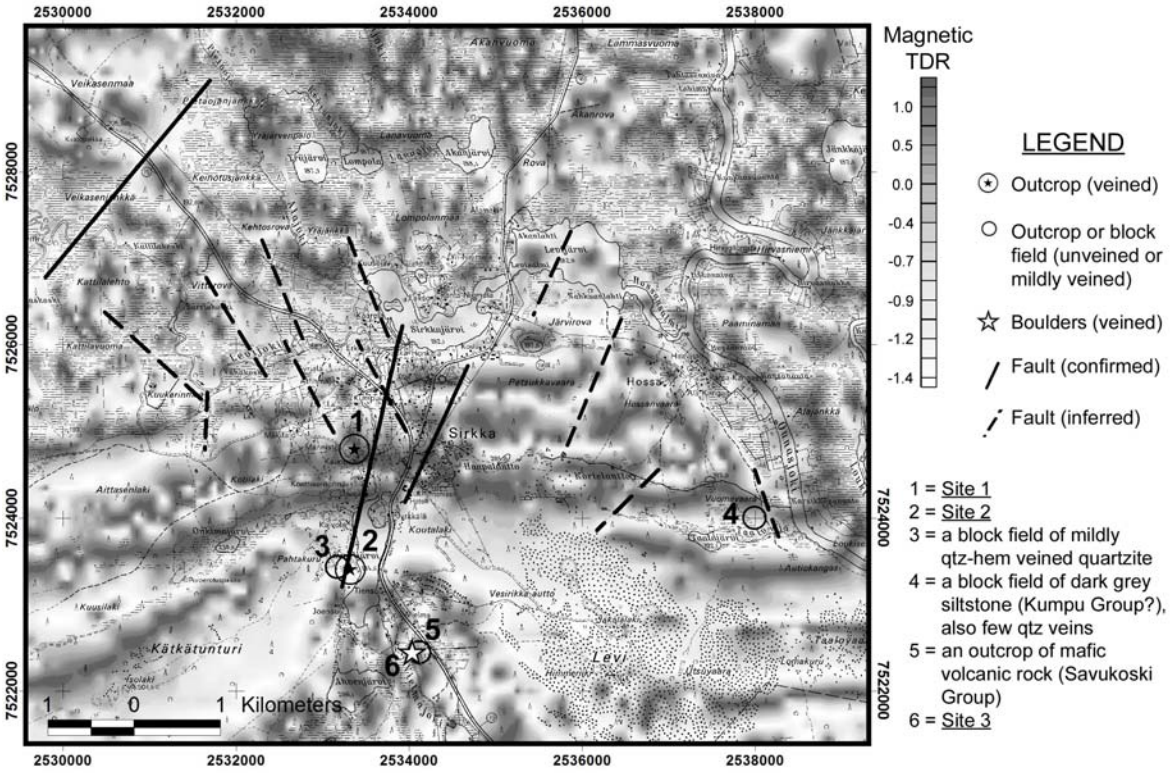

Figure 2. TDR-filtered aeromagnetic map of the study area showing the conjugate pattern of relatively straight faults. TDR filtering equalizes small and large magnetic anomalies enabling to recognise structural discontinuations such as thrusts and faults more easily. Here some magnetic anomalies that are seen in dark grey are disrupted and in places notably displaced by faults.

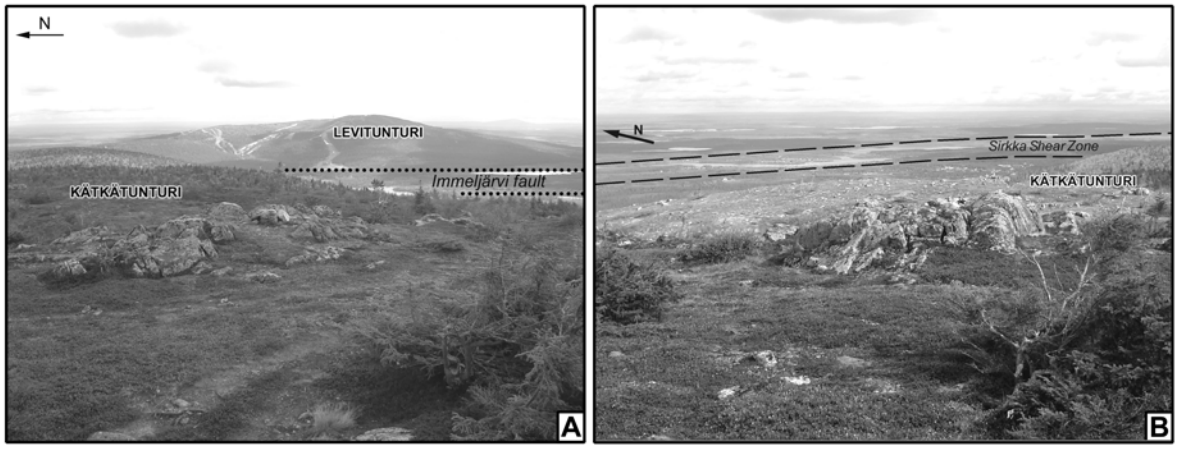

Figure 3. Photographs from atop the quartzite-dominated Kätkätunturi fell towards (A) E to the Immeljärvi valley and (B) NNE (~030º). The Immeljärvi fault that separates the Kätkätunturi fell from the Levitunturi fell is a NNE-striking structure. The intersection between this fault and the approximately E-W-striking Sirkka Shear Zone is located a few kilometres north from the left-hand edge of the Fig. 3A. Compare to Fig. 1.

Crustal tomography in central Fennoscandian Shield

T. Hyvönen*, T. Tiira, A. Korja and K. Komminaho

Institute of Seismology, POB 68, FIN-00014 Helsinki University, Finland
*E-mail: Tellervo.Hyvonen@helsinki.fi

Seismic velocity structure of the crust and the Moho boundary of south-central Finland were inverted by local tomography method using P wave travel time and PMP reflection data. The velocity distribution reveals varying high and low velocity anomalies that can be associated with different geological units of the area. The inverted Moho discontinuity show more detailed structure than previous models.

Keywords: Seismic tomography, V_p, Moho, crust, Finland

A crustal velocity model and a Moho depth map were inverted by the tomography program Jive3D (Hobro 1999) using data from the deep seismic surveys, the permanent station recordings and the SVEKALAPKO passive tomography experiment (Fig. 1; Bock et al. 2001). The variation of the seismic velocities at the surface can be associated with the main geological units. The P wave velocities are varying laterally in the crust: at depth of 10 km between 5.9 and 6.5 km/s, of 20 km between 6.3 and 6.9 km/s, of 30 km between 6.7 and 7.3 km/s, and at depth of 40 km between 6.9 and 7.5 km/s.

Inclusion of the PmP observations from the SVEKALAPKO array allowed 3-D modelling of the Moho boundary between the DSS profiles. The inversion was based on a 3-D tomographic P wave velocity model of the crust (Hyvönen et al. 2006). As the resolution of the inverted model was poor below the depth of 40 km a 1-D velocity model was compiled from 2-D models of the DSS profiles for depths greater than 40 km. All non-controlled source events were relocated with grid search technique by minimizing the travel time residuals between synthetic and observed rays. Lateral velocity resolution was good with cell size of 60 km.

The inverted Moho boundary model differs from the interpolated model (Luosto 1997) in introducing small-scale structural details. The main differences are the nearly 10 km thinner crust north of the Laitila rapakivi area, and the shape of the Moho boundary in the Vyborg rapakivi area. Two large Moho boundary depressions are observed in eastern and south-western Finland. Thinner crust is observed in the Bothnian Bay, in the southern Bothnian Sea and around the Vyborg rapakivi region in south-eastern Finland. The Archean bedrock is usually characterized by higher velocities than the Paleoproterozoic bedrock. The Laitila and Vyborg rapakivi areas and the Central Finland Granitoid Complex are distinguished by higher velocities than the surrounding schist belts: Bothnian, Pirkanmaa and eastern Finland.

References

Bock, G. and the SVEKALAPKO STWG, 2001. Seismic probing of Archean and Proterozoic lithosphere in Fennoscandia. *EOS*, 82, 621, 628-629.

Hobro, J.W.D., 1999. Three-dimensional tomographic inversion of combined reflection and refraction seismic travel time data. PhD thesis, *Department of Earth Sciences, University of Cambridge*, *Cambridge*.

Hyvönen, T., T. Tiira, A. Korja, P. Heikkinen, E. Rautioaho, and the SVEKALAPKO Seismic Tomography Working Group, 2006. A tomographic crustal velocity model of the central Fennoscandian Shield. *Geophys. J. Int. (*in press)

Luosto, U., 1997. Structure of the Earth's Crust in Fennoscandia as Revealed from refraction and Wide-Angle Reflection Studies. Geophysica, 33(1): 3-16.

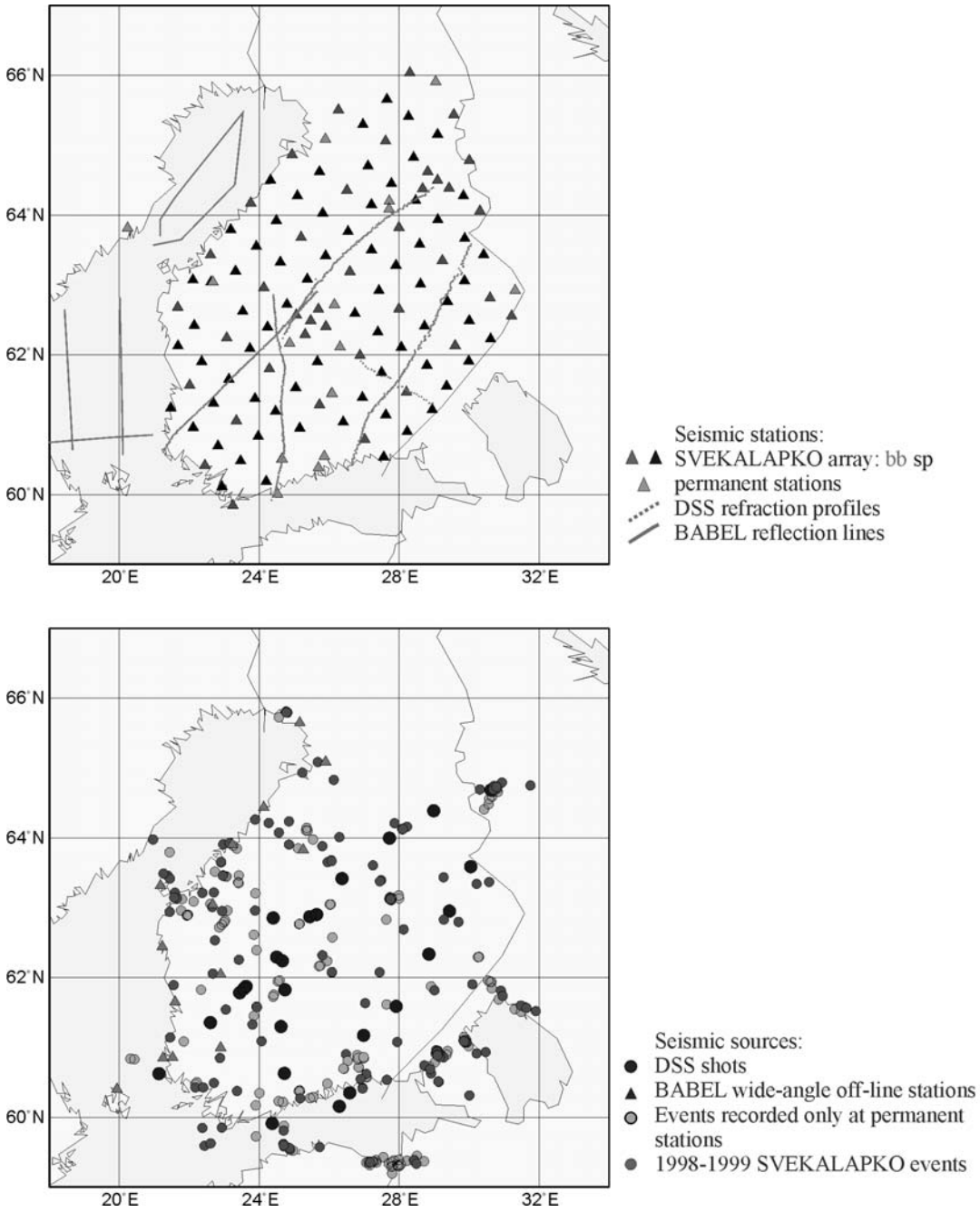

Figure 1. Seismic stations and sources used in the crustal tomography inversions.

Crust-mantle boundary in the central Fennoscandian shield: Constraints from wide-angle P- and S-wave velocity models and results of FIRE reflection profiles

Tomasz Janik[1], Elena Kozlovskaya[2]*,Jukka Yliniemi[2] and FIRE Working Group

[1]Institute of Geophysics, Polish Academy of Sciences, Ks. Janusza 64, PL-01-452 Warszawa, Poland, janik@igf.edu.pl
[2]Sodankylä Geophysical Observatory/Oulu Unit, POB 3000, FIN-90014 University of Oulu, Finland, *E-mail:elena.kozlovskaya@oulu.fi

We present analysis of the crust-mantle boundary in the central Fennoscandian shield based on new P- and S-wave 2-D velocity models of SVEKA'81, SVEKA'91 and FENNIA wide-angle reflection and refraction profiles and on results of a FIRE seismic reflection experiment in Finland. In this area the Moho boundary is difficult to detect using methods based on interpretation of P-waves (near vertical profiling and wide-angle experiments). However, the S-wave reflections from the Moho boundary (SmS) are frequently more pronounced in wide-angle data than the P-wave reflections (PmP). Based on the lateral variations of Vp, Vp/Vs and reflectivity in the lower crust and upper mantle, three main types of the crust-mantle boundary were distinguished.

***Keywords*:** crust, upper mantle, P- and S- wave 2-D raytrace modeling, Vp/Vs ratio, lithological crust-mantle boundary

The origin and evolution of the crust-mantle boundary in the Precambrian areas had been debated over for many years, but still remains not completely understood. The depth to the crust-mantle boundary (the Moho boundary) is usually defined by seismic techniques, e.g. seismic wide-angle reflection and refraction profiling, near-vertical reflection profiling and teleseismic receiver function studies. However, different seismic techniques employed to study the Moho boundary may give incomparable results (Eaton, 2006) and interpretation of these results in terms of rock composition is difficult.

One of such areas is the central part of the Fennoscaldian shield, where the crust-mantle boundary has been studied by all the seismic methods mentioned above. In the 80s-90s the central part of the shield was studied by BALTIC, SVEKA'81, SVEKA'91 and FENNIA wide-angle reflection and refraction profiles (c.f. FENNIA Working Group, 1998; Grad and Luosto, 1987, Luosto et al., 1984, 1990,Yliniemi, 1991). In 1989 a marine seismic survey BABEL recorded more than 2000 km of deep reflection profiles around the Gulf of Bothnia and the Baltic sea (BABEL Working Group, 1990). The crust-mantle boundary was studied by SVEKALAPKO (1998-1999) multidisciplinary passive seismic array experiment (Sandoval et al., 2003, Alinaghi et al., 2003, Yliniemi et al., 2004). In 2001-2003 the project FIRE (Finnish Reflection Experiment) comprised four reflection seismic transects of total length of 2104 km crossing the main geological units of the central part of the Fennoscandian shield (Kukkonen et al., 2006).

This abundant, but sometimes contradicting information about the crust-mantle boundary in the central Fennoscandian shield was the main motivation of our study, in which we tried to explain the apparent inconsistence of the Moho obtained from wide-angle data, receiver function studies and reflection profiling.

For this we made analysis of the crust-mantle boundary in the central Fennoscandian shield using both P- and S-wave wave fields of previous SVEKA and FENNIA wide-angle

reflection and refraction profiles. In the central Fennoscandian Shield the recordings of S-waves demonstrate clear reflections from the Moho boundary (SmS), same or frequently much better quality than P-wave reflections (PmP) due to absence of thick sediments. Therefore, combined analysis of P- and S-waves can be used to estimate depth to the crust-mantle boundary and Vp/Vs ratio in the crust and uppermost mantle. We developed new P- and S-wave velocity models using reprocessing of the old data and compared them to record sections of collocated FIRE profiles and to petrophysical data about seismic velocities in the main types of lower crustal and upper mantle rocks.

The main conclusions from our study can be formulated as follows (Janik et al., submitted):

1) The new combined seismic models of SVEKA transect and FENNIA profile demonstrate pronounced lateral variations of values of Vp, Vs and Vp/Vs ratio in the crust and of the depth to the Moho boundary that can be associated with large blocks of the crust.

2) The low velocity zone (LVZ) was detected at depths of 5-12 km in central and northern parts of FENNIA profile and along all SVEKA transect, with exception for most of the southwestern part.

3) Significant difference in the crustal structure of the south-westren block beneath the SVEKA transect and the southern block beneath the FENNIA profile suggests that these blocks belong to different crustal units and there should be an unexposed boundary separating these units, that should stretch in the NS direction.

4) The deepest Moho (> 60 km) was found beneath the central part of the CFGC.

5) The Moho boundary is overlain by a high-velocity lower crust (HVLC) with Vp>7.15 km/s and Vs>4.0 km/s. The thickness of the HVLC and the value of Vp/Vs ratio in this layer vary from 10 to 30 km and from 1.74 to 1.78, respectively.

6) There is a general agreement between SVEKA and FENNIA models and FIRE1 and FIRE2 sections, regarding the shape and thickness of the lower crust and the Moho depth.

7) Beneath the CFGC thickness of the HVLC is extremely high and two layers can be distinguished there: HVLC1 and HVLC2. The P- and S-wave velocities in the lowermost HVLC2 (Vp>7.3 km/s, Vs>4.15 km/s) are higher than in the uppermost HVLC1 (Vp>7.15 km/s, Vs>4.0 km/s). The values of Vp/Vs are similar (1.76-1.77) within the HVLC1 and the HVLC2. This indicates that both HVLC sub-layers are probably composed of mafic garnet granulites formed by a multi-stage evolution that included both partial melting of the lower crust and magmatic underplating.

8) The HVLC beneath the Archaean-Proterozoic transition and beneath the southern part of the FENNIA profile is composed of one layer (HVLC3) with value of Vp/Vs ratio of 1.74. This suggests that in both cases the HVLC3 is composed of rocks that have reached transition to eclogite facies.

9) Three main types of the Moho boundary were distinguished:

*The first type corresponds to eclogitized lower crust (HVLC3) that overlies peridotitic upper mantle. In this case the Moho boundary coincides with the litholigical crust-mantle boundary.

*The second type corresponds to HVLC2 composed of mafic garnet granulites overlying peridotitic upper mantle, for which the seismic Moho and the petrophysical crust-mantle boundary coincide as well.

*The third type corresponds to the contact of mafic garnet granulites (HVLC2) and eclogities. In this case the Moho and the petrophysical crust-mantle boundary do not coincide and the latter is located deeper than the Moho boundary.

10) The sub-Moho velocities of Vp>8.3 km/s, Vs=4.72-4.73 km/s and Vp/Vs ratio of 1.76-1.77 were detected below southwestern part of the SVEKA transect and the northern part of the FENNIA profile. The values of Vp=8.1 km/s and Vp=8.05 km/s were detected below the southern part of the FENNIA profile and the northeastern part of the SVEKA transect, respectively. The values of Vs and Vp/Vs were not well constrained there.
11) Upper mantle reflectors were detected at the depth of 60-80 km.

Acknowledgements

This study was funded by the Academy of Finland and Polish Academy of Sciences (exchange visitor grants for T. Janik and E. Kozlovskaya). The authors thank Dr. Timo Tiira from the Institute of Seismology of the Helsinki University for the help with transformation of the data of SVEKA'81, SVEKA'91 and FENNIA profiles into ZPLOT format. The assistance of Dr. T. Korja from the Department of Geophysics of Oulu University, who provided materials for a geological map of the area, is highly appreciated. Many thanks for support of E. Gaczyński in preparation of the part of the data. The SVEKA'81 Working Group consists of U. Luosto, E. Lanne, H. Korhonen, A. Guterch, M. Grad, R. Materzok, E. Perchuć. The SVEKA'91 Working Group consists of U. Luosto, M. Grad, A. Guterch, P. Heikkinen, T. Janik, K. Komminaho, C-E. Lund, H. Thybo, J. Yliniemi. The FENNIA Working Group consists of P. Heikkinen, U. Luosto, J. Malaska, M. Grad, T. Janik, P. Maguire, P. Denton, C-E. Lund, A-K. Lefman, J. Yliniemi, K. Komminaho. The FIRE Working Group consists of E. Ekdahl, I. Kukkonen, R. Lahtinen, M. Nironen, A. Kontinen, J. Paavola, H. Lukkarinen, A. Ruotsalainen, J. Lehtimäki, H. Forss, E. Lanne, H. Salmirinne, T. Pernu, P. Turunen, E. Ruokanen, P. Heikkinen, A. Korja, T. Tiira, J. Keskinen, S.-E. Hjelt, J. Tiikkainen, J. Yliniemi, E. Jalkanen, R. Berzin, A. Suleimanov, N. Zamoshnyaya, I. Moissa, A. Kostyuk, V. Litvinenko.

References

Alinaghi A., Bock G., Kind R., Hanka W., Wylegalla K, TOR and SVEKALAPKO Working Groups, 2003. Receiver function analysis of the crust and upper mantle from the North German Basin to the Archaean Baltic Shield. *Geophysical Journal International*, 155, 641-652.

BABEL Working Group 1990. Evidence for early Proterozoic plate tectonics from seismic reflection profiles in the Baltic shield. Nature, 348, 34– 38.

Eaton, D.W. 2006. Multi-genetic origin of the continental Moho: insights from LITHOPROBE. Terra Nova, 18, 1, 34-43.

FENNIA Working Group, 1998. P- and S-velocity structure of the Baltic Shield beneath the FENNIA profile in southern Finland. University of Helsinki, Institute of Seismology, Report S-38, Helsinki 1998.

Grad M. and Luosto U., 1987. Seismic models of the crust of the Baltic Shield along the SVEKA profile in Finland. Annales Geophysicae, 5B, 639-650.

Janik, T., Kozlovskaya, E., Yliniemi, J. 2006. Crust-mantle boundary in the central Fennoscandian shield: constraints from wide-angle P- and S-wave velocity models and new results of reflection profiling in Finland. J. Geoph. Res., submitted.

Kukkonen I.T., Heikkinen P., Ekdahl E., Hjelt S.-E., Yliniemi J., Jalkanen E. and FIRE Working Group, 2006. Aquisition and geophysical characteristics of reflection seismic data on FIRE transects, Fennoscandian Shield. In: GTK Special paper "Finnish Reflection experiment (FIRE) 2001-2005, submitted.

Luosto U., Lanne E., Korhonen H., Guterch A., Grad M., Materzok R., & Perchuć E., 1984. Deep structure of the Earth's crust on the SVEKA profile in central Finland, Annales Geophysicae, 2, 559-570.

Luosto, U., Tiira, T., Korhonen, H., Azbel, I., Burmin, V., Buyanov, A., Kosminskaya, I., Ionkis, V., Sharov, N., 1990. Crust and upper mantle structure along the DSS BALTIC profile in SE Finland. Geophysical Journal International, 101, 89-110.

Sandoval S., Kissling E., Ansorge J. & the SSTWG, 2003. High-resolution body wave tomo-graphy beneath the SVEKALAPKO array. I. A priori 3D crustal model and associated travel time effcets on teleseismic wave fronts. Geophysical Journal International, 153, 75 - 87.

Yliniemi J. 1991. Deep seismic soundings in the University of Oulu. In: Structure and dynamics of the Fennoscandian lithosphere. Institute of seismology, University of Helsinki, Report S-25, pp. 1-6.

Yliniemi J., Kozlovskaya E., Hjelt S-E., Komminaho K., Ushakov A. & the SVEKALAPKO Tomography WG 2004. Structure of the crust and uppermost mantle beneath southern Finland revealed by local events registered by the SVEKALAPKO seismic array. Tectonophysics, 394, 41 – 67.

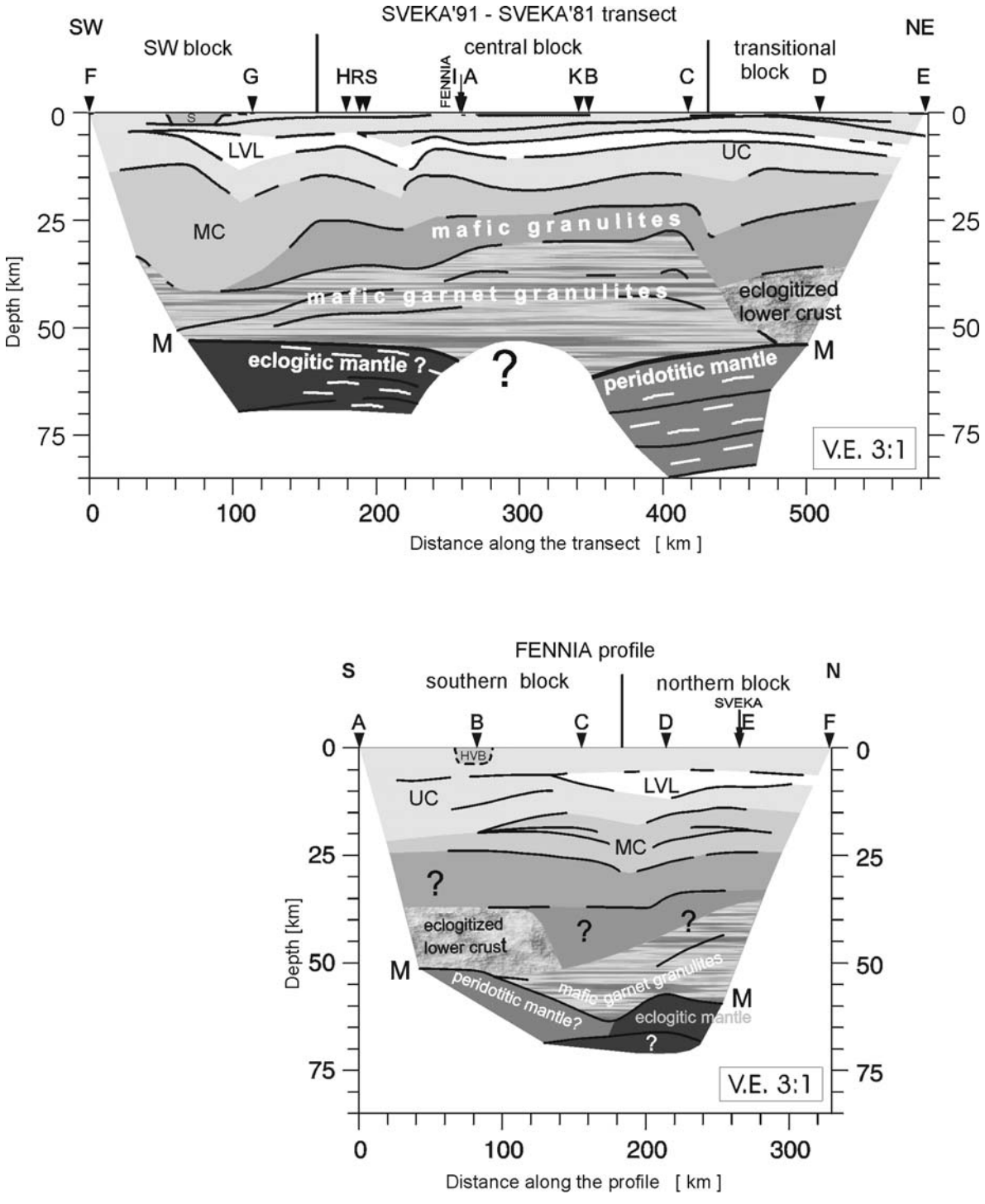

Figure 1. Simplified sketch of the crustal structure along the SVEKA transect and FENNIA profile developed by re-interpretation. Thick lines are velocity discontinuities. Dotted lines show boundaries between four blocks with different structure. Abbreviations: UC – upper crust; MC – middle crust; LVL – low velocity layer; M – Moho boundary. VE denotes vertical exaggeration.

Magnetic fabric investigation on rapakivi granites in Finland

Fredrik Karell

Geological Survey of Finland, FIN-02151 Espoo, Finland
Email: fredrik.karell@gtk.fi

Aeromagnetic data reveal concentric structures associated with rapakivi granites in Finland. Three areas based on their magnetic structures are selected for closer investigation. Geological observations, aeromagnetic interpretation and petrophysical data, including anisotropy of magnetic susceptibility (AMS) are essential tools in this research.

Keywords: Rapakivi granites, magnetic fabric, anisotropy of magnetic susceptibility (AMS), petrophysics

1. Introduction

The main purpose of my research is to determine the intrusion mechanism of rapakivi batholiths in Finland with emphasis on observed field relations and the magnetic fabric. This abstract refers to methods and work done so far. Results concerning the intrusion mechanisms are later discussed in my unfinished PhD thesis. This research project is collaboration between the Department of Geology and Mineralogy at Åbo Akademi University and the Geological Survey of Finland.

Aeromagnetic maps reveal previously unknown concentric structures indicating numerous smaller sub-intrusions building up and forming the Wiborg rapakivi batholith. Is the "homogenous" Wiborg rapakivi batholith divided into distinctive smaller intrusions composed of successive series of amalgamated pulses of granitic magmas? Structures with similar patterns have previously been described in connection with e.g. caldera collapses *(Selonen et al., 2005)*. Primarily, I have selected three smaller (c. 10 kilometers in diameter) and distinct magnetic structures; Ruotsinpyhtää (fig. 1), Ylämaa (fig. 2) and Vehmaa (fig. 3) for closer investigation, based on the aeromagnetic pattern and on published geological maps (*Simonen, 1987; Lindberg & Bergman, 1993*). Ruotsinpyhtää is located in the western part and Ylämaa is located in the eastern part of the Wiborg batholith in SE Finland. The Vehmaa rapakivi batholith is located in SW Finland. Petrology, petrogenesis and isotopic ages of rapakivi granites from the Wiborg batholith are in more detail discussed in works by Rämö and others *(1990; 1994).*

Even though the aeromagnetic data of the three selected areas show distinctive structures, similarities can be found in their size and concentric appearance. The anisotropy of magnetic susceptibility (AMS) in rocks reflects the lineation and foliation of the magnetic fabric. Analyses of the magnetic fabric give an opportunity to follow up the directions of the magma pulses within the concentric structures of the batholiths. In this research of the intrusion mechanisms of rapakivi batholiths, major emphasis will be given on magnetic fabric studies.

Application of the AMS technique can further be used for describing the fabric of oriented cracks, joints and deformation zones which may be relevant for nuclear waste depositing *(Mattson, 2006)*, for the dimension stone industry or engineering geology.

2. Anisotropy of magnetic susceptibility (AMS)

The anisotropy of magnetic susceptibility method is well established as a petrophysical tool to determine lineations and foliations in granitic rocks *(Bouchez, 1997).* Puranen *(1991)* describes the AMS technique and estimates the magnetic fabric within and around the Wiborg rapakivi pluton, which I use as reference data for my studies. Emplacement and intrusion mechanism of granitic plutons have been successfully explained by AMS interpretations *(Wennerström & Airo, 1998; Ferré et al., 1999; McNulty et al. 2000; Titus et al., 2005).*

The magnetic susceptibility, K, is based on an induced change in the applied magnetic field, which is caused by the magnetic properties of the measured specimen. The anisotropy of magnetic susceptibility represents three principal susceptibilities and their directions (K_1 = maximum, K_2 = intermediate, K_3 = minimum) as the axes of an ellipsoid (fig. 4).

The magnetic anisotropy of minerals originates from either grain shape or their crystallographic structure. Magnetite, which shows the highest susceptibility, tends to dominate the magnetic properties and therefore also the anisotropy. If the rock does not include ferrimagnetic magnetite, the anisotropy derives from biotite or other paramagnetic minerals.

3. Fieldwork

Oriented drill core samples are collected from two selected areas, Ruotsinpyhtää and Vehmaa with a portable mini drill. There are 45 sample stations in the Ruotsinpyhtää area within the Wiborg rapakivi batholith and 25 sample stations from the center of the Vehmaa rapakivi batholith. Two and more drill cores are collected from each station. From each drill core 2-4 specimens are sawed to a fixed length of 22 mm. The diameter of the cores are 25 mm, each specimen therefore has a volume of about 11 cm^3. A total amount of 6-12 specimens from each sampling station are achieved. Altogether c. 350 specimens from the Ruotsinpyhtää area and c. 200 from the Vehmaa area are measured. The strike and dip direction of each drill core are measured using a sun compass.

Apart from collecting drill core samples detailed geological observations are made. Also samples for standard petrophysical investigations (density, susceptibility and intensities of remanent magnetization) are collected at each outcrop. A total amount of 150 additional samples for standard petrophysical investigation have been taken throughout the Ruotsinpyhtää area. In the Vehmaa batholith, aligned fragments of fine-grained granitic rock are visible on outcrops around the center of the concentric anomaly pattern, which are compared to the AMS data. At some localities visible foliation are found, which can also be compared with the AMS results.

4. Laboratory work

The AMS measurements of the Ruotsinpyhtää area of the Wiborg rapakivi batholith and Vehmaa rapakivi batholith are performed at the geophysical laboratory of the Geological Survey of Finland using the Kappabridge KLY-3S apparatus. The Kappabridge apparatus is working with magnetic field-intensity at 330 Am^{-1} and operating frequency at 875 Hz. The specimen rotates slowly inside the coil were the susceptibility is measured subsequently about three axes which are manually input. Finally a bulk susceptibility measurement is done. The anisotropy is computed from these measurements. Parameters that are commonly used to describe the magnetic fabric are the degree of anisotropy, P`, the degree of lineation, L, the degree of foliation, F and the ellipsoid shape, T.

Apart from AMS measurements, standard petrophysical measurements are made. Thin sections and geochemical analyses are made to identify compositional varieties of distinctive rapakivi granite types.

5. Preliminary results

Preliminary results show that the different magnetic anomaly patterns from each study area can be described on the basis of their petrophysical properties. A comparison with samples taken in purpose for this research are compared with all Finnish rapakivi granites in the petrophysical database of the Geological Survey of Finland.

Geological observations in the Ruotsinpyhtää area show that the previously unknown concentric magnetic structure consists entirely of dark wiborgite and the inside of the ring structure consists of even-grained rapakivi granite.

Preliminary petrophysical measurements at Ylämaa show strong susceptibility variations between different rapakivi granite types. Dark even-grained rapakivi granite has very high susceptibility and high density in opposite to wiborgite, which has low susceptibility and normal density.

In the Vehmaa batholith the distinctive medium-grained porphyric rapakivi granites from the inner and outer zone *(Selonen et al., 2005)* can also be identified by petrophysical data. Data from the inner zone show high susceptibility and normal density and the outer zone show lower susceptibility and normal density.

6. Conclusions

The concentric magnetic anomaly patterns of the selected areas can be explained by a combination of basic petrophysical measurements, thin section and chemical analysis of the rocks. Preliminary AMS test results from Ruotsinpyhtää and Vehmaa speak for further research concerning the magnetic fabric investigation to determine intrusion mechanisms of the rapakivi granites in Finland.

References

Bouchez, J.L., 1997. Granite is never isotropic: an introduction to AMS studies of granitic rocks. *In: Bouchez, J.L., Hutton, D.H.W., Stephens, W.E. (Eds.), Granite: From Segregation of Melt to Emplacement Fabrics. Kluwer Academic Publishers, Netherlands, pp. 99-112.*

Ferré, E., Wilson, J. & Gleizes, G., 1999. Magnetic susceptibility and AMS of the Bushveld alkaline granites, South Africa. *Tectonophysics, 307, 113-133.*

Lindberg, B. & Bergman, L. 1993. Pre-Quaternary rocks of the Vehmaa map-sheet. Explanation to the Geological map of Finland 1:100000. *Geological Survey of Finland, 56 p. (In Finnish with English summary).*

Mattson, H. 2006. The magnetic anisotropy of rocks across two major deformation zones in the Laxemar and Simpevarp area. *SKB P-06-100. Svensk Kärnbränslehantering AB.*

McNulty, B.A., Tobisch, O.T., Cruden, A.R., & Gilder, S. 2000. Multistage emplacement of the Mount Givens pluton, central Sierra Nevada batholith, California. *Geological Society of America Bulletin, v. 112; no 1; 119-135.*

Puranen, R., 1991. Estimation of magnetic fabrics within and around the Wiborg rapakivi pluton, SE Finland. *Geological Survey of Finland, report of investigation 100, 37 p.*

Rämö, O.T. & Haapala, I., 1990. The rapakivi granites of eastern Fennoscandia: a review with insights into their origin in the light of new Sm-Nd isotopic data. *In: C.F. Gower, T. Rivers and B. Ryan (eds.), Mid-proterozoic Laurentia-Baltica. Geological Association of Canada Special Paper 38, 401-415.*

Rämö, O.T., Haapala, I. & Salonsaari, P., 1994, Rapakivi granite magmatism: implications for lithospheric evolution. *In M. Pajunen (ed.), High temperature-low pressure metamorphism and deep crustal*

structures, Meeting of IGCP Project 304 "Deep Crustal Processes" in Finland, September 16-20, 1994. Geological Survey of Finland, Guide 37, 61-68.

Selonen, O., Ehlers, C., Luodes, H. & Lerssi, J. 2005. The Vehmaa rapakivi granite batholith – an assemblage of successive intrusions indicating a piston-type collapsing centre. *Bulletin of the Geological Society of Finland, Vol. 77, 65-70.*

Simonen, A., 1987. Pre-Quaternary rocks of the map sheet areas of the rapakivi massif in SE Finland. Explanation to the Geological map of Finland 1:100000. *Geological Survey of Finland,* 49 *p. (In Finnish with English summary).*

Wennerström, M. & Airo, M-L., 1998. Magnetic fabric and emplacement of the post-collisional Pomovaara Granite Complex in northern Fennoscandia. *In: Liégeois, J. -P. (ed.) Post-collisional magmatism. An issue in honour of Professor Russell Black EUG, Strasbourg, France, 23-27 March 1997, Symposium 55. Lithos 45 (1-4), 131-145.*

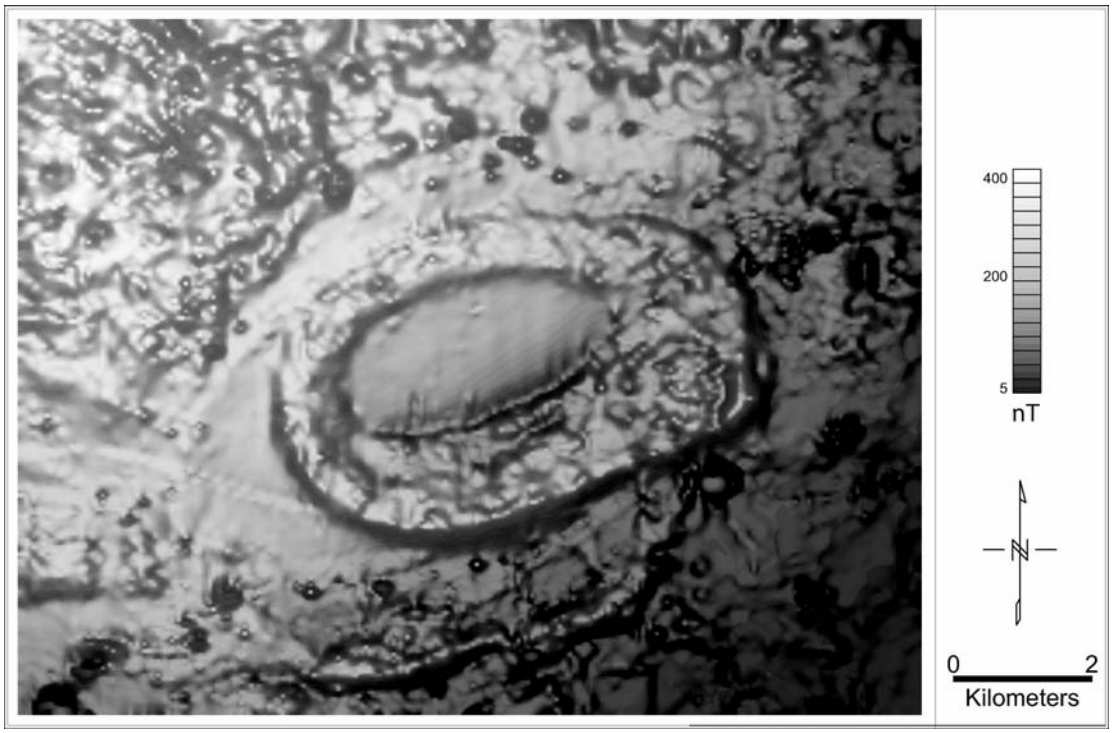

Figure 1. Aeromagnetic image of the Ruotsinpyhtää area in the western part of the Wiborg rapakivi batholith. Aerogeophysical Surveys by Geological Survey of Finland.

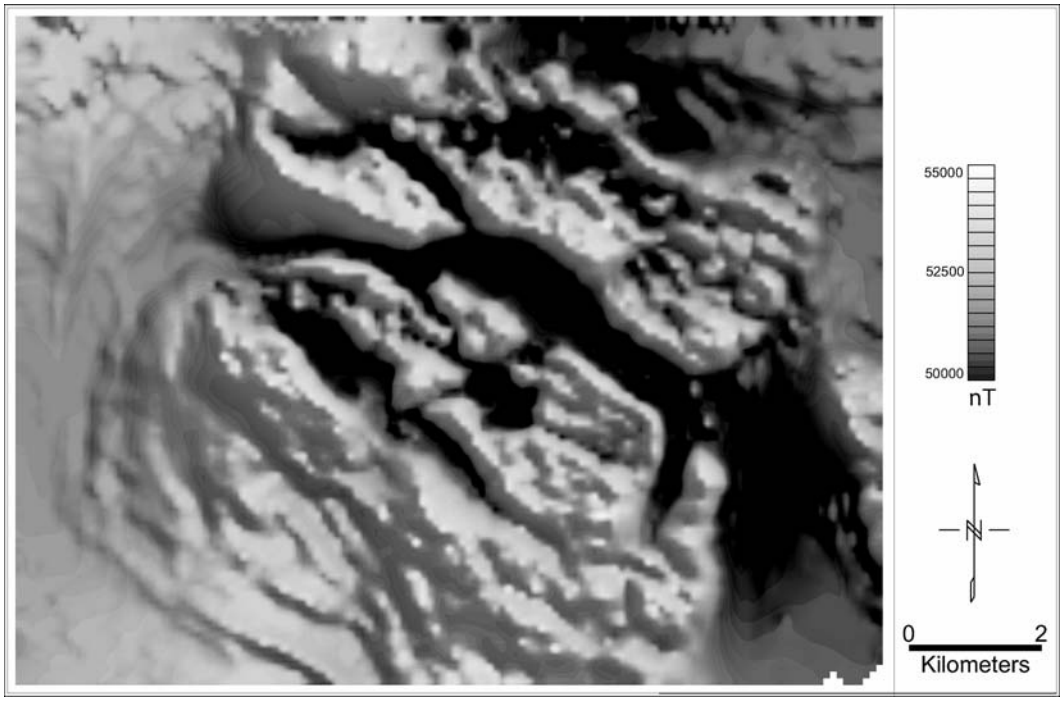

Figure 2. Aeromagnetic total intensity map of the Ylämaa area in the eastern part of the Wiborg rapakivi batholith. Aerogeophysical Surveys by Geological Survey of Finland.

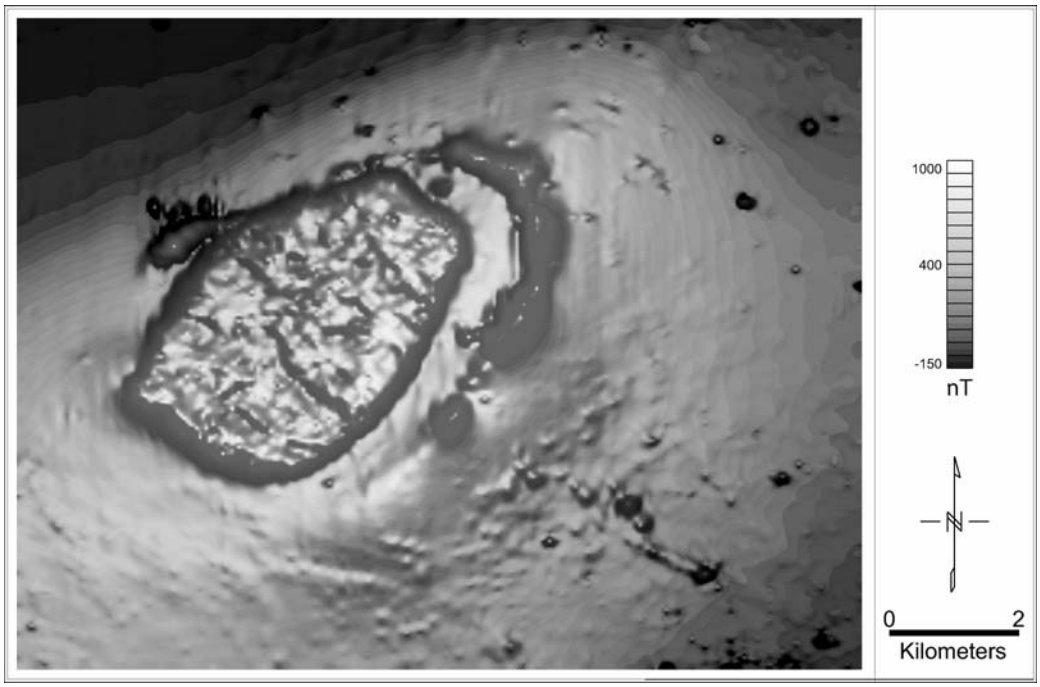

Figure 3. Aeromagnetic image of central Vehmaa batholith. Aerogeophysical Surveys by Geological Survey of Finland.

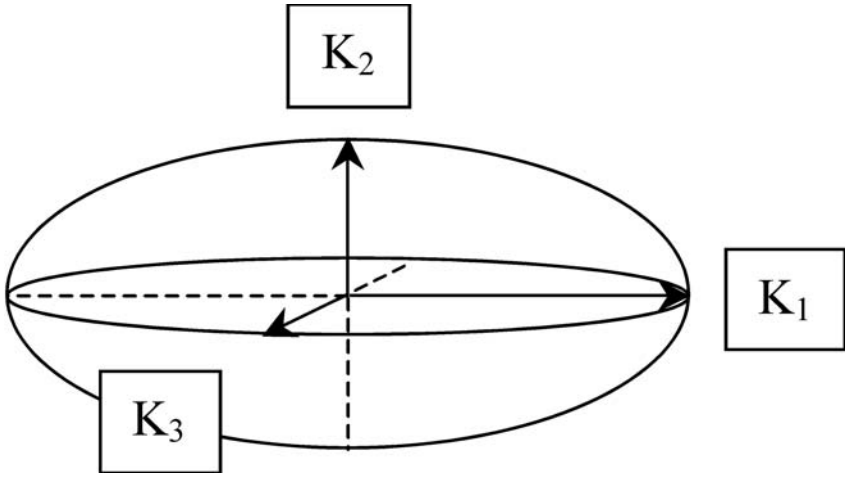

Figure 4. The anisotropy of magnetic susceptibility viewed as an ellipsoid with its principal axes $K_1 \geq K_2 \geq K_3$. K_1 represents the direction of the magnetic lineation, K_3 represents the pole to the magnetic foliation.

Metamorphism of the Archean Tuntsa-Savukoski area, NE-Finland: preliminary results

T. Kivisaari[1]* and P. Hölttä[2]

[1]Department of Geology, University of Helsinki, P.O. Box 64,
FIN-00014 Helsingin yliopisto
[2]Geological Survey of Finland, P.O. Box 96, FIN-02151 Espoo
*E-mail:tiia.kivisaari@helsinki.fi

The Archean Savukoski-Tuntsa area is characterised by horizontal tectonics, manifested by flat-lying foliation that was evidently developed in overthrust folding. Metasediments of the area are staurolite schists and gneisses which sometimes have narrow leucosome veins marking the beginning of melting. Typical mineral assemblage in peraluminous gneisses is st-ky-bt-pl-qtz±grt±crd±chl±ms. Andalusite was found in one locality in the eastern part of the area and sillimanite in the northernmost part of the study area, indicating increasing metamorphic grade to the north. Garnet has a strong compositional zoning indicating two-stage metamorphism. Garnet cores are Ca-richer and Mg-poorer than garnet rims. Thermocalc average PT-calculations show crystallization pressures of around 8 kbars for the garnet cores and 5-6 kbars for the garnet rims at temperatures of ca. 520-620^{o}C. These results indicate Barrovian, low T/P type metamorphism with clockwise decompressional PT path, typical for tectonically thickened crust.

Keywords: Archaean, metamorphic reactions, Lapland, Tuntsa-Savukoski formation

Contemporary crustal motion in Fennoscandia observed with continuous GPS networks

Hannu Koivula, Maaria Tervo and Markku Poutanen

Finnish Geodetic Institute
Geodeetinrinne 2, FIN-02430 Masala, Finland
Hannu.Koivula@fgi.fi

We describe the crustal motion in the Fennoscandian area based on the decade-long time series of permanent GPS networks in Finland and Sweden. Both horizontal and vertical motions can be measured simultaneously with GPS. In most studies, the general motion of the Eurasian plate has been removed to find the intra-plate deformation. In our case, vertical motion due to the post-glacial rebound is dominant, but the rebound causes also detectable horizontal motion.

***Keywords*:** GPS, permanent networks, plate tectonics, intra-plate crustal deformation

1. Introduction

Networks of permanent geodetic GPS (Global Positioning System) stations provide an accurate method to determine present day crustal 3-D deformations. Both horizontal and vertical motions can be measured simultaneously. The horizontal velocities can be measured at a millimeter/year level and vertical rates about 2 times less accurately. This, however, requires time series of several years and stable reference frames.

Global GPS networks are sparse, and can be used together with other space geodetic methods, Satellite Laser Ranging and geodetic VLBI, for monitoring plate tectonics and defining accurate and stable global reference frames. Regional networks, such as the European Permanent GPS Network, EPN, are considerably denser than the global networks. They are used for defining regional reference frames. National GPS networks are used for creating national frames for mapping and GIS purposes. These and other local networks of all scales, down to small km-sized networks are suitable for deformation studies. However, local (or intra-plate) deformation studies may require even denser networks. The observations are to be processed in a global reference frame, which ensures stability over years to detect minor movements.

The Nordic geodetic GPS network consists of national networks of Finland, Sweden, Norway and Denmark (Fig. 1). As an example of the network hierarchy, the Finnish permanent GPS network, FinnRef, consists of 13 GPS stations. One station, Metsähovi, belongs to the global IGS (International GNSS Service) network, which is used for orbit computation of GPS satellites and maintaining of global reference frames. Metsähovi, and three other stations, Vaasa, Joensuu and Sodankylä are part of the European Permanent GPS Network (EPN), and are basic stations for the European reference frame. All FinnRef stations are used for regional studies of Fennoscandian intra-plate deformation as well as creating the national frame EUREF-FIN.

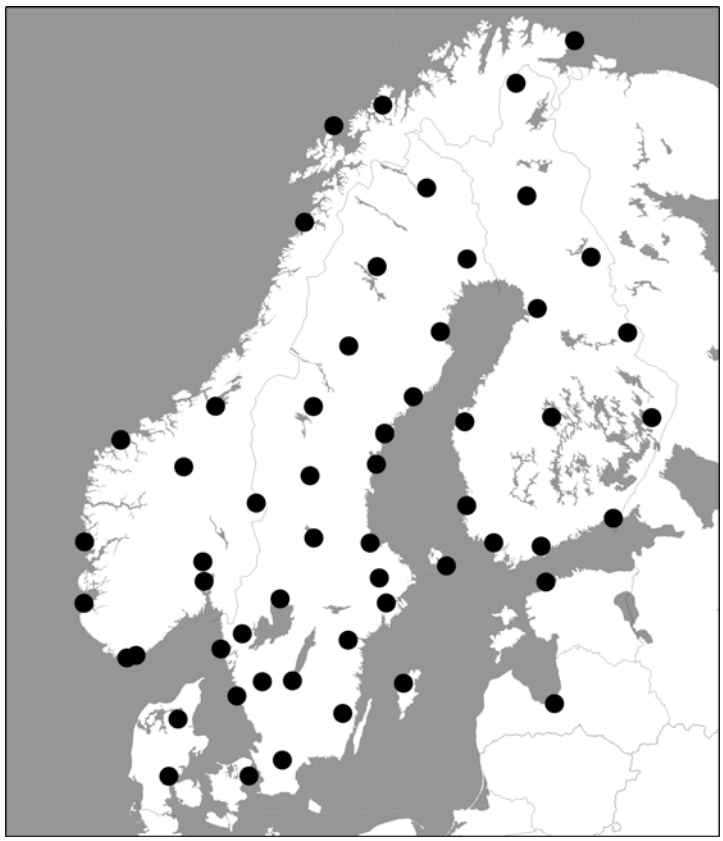

Figure 1. Nordic permanent GPS network. All the sites receive GPS signals 24 hours a day, providing long time series for reference frame creation as well as for deformation studies. Special care has been put into site selection to ensure their stability. The sites in Finland and Sweden are used in the BIFROST project.

Baseline Inferences for Fennoscandian Rebound Observations, Sea Level, and Tectonics (BIFROST) has been a project that was initiated in 1993 taking advantage of tens of permanent GPS stations both in Finland and Sweden. The goal was to measure the present day crustal deformation in Fennoscandia and provide a new GIA (Glacial Isostatic Adjustment) observable for determination of the Earth structure and Fennoscandian ice history. Most of the following results are based on the BIFROST network, but also on the observations and analysis of the FinnRef network, and on the global scale, the IGS solution. The BIFROST results are published in *Milne et al., 2001* and *2004*, *Johansson et al., 2002*, and *Scherneck et. al.,2002*.

2. Plate tectonics and crustal deformation in Fennoscandia

The observed crustal motion includes several components. First of all, there is the general drift of the Eurasian plate, as observed in the global network (Fig. 2). The vectors are relative to the global reference frame ITRF and based on the time series of the IGS

network. One commonly used model to describe the plate tectonics is the NNR-NUVEL 1A (*de Mets et al., 1994*). It takes into account the general drift of a plate, but especially in the margin regions and in the areas of deformation, the model cannot be applied. It applies only the horizontal motion, and therefore cannot be used in the postglacial rebound area either.

In local deformation analysis the global continental drift may be removed, either using the global NNR-NUVEL1A model or velocity vectors computed in the ITRF solution. A standard geodetic solution includes a mean value and a constant rate of a station, an admittance parameter for atmospheric loading and periodic terms with different frequencies. Also a bias parameter needs to be included on times that were expected to influence on the rate estimates. These kind of known interruptions are changes or removals of antennas or antenna radomes etc. Discussion and numerical results are given in *Milne et al. 2001*, and *Johansson et al. 2002*.

In Fig. 3. we show an example of time series obtained from a permanent GPS network. The time series have periodic and non-periodic variability. These are connected to changes in antenna radomes or antennas, heavy snowstorms and frost, and periodic crustal loading effects, sometimes even an artifact coming from data processing. Postglacial rebound is visible in the trend of the vertical component, but also as a change in the networks scale.

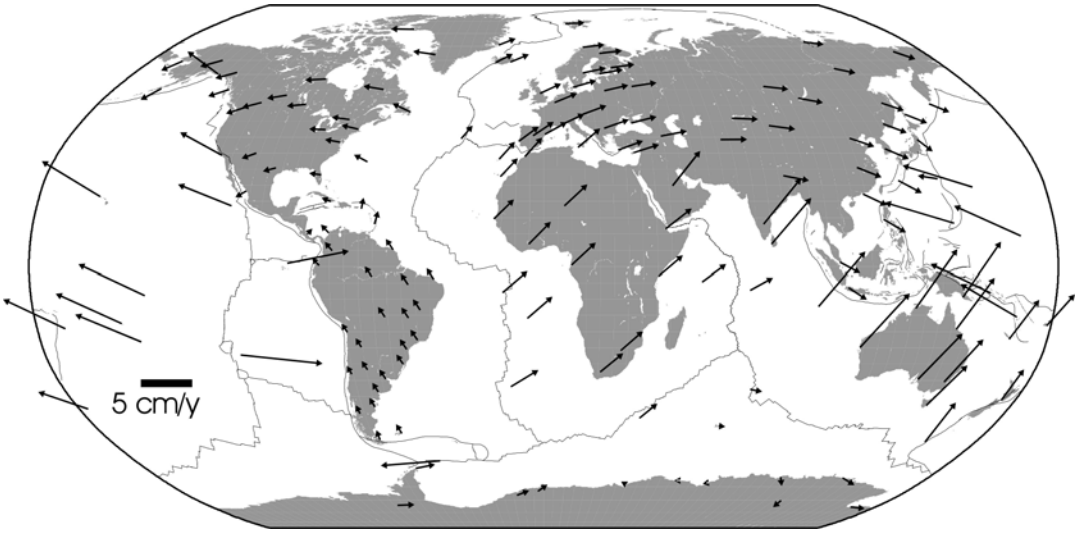

Figure 2. Velocity vectors of stations belonging to the permanent global GPS network. Stations shown are only a sub-set of the global network. Plate boundaries are also indicated.

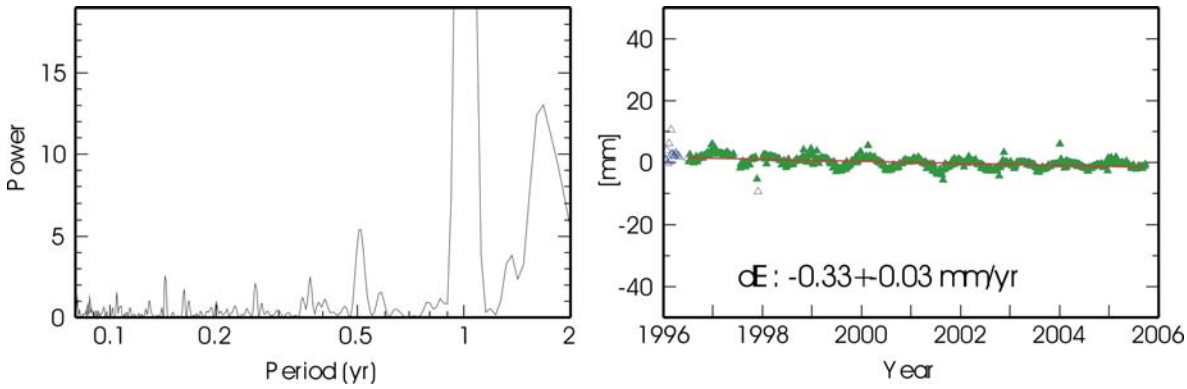

Figure 3. An example of time series of continuous GPS observations. In the right column is time series of the East component of Tuorla station with respect to Metsähovi. In the left column is the Lomb periodogram of the time series. A prominent annual variation can be seen. In some cases outliers, e.g. due to snow accumulation on a radome degrade the rate estimates, especially on the height component.

The amplitude and orientation of the GPS-based horizontal velocity vectors in Fennoscandia (Fig. 4b) are consistent with the GIA model prediction (*Lambeck et. al., 1998*) (Fig. 4a). Horizontal velocities are small in the vicinity of the Gulf of Bothnia, and they tend to radiate outward from this area. The horizontal rates have greater amplitude westward of the Gulf of Bothnia than eastward of this region. The asymmetry is a consequence of several factors. The surface mass (ice plus water) load is not symmetric about the Gulf of Bothnia. Furthermore, deglaciation of Late Pleistocene North American ice sheets and rotational effects produce long-wavelength present-day horizontal deformations in Fennoscandia directed, respectively, toward the northwest and east. (*Milne et. al., 2001, 2004*)

GPS gives rather 3D results than only horizontal direction. In Figure 5 is shown the GIA model prediction and GPS derived present day vertical crustal motions in Fennoscandia. (*Milne et. al., 2001, 2004*).

In *Milne et al. (2001* and *2004*) a conclusion is given that an Earth model that satisfies both the observational and independent geologic constraints has an average viscosity of 5 x 10^{20} to 1 x 10^{21} pascal seconds in the upper mantle and an elastic thickness of the lithosphere of 90 to 170 kilometers. The horizontal GPS results do not show indication of ongoing intra-plate tectonic motion exceeding 1-2 mm/yr across the entire shield area. However, for a more detailed study of the intra-plate deformation a denser set of GPS stations or episodic GPS campaigns are necessary. Detailed 3-D motion with an accuracy of sub-millimeter is achievable in a small local network as demonstrated in *Ahola et al., 2006*.

Combined observation techniques, ever increasing length of time series and eventual re-computation of the whole BIFROST data history with improved algorithms (see e.g. *Lidberg, 2004*) will increase the accuracy.

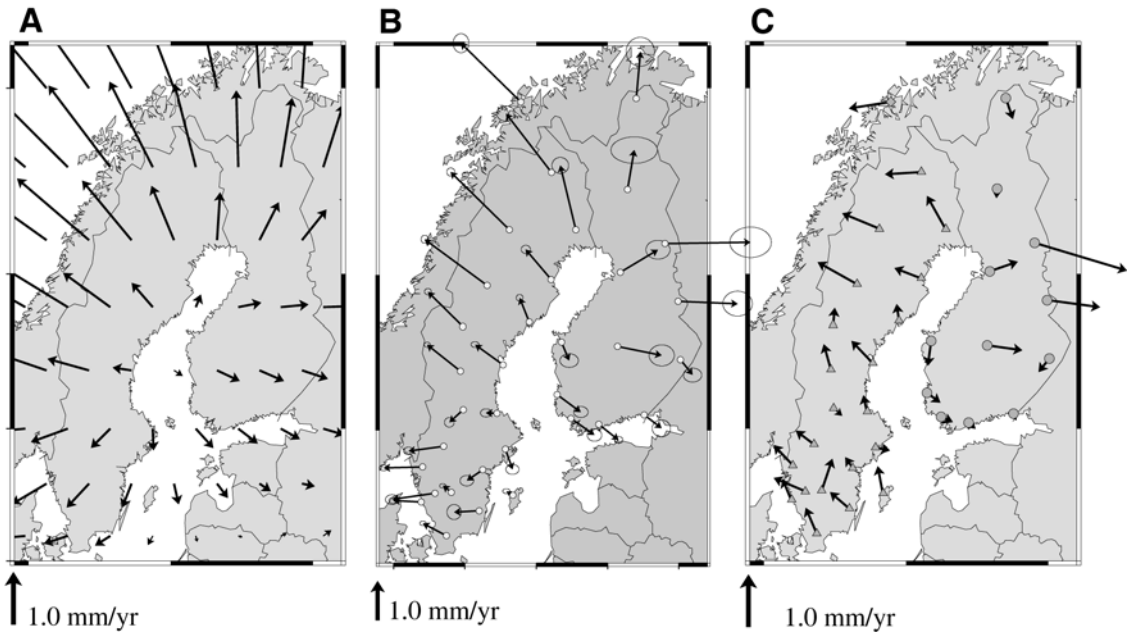

Figure 4. BIFROST prediction of the horizontal present-day crustal motion (a), the velocities determined from GPS observations at each site (b), the error ellipses are 1σ. Residual horizontal deformations at each GPS site when predicted rates are subtracted from observed ones. (*Milne et. al., 2004*)

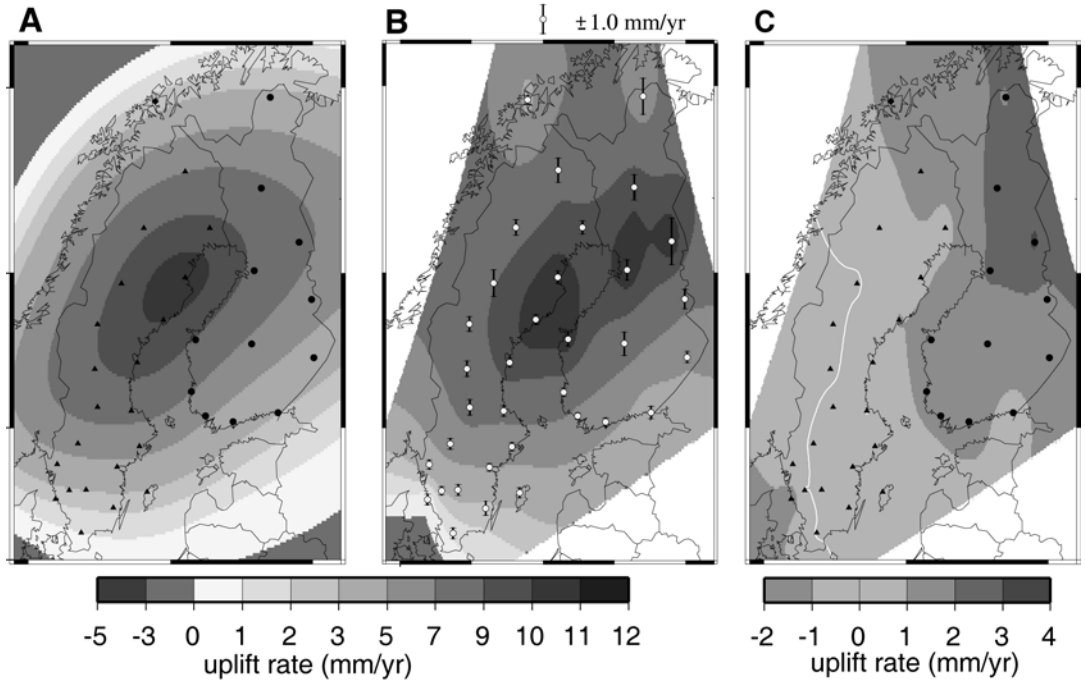

Figure 5. BIFROST prediction of the vertical present-day crustal motion (a), the velocities determined from GPS observations at each site as a contour map (b),. Residual vertical deformations at each GPS site when predicted rates are subtracted from observed ones. (*Milne et. al., 2004*).

3. Future of the networks

Traditionally, geodetic networks of different techniques have been separated, with only a few, if any, common points. There is, however, a great advantage in combining, for example, gravimetric and GPS networks. In addition to the 3-D crustal deformation, one gets also information on gravity changes, important for geodynamic interpretation. During recent years, combined network and observing systems have been discussed and established.

The Nordic Geodetic Commission (NKG) established in 2003 a Task Force with the mission to prepare the plan and the practical implementation of the Nordic Geodetic Observing System (NGOS). The geographic extent of NGOS covers the Nordic region, including Iceland, Greenland and Svalbard, i.e. the area of the ice-covered part of the Northern Europe during the last ice age. (*Poutanen et al., 2005*)

NGOS will be the major channel in the future to coordinate and combine the existing observations and networks in the Fennoscandian area, and act as an interface between the geodetic community and the public. Most of the infrastructure is already in its place, and we already have years of high-quality data available, which can be used for intra-plate deformation studies. On the global level, GGOS (Global Geodetic Observing System) will be in coming decades the geodesy's major contribution in the studies of the Planet Earth.

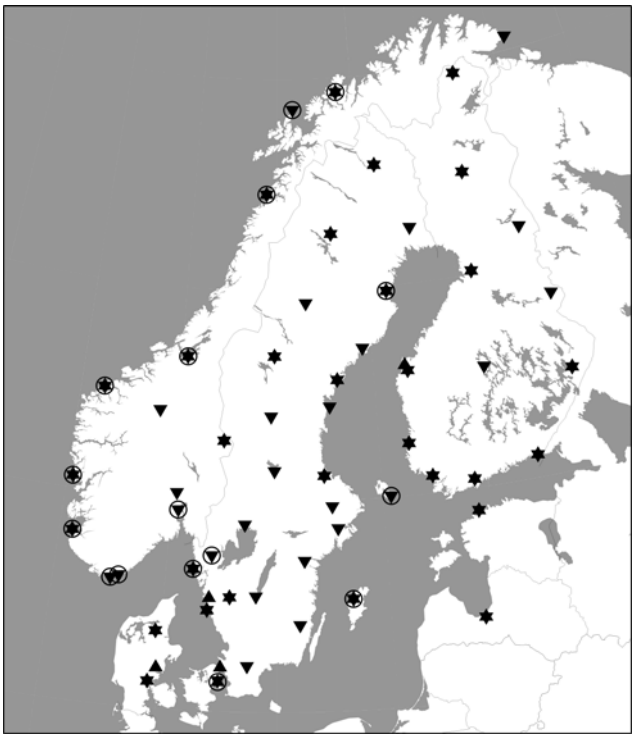

Figure 6. NGOS plan. Absolute gravity points (triangles), Nordic permanent GPS network (upside down triangles) and tide gauges (circles). All absolute gravity points are occupied with a GNSS instrument. (*Poutanen et al., 2005*)

References

Ahola, J., Ollikainen, M., Koivula, H. and Jokela, J., 2006. GPS Operations at Olkiluoto, Kivetty and Romuvaara in 2005. *Working Report* **2006-63**. Posiva Oy.

de Mets, C., Gordon, R.G., Argus, D.F. and Stein, S., 1994. Effect of recent revision to the geomagnetic reversal time scale on estimates of current plate motions. Geophysical Research Letters 21 (20), 2191-2194.

Johansson J.M., Davis, J.L., Scherneck, H.-G., Milne, G.A., Vermeer, M., Mitrovica, J.X., Bennett, R.A., Ekman, M., Elgered, G., Elosegui, P., Koivula, H., Poutanen, M., Rönnäng, B.O. and Shapiro, I.I., 2002. Continuous GPS measurements of postglacial adjustment in Fennoscandia, 1. Geodetic results. Journal of Geophysical Research, 107, B8, doi:10.1029/2001JB000400.

Lambeck K., Smither, C. and Johnston, P., 1998. Sea-level change, glacial rebound and mantle viscosity for Northern Europe. Geophysical Journal International, 103, 102-144.

Lidberg, M., 2004. Motions in the geodetic reference frame—GPS observations. Licentiate's Thesis, Department of Radio and Space Science with Onsala Space Observatory, Chalmers Institute of Technology, Göteborg, Sweden.

Milne G.A., Davis, J.L., Mitrovica, J.X., Scherneck, H.-G., Johansson, J.M., Vermeer, M. and Koivula, H., 2001. Space-Geodetic Constraints on Glacial Isostatic Adjustment in Fennoscandia. Science, Vol. 291, 23 March 2001, pp. 2381-2385.

Milne G.A., Mitrovica, J.X., Scherneck, H.-G., Davis, J.L., Johansson, J.M., Koivula, H. and Vermeer, M., 2004. Continuous GPS measurements of postglacial adjustment in Fennoscandia: 2. Modelling results. Journal of Geophysical Research, 109, B02412, doi:10.1029/2003JB002619.

Poutanen M., Knudsen, P., Lilje, M., Nørbech, T. Plag, H.- P. and Scherneck, H.-G., 2005. NGOS – The Nordic Geodetic Observing System. Nordic Journal of Surveying and Real Estate Research, vol. 2, number 2, 79-100.

Scherneck, H.-G., Johansson, J.M., Elgered, G., Davis, J.L., Jonsson, B., Hedling, G., Koivula, H., Ollikainen, M., Poutanen, M., Vermeer, M., Mitrovica, J.X. and Milne, G.A., 2002. BIFROST: Observing the Three-Dimensional Deformation of Fennoscandia, in Glacial Isostatic Adjustment and the Earth System, edited by J.X. Mitrovica and B.L.A. Vermeersen, Geodynamics Series, Volume 29, American Geophysical Union, Washington, D.C.

BIFROST project members: *J.M. Johansson, J.L. Davis, H.-G. Scherneck, G.A. Milne, M. Vermeer, J.X. Mitrovica, R.A. Bennett, M. Ekman, G. Elgered, P. Elosegui, H. Koivula, M. Poutanen, B.O. Rönnäng, I.I. Shapiro, M. Lidberg, M. Ollikainen, B. Johnsson, G. Hedling*

Electrical conductivity of upper mantle in Fennoscandia

T. Korja[1]*, Kaikkonen, P. [1], Lahti, I. [2], Pedersen, L.B. [3], Smirnov, M. [1], Vaittinen, K. [1], BEAR WG and EMTESZ WG

[1]University of Oulu, Department of Physical Sciences, Geophysics, POB 3000, FIN-90014, University of Oulu,
[2]Geological Survey of Finland, Rovaniemi
[3]University of Uppsala, Department of Earth Sceinces, Uppsala, Sweden
*E-mail: toivo.korja@oulu.fi

Information on electrical conductivity of upper mantle beneath the Fennoscandian Shield and its margins are reviewed and potential implications are discussed.

Key words: magnetotellurics, electromagnetic soundings, electrical conductivity, lithosphere, asthenosphere, upper mantle, Fennoscandia

The first long period electromagnetic soundings in Fennoscandia were completed in early 1980's (e.g. *Jones, 1980, Kaikkonen et al., 1983*). Since then a few additional deep probing studies were carried out (e.g. *Pajunpää, 1988, Rasmusen, 1988*) before the end of the last century. Recent improvements of magnetotelluric instrumentation have made it possible to obtain reliable and good quality data from magnetotelluric profile and array measurements. This is important, in particular, for upper mantle studies because long recording times are needed for deep probing soundings to obtain long period data (needed for upper mantle studies) and to correct for source field effects. As an example, in the recent EMMA work (*Smirnov et al., 2006*) simultaneously nine months long recordings at 12 sites were carried out from Aug 2005 to Jun 2006. These recordings provide information from the depths of several hundreds of kilometres.

In 1998 a large MT array was employed in Fennoscandia as a part of the BEAR research (*Korja et al., 2002*), which, for the first time, provided data over the entire shield (e.g. *Lahti et al., 2005*). Since then several extensive data sets have been collected both in the Fennoscandian Shield (Jämtland - *Korja et al., 2006*; EMMA – *Smirnov et al., 2006*; MT-FIRE – *Vaittinen et al., 2006*) as well as on its margins (TOR – *Smirnov and Pedersen, 2006*; EMTESZ-Pomerania – *Brasse et al., 2006*). A complete list of references to original work used in current work are given in the reference list.

Figure 1 shows the location of deep sounding sites in Fennoscandia. Circles are coloured according to the inferred depth of the top of the upper mantle conductor. Figure 2 shows an example of the depth of the assumed electrical lithosphere-asthenosphere border along a NS-directed profile across Europe.

Results show that in Fennoscandia (and in East European Craton) electrical asthenosphere is either very deep or is absent (or cannot be detected by magnetotellurics) whereas in Central and Southern Europe electrical asthenosphere is much shallower. Rapid transition from thick East European Craton to thinner Phanerozoic Europe coincides with the Trans European Suture Zone.

References

Brasse, H., Cerv, V., Ernst, T., Hoffmann, N., Jankowski, J., Jozwiak, W., Korja, T., Kreutzman, A., Neska, A., Palshin, N., Pedersen, L.B., Schwartz, G., Smirnov, M., Sokolova, E., and Varentsov, I.M., 206.

Probing Electrical Conductivity of the Trans-European Suture Zone. *EOS*, Vol. 87, No. 29, 18 July 2006, p 281 and 287.

Carlsäter, M., 2002. Magnetotelluric measurements in the Swedish Caledonides. *Unpublished M.Sc. thesis, Department of Earth Sciences, University of Uppsala*, Uppsala, Sweden, 33 pp.

Jones, A.G., Olafsdottir, B. and Tiikkainen, J., 1983. Geomagnetic induction studies in Scandinavia. - III. Magnetotelluric observations. *J. Geophys*., 54, 35 - 50.

Jones, A.G., 1980. Geomagnetic induction studies in Scandinavia - I Determination of the inductive response function from the magnetometer array data, *J. Geophys*., 48, 181-194.

Jones, A.G., 1981. Geomagnetic induction studies in Scandinavia. II Geomagnetic depth sounding, induction vectors and coast effect, *J. Geophys*., 50, 23-36.

Jones, A.G., 1982. Observations of the electrical asthenosphere beneath Scandinavia, *Tectonophysics*, 90, 37 - 55.

Jones, A.G., 1983. The electrical structure of the lithosphere and asthenosphere beneath the Fennoscandian shield. *J. Geomagn. Geoelectr*., 35, 811 - 827.

Kaikkonen, P., L.L. Vanyan, S.-E. Hjelt, A.P. Shilovsky, K. Pajunpää, and P.P. Shilovsky, A preliminary geoelectrical model of the Karelian megablock of the Baltic Shield, *Phys, Earth Planet. Inter*., 32, 301-305, 1983.

Koistinen, T., Stephens, M.B., Bogatchev, V., Nordgulen, O., Wennerström, M. &Korhonen, J. 2001. Geological map of the Fennoscandian Shield, scale 1:2 000 000. *Geological Surveys of Finland, Norway and Sweden and the North-West Department of Natural Resources of Russia*.

Korja T., Engels M., Zhamaletdinov A.A., Kovtun A.A., Palshin N.A, Smirnov M.Yu., Tokarev A., Asming V.E., Vanyan L.L., Vardaniants I.L., and the BEAR Working Group, 2002. Crustal conductivity in Fennoscandia - a compilation of a database on crustal conductance in the Fennoscandian Shield. *Earth Planets Space*, 54, 535-558.

Korja, T., Hjelt, S.-E., Kaikkonen, P., Kozlovskaya, E., Lahti, I., Pajunpää, K., Pulkkinen, A., Viljanen A., and BEAR Working Group, 2002. Crust and Upper Mantle beneath Fennoscandia as imaged by the Baltic Electromagnetic Array Research (BEAR). Pp. 41-48 in Lithosphere 2002. Programme and extend abstracts, eds. R. Lahtinen, A. Korja, K. Arhe, O. Eklund, S.-E. Hjelt, and L.J. Pesonen, *Institute of Seismology, University of Helsinki, Helsinki, Finland, Report S-42*, 146 pp. (in English).

Korja, T., Smirnov, M. and Pedersen, L.B., 2006. Electrical conductivity of the Scandinavian Caledonides and the underlying lithosphere, Jämtland, Sweden. *Bull. Geol. Soc. Finland, Special Issue 1*, p. 73.

Korja, T., 2006. How is the European lithosphere imaged by magnetotellurics? Invited review in the *17th Electromagnetic Induction Workshop*, 17.-23.09.2006, El Vendrell, Spain.

Kovtun, A.A., S.A. Vagin, I.L. Vardaniants, N.P Legenkova, O.N. Moiseev, M.Yu. Smirnov, and N.I. Uspenskiy, The crust and upper mantle structure along the profile Suoyarvy-Vyborg according to magnetotelluric data, *Vestnik LGU (Leningrad University)*, 4, No. 25, 25-34, 1988. (in Russian)

Kovtun, A.A., S.A. Vagin, I.L. Vardaniants, L.N. Porokhova, E.L. Kokvina, and N.I. Uspenskiy, Magnetotelluric investigation of the crust and upper mantle structure in the Eastern part of Baltic Shield, in Proceedings of the Jubilee Symposium of the 10 years Finnish-Soviet co-work in geoelectrics, edited by P. Kaikkonen, *Department of Geophysics, University of Oulu, Oulu, Finland, Report,* 18, 47-54, 1992.

Kovtun A.A., S.A. Vagin, I.L. Vardaniants, E.L. Kokvina, and N.I. Uspenskiy, Magnetotelluric investigations of the crust and mantle structure in the eastern part of the Baltic Shield, *Izvestiya Rossiyskoy Akademii Nauk, Physics of Earth*, 3, 32-36, 1994. (in Russian)

Krasnobayeva A.G., B.P. Dyakonov, P.F. Astafjev, O.V. Batalova, V.S Vishnev, I.E. Gavrilova, R.B. Zhuravleva, and S.K. Kirillov, The structure of the north-eastern part of the Baltic shield based on the magnetotelluric data, *Izvestiya Rossiyskoy Akademii Nauk*, *Physics of the Solid Earth*, 6, 65-73, 1981.

Lahti, I., Korja, T., Kaikkonen, P., Vaittinen, K. and BEAR Working Group 2005. Decomposition analysis of the BEAR magnetotelluric data: implications for the upper mantle conductivity in the Fennoscandia Shield. *Geophysical Journal International*, 163, 900-914.

Pajunpää, K., 1988. Application of horizontal spatial gradient method to magnetometer array data in Finland - Preliminary results. *Department of Geophysics, Univ. Oulu, Rep.* No.15, 13 pp.

Rasmussen, T.M., 1988. Magnetotellurics in Southwestern Sweden: Evidence for electrical anisotropy in the lower crust ? *J. Geophys. Res*., 93, B7, 7897 - 7907.

Rasmussen, T.M., R.G. Roberts, and L.B. Pedersen, Magnetotellurics along the Fennoscandian Long Range Profile, *Geophys. J. R. Astron. Soc*., 89, 799-820, 1987

Smirnov, M. and Pedersen, L.B., 2006. Electrical conductivity across the Sorgenfrei-Tornquist Zone. *17th Electromagnetic Induction Workshop*, 17.-23.09.2006, El Vendrell, Spain.

Smirnov, M., Korja, T. and Pedersen, L.B., 2006. Deep lithosphere structure is a target for electromagnetic arrays. Electromagnetic Mini Array (EMMA) project in Fennoscandia. *Bull. Geol. Soc. Finland, Special Issue* 1, p. 150.

Vaittinen, K., Korja, T., Kaikkonen, P. and Lahti, I., 2006. High-resolution magnetotelluric studies of the Archaean-Proterozoic border zone in Fennoscandian Shield, Finland. *Bull. Geol. Soc. Finland, Special Issue* 1, p. 166.

Viljakainen, M., A magnetotelluric study on the electrical conductivity of the upper mantle in the Archaean Kuhmo region, *Unpublished M.Sc. thesis, Department of Geophysics, University of Oulu*, Oulu, Finland, 66 + 10 pp., 1996. (in Finnish)

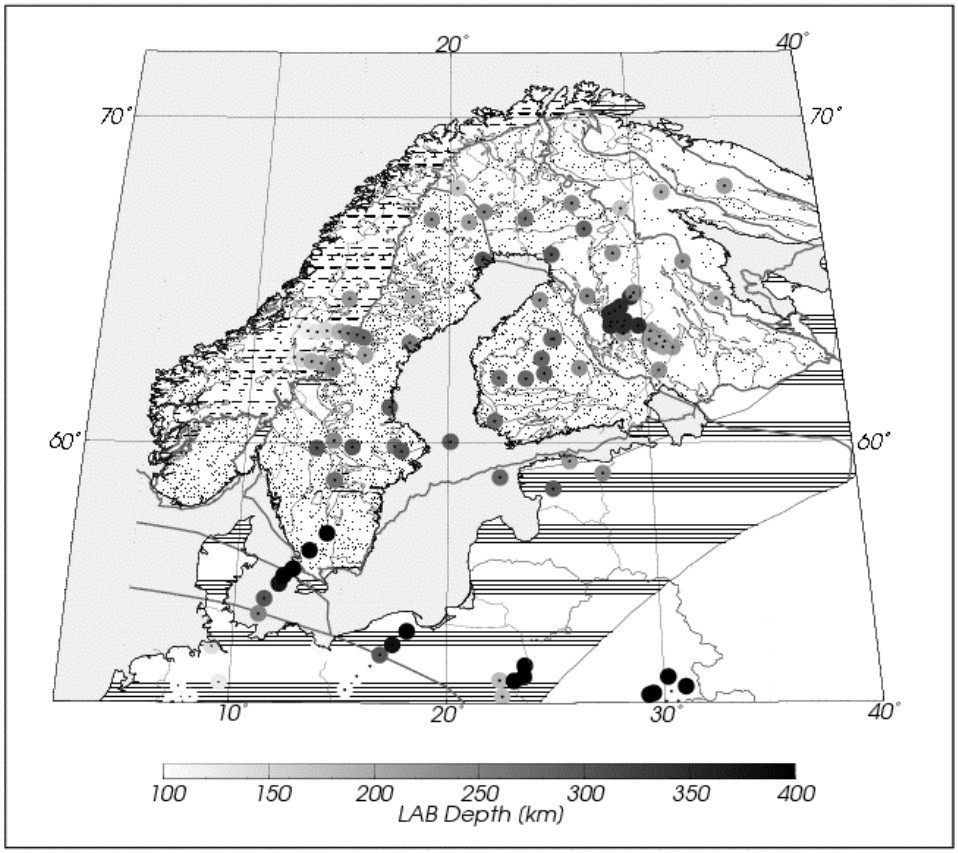

Figure 1. Location of deep electromagnetic sounding sites in Fennoscandia and adjacent regions (circles). Colour of circles denotes depth to upper mantle conductor. Geological map simplified from Koistinen et al. 2001. References for original deep electromagnetic studies are given in text.

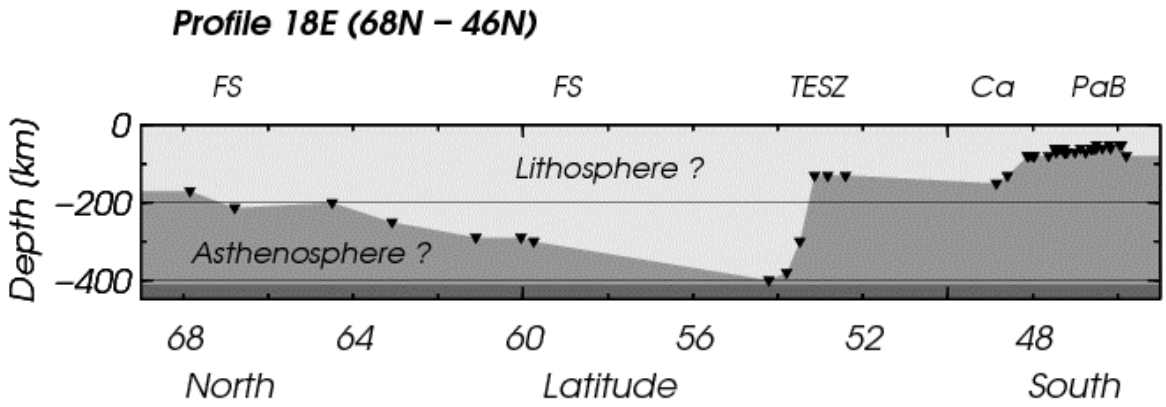

Figure 2. Upper mantle cross-section through Europe (Korja, 2006) showing the depth of the assumed electrical lithosphere-asthenosphere border in Europe. Inverted triangles show the simultaneously location of sampling points.

Post-collisional extension in central Svecofennian, Central Finland

P. Kosunen[1]*, A. Korja [1], M. Nironen[2] and FIRE Working Group

[1]Institute of Seismology, POB 68, 00014 University of Helsinki, Finland
[2]Geological Survey of Finland, POB 96, FIN-02151 Espoo, Finland
*Email: Paula.Kosunen@helsinki.fi

Two deep seismic reflection profiles, FIRE 1 and 3a reveal post-collisional deformation in the Central Finland Granitoid Complex (CFGC) in the central part of the Svecofennian Orogen. In the orogeny, the Proterozoic Central Finland was thickened due to westward stacking of 25 km thick crustal slices. Gravitational collapse took place in the upper parts of the continental stack and it is displayed as shallow, upper crustal extensional structures (3-8 km) cross-cutting the collisional ones.

FIRE 3a is characterized by shallow, SE dipping listric structures, which flatten out between the depths of 8 km and 10 km; these listric structures are imaged as subhorizontal reflections on FIRE 1. The listric reflections broadly correlate with smooth NE trending changes in magnetic anomaly levels. On Fire 1, the subhorizontal reflections are transected by several NW-SE trending,, NE or SW dipping lineaments, which define a graben-horst structure in the uppermost 8 km of the crust. These lineaments are seen as sharp magnetic minima on aeromagnetic anomaly maps. It is likely, that these steeply dipping and listric structures controlled the emplacement of some of the granites of the CFGC, probably under transtensional or extensional tectonic regime.

Keywords: Central Finland, extension, gravitational collapse, reflection seismic line, FIRE

1. Introduction

Extension takes place in several continental environments: continental rifts, back-arcs, core complexes and in collapsing orogens. Extension is either related to diverging plate movements, mantle plume upwelling or gravitational potential energy (GPE) anomalies in the crust (Rey et al. 2001). The mode by which the lithosphere is stretched depends on rheology, thickness of the crust and lithosphere, geothermal gradient, strain rate, type of stress applied, plate boundary forces and time applied. So far, the different modes of extension have not been distinguished in shield areas although extensional environments have been recognised and described in geological literature.

Seismic reflection data has a large role in distinguishing extensional structures in crustal scale, both in modern environments and in the ancient ones. Deep seismic reflection profiles FIRE 1 and 3A image post-collisional, extension-related deformation in the Central Finland Granitoid Complex (CFGC) in the central part of the Svecofennian orogen. The FIRE 1 and 3A profiles cross each other in the Karstula-Saarijärvi area in the CFGC (Fig. 1). As this provides an excellent opportunity to gain a 3D view of the crust, the area was chosen as the starting point for further studies in the ongoing project.

2. Geologic and aeromagnetic features of Central Finland Granitoid Complex

The CFGC comprises 1.89 - 1.88 Ga synkinematic granodiorites and granites, 1.88 Ga postkinematic granites, minor mafic intrusions and various volcanic to subvolcanic rocks; metasedimentary rocks are found in places. The synkinematic granitoids of the complex are more or less deformed and show clear and pervasive foliation or schistosity. The massive, nonfoliated postkinematic granites are the latest intrusives in the complex and post-date the collisional deformation. Two postkinematic granite intrusions, Karstula and Saarijärvi, are

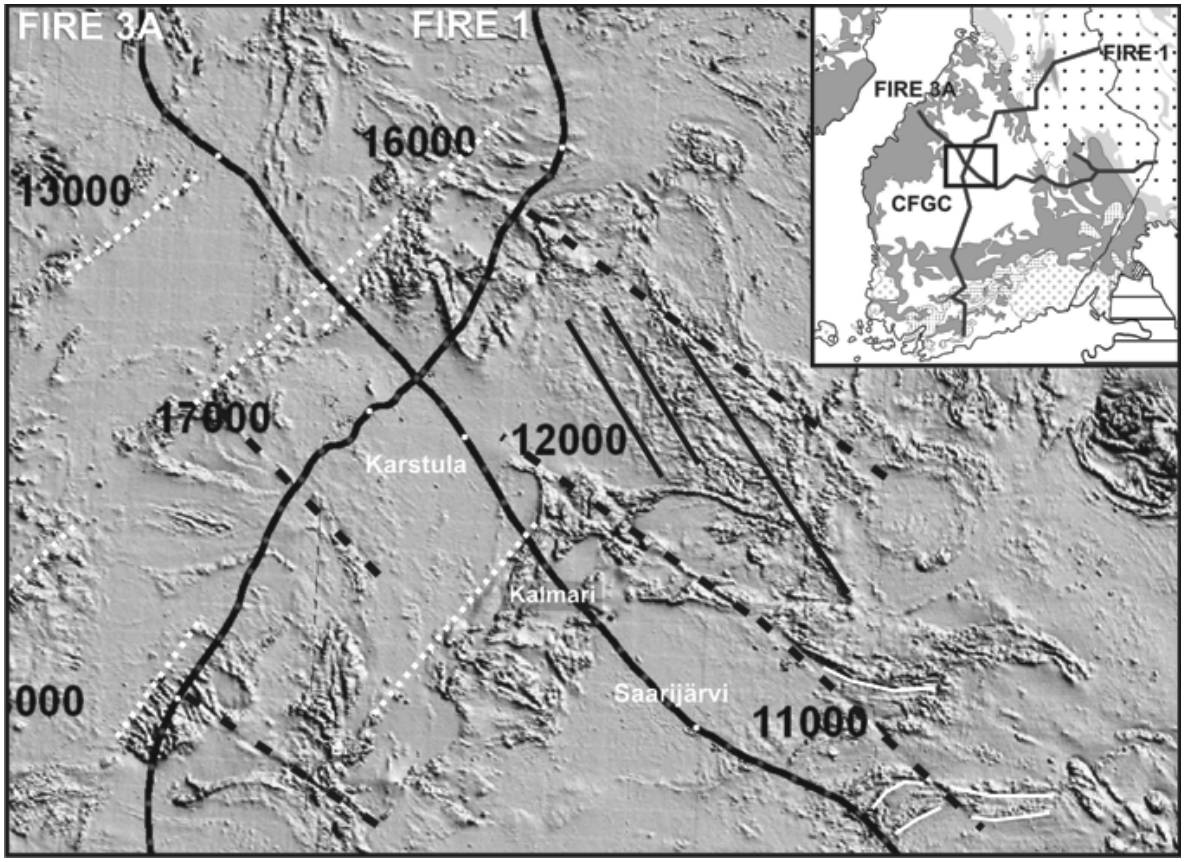

Figure 1. Aeromagnetic anomaly map of the Karstula-Saarijärvi area of the Central Finland Granitoid Complex (Geological Survey of Finland). The numbers indicate CMP for the seismic profiles FIRE 1 and FIRE 3A. Two postkinematic granite intrusions, Karstula and Saarijärvi, and the supracrustal Kalmari sequence are marked on the map. The dashed black lines indicate the SE-trending, linear magnetic minima identified as shear-zones; the solid white lines show bending of the structures along one of them. The solid black lines indicate Riedel fractures. The stipled white lines denote the NE-trending, SE-dipping changes in magnetic anomaly levels.

found in the study area, separated by the Kalmari supracrustal (subvolcanic) sequence (Fig. 1).

On the aeromagnetic anomaly map of the Karstula-Saarijärvi area, the more magnetic mafic and supracrustal rocks of the area form local anomaly maxima in the background composed of granitoid intrusions (Fig. 1). The postkinematic Karstula and Saarijärvi granites are displayed as featureless magnetic minima, flanking the more magnetic Kalmari subvolcanic sequences in between. Several sharp, linear, SE-trending magnetic minima transect the synkinematic granitoids and supracrustal rocks. Field observations identify these lineaments as shear-zones, which in places truncate also the postkinematic granites. Bending of the structures along one of these lineaments indicates right-handed lateral movement along the shear-zone. A less obvious feature in the area are the NE-trending,

SE-dipping changes in magnetic anomaly levels; one of these changes coincides with deformed amphibolites northwest of the Karstula granite.

3. Interpretation of the seismic data

Lahtinen et al. (2005) have suggested the Svecofennian orogen to be a collage of microplates and intervening volcanosedimentary belts. The seismic reflection data reveals that the thick Svecofennian crust (>50 km) is composed of 20-25 km thick crustal slices that have been stacked west-northwestwards. In the CFGC, the collisional structures have been overprinted by extensional deformation.

The deep seismic reflection profiles reveal a three-layered structure of the crust in the CFGC area. On FIRE 1, the upper crust (down to about 8-10 km) is characterized by subhorizontal reflections, which are transected by several relatively steep, NE or SW dipping lineaments. These lineaments define a graben-horst structure in the uppermost 8 km of the crust and seem to correlate with the southeasterly, linear magnetic anomalies and image the shear-zones. The middle crust (from about 10 to 35 km) is segmented by strong reflections that merge into the middle crust - lower crust boundary. The lower crust (down to almost 60 km) is characterized by diffuse, nearly horizontal reflections. In the Karstula – Saarijärvi area, the middle crust is thinner, separated from the thickened lower crust by strong reflections at the depth of 20 to 25 km.

The upper crust along FIRE 3A is characterized by shallow, SE dipping listric structures, which flatten out between the depths of 8 to 10 km; on FIRE 1, these structures are imaged as the subhorizontal reflections. The surface intersects of some of these structures broadly correlate with the NE-trending changes in magnetic anomaly levels. The middle-crustal segments are clearly defined by strong reflections that dip gently southeast and flatten out or become diffuse at the middle crust - lower crust boundary. The middle-crustal reflections are truncated by the upper-crustal ones, on both profiles.

The seismic image indicates the postkinematic Karstula and Saarijärvi granites to be bowl-shaped, relatively shallow (from 2 to 6 km) intrusions that overlie some of the listric structures seen in FIRE 3A. Also, the SW contact of the Karstula granite is tectonic, formed by a SW-dipping shear-zone seen in FIRE 1 and confirmed by field observations. It is interpreted that these structures partly controlled the emplacement of the postkinematic granites, probably under transtensional or extensional tectonic regime.

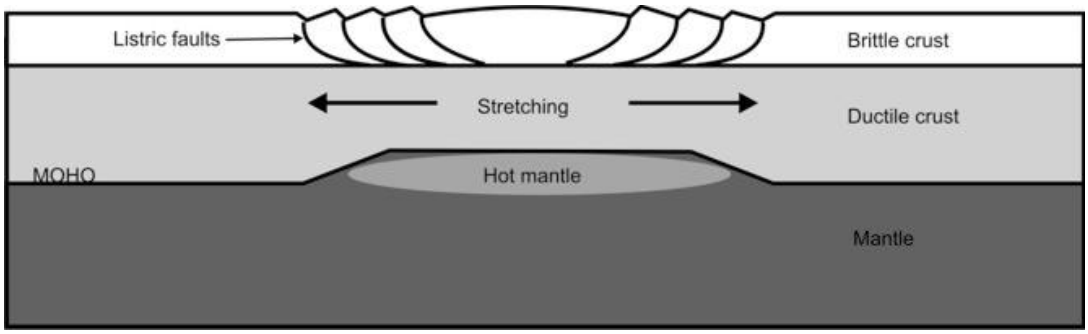

Figure 2. Uniform pure shear model of basin formation after McKenzie (1978) and Coward (1986).

4. Discussion and conclusions

The interpretation of the seismic data and the different reflections in the upper, middle and lower crust are compatible with the rheological models/observations by Meissner 1996 and Coward 1987. The upper crust shows brittle structures, lower crust ductile subhorizontal structures and middle crust large scale listric faults typical of elastic domain. Thinning of the upper and middle crust has been compensated by upwarping of the lower crust and upper mantle. Highly reflective crustal "steps or ladders" found beneath the mafic intrusions are interpreted as magmatic feeder channels whereby melts from the lower crust have risen to the upper crust.

In N-S direction, along FIRE 1, the crustal structure bears a striking similarity to the McKenzie-type uniform pure shear model of basin formation (Fig. 2; McKenzie, 1978; Coward, 1986). As the lithosphere is stretched during continental extension, the ductile lower crust thins by stretching, while the upper crust is broken up and pulled apart by normal faults soling at the brittle-ductile transition zone. In E-W or SE-NW direction, along FIRE 3, the overall crustal structure is asymmetric suggesting extension in simple shear mode (Wernicke 1985; Lister et al., 1991). Both simple and pure shear stress may have coexisted during the extensional event.

The granitoids of the CFGC seems to have intruded the uppermost brittle part of the crust in extensional tectonic setting. The extensional structures may have developed in either active (rift, back-arc) or passive setting (collapse) (Rey et al., 2001). Because the extension is taking place contemporaneous with accretion of the Oskarshamn-Jönköping volcanic belt to the southwestern margin of the Fennoscandian plate, it is suggested that the extension is related to gravitational collapse of the over-thickened Svecofennian crust as previously proposed by Lahtinen et al. 2005.

References

Coward, M.P. 1986. Heterogeneous stretching, simple shear and basin development. Earth and Planetary Science Letters 80: 325-336.

Lahtinen, R., Korja, A. & Nironen, M., 2005. Palaeoproterozoic tectonic evolution. In: Lehtinen, M., Nurmi, P. A. & RÄMÖ, O. T. (eds.) The Precambrian Geology of Finland - Key to the Evolution of the Fennoscandian Shield. Elsevier Science B.V, Amsterdam. pp.418-532.

Lister, G.S., Etheridge, M.A. and Symonds, P.A. 1991. Detachment models for the formation of passive continental margins, Tectonics, 10, 1038-1064.

McKenzie, D., 1978. Some remarks on the development of sedimentary basins. Earth and Planetary Science Letters 40: 25-32.

Meissner, R. 1996. Faults and folds, fact and fiction. Tectonophysics 264: 279-293.

Nironen, M. 2003. Keski-Suomen Granitoidikompleksi, Karttaselitys. Summary: Central Finland Granitoid Complex - Explanation to a map. Geological Survey of Finland, Report of Investigation 157, 45 p.

Rey, P., Vanderhaege, O., Teyssier C., 2001. Gravitational collapse of the continental crust: definition, regimes and modes. Tectonophysics 342: 435-449.

Wernicke, B., 1985. Uniform-sense normal simple shear of the continental lithosphere. Canadian Journal of Earth Sciences 22: 108-125.

POLENET/FI - a multidisciplinary geophysical experiment in Northern Fennoscandia and Antarctica during the International Polar Year 2007-2008

Elena Kozlovskaya[1]*, Markku Poutanen[2] and POLENET/FI colleagues

[1]Sodankylä geophysical observatory/Oulu Unit, POB 3000, FIN-90014, University of Oulu, Finland,
*E-mail: Elena.Kozlovskaya@oulu.fi
[2]Finnish Geodetic Institute, Geodeetinrinne 2, P.O.Box 15, FIN-02431 Masala, Finland,

1. Introduction. International Polar Year 2007-2008

Environmental changes currently observed in Polar Regions are unprecedented in times of modern observation, and there is concern that these rapid changes may continue or even amplify in the coming decades. However, our ability to describe and understand the processes affecting environmental state of the Polar Regions is critically limited by a lack of observations in space and time. Therefore, increasing of multidisciplinary observations in polar region is important for proper understanding these processes.

The First International Polar Year was held in 1882-1883. It was the first international collaborative project aiming to study Polar Regions. During this year an observation station was founded also in Sodankylä (Finland). The next IPY (1932-1933) and the International Geophysical Year (IGY; 1957-1958) produced unprecedented amount of data and new discoveries in many fields of research and fundamentally changed understanding of processes of the polar regions. At present, new technological developments such as information technologies, Earth's observation satellites, autonomous vehicles offer new opportunities for a further understanding of polar systems.

As described in the report by the International Council for Science's (ICSU) IPY Planning Group (Rapley and Bell, 2004), IPY 2007-2008 will be an intense, internationally coordinated campaign that gives expanded attention to the deep relevance of the polar regions to the health of our planet, and serves to establish the ongoing observation systems needed to fully understand the polar regions and their links to the global system. It will include research in both the Arctic and Antarctic, be multi- and interdisciplinary in scope, and be truly international in participation. It will educate and excite the public and help produce the next generation of engineers, scientists, and leaders. A framework such as the IPY can provide the impetus to undertake projects that normally could not be achieved by any single nation.

2. POLENET- Polar Earth Observing Network

POLENET (http://www.ipy.org/development/eoi/proposal-details.php?id=185) -**PO**lar **E**arth Observing **NET**work is a multidisciplinary consortium of activities during the IPY 2007-2009 that aims to dramatically improve the coverage in geodetic, magnetic, and seismic data across the polar regions (both Arctic and Antarctic). The project leader is Prof. Terry Wilson from the Ohio University, USA. The science programme of the POLENET consortium will investigate polar geodynamics, the earth's magnetic field, crust, mantle and core structure and dynamics, and systems-scale interactions of the solid earth, the cryosphere, the oceans and the atmosphere. Activities will be focused on deployment of autonomous observatories at remote sites on the continents and offshore, coordinated with measurements made at permanent station observatories and by satellite campaigns.

Measurements will include GNSS, seismic, gravity (absolute and relative), geomagnetic, tide gauges (at coastal sites), and oceanographic and chemical (at offshore sites). Countries participating in the POLENET are Argentina, Australia, Austria, Belgium, Canada, Chile, Czech Republic, Denmark, Finland, France, Germany, India, Italy, Japan, Luxembourg, New Zealand, Norway, Poland, Russia, Spain, Sweden, Switzerland, South Africa, Ukraine, United Kingdom and United States. The Finnish part of the consortium (POLENET/FI) unites scientists from Finnish Institutions participating in POLENET project (Sodankylä Geophysical Observatory of Oulu University, Finnish Geodetic Institute and Institute of Seismology of Helsinki University). The consortium will concentrate on two topics: POLENET/LAPNET aims a multidisciplinary geophysical experiment in Northern Fennoscandia during IPY and POLENET/GEOD concerns collocated seismic and geodetic measurements in Finland and in Dronning Maud Land, Antarctica.

3. POLENET/GEOD: Collocated seismic and geodetic measurements in Finland and Antarctica

Exploring the core of our planet is essential for understanding the initial differentiation of the Earth, the Earth's thermal history, and the physics and variability of the earth's magnetic field. The inner core shows seismic anisotropy approximately aligned with the earth's rotation pole. Thus seismic phases travelling along polar paths show much smaller travel times than the same phases traversing the inner core along equatorial paths. Observations of polar path seismic waves also suggest that the inner core rotates faster relative to the Earth's mantle and surface at a speed some 100,000 times faster than the drift of continents (Vidale et al., 2000). The phenomenon is caller "differential rotation" of the inner core. Therefore, more detailed observations in polar regions are essential to constrain the distribution of crystal alignment in the inner core and for understanding the dynamics of the core and changes in the Earth's magnetic field.

At present, two main groups of methods are employed for observations of the inner core:

a) methods basing on observations of seismic body waves traveling through the inner core (c.f. Cao et al., 2005)

b) methods based upon quake-driven free oscillations of the planet. These oscillations were previously observed in recordings of strong earthquakes by long-period and broadband seismographs.

Recent developments in superconducting gravimetry provide a new tool to detect free oscillations. This enables study of the processes in the Earth core by mean of multidisciplinary collocated measurements. This has been demonstrated e.g. in connection of the Sumatra-Andamanian earthquake in December 2004 (Park et al, 2005). At present, the effect is at the limit of the method, however, we may expect that in coming years this technique can be used to detect the gravity variations that are partly caused by core convection. GPS measurements have been used in 1 Hz mode to detect large surface movements in the active areas. However, after a major earthquake, the crustal movement is large enough to be detected by a careful spectral analysis on GPS kinematic data in a larger GPS network. Maximum movements can be over 1 cm everywhere on the Earth, as was estimated in connection to the Sumatra-Andamanian case.

The network of permanent seismic stations in Finland consists of 15 broadband (BB) and short-period (SP) stations. The Institute of Seismology of Helsinki University operates 12 stations located primary on the territory of southern Finland. Sodankylä Geophysical

Observatory of Oulu University operates three permanent broadband seismic stations located in the northern part of Finland.
The Finnish Geodetic Institute (FGI) operates 13 permanent GPS stations (CGPS) in Finland, three of which are situated in the vicinity of the SGO broadband seismometer stations OUL, MSF and SGF. The superconducting gravimeter of the FGI is in Metsähovi observatory is collocated with a broadband seismometer of the Institute of Seismology of the University of Helsinki. As the FGI is a member of the Global Geodynamics Network of the superconducting gravimeters, data of the Ny Alesund station on Svalbard will be available. Metsähovi and Ny Alesund are the two Northenmost superconducting gravimeters in the world. Both are also collocated with a CGPS.

Recently defined Nordic Geodetic Observing System (NGOS) as a subset of Global Geodetic Observing System (GGOS) (Poutanen et al, 2005, Beutler et al., 2003) propose absolute gravity measurements to be done on all permanent GPS stations, including the stations mentioned above. As a long-term Nordic co-operation, this will provide a frame for other gravity measurements and a control of temporal changes in gravity and their connection to the postglacial rebound.

Existing GPS, superconducting gravimeter and seismograph stations and satellite observations in Finland and Anctarctica can be used to organize long-term collocated measurements aiming at studying of the inner core within the frame of the POLENET scientific program. In addition, such measurements can be used to study glacial rebound in the Fennoscandian Shield and Antarctica, to improve our current understanding of displacements and stresses for stable cratonic regions and mid-continent deformations and investigate interplate earthquake mechanisms. Since the GPS, gravity measurements and seismic instrumentation share infrastructure, the cost of multidisciplinary observation network is lower than organisation of two separate networks.

4. POLENET/LAPNET- a temporary seismic array research in Northern Fennoscandia during IPY

The POLENET/LAPNET is a sub-project of the POLENET consortium related to POLENET seismic studies in the Arctic regions. POLENET/LAPNET activities will be carried out on the territory of northern Fennoscandia (Finland and Norway). The main target of the POLENET/LAPNET project is to carry out a temporary broadband seismic array research in the area of northern Finland and Norway. The array will consist of 30-35 temporary stations, 3 permanent broadband stations (OUL, SGF and MSF) of Oulu University and two permanent stations (KEV and KIF) operated by the Institute of Seismology of Helsinki University. The array will register teleseismic, regional and local events during 2007-2009. The study will be continuation of the SVEKALAPKO Deep Seismic Tomography project in 1997-1998. The project was carried out by the international team that included researchers from 16 institutions from 9 European countries and Russia (Hjelt and Daily, 1996, Bock et al., 2001). The SVEKALAPKO project resulted in significant scientific output and completely new knowledge about the structure of the upper mantle beneath Finland (Fig.2) (Alinaghi et al., 2003; Sandoval et al. 2003, 2004; Bruneton et al., 2004a,b, Kozlovskaya et al., 2004, Yliniemi et al., 2004, Hjelt et al., 2006, Plomerová et al., 2006, Kozlovskaya et al., submitted).

The research aims to obtain a 3D seismic model of the crust and upper mantle down to 670 km (P- and S-wave velocity models, position of major boundaries in the crust and upper mantle and estimates of seismic anisotropy strength and orientation) in northern

Fennoscandian Shield, in particular, beneath the Arhaean domain of the Fennoscandian Shield. The model will be merged to the seismic model of the previous SVEKALAPKO array research in order to obtain a 3-D model of the crust and upper mantle beneath Finland. The 3-D model can be used to define spatial distribution and depth of the Archaean lithosphere below Finland for the purpose of diamond prospecting. The 3-D model of the crust and upper mantle will be also used to improve registration and location of local earthquakes and understanding of mechanisms of local seismicity in northern Fennoscandia.

The study will also contribute to the POLENET multidisciplinary research in northern Fennoscandia by collecting waveforms of seismic phases travelling through the inner core. The waveform data will be compiled into a database that will be available to world geophysical community via GEOFON Data Center (GeoForschungZentrum Potsdam) and interpreted by different techniques.

References

Alinaghi, A., Bock, G., Kind, R., Hanka, W., Wylegalla, K. & TOR and SVEKALAPKO Working Group 2003. Receiver function analysis of the crust and upper mantle from the North German Basin to the Archaean Baltic Shield, *Geophysical Journal International*, 155, 641 – 652.

Cao, A., Romanowicz, B., Takeuchi, N., 2005. An observation of PKJKP: Inferences on Inner Core Shear Properties. Science, [DOI:10.1126/science.1109134]

Park J., Teh-Ru A. Song, J. Tromp, E. Okal, S. Stein, G. Roult, E. Clevede, G. Laske, H. Kanamori, P. Davis, J. Berger, C. Braitenberg, M. Van Camp, Xiang'e Lei, Heping Sun, Houze Xu, S. Rosat 2005. Earth's Free Oscillations Excited by the 26 December 2004 Sumatra-Andaman Earthquake. Science, vol 308, 1139-1144.

Poutanen M., P. Knudsen, M. Lilje, T. Nørbech, H.-P. Plag, H.-G. Scherneck, 2005. NGOS – The Nordic Geodetic Observing System. Nordic Journal of Surveying and Real Estate Research, accepted.

Beutler G., Drewes H., Reigber C., Rummel, R. (2003): Proposal to establish the Integrated Global Geodetic Observing System (IGGOS) as IAG's First Project. http://www.gfy.ku.dk/~iag/ iggos_prop_june_03.htm.

Bock, G. & SVEKALAPKO Seismic Tomography Working Group 2001. Seismic probing of Fennoscandian lithosphere. EOS, Transactions AGU, 82, 621, 628–629.

Bruneton, M., Farra, V., Pedersen, H. A. & the SVEKALAPKO Seismic Tomography Working Group 2002. Non-linear surface wave phase velocity inversion based on ray theory. Geophysical Journal International, 151, 583–596

Bruneton, M., Pedersen, H.A., Vacher, P., Kukkonen, I.T., Arndt, N.T., Funke, S., Friederich, W., Farra, V., SVEKALAPKO STWG. 2004. Layered lithospheric mantle in the central Baltic Shield from surface waves and xenolith analysis. Earth and Planetary Science Letters, 226, 41-52.

Bruneton, M., H.A. Pedersen, R. Farra, N.T. Arndt, P. Vacher, U. Achauer, A. Alinaghi, J. Ansorge, G. Bock, W. Friederich, M. Grad, A. Guterch, P. Heikkinen, S.E. Hjelt, T.L. Hyvonen, J.P. Ikonen, E. Kissling, K. Komminaho, A. Korja, E. Kozlovskaya, M.V. Nevsky, H. Paulssen, N.I. Pavlenkova, J. Plomerova, T. Raita, O.Y. Riznichenko, R.G. Roberts, S. Sandoval,. I.A. Sanina, N.V. Sharov, Z.H. Shomali, J. Tiikainen, E. Wieland, K. Wylegalla, J. Yliniemi, Y.G. Yurov. 2004. Complex lithospheric structure under the central Baltic Shield from surface wave tomography. Journal of Geophysical Research-Solid Earth, 109 (B10): art.no. B10303. (F)

Hjelt, S-E., Daly, S. & SVEKALAPKO colleagues 1996. SVEKALAPKO. Evolution of Palaeoproterozoic and Archaean Lithosphere. pp. 56 - 67 in Gee, D. & Zeyen, H., (eds): EUROPROBE 1996—Lithosphere Dynamics: Origin and Evolution of Continents, EUROPROBE Secretariate, Uppsala University, p. 138.

Hjelt, S-E., Korja, T., Kozlovskaya, E., Yliniemi, J., Lahti, I., BEAR and SVEKALAPKO Working Groups, 2005. Electrical conductivity and seismic velocity structures of the lithosphere beneath the Fennoscandian Shield. In: D. Gee, R. Stephenson (eds) European Lithosphere Dynamics (in print).

Plomerova, J., Babuska, V., Vecsey, L., Kozlovskaya, E., T. Raita and SVEKALAPKO STWG. 2005. Proterozoic-Archean boundary in the upper mantle of eastern Fennoscandia as seen by seismic anisotropy. Journal of Geodynamics, 41, 4, 369-450.

Vidale, J.E., Dodge, D.A., Earle, P.S. 2000. Slow differential rotation of the Earth's inner core identified by temporal changes in scattering. Nature, 405, 445-448.

Yliniemi, J., Kozlovskaya, E., Hjelt, S-E., Komminaho, K., Ushakov, A. & the SVEKALAPKO Tomography WG 2004. Structure of the crust and uppermost mantle beneath southern Finland revealed by local events registered by the SVEKALAPKO seismic array. Tectonophysics, 394, 41 – 67.

Seismic studies of the upper mantle in the Fennoscandian Shield: main results and perspectives for future research

Elena Kozlovskaya

Sodankylä geophysical observatory/Oulu Unit, POB 3000, FIN-90014, University of Oulu, Finland,
E-mail: Elena.Kozlovskaya@oulu.fi

Main results of seismic studies of the upper mantle in the Fennoscandian Shield are summarized.

Keywords: upper mantle, lithosphere, asthenosphere, seismic studies

1. Introduction

Knowledge of the present-day structure of the Earth's mantle is essential our understanding of plate tectonics and hazards associated with it, as well as of the Earth's thermochemical evolution over long periods of geological time. Several factors including temperature, chemical compositions, presence of the partial melt or water, and anisotropy can influence seismic velocities in the upper mantle; that is why multimethod approach is essential in order to infer its realistic model. A number of different seismic techniques were employed to study the upper mantle beneath the Fennoscandian Shield. Here we present a summary of seismic studies of the upper mantle there, aiming to answer three main questions:

(1) What are the general features of the upper mantle velocity structure beneath the Shield and what is the explanation for seismic velocity anomalies?

(2) Are there any regional seismic boundaries in the upper mantle and what are their origins?

(3) Is there a correlation between seismic structure of the upper mantle and major tectonic units of the Shield?

(4) What is the lithosphere–asthenosphere system beneath different tectonic domains of the Fennoscandian Shield?

2. Structure of the Shield from global seismic tomography models

Over the past two decades, global seismic tomography, a class of inversion techniques for interpreting observations from earthquake records in terms of three-dimensional (3D) variations in Earth's elastic properties, has produced spectacular images of Earth's interior structure**.** Already early studies showed that Precambian cratons, shields, and platforms are marked by fast seismic wave velocities to depths of 200 km (cf. Woodhouse and Dziewonski, 1984). Until a few years ago the results of global tomography were mostly interpreted in terms of spatial variations in temperature. However, it is increasingly evident that a quantitative interpretation of the currently available seismologic and mineral physics data sets cannot be done in the framework of temperature alone and that spatial variations in major element composition must be considered (Trampert and Van der Hilst, 2005). Necessity to get more detailed images of the upper mantle was the motivation for deployment of regional and local passive seismic arrays in different areas of the Earth.

3. Controlled-source seismic experiments

a) Near-vertical reflection profiling. Seismic near-vertical reflection profiling is a major tool to infer structural features in the crust. However, penetration depth of reflection profiling is limited to about 100 km and the method does not provide the velocities in the upper mantle. That is why interpretation of reflection profiling results in terms of upper mantle structure and composition is non-unique. Deep seismic profiling experiments in the main structural provinces within the Shield including Svecofennian, Transscandinavian Igneous Belt, Gothian and Sveconorwegian (BABEL in the Gulf of Bothnia and the Baltic

Sea, Mobil Search in the Skagerrak and MONA LISA in the North Sea) have demonstrated the existence of dipping and sub-horisontal seismic reflectors (down to a depth of 90 km) in the mantle lithosphere beneath the Shield, the Tornquist Zone and the North Sea basins (Balling, 2002). The reflectivity is interpreted to represent fossil, ancient subduction and collison zones with remnant oceanic basaltic crust transformed into eclogite. Another explanation of dipping reflectors beneath the northernmost BABEL profiles was given by Snyder (2002) who proposed that the Archaean block forms a wedge of uppermost mantle rocks embedded in a Proterozoic block and that the Archaean lithosphere is laterally more extensive at depth than at surface.

In 2001-2003 the project FIRE (Finnish Reflection Experiment) comprised four reflection seismic transects crossing the main geological units of the central part of the Fennoscandian shield in Finland (Kukkonen et al., 2006) where the crust is generally very thick. Due to the thick crust, the profiles revealed complicated reflection pattern in the crust and clear Moho boundary in some places, but no dipping and sub-horisontal seismic reflectors in the mantle lithosphere.

b) Wide-angle reflection and refraction profiling. The majority of wide-angle reflection and refraction profiles across the Shield are too short to sample the upper mantle, as they were designed mainly for the purpose of investigating the crust. The studies indicated significant variations of the crustal thickness in the Precambrian parts of the Fennoscandian Shield as well as of sub-Moho P-wave velocities (c.f. Guggisberg and Berthelsen, 1987, Luosto, 1991, 1997, Kozlovskaya et al., 2004). Recently Janik et al. (submitted) re-interpreted previous SVEKA and FENNIA profiles in order to investigate the variations of Vp/Vs ratio on the crust-mantle boundary. The study demonstrated multi-genetic origin and nature of the Moho and different composition of the upper mantle beneath the central and southern parts of the Shield.

The only one long-range FENNOLORA profile of total length of 1900 km in Sweden was a part of the European Geotraverse. The reflected and refracted body waves were observed at offsets up to 1800–2000 km, which made it possible to penetrate the upper mantle up to depths of 200 km. A characteristic feature of the upper mantle model of the profile by) is thin layering with alternation of low velocity and high velocity zones. The more recent model by Pavlenkova and Pavlenkova (2006) clearly shows that the uppermost mantle structure changes from the north to south. The southern part of the profile is characterised by higher velocities beneath the Moho (up to 8.3 km/s). At depths of 80–100 km, a low velocity layer was revealed that corresponds roughly to the low velocity layer identified by Abramovitz et al. (2002). In the northern part of the profile, the uppermost mantle velocities are lower (8.1–8.2 km/s) and there are no clear low velocity layers. The velocities in the depth interval of 100–200 km are nearly constant along the entire profile.

For the central and southern parts of the Shield, Yliniemi *et al.* (2004) presented results of forward raytrace modelling of reflected and refracted P-waves of the strongest local events registered by the SVEKALAPKO array at offsets up to 850 km. They reported two types of mantle reflections: sub-horizontal and gently dipping reflectors below the Moho at a depth of 70-90 km, and phases originating from a depth of 100-130 km. Based on the irregular character of reflectors of the first group, on their different spatial orientation and on a correlation with Moho offsets, they interpreted the boundaries of the first group as relicts of ancient subduction and collision processes. The boundaries of the second group can be explained either by a wedge of Archeaan mantle lithosphere embedded into the Proterozoic mantle or by the lower boundary of the mechanically strong lithosphere. This explanation

is in accord with receiver function study by Alinaghi *et al.* (2003), who did not identify any upper mantle discontinuities except for global ones at 410 km and 660 km. Generally, controlled-source seismic experiments demonstrated that the uppermost mantle is heterogeneous and that the reflectivity in the upper mantle has different origin.

4. Teleseismic array studies: the TOR and SVEKALAPKO projects

Dense 2-D arrays of broadband seismic instruments have proved to be the most effective mean to study the deep mantle (Trampert and Van der Hilst, 2005). In the Fennoscandian Shield two such experiments have been completed.

The main aim of the TOR passive teleseismic array research (1996-1997) was to study the lithospheric–asthenospheric boundary structure under the Sorgenfrei–Tornquist Zone, across northern Germany, Denmark and southern Sweden (Gregersen et al., 1999). The SVEKALAPKO (1998-1999) multidisciplinary passive seismic array research covered the central and southern part of the Shield from 59^0 to 68^0 N and 18^0 to 34^0 E. The study aimed to find the signatures of the Proterozoic-Archaean suture in the upper mantle and to study lithosphere-asthenosphere system beneath the central and southern parts of the Shield (Hjelt et al., 2006).

Results of receiver function studies: Comparison between stacked receiver functions from the TOR (Teleseismic Tomography of TORnquist Zone) and SVEKALAPKO arrays indicates that the difference between arrival times of the converted P410 and P660 phases increases below the Shield due to a cooler upper mantle (Alinaghi et al., 2003). The pronounced asthenosphere beneath central Europe terminates at the southern edge of the Shield and cannot be identified in the SVEKALAPKO data. Altogether the TOR seismic experiment documents a surprisingly sharp boundary of the BS in the upper mantle and the change in crustal thickness across TESZ along the TESZ in Denmark (e.g. Wilde-Piórko *et al.* 1999). The pronounced asthenosphere beneath the approximately 100 km continental lithosphere of west-central Europe abruptly terminates along the Trans-European Suture Zone (TESZ).

Results of high-resolution body-wave tomography: The P- and S-wave velocity models across the TESZ show two sharp and distinct increases in depth to velocities which are low compared to IASP'91 reference model, as one move from South to North (Artlitt et al., 1999, Shomali et al., 2006). The location and sharpness of these boundaries suggests that these features are, at least partially, compositional in origin, presumably related to mantle depletion. A sharp and steep subcrustal boundary is found roughly coincident with the southern edge of Sweden, at the Sorgenfrei–Tornquist Zone. Another less significant transition was recognised more or less beneath the Elbe-lineament.

The major result obtained from the SVEKALAPKO body-wave tomography indicates P- and S-wave velocity variations of up to 4%, as compared with the IASP'91 model (Sandoval et al. 2003, 2004). The positive P-wave velocity anomaly seems to extend down to 300 km, without any indication of an asthenospheric low-velocity layer. This is proved also by surface wave analysis. The Archaean-Proterozoic suture zone has no continuation at upper mantle depths. Instead, a laterally and vertically heterogeneous structure of the subcontinental lithospheric mantle (SCLM) in the contact zone of Archaean and Proterozoic domains beneath the SVEKALAPKO area has been revealed by both teleseismic and local event studies.

Surface wave studies: In spite of long wavelength, surface wave studies have certain advantage over teleseismic body wave tomography, as they allow estimation of the

absolute values of S-wave velocity in the upper mantle that are directly comparable to values estimated by petrophysical studies of upper mantle rocks. The study by Cotte et al. (2002) indentified the the pronounced zone of low S-wave velocity beneath central Europe that can be associated with the asthenosphere. This layer abruptly terminates at the southern edge of the Shield and cannot be identified in the data of the SVEKALAPKO array (Bruneton et al., 2004). Generally, the S-wave velocities beneath the SVEKALAPKO array are higher than beneath the TOR array, which is mainly due to temperature variations. The 3-D S-wave velocity model obtained for the SVEKALAPKO area (Bruneton et al. 2004a) shows both lateral and vertical S-wave velocity variations (+-3%) that can be explained either by variations of composition of upper mantle rocks or by seismic anisotropy.

Seismic anisotropy studies: Anisotropy of seismic velocities can result for various reasons, e.g. from oriented fractures in the upper crust, from alternating layers with different isotropic velocities, or, be due to the alignment of crystals of rock-forming minerals in a stress field. According to the analysis of Plomerová *et al.* (2001, 2002, 2006) the main source of the large-scale anisotropy beneath the Fennoscandian Shield has to be in the upper mantle, caused especially by its large-scale fabric due to preferred orientation of olivine. The anisotropy reflects frozen-in olivine fabrics, most probably created during early stages of the evolution of the European continent. Joint analysis of shear-wave splitting parameters and directional dependence of teleseismic P residuals based on data from the seismic experiment TOR across the Trans-European Suture Zone revealed different lithosphere thickness and different orientation of seismic anisotropy in the mantle lithosphere which identify three domains separated by the STZ between Denmark and southern Sweden and the Thor Suture between northern Germany and Denmark (Babuška and Plomerová, 2004). Anisotropic upper mantle structure was obtained from combined analysis of S-wave splitting parameters and direction-dependent P-wave residuals registered by the SVEKALAPKO array. In particular, strong anisotropy and uniform orientation of anisotropic material in the upper mantle was revealed beneath the Archaean domain. On the contrary, the anisotropic pattern corresponding to the Proterozoic domain (Fig. 11) is more heterogeneous and weakly anisotropic (Plomerová *et al*. 2006, Vescey *et al*. submitted). Both large Archaean and Proterozoic tectonic units of the eastern part of the Shield seem to be composed of several smaller lithospheric domains with different orientation of large-scale mantle fabric that may result from different geological history.

9. Conclusions

1) The Fennoscandian Shield is generally characterized by lower than in standard Earth models seismic velocities. The velocity heterogeneities are most probably explained either by compositional variations or by seismic anisotropy.

2) The most pronounced regional seismic boundaries beneath the Shield are the Moho boundary and global 410 and 660 km discontinuities. The other boundaries in the upper mantle are observed locally and may have different origin.

3) Clear correlation between seismic structure of the upper mantle and surface position of major tectonic boundaries has been revealed in the TESZ. In addition, reflection profiling between inclined upper mantle reflectors (down to 80-90 km) and tectonic sutures in some other areas of the Shield. At the moment, seismic studies did not reveal systematically higher velocities in the upper mantle of the Archean domain than in the Proterozoic domain.

4) The asthenosphere assotiated with low seismic velocities and partially molten rocks abruptly terminates beneath the northen margin of the TESZ. The low velocities associated with partially molten rocks have not been revealed by the SVEKALAPKO study.
It should be noted that the architecture of the Fennoscandian deep lithosphere is not yet completely known, due to inadequate spatial sampling by passive seismic arrays. The SVEKALAPKO and TOR seismic arrays were relatively small compared to the size of the Shield. As a result, the array studies provided detailed images of the upper mantle, but only from several limited regions. Total coverage is therefore required for the detailed understanding of the structure of deep lithosphere/upper mantle of the Shield. Among the most interesting problem remaining is to define the structure and geometry of the transition between the cratonic and oceanic lithosphere and to investigate the effect of realistic lithosphere structure on the processes of isostatic adjustment. On-going interpretation of the data of Swedish National Seismological Network and results of future POLENET/LAPNET passive seismic experiment (Kozlovskaya and Poutanen, this edition) will help to solve this problems.

References

Alinaghi, A., Bock, G., Kind, R., Hanka, W., Wyllegalla,K., TOR and SVEKALAPKO Working Groups. 2003. Receiver function analysis of the crust and upper mantle from the North German Basin to the Archean Baltic Shield. Geoph. J. Int., 155, 641-652.

Arlitt, R., Kissling, E., Ansorge, J. and TOR Working Group. 1999. Three-dimensional crustal structure beneath the TOR array and effects on teleseismic wavefronts. Tectonophysics, 314, 1-3, 309-319.

Babuška, V., Plomerová, J., 2004. Sorgenfrei-Tornquist Zone as the mantle edge of Baltica lithosphere: new evidence from three-dimensional seismic anisotropy. Terra Nova 16, 243-249.

Balling, N., 2000. Deep seismic reflection evidence for ancient subduction and collision zones within the continental lithosphere of northwestern Europe. Tectonophysics, 329, 269-300.

Bruneton, M., Farra, V., Pedersen, H., and the SVEKALAPKO STWG, 2002. Non-linear surface wave phase velocity inversion based on ray theory. Geoph . J. Int., Geoph J. Int.,151, 2, 583-596.

Bruneton, M., Pedersen, H.A., Vacher, P., Kukkonen, I.T., Arndt, N.T., Funke, S., Friederich, W., Farra, V., SVEKALAPKO STWG. 2004. Layered lithospheric mantle in the central Baltic Shield from surface waves and xenolith analysis. Earth and Planetary Science Letters, 226, 41-52.

Bruneton, M., H.A. Pedersen, R. Farra, N.T. Arndt, P. Vacher, U. Achauer, A. Alinaghi, J. Ansorge, G. Bock, W. Friederich, M. Grad, A. Guterch, P. Heikkinen, S.E. Hjelt, T.L. Hyvonen, J.P. Ikonen, E. Kissling, K. Komminaho, A. Korja, E. Kozlovskaya, M.V. Nevsky, H. Paulssen, N.I. Pavlenkova, J. Plomerova, T. Raita, O.Y. Riznichenko, R.G. Roberts, S. Sandoval,. I.A. Sanina, N.V. Sharov, Z.H. Shomali, J. Tiikainen, E. Wieland, K. Wylegalla, J. Yliniemi, Y.G. Yurov. 2004. Complex lithospheric structure under the central Baltic Shield from surface wave tomography. Journal of Geophysical Research-Solid Earth, 109 (B10): art.no. B10303. (F)

Cotte, N., Pedersen, H.A. and TOR Working group, 2002. Sharp contrast in lithospheric structure across the Sorgenfrei-Tornquist Zone as inferred by Rayleigh wave analysis of TOR1 project data. Tectonophysics, 360, 1-4, 75-88.

Gregersen, S., Pedersen, L.B., Roberts, R.G., Shomali, H., Berthelsen, A., Thybo, H., Mosegaard, K., Pedersen, T., Voss, P., Kind, R., Bock, G., Gossler, J., Wylegala, K., Rabbel, W., Woelbern, I., Budweg, M., Busche, H., Korn, M., Hock, S., Guterch, A., Grad, M., Wilde-Piorko, M., Zuchniak, M., Plomerova, J., Ansorge, J.,Kissling, E., Arlitt, R., Waldhauser, F., Ziegler, P., Achauer, U., Pedersen, H., Cotte, N., Paulssen, H., Engdahl, E.R., 1999. Important findings expected from Europe's largest seismic array. Eos Trans. AGU 80 (1 and 6).

Hjelt, S-E., Korja, T., Kozlovskaya, E., Yliniemi, J., Lahti, I., BEAR and SVEKALAPKO Working Groups, 2006. Electrical conductivity and seismic velocity structures of the lithosphere beneath the Fennoscandian Shield. In: D. Gee, R. Stephenson (eds) European Lithosphere Dynamics (in print)

Kozlovskaya, E., Elo, S., Hjelt, S.-E., Yliniemi, J., Pirttijärvi, M., SVEKALAPKO STWG, 2004. 3D density model of the crust of southern and central Finland obtained from joint interpretation of SVEKALAPKO crustal P-wave velocity model and gravity data. Geoph . J. Int., 158, 827-848.

Kukkonen I.T., Heikkinen P., Ekdahl E., Hjelt S.-E., Yliniemi J., Jalkanen E. and FIRE Working Group, 2006. Aquisition and geophysical characteristics of reflection seismic data on FIRE transects, Fennoscandian Shield. In: GTK Special paper "Finnish Reflection experiment (FIRE) 2001-2005, submitted.

Plomerová, J., Arvidsson, R., Babuška, V., Granet, M., Kulhánek, O., Poupinet, G., Šílený, J., 2001. An array study of lithospheric structure across the Protogine zone, Varmland, south-central Sweden - signs of a paleocontinental collision, Tectonophysics 332, 1-21.

Plomerová, J, Babuška, V, Vecsey, L., Kouba, D., TOR Working Group, 2002. Seismic anisotropy of the lithosphere around the Trans-European Suture Zone (TESZ) based on teleseismic body-wave data of the TOR experiment. Tectonophysics 360, 89-114.

Plomerova, J., Babuska, V., Vecsey, L., Kozlovskaya, E., T. Raita and SVEKALAPKO STWG. 2006. Proterozoic-Archean boundary in the upper mantle of eastern Fennoscandia as seen by seismic anisotropy. Journal of Geodynamics, 41, 4, 369-450.

Sandoval, S., Kissling, E., Ansorge, J. and the SVEKALAPKO STWG, 2003. High-Resolution body wave tomography beneath the SVEKALAPKO array: I. A-priori 3D crustal model and associated traveltime effects on teleseismic wavefronts. Geoph . J. Int., 153, 75-87.

Sandoval, S., Kissling, E., Ansorge, J. and the SVEKALAPKO STWG, 2004. High-Resolution body wave tomography beneath the SVEKALAPKO array: II. Anomalous upper mantle structure beneath central Baltic Schield. Geoph . J. Int., 157, 200-214.

Snyder, D. B., 2002. Lithospheric growth at margins of cratons. Tectonophysics, 355, 1-4, 7-22.

Trampert, J., Vander Hilst, R.D. 2005. Towards a Quantitative Interpretation of Global Seismic Tomography. In: Earth's Deep Mantle: Structure, Composition, and Evolution. AGU Geophysical Monograph Series, 160.

Yliniemi, J., Kozlovskaya, E., Hjelt, S.-E., Komminaho, K., Ushakov, A. and SVEKALAPKO Seismic Tomography Working Group. 2004. Structure of the crust and uppermost mantle beneath southern Finland revealed by analysis of local events registered by the SVEKALAPKO seismic array. Tectonophysics, 394, 41-67.

Vecsey, L., Plomerova, J., Kozlovskaya, E., Babuska, V. 2006. Shear-wave splitting as a diagnostic of varying upper mantle structure beneath eastern Fennoscandia. Tectonophysics, submitted.

Wilde-Piorko, M., Grad, M. and POLONAISE Working Group. 1999. Regional and teleseismic events recorded across the TESZ during POLONAISE'97, Tectonophysics, 314, 1-3, 161-174.

Woodhouse, J. H. and A. M. Dziewonski,1984. Mapping the upper mantle: Three dimensional modelling of Earth structure by inversion of seismic waveforms, J. Geophys. Res, 89, 5953–5986.

Composition of the crust and upper mantle derived from joint inversion of receiver function and surface wave phase velocity of SVEKALAPKO teleseismic records

Elena Kozlovskaya[1], Grigoriy Kosarev[2], Igor Aleshin[2], Jukka Yliniemi[1], Oksana Riznichenko[2] and Irina Sanina[3]

[1]Sodankylä Geophysical Observatory/Oulu Unit, University of Oulu, Finland
[2]Institute of Physics of the Earth RAS, Moscow, Russia
[3]Institute of Geospheres Dynamics RAS, Moscow, Russia

1. Introduction

In the 80-90th of the last century the Earth's crust and upper mantle of the Fennoscandian Shield has been intensively studied by controlled-source seismic experiments (CSS). They indicated significant variations of the thickness and structure of the crust in the central part of the Shield and showed that the latter is essentially three-dimensional one. The CSS experiments also demonstrated that the Moho boundary is not always easily detectable by the methods based upon interpretation of P-waves (e.g. near vertical reflection profiling and wide-angle reflection and refraction experiments). The problem can be solved if combined analysis of both P- and S-wave reflections in the wide-angle data is used (Janik et al., submitted). Such interpretation provides also the variations of Vp/Vs ratio that are used to derive compositional variations in the crust and upper mantle and different types of crust-mantle transition. Another method of the determination of the crust-mantle boundary and Vp/Vs ratio in the crust is usage of teleseismic P- to S- converted waves (P-wave receiver functions). The method was used by Bock et al. (2001) and Alinaghi et al. (2003) to determined the Moho depth and spatial variations of averaged Vp/Vs ratio within the crust beneath the central Fennoscandian Shield. However, the teleseismic P-wave receiver functions alone cannot be used to evaluate variations of S-wave velocities with depth and to obtain detailed structure of the crust. The problem can be solved if P-wave receiver functions are interpreted together with other data sets (Vinnik et al., 2004).

2. Method

We made inversion of P-receiver functions of 30 broadband SVEKALAPKO stations (including RUKSA small aperture array in Russian Karelia) jointly with Rayleigh phase velocities, determined by Bruneton et al. (2004), and Ps traveltimes from the 410- and 660-km discontinuities and constructed 3D S-wave velocity model from 1D velocity distributions under BB stations. The technique makes it possible to estimate absolute values of S-wave velocity in the crust and upper mantle that are directly comparable to values estimated by studies on rock samples.

3. Results

a) Crustal structure. the S-wave velocity model revealed several low S-wave velocity anomalies in the uppermost crust (down to 2 km) that correlate with the Kainuu shist belts within the Archean Domain and with Pirkkala shist belt in the Proterozoic domain). Archean granitoids, Proterozoic Central Finland Granitoid complex (CFGC) and Wyborg rapakivi batholith have generally higher S-wave velocities, while Proterozoic shists and migmatites generally have lower S-wave velocities in the upper crust. In the middle crust

the model shows a number of higher and low velocity heterogeneities; however, not all of them can be correlated with the surface geology. At a depth of 30 km the most pronounced feature is a NS stretching high S-wave velocity zone below the Outokumpu area (OA), Kuhmo Greenstone Belt (KB) and Kainuu Shist Belt (KSB).

b) The Moho boundary. To define the depth to the Moho boundary from 1-D velocity models, we used the following criteria selected on the base of analysis of previous wide-angle profiles (Janik et al., submitted): first, the Vp should be more than 8.0 km/s, second, the Vs should be more than 4.5 km/s. The maximum crustal thickness of 64 km occurs beneath the CFGC, which is in agreement with the result by Alinaghi et al. (2006). A secondary maximum trough, with crustal thickness up to 60 km, stretches along the OA, KB and KSB.

c) S-wave velocities in the upper mantle. The absolute values of S-wave velocities in the upper mantle at a depth of 66-72 km generally vary from 4.6 km/s to 4.8 km/s. Our result does not show systematically higher velocities beneath Archean Domain. The area with highest velocities (up to 4.8 km/s) is seen to the both sides of the surface trace of Archean and Prorerozoic domains. The area is limited from the East by the KB. These velocities agree with the value estimated from highly depleted lherzolite and harzburgite xenoliths from eastern Finland (Kukkonen *et al.* 2003, Bruneton *et al.* 2004). The lowes S-wave velocities in the Proterozoic domain are found beneath the western part of CFGC, with agrees with the result by Bruneton et al. (2004).

d) Analysis of Vp/Vs ratio in the high-velocity lower crust (HVLC) and upper mantle. In order to infer compositional changes at the crust-mantle boundary, we compared S-wave velocity models and Vp/Vs ratio to pertophysical data about seismic velocities in main types of lower crustal and upper mantle rocks. Our analysis shows two types of the HVLC corresponding to mafic garnet granulites and eclogites, which are present both in Archean and Proterozoic domains. This agrees also with results by Janik et al (submitted). The most interesting feature in the upper mantle is a zone of high Vp/Vs stretching from the OA along the KB and KB. We interpret these high Vp/Vs values as corresponding to eclogites, because upper mantle peridotites have generally low Vp/Vs ratio.

References

Alinaghi, A., Bock, G., Kind, R., Hanka, W., Wylegalla, K, TOR and SVEKALAPKO Working Groups, 2003. Receiver function analysis of the crust and upper mantle from the North German Basin to the Archaean Baltic Shield. Geoph. J. Int., 155, 641-652.

Bock, G. & SVEKALAPKO Seismic Tomography Working Group 2001. Seismic probing of Fennoscandian lithosphere. EOS, Transactions AGU, 82, 621, 628–629.

Bruneton, M., H.A. Pedersen, R. Farra, N.T. Arndt, P. Vacher, U. Achauer, A. Alinaghi, J. Ansorge, G. Bock, W. Friederich, M. Grad, A. Guterch, P. Heikkinen, S.E. Hjelt, T.L. Hyvonen, J.P. Ikonen, E. Kissling, K. Komminaho, A. Korja, E. Kozlovskaya, M.V. Nevsky, H. Paulssen, N.I. Pavlenkova, J. Plomerova, T. Raita, O.Y. Riznichenko, R.G. Roberts, S. Sandoval,. I.A. Sanina, N.V. Sharov, Z.H. Shomali, J. Tiikainen, E. Wieland, K. Wylegalla, J. Yliniemi, Y.G. Yurov. 2004. Complex lithospheric structure under the central Baltic Shield from surface wave tomography. Journal of Geophysical Research-Solid Earth, 109 (B10): art.no. B10303. (F)

Janik, T., Kozlovskaya, E., Yliniemi, J. 2006. Crust-mantle boundary in the central Fennoscandian shield: constraints from wide-angle P- and S-wave velocity models and new results of reflection profiling in Finland. J. Geoph. Res., submitted.

Luosto, U. 1991. Moho depth map of the Fennoscandian Shield based opn seismic refraction data. pp. 43 - 49 in Korhonen, H. & Lipponen, A. (eds.): Structure and dynamics of the Fennoscandian lithosphere. Institute of Seismology, University of Helsinki, Report S-25.

Sandoval, S., Kissling, E., Ansorge, J. & the SSTWG, 2003. High-resolution body wave tomo-graphy beneath the SVEKALAPKO array. I. A priori 3D crustal model and associated travel time effcets on teleseismic wave fronts. Geophysical Journal International, 153, 75 - 87.

Vinnik, L.P., Reigber, C. Aleshin, I.M., Kosarev, G.L., Kaban, M., Oreshin, S.I. and Roecker, S.W. 2004. Receiver function tomography of the central Tien Shan, EPSL, 225, 131-146.

Modelling the thermal evolution of a Precambrian orogen: high heat production migmatitic granites of southern Finland

I.T. Kukkonen[1]* and L.S. Lauri[2]

[1]Geological Survey of Finland, P.O. Box 96, FI-02151 Espoo, Finland
[2]Department of Geology, P.O. Box 64, FI-00014 University of Helsinki, Finland
*E-mail: ilmo.kukkonen@gtk.fi

We present results of geochemical and thermal modelling of southern Finland, which is characterized by high heat production migmatitic granites. Our results suggest that the thermal evolution of the study area can be modelled as a process of crustal thicknening in a plate collision at ca. 1860 Ma ago, followed by conductive heating of the crust. Applying heat production values constrained by geochemical data in southern Finland, and a relatively low mantle heat flow, temperatures at 30-50 km depths exceed the wet solidus of metasediments about 10-30 Ma after the collision. The results explain the high temperature-low pressure metamorphism in southern Finland as a natural consequence of the crustal thicknening (at least 60 km), which resulted in increased total heat production of the crust and lead to higher temperatures during the orogeny.

Keywords: Paleoproterozoic, Svecofennian, Finland, modelling, heat sources, U, Th, migmatite

1. Introduction

Thermal evolution of a Paleoproterozoic orogen is a difficult modelling target. The events that took place close to 2 Ga ago have left traces that are few and of limited extent. Rocks at the present surface level have been equilibrated at depths of 10-25 km and important geological evidence may have been swept away by exhumation processes. Further, the validity of the present-day tectonic processes as analogues in modelling the Paleoproterozoic orogens may be questioned due to higher Paleoproterozoic mantle temperatures, higher buoyancy of plates, and higher radiogenic heat production. A typical problem in modelling the thermal evolution of a Precambrian orogen is how to constrain the heat sources that drive the high temperature-low pressure metamorphism and contribute to the origin of the high heat production granitoids.

In this study we have investigated the thermal evolution of southern Finland, which was affected by the Svecofennian orogeny at 1.89–1.87 Ga and experienced another granite and migmatite-forming phase at 1.85–1.79 Ga. In southern Finland the metamorphic peak is of the high temperature but relatively low pressure type (e.g., *Korsman et al., 1984; Väisänen et al., 2002; Mouri et al., 2005*). On the present surface level most of the rocks record amphibolite facies conditions (4–5 kbar, 650–700 °C), but granulite facies rocks are also found (6 kbar, up to 800 °C). Considerable crustal thickening took place in this area at about 1.87-1.85 Ga ago, possibly as a result of collision(s) and thrusting of arc-type crustal plates (e.g., *Nironen, 1997; Korsman et al., 1999; Nironen et al., 2002*). These processes induced heating and partial melting in middle and lower crust, generating an extensive belt of migmatitic K-rich granitoids with high radiogenic heat production rate (average 3.1 μW m^{-3}). The 1.85–1.79 Ga late orogenic granites of southern Finland are typical examples of anatectic granites found in continental collision zones. They occur as migmatizing dikes and xenolith-bearing granite masses of varying sizes in a ca. 150 km wide zone that extends from the Åland archipelago in the west to the Puruvesi area in the east. The granites are peraluminous with A/CNK values > 1.0, but not all of them are S-type as defined by *Chappell and White (1974)*. The variation in the geochemical composition of

these granites suggests that they were derived from multiple sources, i.e. via partial melting of both metasedimentary (pelitic and quartzofeldspathic) and meta-igneous rocks, a plausible scenario based on melting experiments (see e.g., *Johannes and Holtz, 1996* and references therein).

2. Geochemical modelling

The late orogenic granites of southern Finland are enriched in heat-producing elements (U, Th, K) compared to the average upper crustal values (2.7 ppm U and 9.6 ppm Th; *Rogers and Adams, 1969*). For modelling purposes we have divided the late orogenic granites into "I-type" (A/CNK < 1.1) and "S-type" (A/CNK > 1.1) groups that may reflect the source, i.e. the I-type group was derived from quartzofeldspathic material that may have been volcanic in origin and the S-type group was derived from pelitic sedimentary material. The average whole rock contents of U and Th are 8.2 ppm and 21.0 ppm in the I-type group and 5.0 ppm and 10.8 ppm in the S-type group (Table 1; *GTK Lithogeochemistry Database*). The corresponding average values for the potential source rocks are 2.6 ppm U and 8.5 ppm Th in felsic synorogenic granitoids, 3.4 ppm U and 10.9 ppm Th in felsic synorogenic volcanic rocks and 2.9 ppm U and 11.9 ppm Th in metasedimentary rocks (Table 1). Accessory minerals such as zircon, monazite and apatite incorporate U and Th in their lattice. These values can be calculated to evaluate how much U is situated outside the lattice of these refractory accessory minerals and thus easily incorporated into anatectic melts (Table 1; see also *Friedrich et al., 1987*). The amount of Th outside the lattice of the refractory accessory minerals is harder to estimate, so in this study it is assumed that all Th that isn't incorporated in zircon and apatite is bound to monazite. This assumption may not be altogether realistic if the rock contains also allanite, however, in peraluminous, low-Ca granites such as the late orogenic granites of southern Finland monazite is more stable than allanite (e.g., *Cuney and Friedrich, 1987*).

Table 1. Average U and Th contents in rock types of southern Finland

U and Th content/ppm	Felsic syn-orogenic granitoids		Felsic volcanic rocks		Sedimentary rocks		I-type late orogenic granites		S-type late orogenic granites	
	U	Th	U	Th	U	Th	U	Th	U	Th
Whole rock	2.6	8.5	3.4	10.9	2.9	11.9	8.2	21.0	5.0	10.8
Zircon	0.2	0.1	0.3	0.2	0.2	0.1	0.2	0.2	0.3	0.1
Monazite	0.5	8.0	0.6	10.5	0.7	11.5	1.2	20.6	0.6	10.4
Apatite	0.2	0.4	0.1	0.3	0.2	0.3	0.1	0.1	0.1	0.3
In refractory accessories	0.9		1.0		1.1		1.7		1.0	
Easily leachable	1.7		2.4		1.8		6.5		4.2	
Th/U	3.3		3.2		4.1		2.6		2.2	

It is assumed here that all mobile U, accounting for 2/3 of the total whole-rock U, enters the first melt in a system undergoing partial melting and is subsequently diluted when the melting progresses. In addition, 50% of zircon present in the source is melted, adding 0.1 to 0.15 ppm U in the mobile U budget. Melting of monazite is assumed to add another 0.2 ppm U in the mobile U budget. The behaviour of Th in partial melting is harder to

constrain, but based on Th/U ratios of the potential source rocks and the granites it is assumed that 40 % of Th present in the source enters the first melt and is subsequently diluted in the partial melting process. If a maximum of 20% partial melting is assumed, based on modelling of *Stålfors and Ehlers (2006)* on the late orogenic granites of Nauvo and Hämeenlinna, U contents exceeding 10 ppm and Th contents exceeding 20 ppm are easily obtained by partial melting of Svecofennian synorogenic rock types.

3. Thermal modelling of plate collisions

We have modelled the thermal consequences of crustal thickening in a plate collision. The colliding plates may have represented arc-type or continental-type of crust. In the models we start from simple plates (crust 30 km thick) with the upper crust comprising sediments, volcanic rocks and synorogenic granitoids. The lower crust has a mafic (basaltic) composition, and the upper mantle is naturally ultramafic. By stacking 10-20 km thick pieces of such crust and calculating the subsequent thermal evolution of the stack we can model the Svecofennian orogen in southern Finland. The thickening of crust leads to uplift and erosion, which are included in the models. On one hand, stacking increases the total crustal heat production, but on the other hand, erosion effectively removes heat sources from the system. The mutual relationship of these processes is a key factor affecting the pT evolution of the crust. Our models are 1-dimensional conductive numerical simulations, which were calculated using the finite difference code *Processing Shemat* (*Clauser, 2003*). Temperature in the stack was calculated at 5 Ma intervals.

The crustal heating can be attributed to several factors. The most important ones are crustal heat production, differentiation of crustal heat sources by partial melting, upward transport of melts, latent heat of melts, original and final thicknesses of the crustal stack, applied exhumation rate, and mantle heat flow density.

Modelling results of a crustal stack are shown in Fig. 1. Immediately after collision the crust was up to 60 km thick. The applied heat production values correspond to present-day concentrations of U, Th and K (but corrected for the higher values at 1.9-1.8 Ga ago). Modelling results indicate that temperatures up to 600-850 ºC are achieved at 30-50 km depths about 10-30 Ma after the collision. Such temperatures are above the solidus of wet (down-thrusted) sediments and volcanic rocks and also dehydration melting temperatures of micas are exceeded. Intrusion of melts to the upper-middle crust (15-30 km depth) transports heat producing elements upwards, and together with the latent heat of the melts provides an extra source of heat resulting in a higher amphibolite facies – granulite facies metamorphic conditions.

A critical issue in modelling is to correctly select the heat production values in the produced melt and restite. These depend on the source rock composition, the proportion of melt produced and the fraction of heat producing elements ending in the melts. Uranium is very mobile and we can estimate that about two thirds of it is lost to a granitic melt extracted from a metasedimentary source rock (20% melting assumed), whereas Th and K are much more conservative, and much smaller fractions of these elements enter the melt phase. Exact data is not available, but we estimate that about 15 % of Th and 30 % of K would enter the melt. The fractioning between melt and restite is an important factor controlling the final distribution of heat production in the crust and the thermal development of crust.

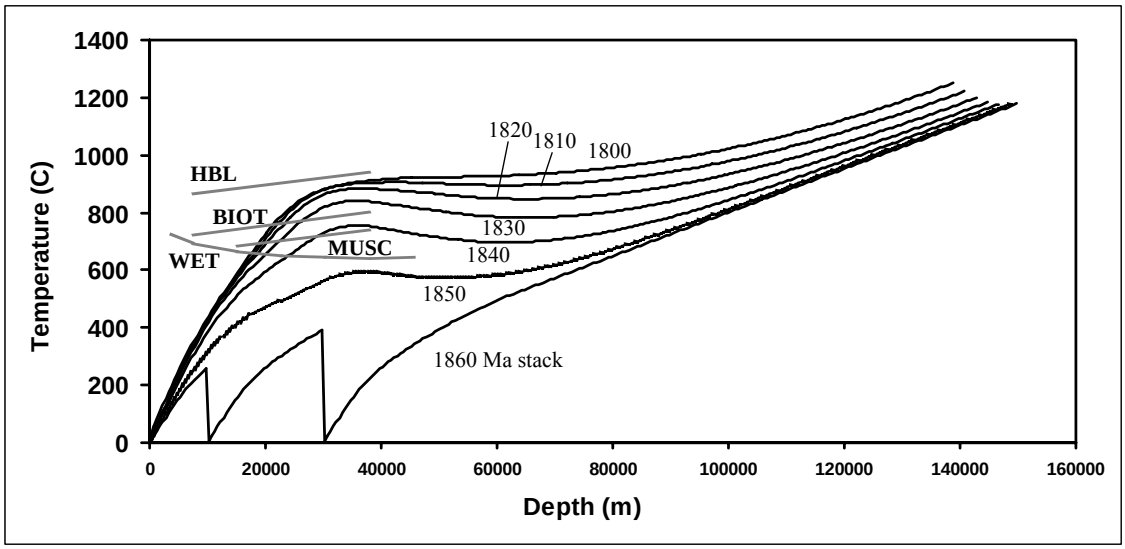

Figure 1. An example of modelling the thermal evolution of southern Finland between 1860 Ma and 1800 Ma. A thick crust (60 km) is formed at 1860 Ma by collisional stacking. The stacked layers inherit their original geotherms. Subsequent heating of the crust takes place by conductive heat transfer, and the main heat sources are the radiogenic heat from U, Th and K and the mantle heat flow (18 mW m^{-2}). Heat production values were constrained by geochemical data, and an exhumation rate of 1 km/5 Ma was applied. The curve 'WET' represents the wet solidus of metasediments, and 'MUSC', 'BIOT' and 'HBL' the onset of dehydration melting of muscovite, biotite and hornblende, respectively. The model results indicate that temperatures sufficiently high to generate granitic melts are easily achieved about 10-30 Ma after collision.

4. Conclusions

The model discussed here is able to explain the thermal evolution of southern Finland due to a collisional thrusting event, which took place at about 1860-1870 Ma ago. The major factor responsible of crustal heating and generation of the migmatitic granites is the increase of the total heat production of the crust due to collisional stacking.

Applying heat production values constrained by geochemical data in southern Finland, and a relatively low mantle heat flow, temperatures at 30-50 km depths exceed the wet solidus of metasediments about 10-30 Ma after the collision. The results explain the high temperature-low pressure metamorphism in southern Finland as a natural consequence of the crustal thickening (at least 60 km), which resulted in increased total heat production of the crust and higher temperatures during the orogeny.

References

Chappell, B.W., White, A.J.R., 1974. Two contrasting granite types. *Pacific Geol. 8, 173–174.*

Clauser, C. (ed.), 2003. Numerical simulation of reactive flow in hot aquifers. Springer, Berlin, 332 p.

Cuney, M., Friedrich, M., 1987. Physicochemical and crystal-chemical controls on accessory mineral paragenesis in granitoids: implications for uranium metallogenesis. Bull. Mineral. 110, 235–247.

Friedrich, M.H., Cuney, M., Poty, B., 1987. Uranium Geochemistry in Peraluminous Leucogranites. Uranium, 3, 353–385.

Johannes, W., Holtz, F., 1996. Petrogenesis and Experimental Petrology of Granitic Rocks. Springer-Verlag, Berlin, Germany, 335 p.

Korsman, K., Hölttä, P., Hautala, T., Wasenius, P., 1984. Metamorphism as an indicator of evolution and structure of crust in eastern Finland. Geol. Surv. Finland, Bull. 397.

Korsman, K., Korja, T., Pajunen, M., Virransalo, P. & GGT/SVEKA Working Group, 1999. The GGT/SVEKA transect: structure and evolution of the continental crust in the Paleoproterozoic Svecofennian orogen in Finland. Int'l Geol. Rev. 41, 287–333.

Mouri, H., Väisänen, M., Huhma, H., Korsman, K., 2005. Sm–Nd garnet and U–Pb monazite dating of high-grade metamorphism and crustal melting in the West Uusimaa area, southern Finland. GFF 127, 123–128.

Nironen, M., 1997. The Svecofennian Orogen: a tectonic model. Precambrian Res. 86, 21–44.

Nironen, M., Lahtinen, R., Korja, A., 2002. Paleoproterozoic Tectonic Evolution of the Fennoscandian Shield – Comparison to Modern Analogues. Institute of Seismology, University of Helsinki, Rep. S–42, 95–97.

Rogers, J.J.W., Adams, J.A.S., 1969. Geochemistry of uranium. In: Wedepohl, K.H. (Ed.), Handbook of Geochemistry, Sect. II, 5. Springer, Berlin, pp. 92E1–92E5.

Stålfors, T., Ehlers, C., 2006. Emplacement mechanisms of late-orogenic granites: structural and geochemical evidence from southern Finland. Int. J. Earth Sci. 95, 557–568.

Väisänen, M., Mänttäri, I., Hölttä, P., 2002. Svecofennian magmatic and metamorphic evolution in southwestern Finland as revealed by U-Pb zircon SIMS geochronology. Precambrian Res. 116, 111–127.

Geochemistry of coherent andesites at Palvajärvi, Paleoproterozoic Tampere Belt, southern Finland: evidence for alteration, petrogenesis and tectonic setting

Yrjö Kähkönen

Department of Geology, P.O. Box 64, FI-00014 University of Helsinki, Finland
Email: yrjo.kahkonen@helsinki.fi

Thirty four samples from seven coherent andesite units (ca. 1.89 Ga) distinguished at Palvajärvi, Tampere Belt, were analysed for major and trace elements with XRF and ICP-MS methods. The units show largely similar geochemical characteristics but there are also differences. The LIL elements have been mobile in post-depositional processes. The variation in the composition is largely controlled by fractional crystallization. There seem to have been differences in the sources of partial melting or in the degree of partial melting. The results substantiate the idea that the bulk of the Tampere Belt volcanism took place at an active continental margin rather than in an immature oceanic arc. In studies concerning geochemistry of ancient volcanic rocks, high-quality determinations on immobile trace elements have a key position.

Keywords: Proterozoic, geochemistry, alteration, subduction, andesite, Tampere, Palvajärvi

1. Introduction

Geochemistry of metamorphosed volcanic rocks provides means for their classification and discussion on their petrogenesis as well as clues to the tectonic setting of eruption. However, mobility of major and trace elements during weathering, hydrothermal processes, and metamorphism is possible and may result in significant compositional changes and erroneous interpretations. In particular, LIL elements (K, Rb, Ba, Sr) are well known for their mobility whereas elements such as REE, Y, Th, Ta, Nb Ti, Zr, and Hf are less mobile or practically immobile.

This paper briefly considers selected geochemical aspects of a set of 34 medium-grade andesitic samples from the Paleoproterozoic Tampere belt, southern Finland, which have been analysed for major and trace elements. The results show considerable mobility of LIL elements and emphasize the importance of high-quality immobile element determinations as an integral part of studies concerning geochemistry of ancient volcanic rocks.

2. Geological setting

The Tampere Belt (Fig. 1) lies in the centre of the Svecofennian domain of Finland and Sweden, which evidently developed by growth and accretion of volcanic arc systems some 2.0-1.9 Ga ago. The Tampere Belt is one of the best-preserved Svecofennian volcanic-sedimentary belts and was mainly metamorphosed in low-T amphibolite to greenschist/amphibolite facies conditions. It is mainly composed of 1.905-1.89 Ga volcanic and related sedimentary rocks that were probably deposited in a setting of volcanic arc but the belt also contains slightly older turbidites as well as a unit characterized by EMORB-like pillow basalts, which seems to stratigraphically underlie the turbidites (*Kähkönen, 2005*). The migmatitic Pirkanmaa belt (also known as the Vammala belt) to the south is interpreted to represent the subduction complex of this arc system.

Structurally, the central part of the Tampere belt is characterised by a major synform/syncline with a mainly E-W trending hinge zone, subhorizontal fold axis,

subvertical axial planes, and deeply plunging stretching lineation. The 6-7 km thick succession in the southern limb shows evolution from submarine fan environments to partly subaerial volcanic-dominated environments. The upper part is characterized by the 2 to 2.5 km thick Pulesjärvi-Kolunkylä Complex (ca. 1.89 Ga), which consists of essentially coherent andesitic units interlayered with pyro- and volcaniclastic strata.

In the Palvajärvi profile, seven essentially coherent andesitic units have been identified in the Pulesjärvi-Kolunkylä Complex. The units are up to ~0.5 km thick and principally consist of plagioclase ± uralite (originally pyroxene) porphyritic rocks. Although mainly coherent, the units, particularly at their upper and lower margins, show fragmental features that in many cases can be interpreted as globular peperites formed in situ by magma/wet sediment interaction (see, e.g., Skilling et al., 2002).

3. Samples and analytical methods

After a petrographic study, 34 samples were selected for analyses that were performed at the Geoanalytical Laboratory of the Washington State University, Pullman, USA. The major elements and a part of trace elements were determined by XRF and a part of trace elements by ICP-MS.

4. Major and trace element geochemistry

The analysed rocks are mainly high-K to shoshonitic andesites and basaltic andesites (Figure 2) or, according to the Zr/Ti vs. Nb/Y diagram, basalts, basaltic andesites, andesites and trachyandesites (*Kähkönen, 2004*). The K_2O vs. SiO_2 trend slopes positively but is widely dispersed. Similarly, the K_2O vs. Zr diagram (Figure 3) shows wide variation from the generally positive trend. Instead, the dispersion in the Th vs. Zr diagram is minor (Figure 4); the same concerns, e.g., LREE vs. Zr diagrams with a few exceptions (figures not shown). The general trend in the Cr vs. Zr diagram is subvertical (Figure 5) whereas the Eu:Eu* ratio decreases slightly with increasing Zr contents (*Kähkönen, 2004*). The P_2O_5 vs. Zr trend is convex upward with a P_2O_5 maximum at ca. 130 ppm Zr (*ibid.*).

In the Ti vs. Zr diagram the Palvajärvi andesites fall in the field of arc lavas and in the NMORB-normalized multielement variation diagrams they show depletions in Ta and Nb typical of subduction-related magmas (*Kähkönen, 2004*). According to the Th/Yb vs. Ta/Yb diagram, a setting of an active continental margin is more probable than that of an immature oceanic island arc (Figure 6).

5. Discussion

The wide dispersion from a linear trend in the K_2O vs. Zr diagram, compared with the limited dispersion in the Th vs. Zr diagram, indicates that potassium (and other LIL elements) was mobile during post-depositional processes. Once again, classifications based on LIL elements should be used with care. However, although compositional changes are pronounced in individual samples, the general idea of a high-K to shoshonitic character of the Palvajärvi andesites, based on Figure 2, seems justified according to the immobile trace element data.

The increase in Th, the steep decrease in Cr, and the decrease in Eu:Eu* with increasing Zr are evidently controlled by fractional crystallisation of mafic phases and plagioclase. The primary magmas were possibly formed as partial melts of the mantle. The convex-upward P_2O_5 vs. Zr trend indicates fractionation of apatite at late stages.

A more detailed examination of Figure 5 suggests differences between certain units. As compared with the other Palvajärvi andesites with similar Cr contents, the rocks of the two uppermost units (F and G) tend to be lower in zirconium. Therefore, the Palvajärvi andesites are not strictly comagmatic and there may be differences in the sources or degree of partial melting. It is also evident that indentification of these differences requires a tight stratigraphic control during sampling and numerous high-quality trace element determinations on the andesite units.

Conclusions

The seven coherent andesite units distinguished in the Pulesjärvi-Kolunkylä Complex at Palvajärvi show largely similar geochemical characteristics but there are also differences. The variation in the composition is largely controlled by fractional crystallization. The LIL elements have been mobile in post-depositional processes and compositional changes have been pronounced in individual samples. The Palvajärvi andesites are not strictly comagmatic but show differences either in the sources of or in the degree of partial melting. These differences were identified by a tight stratigraphic control during sampling and sufficient amount of high-quality trace element determinations. The Palvajärvi andesites were formed in an active continental margin rather than in an immature island arc.

Acknowledgements

This study was significantly supported by a grant from the Finnish Cultural Foundation.

References

Kähkönen, Y., 1989. Geochemistry and petrology of the metavolcanic rocks of the early Proterozoic Tampere Schist Belt, southern Finland. *Geological Survey of Finland, Bulletin* **345**, 104 p.

Kähkönen, Y., 2004. Subduction-related volcanism in the Paleoproterozoic Tampere belt, southern Finland: evidence from the Palvajärvi area. IAVCEI General Assembly 2004, Pucón – Chile, November 14-19. Abstracts, s07a_pt_078 [CD-ROM].

Kähkönen, Y., 2005. Svecofennian supracrustal rocks. In: Lehtinen, M., Nurmi, P. and Rämö, T. (eds.), Precambrian Bedrock of Finland Key to the Evolution of the Fennoscandian Shield. Elsevier, Amsterdam, 343-406.

Le Maitre, R.W. (ed.), 1989. A Classification of Igneous Rocks and Glossary of Terms. Blackwell, Oxford. 193 p.

Skilling, I.P., White, J.D.L. and McPhie, J., 2002. Peperite: a review of magma-sediment mingling. Journal of Volcanology and Geothermal Research 114, 1-17.

Pearce, J., 1983. Role of subcontinental lithosphere in magma genesis at active continental margins. In: Hawkesworth, C.J. and Norry, M.J. (eds.) Continental Basalts and Mantle Xenoliths. Shiva, 230-249.

Pearce, J.A., 1996. A User's guide to basalt discrimination diagrams. Geological Association of Canada, Short Course Notes 12, 79-113.

Tatsumi, Y. and Eggins, S., 1995. Subduction Zone Magmatism. Blackwell, Cambridge. 211 p.

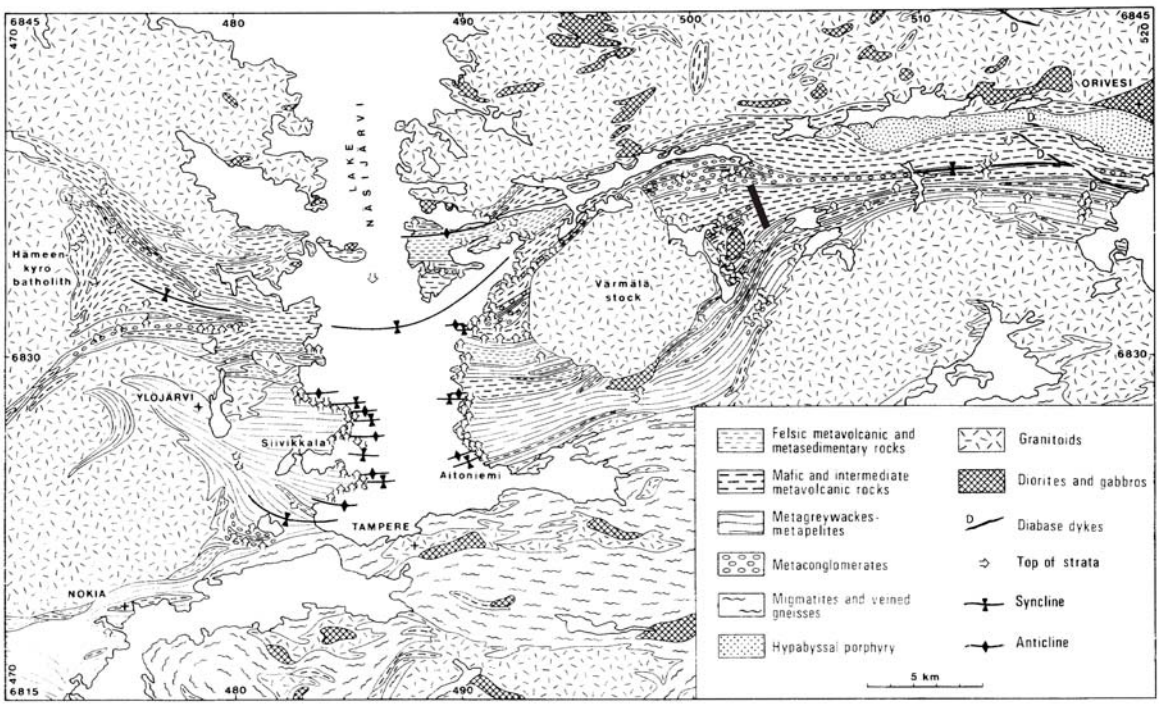

Figure 1. Lithological map of the central Tampere belt with top of strata observations and a simplified structural interpretation. Slightly modified from Kähkönen (*1989*). The thick black line east of the Värmälä stock shows the sampled part of the Palvajärvi profile.

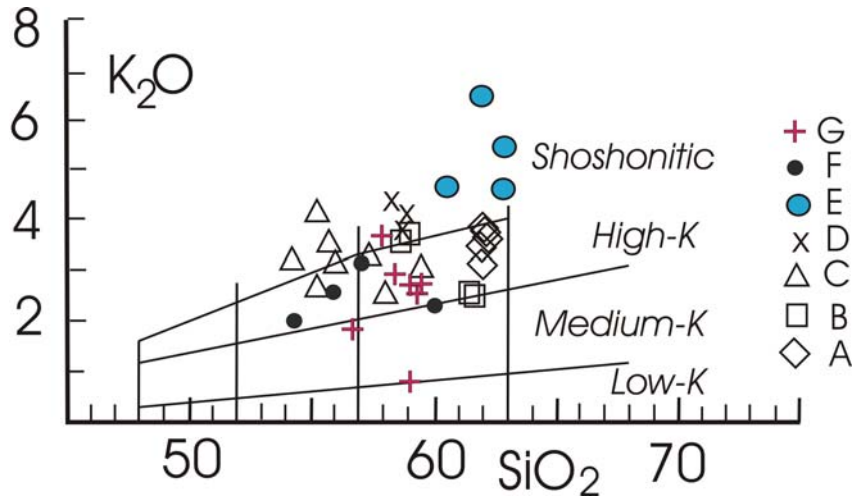

Figure 2. K_2O vs. SiO_2 diagram of the Palvajärvi andesites. The two lower field boundaries are from Le Maitre et al. (*1989*), the uppermost one has been simplified from Tatsumi and Eggins (*1995*). A to F with symbols of the units: A is the lowermost and F the uppermost unit.

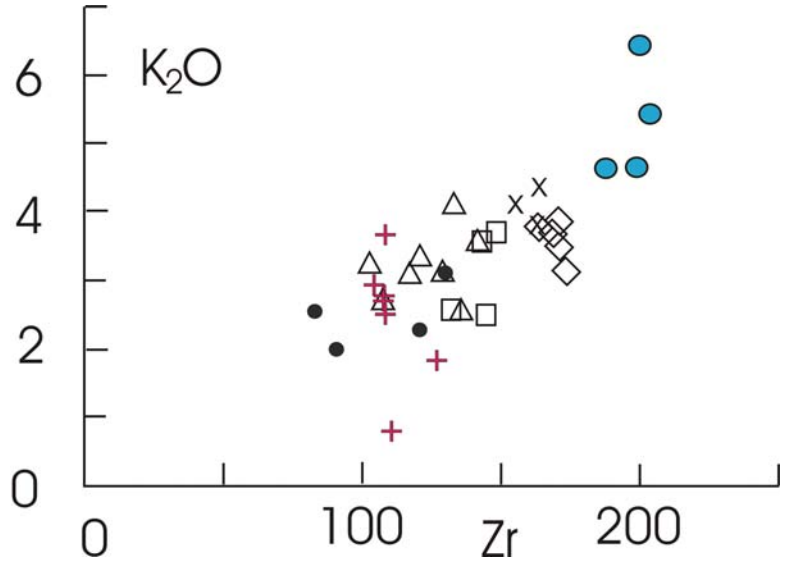

Figure 3. K_2O vs. Zr diagram of the Palvajärvi andesites. Unit symbols as in Figure 3.

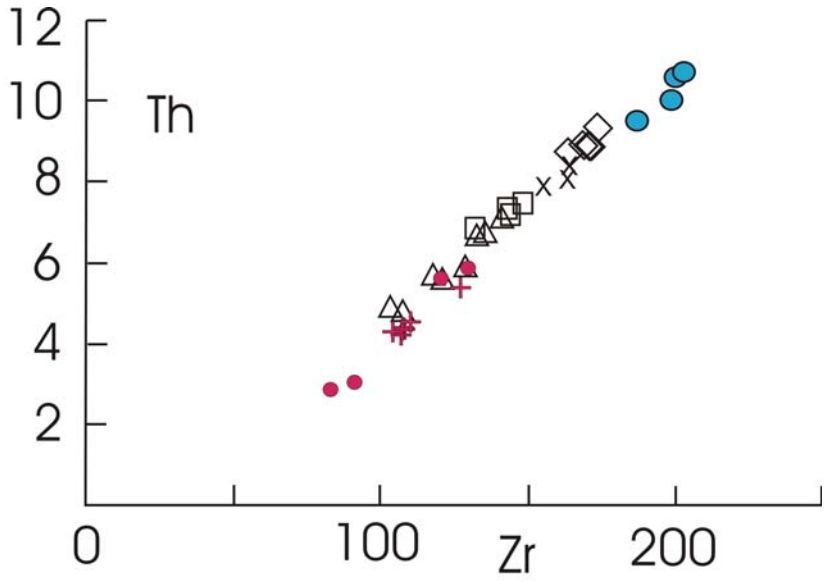

Figure 4. Th vs. Zr diagram of the Palvajärvi andesites. Unit symbols as in Figure 3.

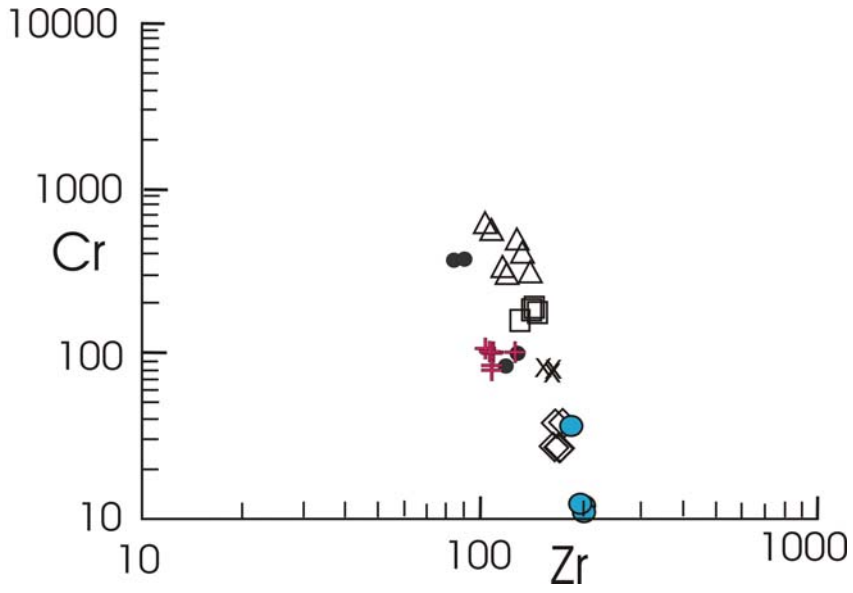

Figure 5. Cr vs. Zr diagram of the Palvajärvi andesites. Unit symbols as in Figure 3.

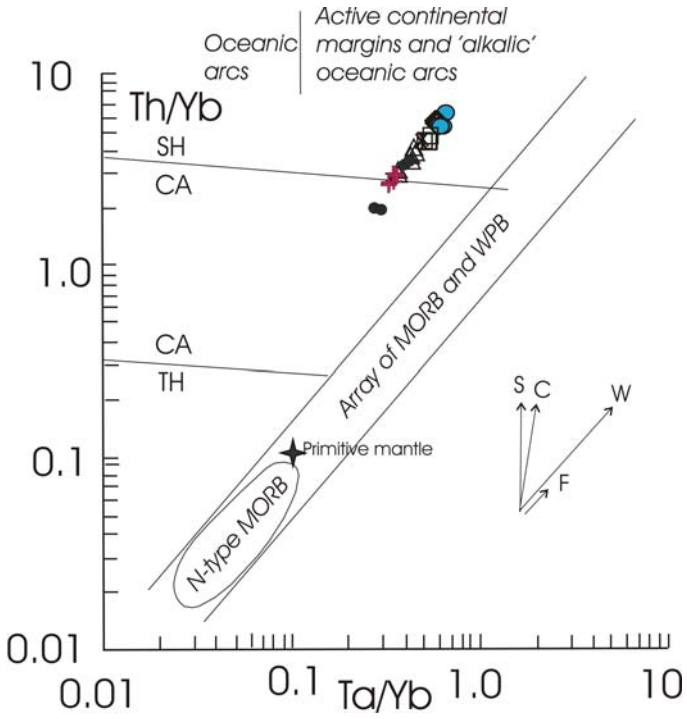

Figure 6. Th/Yb vs. Ta/Yb diagram of the Palvajärvi andesites. Unit symbols as in Figure 3. The fields and vectors from Pearce (*1983*); s = subduction zone enrichment, c = crustal contamination, w = within plate enrichment, f = fractional crystallization (for F = 0.5).

Continent formation: the Fennoscandian perspective

Raimo Lahtinen[1]*, Annakaisa Korja[2] and Mikko Nironen[1]

[1]Geological Survey of Finland POB 96, FIN-02151 Espoo, Finland
[2]Institute of Seismology, POB 68, FIN-00014 University of Helsinki, Finland
*Email: raimo.lahtinen@gtk.fi

The Archaean Karelian Craton of the Fennoscandian Shield is dominantly Neoarchaean in age (2.8-2.6 Ga) and cratonized at 2.6 Ga but the preceding continental evolution is not known. The main lateral growth of Fennoscandia occurred at 1.9-1.8 Ga ago and included amalgamation of several microcontinents (2.1-2.0 Ga) and island arcs (2.0-1.83 Ga). The complexity of this stage can be compared with the future squeezing of the Indonesian archipelago between Eurasia and Australia.

Keywords: Fennoscandia, crustal growth, Precambrian, lithosphere

1. Continents

Continents are portions of the Earth's crust characterized by a stable platform of Precambrian metamorphic and igneous rock, which extend laterally as submarine continental shelf (~ 30% of total continental area). The continental crust extends vertically down to the Moho and coupled with the lithospheric mantle (subcontinental lithospheric mantle – SCLM) moves across the Earth´s surface as a plate. The continental crust is normally divided seismically into upper, middle and lower crust. Sometimes, however, the lower crust has abnormally high velocities (> 7.3 km/s) in its basal parts under continents and at the continent-ocean transition zone. The continental crust constitutes only ~ 0.6% of the silicate Earth but it is the major reservoir of the Earth`s incompatible elements, enriched in the upper crust. The upper crust is considered to be formed due to intracrustal differentiation including partial melting, crystal fractionation and mixing. The overall Nb depletion of the average crust indicates a major contribution from subduction processes. Subduction processes bring basaltic magmas to the base of the crust. Since overall composition of the whole crust is not basaltic it needs a return of mafic and ultra-mafic component into the convecting mantle. Crustal growth models vary between main growth of continental crust in the Archean and progressively or stepwise crustal growth through time.

Most scientists agree that modern-type plate tectonics have been operating at least since Neoproterozoic. Crustal growth since then has been dominated by convergent margin volcanism and related magmatism balanced by recycling through sediment subduction, subduction erosion, and delamination. Accretionary orogens increase continental crust laterally with arc-arc collisions, growth of accretionary wedges in the fore arc (oceanic plateaus, sediments etc), and extension and sedimentation in the back arc. Collisional orogenesis involves continent-arc/continent collision that stitches two continents into one and is often associated with magmatic underplating leading to formation of high velocity lower crust and a felsic input into the upper crust. Plume magmatism produces mafic input both in the lower crust and onto the surface, and can also cause felsic magmatism by partial melting of the lower crust. Anyhow, the net crustal mass input from (Meso-)Neoproterozoic to present appears to be only 10-20% or less.

There is still a controversy about when plate tectonics started but subduction-type processes may have started to operate in Neoarchean or as early as 3.8 Ga ago. A major issue is how the exponential decline of Earth's radiogenic heat production has affected the formation and evolution of continental crust and the style of plate interaction. Altogether, the Archean Earth was different from modern Earth, and the tectonic interactions between segments of lithosphere have been affected by secular changes due to cooling. It has been suggested that the continental crust generated during the Archean is more mafic in overall composition than younger crust. Seismic data, on the contrary, suggest that the Archean middle and lower crust is more felsic than its Proterozoic and Phanerozoic counterparts.

The overall felsic nature of the Archean crust, with the voluminous TTG-suite rocks, characteristic to Archean, indicates large amounts of recycling of mafic residue to the mantle. Possible mechanisms for this recycling include a) delamination of eclogitic residue, after melting of basaltic lower crust, or b) flat-subduction and melting of the slab with recycling of the slab residue into the mantle. The first model implies "diapiric" extension and collapse leading to vertical dome-and-keel structures, characteristic for many Archean areas. This model indicates that most of the lower and middle crust would have been molten during collapse and, thus, would record mainly structures related to younger post-cooling events. The second model implies both horizontal and vertical structures and at least partly crystalline lower and middle crust. All in all, models explaining the formation of the Archean continental crust should also explain the formation of the thick, depleted Archean lithospheric mantle, has it formed by stacking, growing above or growing from below?

2. Fennoscandian perspective

The Fennoscandian Shield is composed dominantly of Archean rocks in the east and Paleoproterozoic rocks in the central and southern part. Mesoproterozoic arc-related rocks are found in the SW and anorogenic rocks of similar age in the central part (not discussed). The Paleoproterozoic orogenic evolution (1.92-1.79 Ga) for the Fennoscandia includes five orogenies: Lapland-Kola, Lapland-Savo, Svecofennian, Svecobaltic and Nordic orogenies. The four latter ones are part of the Svecofennian orogeny or orogenic cycle. Orogenic collapse and stabilization of Fennoscandia between 1.79 and 1.77 Ga were followed by the Gothian evolution at the southwestern margin of the newly formed continent at 1.73-1.55 Ga.

The following pre-1.92 Ga components within the Fennoscandia are identified: Karelian, Kola and Norrbotten Archean age cratons; Keitele, Bergslagen and Bothnia >2.0 Ga age microcontinents; Kittilä ~2.0 Ga island arc; and Savo, Knaften, Inari and Tersk ~1.95 Ga island arcs. The Archean Norbotten and Kola cratons are not discussed here. The Archean Karelian craton, nucleus for the Fennoscandia, exemplified a long period of rifting between 2.5 and 2.1 Ga leading finally to continental break-up at 2.06 Ga. The part of the Karelian Craton crosscut by the FIRE reflection lines can be divided into three main domains. In the east is the non-stretched Archean core and to the west, in the Archean-Proterozoic boundary zone, the stretched Archean craton margin and its cover. The latter area shows effects of both Paleoproterozoic rifting and passive margin formation, and thin to thick-skin style deformation due to continent-continent collision during Lapland-Savo orogeny. The third area covers the central Lapland part of the Karelian craton, characterized by a failed rift with a prolonged Paleoproterozoic history.

The Archean Karelian Craton is dominantly Neoarchean (2.6-2.8 Ga) in age but some older (3.0-3.5 Ga) ages have been found, especially at the western edge of the craton. The overall exhumation level is rather deep and represented by amphibolite- to granulite-facies high-grade complexes, characterized by TTG gneisses and granitoids. Within the gneiss terranes there are also remnants of lower metamorphic grade in a few small, narrow and shallow greenstone belts. The thin greenstone belts show often steeply dipping structures whereas more gently dipping structures characterizes the high-grade complexes.

The Archean crustal evolution of the Karelian craton remains still unresolved and both oceanic plateau and island arc accretion models are viable; maybe they both operated at the same time. The widely occurring and overprinting 2.63 Ga metamorphism, possibly related to structural exhumation, suggests that both the Archean crust and the lithospheric mantle stabilized at 2.6 Ga. The 240 km thick lithosphere of the non-stretched part of the Karelian craton suggests similar thickness for the whole Karelian craton before Paleoproterozoic, although the mechanism for the formation of this thick lithosphere is not known.

Between 2.45-1.98 Ga the majority of the Paleoproterozoic crustal additions to the Karelian crust have been mafic intrusions, sills and dykes occurring widely in the Karelian craton. Mafic magmatisms at 2.45-2.1 Ga have been related to mantle plumes but some magmas show a convective mantle signature. Lateral additions include sedimentary rocks and the Kittilä 2.0 Ga juvenile arc thrust on the Karelian craton during the Lapland-Savo orogeny. At the Archean-Proterozoic boundary zone the Karelian margin has been involved in a crustal "crocodile structure" where Paleoproterozoic material was both obducted on to the margin and subducted beneath it. Lateral accretion of the Keitele microcontinent and Savo arc to the Karelian margin resulted in thickening of the crust+lithospheric mantle in an Archean-Proterozoic continent-arc/continent collision zone. Magmatic additions during 1.87-1.79 Ga to the Karelian craton margin include enriched-type mafic magmas from the sub-continental lithospheric mantle and felsic magmas dominantly from the Archean lower crust.

The Svecofennian Orogen is one of the largest Paleoproterozoic orogens in the world covering over 1 mill. km^2. The main growth of Fennoscandia occurred during multiple orogenic evolution of the Svecofennian orogeny or orogenic cycle at 1.9-1.8 Ga. The major lateral growth of the Fennoscandia at ~ 1.9 Ga involved ~2.0 Ga microcontinents and 2.0-1.95 Ga island arcs. For example the Keitele microcontinent seems to have been 25-35 km thick before crustal scale duplexing during Lapland-Savo orogen. Both the Fennian and Svecobaltic orogenies have further modified the Keitele microcontinent. The juvenile 1.95-1.90 Ga parts of the Svecofennian domain include arc terranes and accretionary wedges as imaged on the BABEL and FIRE profiles. The stabilization of the continent has-started in the central part of the Archean-Proterozoic boundary zone at 1.87 Ga and final stabilization in the outboard areas has occurred at 1.79-1.77 Ga. A stable cratonic platform has formed between 1.79 and 1.6 Ga.

A noticeable feature is that the sub-continental lithospheric mantle below the Paleoproterozoic in the central part of the Svecofennian domain is also very thick (total thickness of lithosphere ~ 240 km) and seems to correlate with the large crustal thickness, e.g in the Keitele microcontinent and Archean-Proterozoic boundary zone. Preliminary data on 1.90 – 1.87 Ga age mafic magmatism indicate a non-convective mantle origin favouring sub-continental lithospheric mantle source. Thus, we propose that in addition to crustal duplexing, also lithospheric mantle duplexing has occurred. This implies crust-mantle decoupling; both crust and mantle act as stiff bodies during lithosphere-scale stacking.

Petrology of the Svecofennian late orogenic granites with emphasis on the distribution of uranium

Lauri, L.S.[1]*, Cuney, M.[2], Rämö, O.T.[1], Brouand, M.[2] and Lahtinen, R.[3]

[1]Department of Geology, P.O. Box 64, FI-00014 University of Helsinki, Finland
[2]CNRS–CREGU, BP 23, 54501 Vandoeuvre, France
[3]Geological Survey of Finland, P.O. Box 96, FI-02151 Espoo, Finland
*E-mail: laura.lauri@helsinki.fi

The 1.85–1.79 Ga Svecofennian late orogenic granites of southern Finland constitute a positive overall anomaly in radiometric maps and are known to host some uneconomic U deposits. The granites are peraluminous and leucocratic, and they show considerable petrographic variation. Major minerals are K-feldspar, plagioclase, quartz, and biotite, common accessories include garnet, cordierite, zircon, monazite, magnetite, hematite, uraninite, and uranothorite. Geochemically, the granites classify as syn-collisional and volcanic arc granites indicating variable metasedimentary to igneous sources. Isotope geological studies indicate that the source or sources may have been enriched in U and that post-crystallization processes did not markedly disturb the isotope systematics.

Keywords: Finland, Svecofennian, uranium, Pb isotopes, Nd isotopes, Sr isotopes

1. Introduction

The Arc complex of southern Finland (*e.g., Korsman et al., 1997*) represents a magmatic arc ~1.90–1.87 Ga in age that was accreted to the present central Finland during the Svecofennian orogeny at ~1.88 Ga (*e.g., Lahtinen and Huhma, 1997; Nironen, 1997*). The arc complex is depicted as a 150–200 km wide EW-trending zone through southern Finland (Fig. 1). The arc complex of southern Finland is characterized by migmatizing leucogranites (”microcline granites”) that are 1.85–1.79 Ga in age, and thus late orogenic in respect to the main Svecofennian deformation (*e.g., Ehlers et al., 1993; Kurhila et al., 2005; Rämö et al., 2005*). This granite and migmatite-forming event coincides with low-P, high-T metamorphism, including also granulite facies domains, in southern Finland (*e.g., Korsman et al., 1984; Van Duin, 1992; Väisänen et al., 2002; Kurhila et al., 2005*; *Mouri et al., 2005*). Whether there was a causal connection between granite genesis and granulite facies metamorphism is still unknown. The granites form regional positive anomalies in U- and Th-radiation maps and also show somewhat elevated contents of U and Th in the whole rock analyses. Many previously known, thus far uneconomic, U deposits are found within these granites (e.g., Palmottu, Käldö and Junninsuo).

2. Petrography and whole-rock geochemistry

In the outcrop the late orogenic granites vary from thin veins and dikes within migmatitic supracrustal rocks to large, relatively homogeneous batholiths of igneous appearance. Compared to U-bearing granites worldwide, the granites seem relatively little altered but in microscopical scale the rocks commonly show signs of deformation and brittle fracturing associated with hydrothermal alteration (e.g., silicification, episyenitization). Major minerals in the late orogenic granites are K-feldspar, quartz, and plagioclase. The feldspars may be present as euhedral phenocrysts in which case the rock has a porphyritic appearance, but equigranular types are also common. K-feldspar probably crystallized initially as orthoclase, but most crystals are now microcline. Plagioclase occurs both as subhedral to euhedral crystals and in the form of anhedral, hydrothermal albite that has

replaced the rims of the phenocrysts and fills fractures. Quartz and feldspars commonly form micrographic and myrmekitic intergrowth textures. The most common mafic silicate is biotite. Muscovite, garnet, cordierite, and tourmaline are also found. Magmatic U-bearing accessory minerals include apatite, zircon, monazite, allanite, uraninite, and uranothorite. Common opaque minerals are magnetite, hematite, and sulphides. Rutile needles are commonly found within biotite crystals. Alteration products and metamorphic minerals like epidote, clinozoisite, sericite, chlorite and Fe-hydroxide (goethite) are common. Some samples contain carbonate minerals, sillimanite and fluorite.

SiO_2 values in the lateorogenic granites vary mostly from 68 wt% to 76 wt%, although altered samples may show values both lower and higher than these. The granites are peraluminous (Fig. 2), however, a major part of the samples falls below A/CNK=1.1, thus showing that these granites are not strongly peraluminous or uniformly S-type (as defined by Chappell and White, 1974). At least some of them may have been derived from I-type sources. K_2O/Na_2O varies from 0.2 to 4.4. Some samples have high contents of K_2O (7-9 wt.%), which, coupled with the low SiO_2 values, suggest that these samples have suffered from leaching of silica (episyenitization). In most of the samples, $MgO+FeO+TiO_2$ values are low – those with higher values of Fe may indicate the presence of restitic garnet and biotite. Trace elements show scattered values similar to the variation seen in some major elements. Ba varies between 20 and 4160 ppm, Nb between 0.1 and 270 ppm, Rb between 6 and 440 ppm, Sr between 15 and 1000 ppm, Y between 1 and 128 ppm, and Zr between 3 and 1244 ppm. In granite classification diagrams based on trace elements the lateorogenic granites fall into the fields of collisional granites and island arc granites (Fig. 3), possibly also reflecting the igneous to sedimentary source variation. Also A-type affinity has been suggested for some plutons (Jurvanen et al., 2005). Most samples show some fractionation of LREE from HREE and a negative Eu anomaly (Eu/Eu*). The few samples with a positive Eu anomaly may represent eutectic in situ melts of the host gneisses. U and Th values vary from <1 ppm in unmineralized to >1000 ppm in mineralized samples. The samples with higher U show Th/U values <<4, suggesting that uraninite (or its secondaries), rather than monazite, may be the dominant uraniferous phase.

3. Isotope geology

Whole-rock samples of granites analysed for Nd isotopes show an outstandingly large variation in Sm and Nd concentrations and $^{147}Sm/^{144}Nd$ ratios. The initial ε_{Nd} values (at 1830 Ma) fall into three groups (Fig. 4a). The first group shows slightly negative initial ε_{Nd} values (ca. –1 to 0) that are consistent with published values from the late orogenic granites all over the province (e.g., *Kurhila et al., 2005; Mouri et al., 2005; see also Rämö et al., 2005*). In the second group, the initial ε_{Nd} values are slightly more negative and cluster around –2.5, possibly indicating a stronger metasedimentary component in the source. The third group consists of samples with disturbed Nd isotope systematics (Fig. 4a). The T_{DM} model ages (after *DePaolo, 1981*) are on the order of 2.3-2.5 Ga, save for samples with anomalous (beyond chondritic) $^{147}Sm/^{144}Nd$ ratios. On a Sm-Nd isochron diagram, five samples with similar ε_{Nd} values define a trend corresponding to an age of 1836±41 Ma (Fig.4b). This suggests that the Sm-Nd system in these granites has remained closed since their crystallization ~1830 Ma ago.

In the Rb-Sr space, Sr isotope data on plagioclase and apatite fractions extracted from the mineralized granites define a trend corresponding to a poorly defined age of 1782±120 Ma, yet compatible with the overall crystallization age of the granites. Apatite fractions have

varying Rb/Sr ratios ($^{87}Rb/^{86}Sr$ 0.4 to 8) and their initial (at 1830 Ma) $^{87}Sr/^{86}Sr$ values (0.7040–0.7096) point to the involvement of crustal material in their petrogenesis.
Pb isotope composition of meticulously leached K-feldspar fractions separated from the granites implies very high and extremely varying uranogenic Pb isotope ratios with $^{206}Pb/^{204}Pb$ between 16 and 24 and $^{207}Pb/^{204}Pb$ between 15.4 and 16.8. In contrast, the thorogenic ratio $^{208}Pb/^{204}Pb$ is almost constant around 35.5. Uranogenic Pb isotope ratios corrected for in situ radiogenic growth since 1830 Ma do not correlate with Pb concentrations (60-135 ppm) or U/Pb ratios (0.0007–0.0137) of the leached feldspar fractions. These observations imply that the magmas from which the feldspars crystallized may have been variably enriched in uranogenic Pb and were derived from a high-U/Th source.

References

Chappell, B.W., White, A.J.R., 1974. Two contrasting granite types. *Pacific Geol. 8, 173–174.*

Debon, F., Le Fort, P., 1982. A chemical-mineralogical classification of common plutonic rocks and associations. Transactions of the Royal Society of Edinburgh: Earth Sciences, vol.73(3), 135–149.

DePaolo, D.J., 1981. Neodymium isotopes in the Colorado Front Range and crust-mantle evolution in the Proterozoic. Nature 291, 684–687.

DePaolo, D.J., Wasserburg, G.J., 1976. Nd isotopic variations and petrogenetic models. Geophys. Res. Lett. 3, 249–252.

Ehlers, C., Lindroos, A., Selonen, O., 1993. The late Svecofennian granite-migmatite zone of southern Finland – a belt of transpressive deformation and granite emplacement. Precambrian Res. 64, 295–309.

Jurvanen, T., Eklund, O., Väisänen, M., 2005. Generation of A-type granitic melts during the late Svecofennian metamorphism in southern Finland. GFF vol. 127, 139–147.

Korsman, K., Hölttä, P., Hautala, T., Wasenius, P., 1984. Metamorphism as an indicator of evolution and structure of the crust in Eastern Finland. Geol. Surv. Finland, Bull. 328.

Korsman, K., Koistinen, T., Kohonen, J., Wennerström, M., Ekdahl, E., Honkamo, M., Idman, H., Pekkala, Y. (Eds.), 1997. Suomen kallioperäkartta – Bedrock map of Finland 1:1 000 000. Espoo: Geol. Surv. Finland.

Kurhila, M.I., Vaasjoki, M., Mänttäri, I., Rämö, O.T., Nironen, M., 2005. U–Pb ages and Nd isotope characteristics of the lateorogenic, migmatizing microcline granites in southwestern Finland. Bull. Geol. Soc. Finland, 77, 105–128.

Lahtinen, R., Huhma, H., 1997. Isotopic and geochemical constraints on the evolution of the 1.93–1.79 Ga Svecofennian crust and mantle in Finland. Precambrian Res. 82, 13–34.

Mouri, H., Väisänen, M., Huhma, H., Korsman, K., 2005. Sm–Nd garnet and U–Pb monazite dating of high-grade metamorphism and crustal melting in the West Uusimaa area, southern Finland. GFF 127, 123–128.

Nironen, M., 1997. The Svecofennian orogen: a tectonic model. Precambrian Res. 86, 21–44.

Pearce, J.A., Harris, N.B.W., Tindle, A.G., 1984. Trace element discrimination diagrams for the tectonic interpretation of granitic rocks. J. Petrol. 25, 956–983.

Rämö, O.T., Halla, J., Nironen, M., Lauri, L.S., Kurhila, M.I., Käpyaho, A., Sorjonen-Ward, P., Äikäs, O., 2005. EUROGRANITES 2005—Proterozoic and Archean Granites and Related Rocks of the Finnish Precambrian.Eurogranites 2005 Field Conference, September 11–17, 2005. Publications of the Department of Geology A1, 130 p.

Väisänen, M., Mänttäri, I., Hölttä, P., 2002. Svecofennian magmatic and metamorphic evolution in southwestern Finland as revealed by U-Pb zircon SIMS geochronology. Precambrian Res. 116, 111–127.

Van Duin, J.A., 1992. The Turku granulite area, SW Finland: a fluid-absent Svecofennian granulite occurrence. Ph.D. Thesis, Vrije Universiteit, Amsterdam, 234 p.

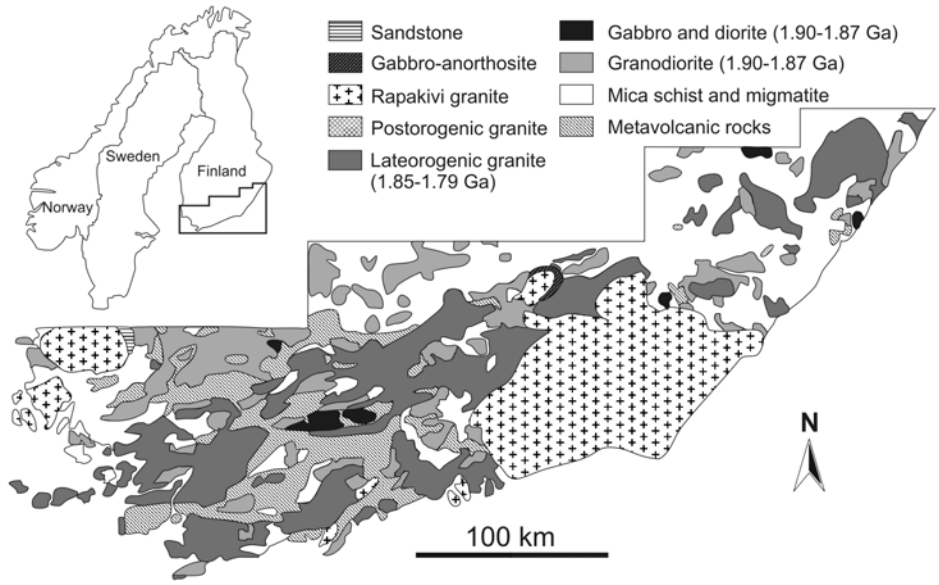

Figure 1. Geologic map of southern Finland. Modified after *Korsman et al. (1997)* and *Rämö et al. (2005)*.

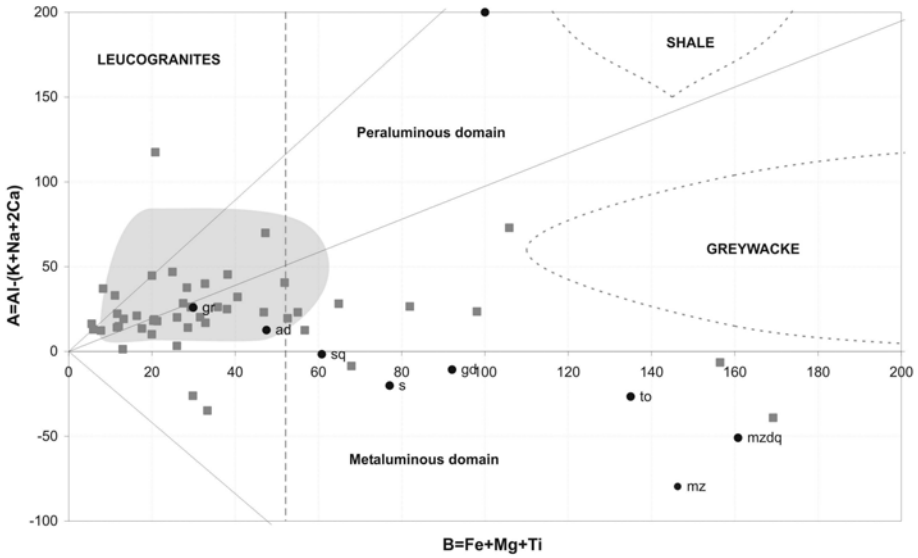

Figure 2. A vs. B diagram (*Debon and Le Fort, 1982*) of the late orogenic granite samples (squares = new samples, gray field = samples from the GTK Lithogeochemistry Database).

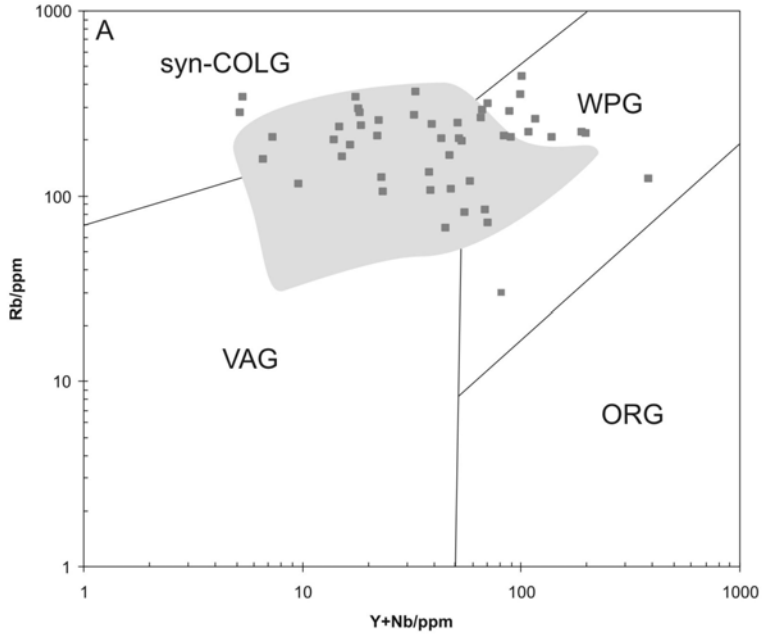

Figure 3. Late orogenic granites plotted into the granite classification diagram of *Pearce et al., (1984)*. VAG = volcanic arc granites, WPG = within-plate granites, syn-COLG = syn-collisional granites, ORG = ocean ridge granites.

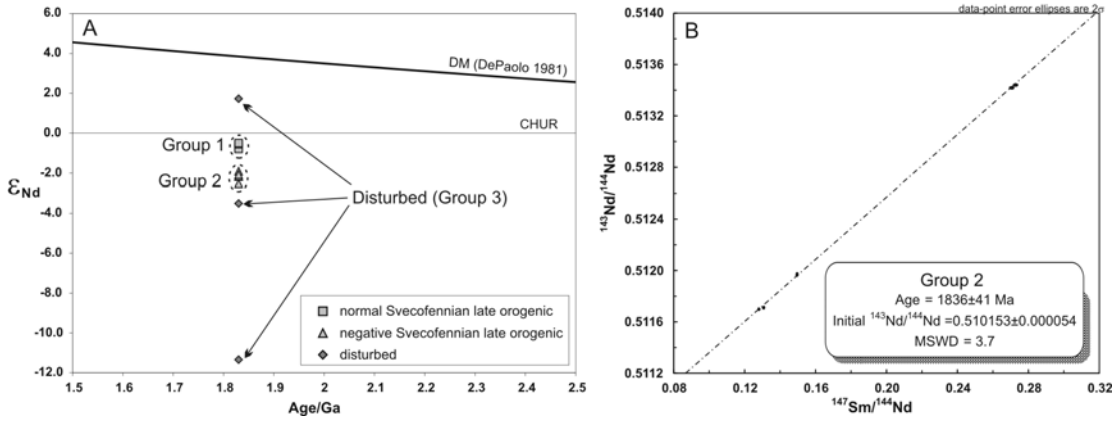

Figure 4. (A) ε_{Nd} vs. age diagram for the late orogenic granites. DM = depleted mantle (*DePaolo, 1981*), CHUR = Chondritic Uniform Reservoir (*DePaolo and Wasserburg, 1976*), (b) Sm-Nd errorchron defined by five samples with initial ε_{Nd} val

Neoarchean growth of the Karelian craton: New evidence from U–Pb and Lu–Hf isotopes in zircons

L.S. Lauri[1]*, T. Andersen[2], P. Hölttä[3], H. Huhma[3] and S. Graham[2]

[1]Department of Geology, P.O. Box 64, FI-00014 University of Helsinki, Finland
[2]Department of Geosciences, University of Oslo, P.O. Box 1047 Blindern, N-0316 Oslo, Norway
[3]Geological Survey of Finland, P.O. Box 96, FI-02151 Espoo, Finland
*E-mail: laura.lauri@helsinki.fi

Zircons from Archean rocks from the Pudasjärvi and Koillismaa blocks of Finland have been dated by SIMS and LAM-ICPMS U-Pb. Zircons from a tonalite and a granite in the Koillismaa block yield emplacement ages of 2805±7 Ma and 2711±15 Ma, whereas zircons from igneous rocks in the Pudasjärvi block yield emplacement ages between 2864±10 and ca. 2660 Ma. Ages younger than ca. 2700 Ma reflect high-grade metamorphism and migmatization that is present throughout the Karelian province. Paleoarchean inherited zircons are present in both areas, however, the major period of crustal growth in both blocks was in the Neoarchean. Zircon initial $^{176}Hf/^{177}Hf$ ratios indicate the participation of the depleted mantle in the petrogenesis of the tonalites in the core of the Pudasjärvi block at ~2850 Ma. Initial Hf isotope variations in zircon from other rocks in both terranes suggest mixing between depleted mantle and an older crustal lithology during petrogenesis. Probable crustal contaminants are indicated by the xenocrystic zircons in the Koillismaa block granitoids which yield U-Pb ages between 2900 and 3450 Ma and low initial Hf isotope ratios. The low initial Hf isotope ratios for these zircons are particularly intriguing as they indicate melting of a crustal source with limited input from the depleted mantle.

Keywords: Archean, Finland, Karelia, zircon, U-Pb, Lu-Hf

1. Introduction

The Archean core of the Fennoscandian shield has a history spanning from Mesoarchean (3200-2800 Ma) to Neoarchean (2800-2500 Ma), with one reported Paleoarchean (3500 Ma) rock unit (*Mutanen and Huhma, 2003*). Paleoarchean ages have also been recently obtained from xenoliths in kimberlites, indicating that the lower crust in the Karelian province is up to 3.5 Ga in age (Peltonen et al., 2006). Limited occurrences of >3.0 Ga old rocks (*e.g., Kröner et al., 1981; Paavola, 1986; Lobach-Zhuchenko et al., 1993; Mutanen and Huhma, 2003*) are surrounded by voluminous occurrences of 2.9–2.7 Ga old rocks (*e.g., Vaasjoki et al., 1999 and references therein; Hölttä et al., 2000; Luukkonen, 2001; Mänttäri and Hölttä, 2002; Käpyaho et al., 2006; Lauri et al., 2006*). This study focuses on the Neoarchean evolution of the NW Karelian province of the Fennoscandian shield in the light of U–Pb ages and Hf isotopes in zircons.

The northwestern part of the Karelian province (Fig. 1) hosts the oldest rocks in the Fennoscandian shield. These >3.1 Ga occurrences (Siurua; *Mutanen and Huhma, 2003*; Varpaisjärvi; *Paavola, 1986*) are found in central parts of the Archean blocks of Pudasjärvi and Iisalmi, which mostly consist of Neoarchean rocks. The Koillismaa area east of the Pudasjärvi block consists of Neoarchean rocks according to published age determinations (*Lauri et al., 2006*).

The Pudasjärvi and Koillismaa blocks are composed of strongly migmatized amphibolites, tonalite-trondhjemite-granodiorite (TTG) gneisses, sanukitoids, Neoarchean leucogranites and limited occurrences of paragneisses and greenstones (*e.g., Räsänen et al., 2004*). Reported ages for the tonalites cluster around 2.8 Ga and for the granites around 2.7 Ga (*Lauri et al., 2006*). Granulite facies metamorphism and migmatization affected both

blocks at ~2.69–2.65 Ga (*Mutanen and Huhma, 2003; Lauri et al., 2006*). This Neoarchean granulite facies metamorphic event took place over the entire western Karelian province, as similar metamorphic ages are reported from the Iisalmi (*Hölttä et al., 2000; Mänttäri and Hölttä, 2002*) and Kuhmo blocks (*Käpyaho et al., in review*).

In this study we have chosen a diverse suite of 2800–2700 Ma samples to investigate the growth of the Karelian Province. The rocks include tonalites, granite, diorite, and a migmatitic amphibolite with two generations of leucosome from the Pudasjärvi and Koillismaa blocks in the western Karelian craton. The samples were chosen to provide a wide range in age and composition of the Neoarchean rock types found in the Pudasjärvi and Koillismaa blocks.

2. U-Pb and Lu-Hf isotope systematics of zircons

Zircon U/Pb isotope ratios in samples A1809, A1810 and A1811 were measured using the Cameca ims1270 secondary ion mass spectrometry (SIMS) at the Nordsim Laboratory, Sweden and following analytical protocols of *Whitehouse et al. (1997, 1999)*. U–Pb dating of the remaining samples, and all Lu–Hf isotope analyses were made by laser ablation ICPMS, using a *Nu Plasma* HR multicollector ICPMS operated in the static mode, with a New Wave/Merchantek LUV-213 laser microprobe at the Department of Geosciences, University of Oslo. Procedures for standardization and data reduction are similar to those described by *Jackson et al. (2004)* for U-Pb and *Andersen et al. (2002)* for Lu-Hf. Reference zircons for U-Pb analysis were GJ-Yellow (a 609 Ma zircon supplied by *E. Belousova, Macquarie University, Australia*) and a multi-grain zircon separate from sample A382 Voinsalmi, dated to 1890±3 Ma by ID-TIMS U–Pb (*Patchett and Kouvo, 1986*).

U–Pb age data are summarized in Table 1. Except for sample A1611, which shows a homogeneous group of concordant zircons dated at 2690 ± 6 Ma, zircon populations are heterogeneous, with evidence of both inheritance and post-emplacement lead-loss. The preferred emplacement ages are based on groups of concordant zircons or on upper intercepts of late lead loss lines (Table 1). Samples A1534 (2864 ± 10 Ma) and A1661 (2805 ± 7 Ma) give the oldest ages, the latter is identical within uncertainty to the published TIMS U–Pb age for the same sample (*Lauri et al., 2006*). The age of sample A1611 (2690 ± 6 Ma) is also consistent with the published TIMS age for the same sample (2703 ± 3 Ma; *Mutanen and Huhma, 2003)*. In a previous study $^{207}Pb/^{206}Pb$ ages of ca. 2.72-2.73 Ga were obtained for sample A1657 (Lauri et al., 2006), however, the new LA-ICPMS age of 2711 ± 15 Ma is in good agreement with the TIMS age of 2711 ± 9 Ma for another leucogranite in Koillismaa (*Lauri et al., 2006)*. Of the three samples from Ärrönperä, the host amphibolite (A1809) at ca. 2.73 Ga is significantly older than either of the two generations of neosomes (A1810: ca. 2.68 Ga, A1811: ca. 2.66 Ga), in agreement with relative age relationships observed in the field.

Most of the inherited zircons in the samples are strongly discordant, indicating a complex lead-loss history, and suggesting ages well in excess of 3000 Ma, and perhaps older than 3450 Ma. Sample A1661 has the most complex inheritance pattern, including a concordant zircon at 3140 ± 27 Ma, and a group of significantly older discordant grains.

Time-corrected $^{176}Hf/^{177}Hf$ ratios are shown relative to growth curves for global reservoirs on Fig. 2. The most radiogenic zircons in A1534 and A1811 overlap the depleted mantle growth curve, and most grains from samples have positive ε_{Hf} values, with an average of +3.2 ± 3.5 (2σ) for A1534. Initial $^{176}Hf/^{177}Hf$ in these zircons are similar to published values from 2600–2800 Ma felsic rocks from Finland (*Patchett et al., 1981*; *Vervoort and*

Patchett, 1996). Zircons in the other fives samples show lower initial $^{176}Hf/^{177}Hf$, with a strong tendency towards negative ε_{Hf} values. In A1611, A1657, A1809 and A1810 magmatic zircons the ε_{Hf} range between 1 and –8. Inherited zircons in A1661 and A1657 have ε_{Hf} in the range of –4 to –10, plotting within a band in the diagram defined by $^{176}Lu/^{177}Hf = 0.010$. Model ages for these zircons suggest extraction ages from the depleted mantle between 3600–3850 Ma.

3. Discussion and conclusions

In a classic Hf isotope study partly based on samples from the Fennoscandian shield *Patchett et al. (1981)* concluded that pre-3.0 Ga rocks worldwide were largely derived from an unfractionated mantle, and that by 2.8 Ga, measurable Hf isotope heterogeneity had been developed in the mantle. Whole-rock Nd isotope determinations also indicate the presence of old crustal and a juvenile ~2.8 Ga mantle components in the formation of the Pudasjärvi and Koillismaa blocks (*Mutanen and Huhma, 2003; Lauri et al., 2006; H. Huhma, unpubl.*).

Igneous zircons with $\varepsilon_{Hf} \geq +4$ must have crystallized from magmas containing a significant component from a depleted mantle source at 2800 – 2600 Ma, which demonstrates that depleted mantle reservoir existed, and contributed to the genesis of Fennoscandian crust at 2.8 Ga and later. On the other hand, the least radiogenic 2600–2800 Ma magmatic zircons, and the inherited zircons in A1657 and A1661 must have been derived from a component with a considerable crustal residence time. Judging from the Hf isotopic compositions of inherited zircons, this crustal source resembles Eoarchean- to Paleoarchean material that has been identified in Acasta, Amitsoq and the younger zircon population in the Jack Hills metasediments. The systematic differences in initial $^{176}Hf/^{177}Hf$ of magmatic zircons between samples from Koillismaa and Pudasjärvi (Fig. 2) indicate that magmas in the Koillismaa block contain a larger proportion of material derived from old crustal rocks than do their counterparts in Pudasjärvi. Possible explanations may be differences in deep crustal structure between the two blocks at ca. 2800 Ma, or different styles of magmatic evolution. Old crustal rocks need to be present at depth, and mantle-derived magmas will need time to interact with the crust in order to aquire a crustal Hf isotope signature.

Acknowledgements

This work has received economic support from the University of Oslo, the Geological Survey of Finland and the University of Helsinki. This is Contribution no. 1 from the University of Oslo Isotope Geology Laboratory.

References

Amelin, Y.,Lee, D.-C., Halliday, A.N. and Pidgeon, R.T., 1999. Nature of the Earth's earliest crust from hafnium isotopes in single detrital zircons. *Nature 399, 252-255*.

Amelin, Y., Lee, D.-C. and Halliday, A.N., 2000. Early-middle Arcahean crustal evolution deduced from Lu-Hf and U-Pb istopic studies of single zircon grains. Geochim. Cosmochim. Acta 64, 4205-4225.

Andersen, T., Griffin, W.L. and Pearson, N.J., 2002. Crustal evolution in the SW part of the Baltic Shield: The Hf isotope evidence. J. Petrol. 43, 1725-1747.

Blichert-Toft, J. and Albarède, F., 1997. The Lu-Hf geochemistry of chondrites and the evolution of the mantle-crust system. Earth Planet. Sci. Lett. 148, 243-258.

Blichert-Toft, J., Albarède,F., Rosing, M., Frei, R. and Bridgwater, D., 1999. The Nd and Hf isotopic evolution of the mantle through the Archaean. Results from the Isua supracrustals, West Greenland, and from the Birimian terranes of West Africa. Geochim. Cosmochim. Acta 63, 3901-3914.

Griffin, W.L., Pearson, N.J., Belousova, E., Jackson, S.E., van Achterbergh, E., O'Reilly, S.Y. and Shee, S.R., 2000. The Hf isotope composition of cratonic mantle: LAM-MC-ICPMS analysis of zircon megacrysts in kimberlites. Geochim. Cosmochim. Acta 64, 133-147.

Hölttä, P., Huhma, H., Mänttäri, I. and Paavola, J., 2000. P-T-t development of Archaean granulites in Varpaisjärvi, central Finland. II. Dating of high-grade metamorphism with the U–Pb and Sm–Nd methods. Lithos 50, 121–136.

Jackson, S.E., Pearson, N.J., Griffin, W.L. and Belousova, E.A., 2004. The application of laser ablation-inductively coupled plasma-mass spectrometry to in-situ U-Pb zircon geochronology. Chem. Geol. 211, 47-69.

Käpyaho, A., Hölttä, P., Whitehouse, M. U-Pb zircon geochronology of Neoarchaean migmatites in the Kuhmo and Lieksa districts, western part of the Karelian craton. Bull. Geol. Soc. Finland (in review).

Käpyaho, A., Mänttäri, I. and Huhma, H., 2006. Growth of Archaean crust in the Kuhmo district, eastern Finland: U–Pb and Sm–Nd isotope constraints on plutonic rocks. Precambrian Res. 146, 95–119.

Kröner, A., Puustinen, K. and Hickman, M., 1981. Geochronology of an Archaean tonalitic gneiss dome in northern Finland and its relation with an unusual overlying volcanic conglomerate and komatiitic greenstone. Contrib. Mineral. Petrol. 76, 33–41.

Lauri; L.S., Rämö, O.T., Huhma, H., Mänttäri, I. and Räsänen, J., 2006. Petrogenesis of silicic magmatism related to the ~2.44 rifting of Archean crust in Koillismaa, eastern Finland. Lithos 86, 137–166.

Lobach-Zhuchenko, S.B., Chekulayev, V.P., Sergeev, S.A., Levchenkov, O.A. and Krylov, I.N., 1993. Archaean rocks from southeastern Karelia (Karelian granite-greenstone terrain). Precambrian Res. 62, 375–397.

Luukkonen, E.J., 2001. Lentiiran kartta-alueen kallioperä. Summary: Pre-Quaternary rocks of the Lentiira map sheet area. Suomen geologinen kartta – Geological map of Finland 1:100 000: Kallioperäkarttojen selitykset, Explanation to the maps of Pre-Quaternary rick, lehti – sheet 4414 + 4432. Geological Survey of Finland. (in Finnish, with English summary)

Mänttäri, I. and Hölttä, P., 2002. U–Pb dating of zircons and monazites from Archean granulites in Varpaisjärvi, Central Finland: Evidence for multiple metamorphism and Neoarchean terrane accretion. Precambrian Res. 118, 101–131.

Mutanen, T. and Huhma, H., 2003. The 3.5 Ga Siurua trondhjemite gneiss in the Archean Pudasjärvi Granulite Belt, northern Finland. Bull. Geol. Soc. Finland 75, 55–68.

Paavola, J., 1986. A communication on the U–Pb and K–Ar age relations of the Archaean basement in the Lapinlahti-Varpaisjärvi area, central Finland. Geol. Surv. Finland, Bull. 339, 7–15.

Patchett, J. and Kouvo, O., 1986. Origin of continental crust of 1.9-1.7 Ga age: Nd isotopes and U-Pb zircon ages in the Svecokarelian of South Finland. Contrib. Mineral. Petrol. 92, 1-12.

Patchett, P.J., Kouvo, O., Hedge, C.E. and Tatsumoto, M., 1981. Evolution of continental crust and mantle heterogeneity: evidence from Hf isotopes. Contrib. Mineral. Petrol. 78, 279–297.

Peltonen, P., Mänttäri, I., Huhma, H., Whitehouse, M.J., 2006. Multi-stage origin of the lower crust of the Karelian craton from 3.5 to 1.7 Ga based on isotopic ages of kimberlite-derived mafic granulite xenoliths. Precambrian Res. 147, 107-123.

Räsänen, J., Iljina, M., Karinen, T., Lauri, L., Salmirinne, H. and Vuollo, J. 2004. Geologic map of the Koillismaa area, northeastern Finland, 1:200 000. Geological Survey of Finland.

Vaasjoki, M., Taipale, K. and Tuokko, I., 1999. Radiometric ages and other isotopic data bearing on the evolution of Archaean crust and ores in the Kuhmo-Suomussalmi area, eastern Finland. Bull. Geol. Soc. Finland 71, 155–176.

Vervoort, J.D. and Patchett, P.J.,1996. Behaviour of hafnium and neodymium isotopes in the crust: Controls from Precambrian crustally derived granites. Geochim. Cosmochim. Acta 60, 3717-3733.

Vervoort, J.D. and Blichert-Toft, J., 1999. Evolution of the depleted mantle: Hf isotope evidence from juvenile rocks through time. Geochimica et Cosmochimica Acta 63, 533-556.

Vervoort, J.D., Patchett, P.J., Gehrels, G.E. and Nutman, A.P., 1996. Constraints on early Earth differentiation from hafnium and neodymium isotopes. Nature 379, 624-627.

Whitehouse, M.J., Claesson, S., Sunde, T. and Vestin, J., 1997. Ion-microprobe U-Pb zircon geochronology and correlation of Archaean gneisses from the Lewisian Complex of Gruinard Bay, north-west Scotland. Geochim. Cosmochim. Acta 61, 3329-4438.

Whitehouse, M.J., Kamber, B.S. and Moorbath, S., 1999. Age significance of U-Th-Pb zircon data from early Archaean rocks of west Greenland – a reassessment based on combined ion-microprobe and imaging studies. Chem. Geol. 160, 201-204.

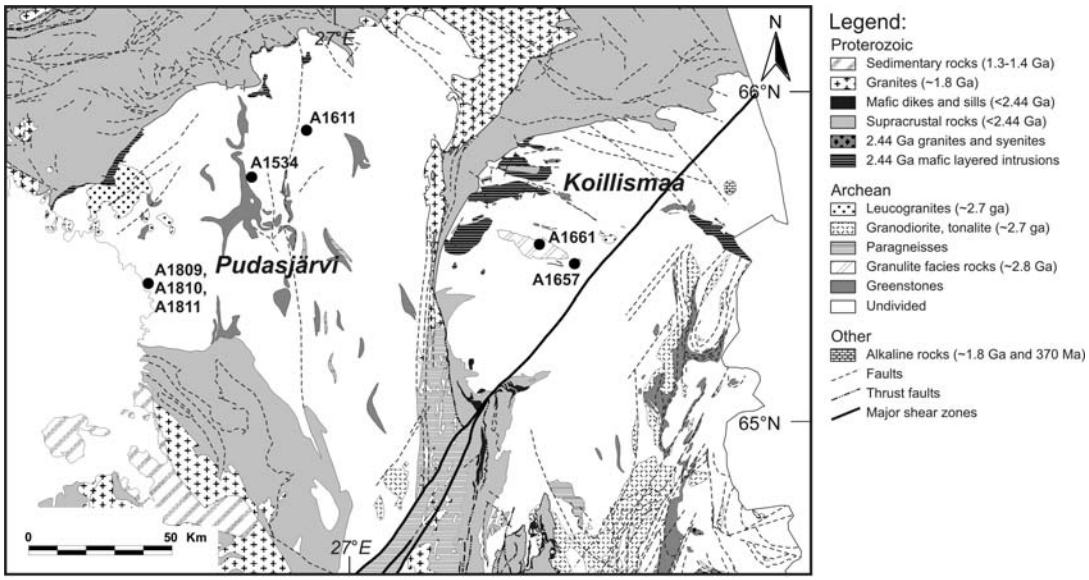

Figure 1. Geologic map of the northwestern Karelian province in Finland. Sampling locations are marked with black dots. Simplified from *Korsman et al. (1997)* and *Räsänen et al. (2004)*.

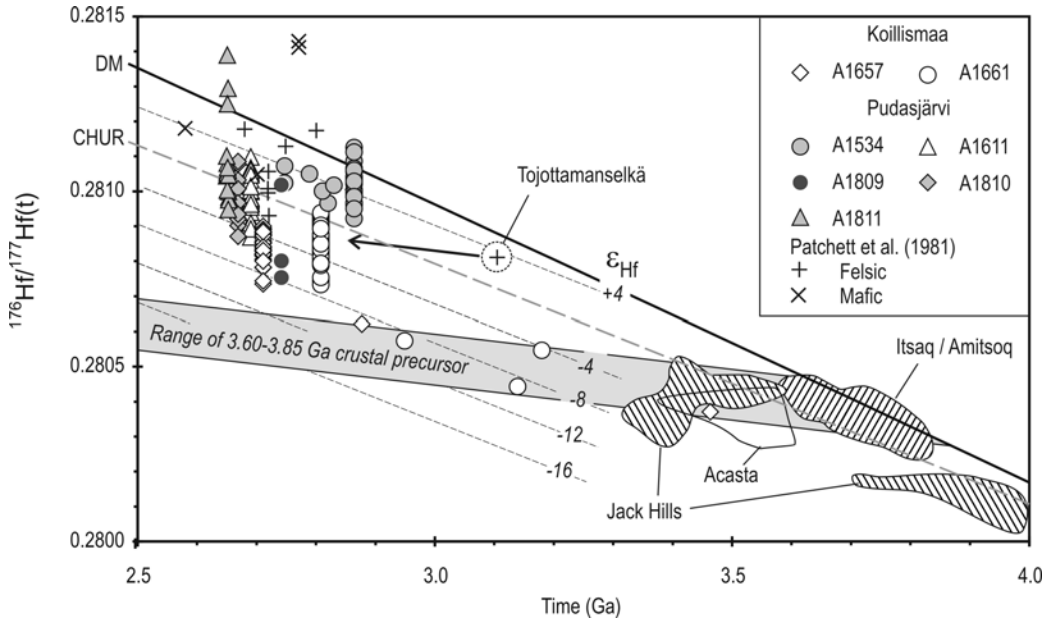

Figure 2. Time-corrected $^{176}Hf/^{177}Hf$ of zircons from the Archean of Finland plotted against U–Pb age, data from the present study and from *Patchett et al. (1981)*, compared to primitive mantle (CHUR; *Blichert-Toft and Albarède, 1997*) and depleted mantle (DM; *Griffin et al., 2000*). Labeled contours parallel to the CHUR curve are lines of equal ε_{Hf}. The shaded field represents the evolution of $^{176}Hf/^{177}Hf$ with time for a Paleo- to Eoarchean crustal reservoir derived from a depleted mantle source at 3600–3850 Ma, at $^{176}Lu/^{177}Hf$ ratio of 0.010. Fields for Eoarchean and Paleoarchean rocks: Jack Hills conglomerate, Australia (*Amelin et al., 1999*), Itsaq (Amitsoq) orthogneisses, Greenland (*Vervoort and Blichert-Toft, 1999; Vervoort et al., 1996, Blichert-Toft et al., 1999*), Acasta gneiss, Canada (*Amelin et al., 1999, 2000*).

Geochemistry of basalt dykes and lavas from Inkoo and Lake Ladoga: Widespread 1.53–1.46 Ga high-Ti and-Zr magmatism in southern Fennoscandian Shield?

A.V. Luttinen[1]*, V. Lobaev[2], O.T. Rämö[1], M. Cuney[3], B.G.J. Upton[4], V. Lindqvist[1]

[1]Department of Geology, P.O.Box 64, 00014-University of Helsinki, Finland
[2]VSEGEI, 74 Sredny pr., 199106, Saint-Petersburg, Russia
[3]UMR CNRS 7566 G2R-CREGU, Université H. Poincaré, BP 239, 54506 Vandoeuvre, France
[4]Department of Geology and Geophysics, University of Edinburgh, Edinburgh EH9 3JW, U.K.
*E-mail: arto.luttinen@helsinki.fi

The Kopparnäs dyke swarm (Inkoo) and the Salmi basalts (Lake Ladoga) constitute a geochemically distinctive group of high-Ti and -Zr basalts that are readily distinguished from other Post-Svecofennian mafic magmas. They may record a single widespread (>500 km) magmatic event along the southern margin of the Fennoscandian Shield at 1.53–1.46 Ga and we designate them tentatively as the Lake Ladoga Igneous Suite.

Keywords: flood basalt, dyke swarm, basin, rifting, rubbly pahoehoe, Mesoproterozoic

1. Introduction

Post-Svecofennian mafic dykes and sills and less abundant lavas crop out over a fan-shaped area extending from the Pasha-Lake Ladoga Basin, Russia, across southern Finland to southern and central Sweden (Fig. 1). The Post-Svecofennian mafic magma suites have been traditionally divided into Subjotnian, Jotnian, and Postjotnian groups based on their age relationship to the rift-filling Mesoproterozoic (Jotnian) sedimentary sequences. However, recent geochronological results have complicated the picture of the spatial and temporal development of the rift basins and associated magmatism (e.g. *Rämö et al., 2004, Söderlund et al., 2005*). Here we review recently obtained geochemical data for "Jotnian" Salmi basalts from the Pasha-Lake Ladoga Basin (*Lobaev, 2005, Rämö and Upton., in prep.*) and undated mafic dykes from Kopparnäs, Inkoo (*Luttinen and Kosunen, 2006*), and compare these suites with other Post-Svecofennian 1.65–1.25 Ga mafic magma suites.

2. Mode of occurrence and age constraints

In the Ladoga Lake region, Post-Svecofennian basalt lavas are found along the north-eastern and eastern shore of Lake Ladoga and basaltic cobbles are found on the Valaam Island. The differentiated Valaam Sill is exposed in the Valaam archipelago. Several phases of mafic magmatism have been distinguished in the area: at least two stages of basaltic lava eruption were associated with sedimentation in the Pasha-Lake Ladoga basin after the emplacement of the 1.55–1.53 Ga Salmi rapakivi intrusion. Drill-core data show that the lower suite of Salmi basalts is up to 130–140 m thick and consists of 2–9 basalt flows. The thickness of individual flow units varies from ~50 m at the base (at Karkku) to ~8 m. The upper suite is up to 90 m thick and consists of 1–6 relatively thin flows (5–20 m). A sedimentary intercalation between the two suites indicates a pause in volcanic activity, whereas the lavas composing each suite appear to have been emplaced in rapid succession. The Salmi basalts exhibit characteristic morphological features of rubbly pahoehoe; i.e. an internal structure of inflated pahoehoe combined with a flow-top breccia (cf. *Keszthelyi et al., 2006*). The intrusion of the Valaam Sill at 1.46 Ga (*Rämö et al.,*

2004) represents the final magmatic phase in the Lake Ladoga area and provides a minimum age for the Salmi basalts.

The Kopparnäs basalt dyke swarm is exposed over a distance of 2 km along the coast of the Gulf of Finland ~40 km west of Helsinki. The swarm is composed of numerous en echelon segments; the overall strike of the near vertical dykes is E-W. The maximum width of the generally lens-shaped segments is ca. 2 m. The Kopparnäs dykes are mainly aphanitic and aphyric. Some wide segments have a porphyritic appearance due to weakly oriented plagioclase laths. Inclusions of wall-rock granitoids, gneisses, and gabbroids are fairly abundant and mainly represent dislocated bridges. The undated Kopparnäs swarm has been regarded as coeval with the nearby 1.65 Ga Obbnäs rapakivi intrusion (*Kosunen, 2004*). However, recent palaeomagnetic measurements of the Kopparnäs dykes yield a transitional palaeopole between the 1.65 Ga and 1.25 Ga poles (*Satu Mertanen, personal communication, 2006*).

3. Geochemistry

The Salmi basalts have highly amygdaloidal bases and flow tops, typical of pahoehoe lavas. Accordingly, many of the analysed samples are strongly altered (*Lobaev, 2005*). The least altered samples from the massive interior parts of the flows are compositionally uniform, have fairly low loss on ignition-values, contain unaltered olivine, and probably correspond quite well to magma composition. Although clinopyroxene is universally replaced by tremolite-actinolite in the Kopparnäs dykes, notably uniform concentrations and ratios of elements, including alkali metals, suggest that postmagmatic processes have not significantly affected the overall whole-rock compositions. Geochemically, the least altered Salmi basalts and the Kopparnäs dykes are notably similar and represent fairly evolved basalt magmas with low MgO (Salmi 3.8–4.7 wt.%, Kopparnäs ~5 wt.%) (Fig. 2a). They have relatively high contents of K_2O (1.0–2.1 wt.%) and Na_2O (2.4–3.0 wt.%) and plot within or close to the alkaline field in the TAS diagram at SiO_2 of 45–50 wt.%, but abundant normative hypersthene indicates a tholeiitic affinity. The rocks are markedly rich in incompatible high field strength elements, such as TiO_2 (3.7–5.0 wt.%), P_2O_5 (1.0–1.5 wt.%), Zr (360–540 ppm), Nb (32–55 ppm), Th (2.7–5.0 ppm), and Ce (100–180 ppm) (Fig. 2). Overall, they can be classified as high-Ti and -Zr basalts with 'transitional' alkaline–tholeiitic compositions.

On the basis of their compositional uniformity, the Kopparnäs dykes probably represent a single intrusive event. The Salmi basalts can be subdivided into two groups which may correlate with individual eruptions or different magma plumbing systems. The least altered samples of the Salmi basalts mainly have TiO_2 of 3.7–4.0 wt.% and Zr of 360–440 ppm. A single flow at the base of the lower suite has higher TiO_2 and Zr contents of 4.4 wt.% and 510 ppm, respectively, and is notably similar to the Kopparnäs magma (TiO_2 4.6–5.0 wt.%, Zr 480–540 ppm). The division of Salmi basalts into two subgroups is further supported by geochemical data on the basaltic cobbles from the Valaam Island (*Rämö and Upton., in prep.*). It is unclear whether all samples with relatively higher TiO_2 and Zr contents represent the same flow or several flows, however.

4. Comparison of Post-Svecofennian mafic magma suites

Geochemical comparison of the Salmi basalts and the Kopparnäs dykes with other Post-Svecofennian mafic magma suites is hampered by the small number of published high-

precision trace element analyses. The available data show that the Salmi basalts and the Kopparnäs dykes constitute a distinctive group of rocks which we designate here as the Lake Ladoga Igneous Suite (LLIS) (Fig. 2). The diagnostic attributes of LLIS include a marked enrichment of incompatible elements, e.g. TiO_2, Zr, and Nb, at given MgO and high Nb/Y and Zr/Y values (Fig. 2). A few high-Ti and -Zr dykes from the Åland-Åboland dyke swarm exhibit broadly similar compositions, but these rocks are believed to be significantly older, and are also distinguished from the LLIS based on their lower Nb and Nb/Y (Fig. 2b). The "Jotnian" ≥1.46 Ga basalts from the Dalarna (Sweden) represent the most likely temporal correlatives of the LLIS basalts, but their low-Ti and -Zr compositions suggest derivation from different magma sources. The lack of published geochemical data hinders comparison with the 1.46 Ga Tuna dolerites from the Dalarna (*Söderlund et al., 2005*).

5. Conclusive remarks

Geochemical data for the 1.53–1.46 Ga Salmi basalts and the undated Kopparnäs dykes show them to be markedly similar to each other and different from other Post-Svecofennian 1.65–1.25 Ga mafic magma suites. Based on geochemical and palaeomagnetic (*Satu Mertanen, personal communication, 2006*) affinities, we speculate that these occurrences of high-Ti and -Zr basalt constitute the Lake Ladoga Igneous Suite, which was associated with rifting close to the southern margin of the Fennoscandian Shield. The position of the Kopparnäs swarm midway between the ≥1.46 Ga basalts and sedimentary basins in the Dalarna (Sweden) and Lake Ladoga (Russia) indicates that 1.53–1.46 Ga rifting and magmatism extended across the southern Fennoscandian Shield. Geochemical and geochronological data for the Post-Svecofennian magma suites are insufficient for more detailed evaluation of the volume and distribution of individual 1.53–1.46 Ga magma suites. The available data indicate, however, that basalts belonging to the Lake Ladoga Igneous Suite were emplaced over an area of >500 km wide. Preliminary Nd isotopic data for the Salmi basalts and the basaltic cobbles (ε_{Nd} at 1.46 Ga -4 to -5; *Rämö and Upton., in prep.*) imply that the magmas that erupted in the Lake Ladoga area include a significant component of Pre-Svecofennian lithospheric material, whereas the Kopparnäs dykes have more radiogenic Nd composition (ε_{Nd} at 1.46 Ga ca. -2; *Kosunen*, *2004*). The Nd isotopic variation could record contamination of basalts during their ascent through the lithosphere, or derivation of primary melts from different sources. A contamination model is supported by the fact that the Kopparnäs magma has somewhat lower SiO_2 and higher MgO than the Lake Ladoga basalts.

The occurrence of rubbly flow top breccias, similar to those of the Salmi basalts, has been recently recognised in some large igneous provinces and their origin has been ascribed to extremely high eruption rates (up to 10^6 m^3s^{-1}; *Keszthelyi et al., 2006*). Development of a thick flow top breccia facilitates transportation of rubbly pahoehoe lava over great distances. Assuming that the Kopparnäs dyke swarm represents a larger feeder system of such voluminous and violently erupted lava flows in the Gulf of Finland area, the volume of preserved basalts may radically underestimate the original volume of erupted magma in the Lake Ladoga Igneous Suite.

References

Andersson, U.B., 1997. The sub-jotnian Strömsbro granite complex at Gävle, Sweden. *GFF* 119, 159-167.

Andersson, U.B., Neymark, L.A., and Billström, K., 2002. Petrogenesis of Mesoproterozoic (Subjotnian) rapakivi complexes of central Sweden: implications from U-Pb zircon ages, Nd, Sr and Pb isotopes. *Trans. R.. Soc. Edinburg Earth. Sci.* 92, 201-228.

Haapala, I., Rämö, O.T. and Frindt, S., 2005. Comparison of Proterozoic and Phanerozoic rift-related basaltic-granitic magmatism. *Lithos* 80, 1-32.

Keszthelyi, L., Self S., Thordarson T., 2006. Flood lavas on Earth, Io and Mars. *J. Geol. Soc.* 163, 253-264.

Kosunen, P., 2004. Petrogenesis of Mid-Proterozoic A-type granites: Case studies from Fennoscandia (Finland) and Laurentia (New Mexico). *Unpubl. PhD thesis, Univ. Helsinki, Department Geol.*, 21 p.

Lindberg, B., Eklund, O. and Suominen, V., 1991. Middle Proterozoic Subjotnian diabases and related ma-fic rocks in the archipelago of southwestern Finland. In I. Laitakari (Ed.), Fennoscandian meeting and excursion on Precambrian dyke swarms, Finland, June 10-15, 1991, *IGCP-257 Tech. Rep.* 4, 18-30.

Lobaev, V., 2005. Mineralogical and petrogeochemical characteristics of the Mesoproterozoic Pasha – Ladoga volcanic-sedimentary basin and its basement (Baltic Shield, Russia). Inferences on the gene-sis of unconformity related uranium deposits. *Unpubl. PhD thesis, Univ. Henri Poincaré Nancy-I*, 292 p.

Luttinen, A. and Kosunen, P., 2006. The Kopparnäs dyke swarm from Inkoo, southern Finland: new evidence for Jotnian magmatism in SE Fennoscandian Shield. In E. Hanski, S. Mertanen, T. Rämö, and J. Vuollo (Eds.), Dyke Swarms - Time Markers of Crustal Evolution. *A.A. Balkema* (in press).

Nyström, J.O., 2004. Geochemistry, origin and tectonic setting of the Jotnian basalts in central Sweden. *Final Report, Project 03-1116/2001. Geol. Surv. Sweden*, 34 p.

Rämö, O.T., 1990. Diabase dyke swarms and silicic magmatism – Evidence from the Proterozoic of Finland. In A.J. Parker, P.C. Rickwood & D.H. Tucker (Eds.), Mafic dykes and emplacement mechanisms. Rotterdam–Brookfield, *A.A. Balkema*., 185-199.

Rämö, O.T., Mänttäri, I., Kohonen, J., Upton, B.G.J., Vaasjoki, M., Luttinen, A.V., Lindqvist, V., Lo-baev, V., Cuney, M. and Sviridenko, L.P., 2004. The Lake Ladoga basin; preliminary insights into geochronology, igneous evolution, and tectonic significance. In C. Ehlers, O. Eklund, A. Korja, A. Kruuna, R. Lahtinen, and L.J. Pesonen (Eds.), Lithosphere 2004 – Third Symposium on the Structure, Composition and Evolution of the Lithosphere in Finland. Programme and Extended Abstracts, Espoo, Finland, November 9-10, 2006 *Inst. Seismology, Univ. Helsinki, Report S-45,* 105-106.

Söderlund, U., Isachsen, C.E., Bylund, G., Heaman, L.M., Patchett, P.J., Vervoort, J.D. and Andersson, U.B., 2005. U-Pb baddeleyite ages and Hf, Nd chemistry constraining repeated mafic magmatism in the Fennoscandian Shield from 1.6 to 0.9 Ga. *Contrib. Mineral Petrol.* 150: 174-194.

Solyom, Z., Lindqvist J.-E. and Johansson, I., 1992. The geochemistry, genesis, and geotectonic setting of Proterozoic mafic dyke swarms in southern and central Sweden. *GFF* 114, 47-65.

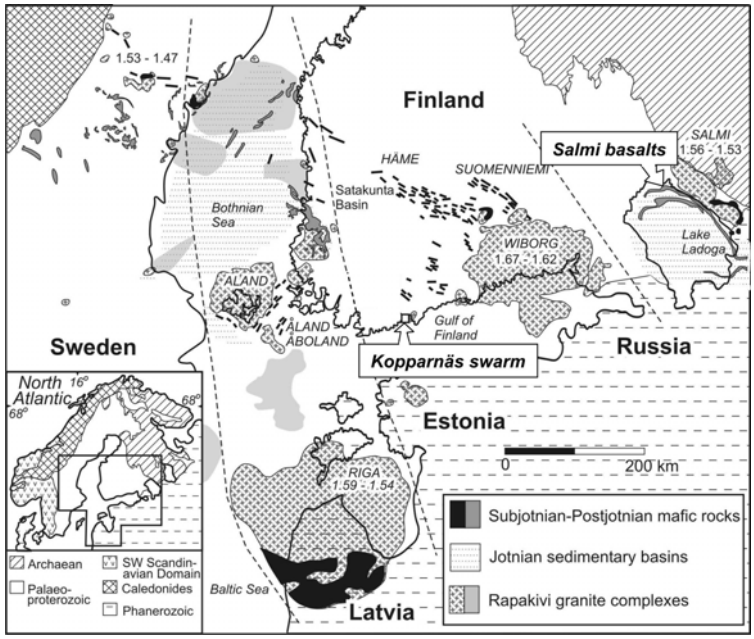

Figure 1. Schematic geological map of southern Fennoscandian Shield showing the distribution of rapakivi granite complexes (ages indicated in Ga) and Subjotnian to Postjotnian mafic rocks. The Kopparnäs dyke swarm and the Salmi basalts are depicted. Dashed lines indicate assumed zones of coeval magmatism. Modified after *Haapala et al*. (2005).

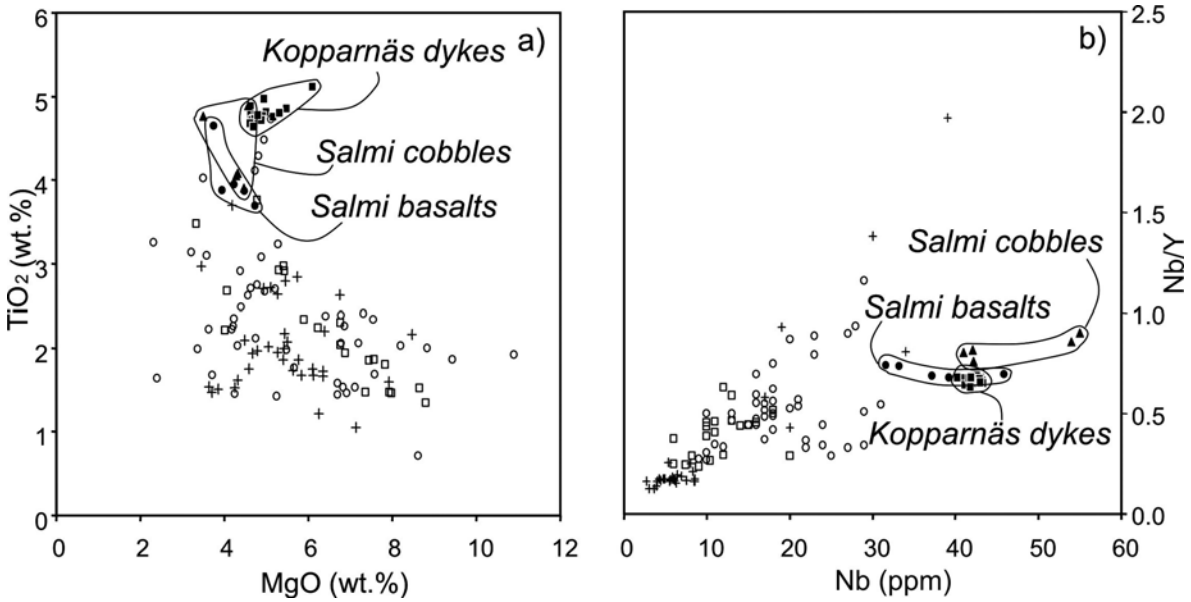

Figure 2. Variation of a) TiO2 vs. MgO and b) Nb vs. Nb/Y for the Kopparnäs dykes, Salmi basalts, and basaltic cobbles from the Valaam Island. Compositions of ~1.65–1.58 Ga (Subjotnian; open circles), ~1.53–1.46 Ga (Jotnian, crosses), and ~1.26 Ga (Postjotnian, open squares) mafic magma suites are shown for comparison. Data sources: Rämö (1990), Lindberg et al. (1991), Solyom et al. (1992), Andersson (1997), Andersson et al. (2002), Nyström (2004), Lobaev (2005), Luttinen and Kosunen (2006), Rämö and Upton. (in prep.), Peltonen (unpubl.).

FIRE 2 & 2A profile: interpretation and correlation to surface geology

Mikko Nironen[1]* and Annakaisa Korja[2]

[1]Geological Survey of Finland POB 96, FIN-02151 Espoo, Finland
[2]Institute of Seismology, POB 68, FIN-00014 University of Helsinki, Finland
*Email: mikko.nironen@gtk.fi

The FIRE 2 and 2A reflection seismic profiles run across the main geologic units of southern Finland. The changes in the reflectivity patterns can be associated with changes in geological units at surface in the scale of a hundred meters. A crustal scale pop-up structure is identified in the area of the Tampere and Pirkanmaa Belts, and an extensional core complex structure within the Uusimaa Belt.

Keywords: Svecofennian, crust, seismic reflection, FIRE

In the 1:1 000 000 geological map of Finland (*Korsman et al. 1997*) the Svecofennian Domain has been divided into Arc complex of southern Finland, Arc complex of western Finland, and Primitive arc complex. In line with the proposed division of arc complexes, recent isotopic and geochemical studies (*Lahtinen and Huhma 1997, Rämö et al. 2001*) suggest the presence of two or three terranes with slightly different Nd isotopic signatures in southern Finland. This is consistent with the interpretations based on geophysical data (*Korja et al. 1993, Korja and Heikkinen 2005*). Several plate tectonic models have been proposed to explain the current geometry of the Svecofennian Domain (*e.g. Lahtinen 1994, Nironen 1997, Lahtinen et al. 2005*).

The FIRE 2 and 2A reflection seismic profiles run across the main geologic units of southern Finland that are from north to south: the Central Finland Granitoid Complex, the Tampere Belt, the Pirkanmaa Belt, the Häme Belt, and the Uusimaa Belt (Fig. 1).

Nironen et al. (*2006*) have described the correlation of the seismic reflectivity with the surface structures and lithological changes. In general, the changes in the reflectivity patterns can be associated with changes in geological units at surface, although this applies to structures more than lithological variation. The upper crustal reflections correlate well with surface geology in the scale of a hundred meters. The uppermost crust hosts blocks with distinct reflectivity patterns; the block boundaries partly correlate with the established lithological boundaries and partly suggest modifications. The boundary between the Arc complex of western Finland and Arc complex of southern Finland coincides with the boundary between the Pirkanmaa and Häme Belts.

A crustal scale pop-up structure is interpreted in the area of the Tampere and Pirkanmaa Belts. The data suggests that the boundary between the Arc complex of western Finland and the Arc complex of southern Finland is a detachment that partly overlays the pop-up structure as well as other contractional structures. In areas dominated by plutonic rocks horst and graben structures with planar, moderately to steeply dipping normal faults seem to be characteristic. An extensional core complex structure was interpreted within the Uusimaa Belt. Late brittle faulting displaces the ductile deformation structures in the entire FIRE 2 & 2A area.

In crustal scale, southern Finland is modelled to consist of two continental units, and a sedimentary-dominated accretionary complex squeezed between these two units. In addition, the refraction seismic FENNIA profile together with reflectivity patterns suggests

a mafic body at the base of the crust below the accretionary complex. We interpret this mafic body as a trapped remnant of oceanic crust.

References

Korja, A., Heikkinen, P., 1995. Proterozoic extensional tectonics of the central Fennoscandian Shield: Results from the Baltic and Bothnian Echoes from the Lithosphere experiment. *Tectonics* 14, 504-517.

Korja, A., Korja, T., Luosto, U., Heikkinen, P., 1993. Seismic and geoelectric evidence for collisional and extensional events in the Fennoscandian Shield – implications for Precambrian crustal evolution. *Tectonophysics* 219, 129-152.

Korsman, K., Koistinen, T., Kohonen, J., Wennerström, M., Ekdahl, E., Honkamo, M., Idman, H., Pekkala, Y. (editors), 1997. Suomen kallioperäkartta – Berggrundskarta över Finland- Bedrock map of Finland 1 : 1 000 000. *Geological Survey of Finland, Espoo, Finland*.

Lahtinen, R. 1994. Crustal evolution of the Svecofennian and Karelian domains during 2.1-1.79 Ga, with special emphasis on the geochemistry and origin of 1.93-1.91 Ga gneissic tonalites and *associated supracrustal rocks in the Rautalampi area, central Finland. Geological* Survey of Finland, Bulletin 378, 128 p.

Lahtinen, R., Huhma, H., 1997. Isotopic and geochemical constraints on the evolution of the 1.93–1.79 Ga Svecofennian crust and mantle. *Precambrian Research* 82, 13–34.

Lahtinen, R., Korja, A., Nironen, M., 2005. Paleoproterozoic tectonic evolution. In: Lehtinen, M., Nurmi, P.A., Rämö, O.T. (editors). Precambrian Geology of Finland – Key to the Evolution of the Fennoscandian Shield. *Developments in Precambrian Geology, Volume 14*. Elsevier, Amsterdam, 481-531.

Nironen, M., 1997. The Svecofennian Orogen: a tectonic model, *Precambrian Research*, 86, 21–44.

Nironen, M., Korja, A., Heikkinen, P. and the FIRE Working Group, 2006. A geological interpretation of the upper crust along FIRE 2 and FIRE 2A. In: Kukkonen, I.T., Lahtinen, R. (editors). Finnish Reflection Experiment FIRE 2001-2005. *Geological Survey of Finland, Special Paper* 43, 77-103.

Rämö, O.T., Vaasjoki, M., Mänttäri, I., Elliott, B.A., Nironen, M., 2001. Petrogenesis of the post-kinematic magmatism of the Central Finland Granitoid Complex I : radiogenic isotope constraints and implications for crustal evolution. *Journal of Petrology* 42, 1971–1993.

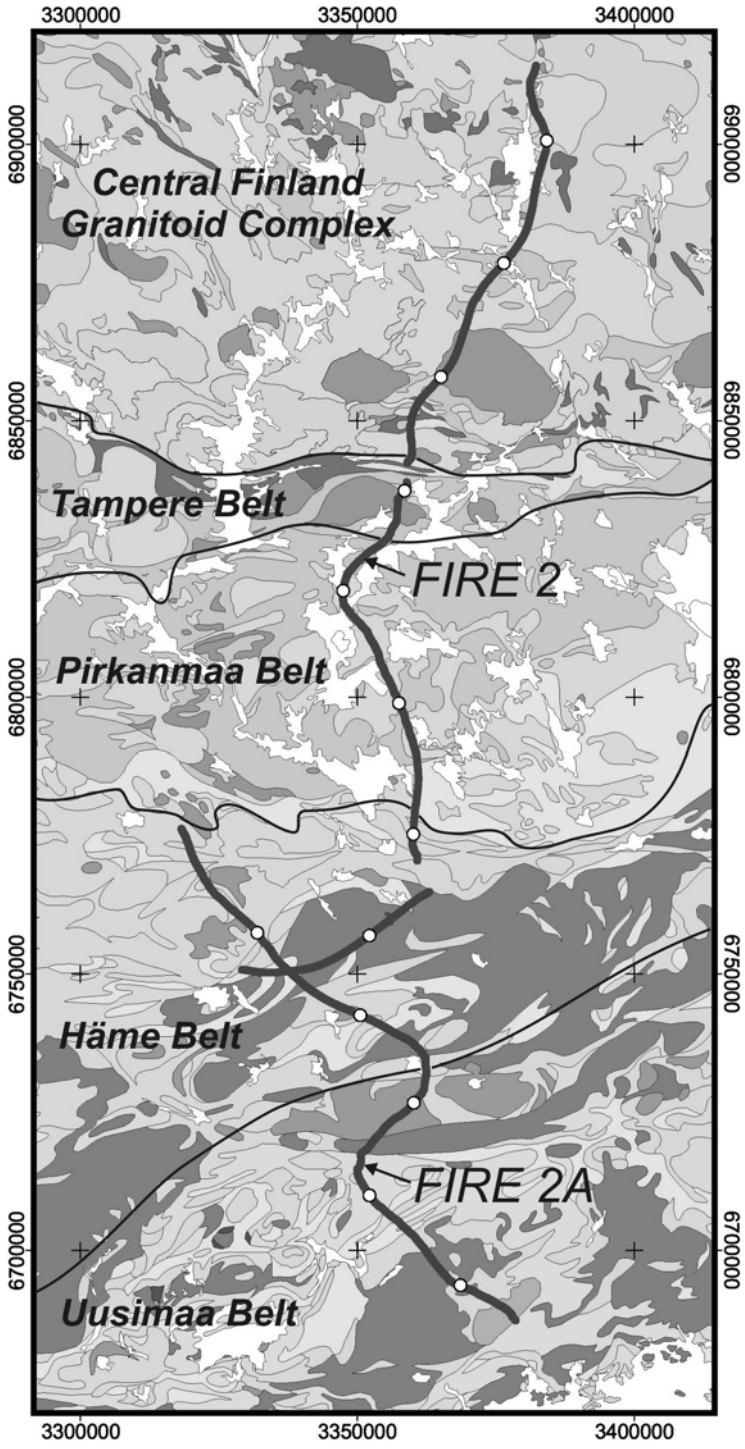

Figure 1. Geological map around the FIRE 2 & 2A profile showing the geological units (based on *Korsman et al. 1997*).

Rheology of the lithosphere and models of postglacial rebound

K. Moisio[1]* and J. Mäkinen[2]

[2]Department of Geophysics, University of Oulu, P.O.Box 3000, FIN-90014 Oulu, Finland
[2]Finnish Geodetic Institute, Geodeetinrinne 2, FIN-02430 Masala, Finland
*Email: Kari.Moisio@oulu.fi, Jaakko.Makinen@fgi.fi

We discuss the rheology of the lithosphere and its role in modelling postglacial rebound.

Keywords: Lithosphere, rheology, postglacial rebound, glacial isostatic adjustment

1. Rheology of the lithosphere

Rheology is defined as deformational behaviour of materials and it involves all mechanisms that deform materials. Generally rheology can be studied from a microscopic and a macroscopic point of view (Ranalli, 1995). In the microscopic approach deformation is analysed at the atomic and lattice structure levels. These studies are constrained by laboratory experiments and microscopic observations of deformed rocks. In the macroscopic approach the relationship between stress and strain and their time derivatives are described. Geophysical and geological observations like the flexure of the lithosphere in response to surface loads at various timescales (sediments, volcanoes, seamounts, ice sheets etc.) can be considered from the macroscopic viewpoint.

Rheological equations describing deformation, i.e., describing the relationship between stress and strain, are called constitutive equations. They are always functions of intrinsic, i.e., material parameters, and of extrinsic, i.e., environmental parameters. In the lithosphere probably most important mechanisms of deformation are brittle, elastic and viscous ones. Viscous deformation is also often referred as ductile deformation. Fundamental difference between elastic and viscous deformation is that for an elastic material strain is related to total stress, whereas for a viscous material the strain rate is related to deviatoric stress (deviation of stress tensor from pressure). The time scale of the deformation is also significant factor, especially in the mantle. At the time scales of 1 to 10000 s the mantle can be considered to be nearly elastic, whereas at time scale of 10^{11} to 10^{17} s the mantle behaves as viscous fluid.

Elastic behaviour is characterized by linear proportionality between stress and strain. In an ideal elastic material strain is also fully recoverable. Rocks in low temperature and low pressure, i.e., the upper lithosphere can be considered elastic. Elastic wave theory is applicable to seismic waves at the timescale of seconds and hours. The whole Earth behaves elastically at high frequencies. The Preliminary Reference Earth Model (PREM) is constrained by seismic body waves together with surface waves, free oscillations and anelastic attenuation.

Viscous models are applied for the deformation of the mantle, but it can also observed in crustal rocks, for example as folds. Either the Newtonian or the non-Newtonian description can be used. A Newtonian fluid has a linear relationship between strain rate and stress, whereas a non-Newtonian fluid has a non-linear relationship. In addition, between elastic and viscous deformation a stage of transient, i.e., time dependent flow, can exist. Combinations of these three phases can be modelled with analogue models like the Maxwell's viscoelastic body and the Burgers general linear body (*Mase 1970*, *Ranalli*

1995). These models are linear. However, from laboratory experiments it is known that for silicate polycrystals in high temperatures the most common creep relation between stress and strain rate is nonlinear, exhibiting a power-law dependence where strain rate is proportional to the n^{th} power of stress.

The two most important classes of creep mechanism are diffusion creep and dislocation creep (see e.g., *Tsenn and Carter 1987*, *Ranalli 1995*, *Turcotte and Schubert, 2003*). Diffusion creep results from diffusion of atoms and crystal lattice vacancies through the interior of crystal grains or along grain boundaries subjected to a deviatoric stress. Diffusion is a thermally activated process. It has a linear relationship between stress and strain rate and therefore it can be considered equivalent to Newtonian fluid flow. In higher stress regimes dislocation creep is often dominant, although some amount of diffusion creep can also be influential to the overall strain rate. Dislocation creep is a result of a motion of dislocations in the crystal lattice structure. Dislocations are defined as imperfections in the crystal structure. These mechanisms are also thermally activated. For the dislocation glide, activation can also be attained by an increase in stress. This means that there is a finite strength in the rocks deforming in such a manner. Ductile creep occurs only when this critical value is exceeded either by change in temperature and/or stress. At high temperatures creep is a result of thermal activation only, and the strength of the rock has vanished. Deformation beyond this point is characterised by some viscous flow, dependent on physical and the mechanical conditions. Dislocation creep has an exponential dependence on temperature and pressure, with the non-linear stress and strain rate relationship in a power-law form. Dislocation creep can be considered equivalent to non-Newtonian flow, if the required activation level is exceeded.

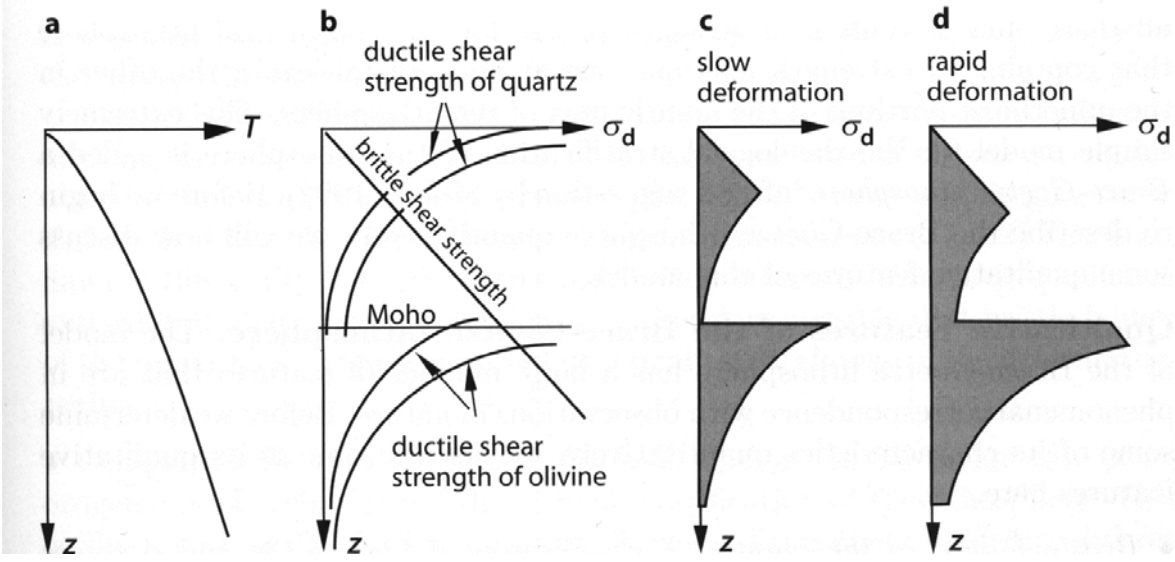

Figure 1. Brace-Goetze rheological model of the lithosphere. a) Temperature T at depth z. b) Shear strength due to brittle failure (straight line) and viscous strength (curved lines) for two different strain rates for quartz and olivine. Curve with higher strength corresponds to a higher strain rate. c) Strength profile for low strain rate. d) Strength profile for high strain rate. Shaded area gives by integration the vertically integrated strength. σ_d is differential stress (taken from *Stuwe, 2002*) .

Failure of material takes place when permanent deformation occurs. Material fails when the deviatoric stress reaches a certain critical value called the yield strength or the yield stress. Failure can occur either as a discontinuous deformation, i.e., fracturing, or as a continuous irrecoverable deformation, i.e., plastic flow (*Ranalli, 1995*). Material that fails by fracturing is called brittle and material that fails by a plastic flow is often also termed as ductile. Yielded flow and fluid flow can be considered similar, with the exception that the former flow occurs only when the yield stress is reached. Earthquakes, faulting and folding are thought to be examples of fracturing and plastic flow, which thus have a major role in geodynamics, especially in the upper lithosphere.

Two different modes of brittle failure can be distinguished: sliding along existing fracture planes, and shear fracture. Combining Amonton's law and the Navier-Coulomb criterion, we can derive a widely used relation for describing brittle failure. This is often presented as Byerlee's law, which can be written in terms of the principal stress difference, of lithostatic pressure and of pore fluid pressure (see e.g., *Sibson 1974* and *Ranalli 1995*). To be exact, this relation is not a constitutive equation, as it does not give a relationship between stress and strain. Instead, it defines the critical state of stress required for failure to occur.

Using constitutive equations, composition and temperature, rheological profiles for the lithosphere can be constructed. A simple rheological model, where the rheological strength of the lithosphere was calculated based on brittle and viscous deformation is shown in Fig. 1. Straight lines and line sections in Fig. 1bcd correspond to brittle failure, with a linear relationship between stress and strain. Curved lines correspond to viscous (ductile) deformation with a power-law dependence between stress and strain rate. Characteristic feature of the curved lines is the decrease of strength towards higher temperatures. In Fig. 1b the effect of different strain rate on ductile strength can be seen. Material that has the lowest strength is assumed to control the deformation at a given depth. Making this assumption we can end up with the strength profile of either Fig. 1c or Fig. 1d. The vertically integrated strength gives the total force required to deform the entire lithosphere, which is useful when considering e.g. deformation of the continental plates.

Ranalli (1994) describes the rheology of the lithosphere with a coupled viscous, elastic and brittle model (Fig. 2). The downward bent elastic lithosphere has a stress-free layer in the middle of the lithosphere. Above this point the stresses are compressive and below this depth point the lithosphere is under extension. Brittle areas are shown by linearly growing straight lines in the upper part. Elastic stresses are shown by straight lines that go from positive to negative stresses in the middle of the figure (compression to extension, respectively). Viscous deformation is shown by curved lines. The elastic section of the lithosphere is therefore restricted to thickness h in Fig. 2a and to thicknesses h_1 and h_2 in Fig. 2b. Note that this model shows show the stress state instead of strength which is displayed in Fig. 1.

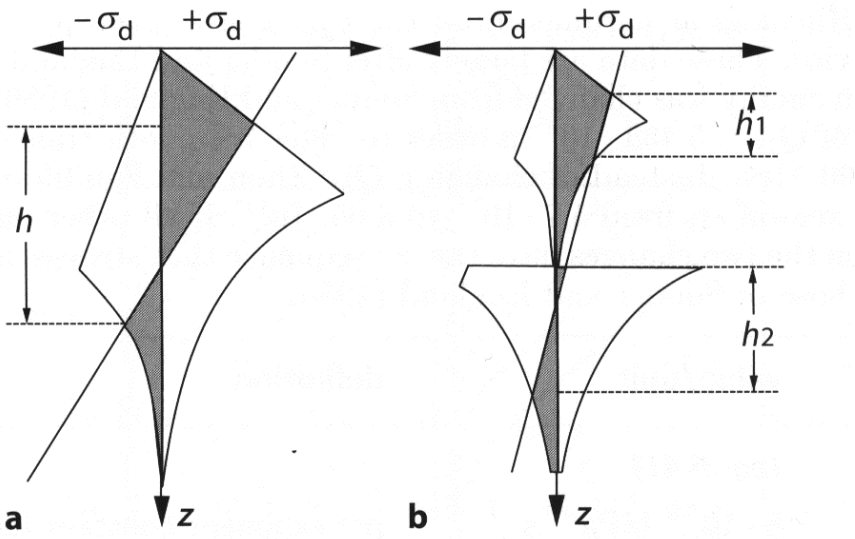

Figure 2. Rheology of the lithosphere with elastic, viscous, and brittle constitutive equations. a) Strength profiles together with elastic stresses for quartz and b) for quartz and olivine mineralogy. This model shows actually stress state instead of the failure envelopes shown in Fig. 1 (taken from *Stuwe, 2002*).

Lithospheric rheology can furthermore be analysed with models where structural models with rheologically different layers are subjected to tectonic stresses. Lithospheric stress conditions and areas of possible deformation can be located (e.g., *Moisio and Kaikkonen, 2004*)

2. Models of Postglacial Rebound

Since Peltier (1974), a kind of rheological standard for the quantitative modelling of the response of the Earth to the waxing and waning of the ice sheets (Postglacial Rebound PGR or Glacial Isostatic Adjustment GIA) has emerged. New developments, simplifications and refinements are typically discussed relative to this standard model. Its features are:

1) The Earth is spherical, self-gravitating, and spherically symmetric. For regional modelling in Fennoscandia, spherical effects are small and most aspects can be adequately treated using a layered half-space (e.g., *Wolf, 1986*). In either case, the rheological stratification can be described as 1-D.
2) The lithosphere is elastic. Its shear modulus is taken to be constant, typically 64 GPa. Thickness is solved for.
3) Upper mantle down to 670 depth has linear Maxwell rheology, where the elastic properties are taken from seismic models (now usually PREM). The viscosity is solved for, may have several layers.
4) Lower mantle down to the mantle-core boundary, treated as the upper mantle.
5) Inviscid core.

The observational data are for this modelling are multitudinous:

a) Relative ancient sea level data and tilt of ancient shorelines.
b) Ancient and present-day earthquakes in the glaciated areas.
c) Contemporary vertical motion and tilt from geodesy (repeated levelling, GPS), tide gauges, lake levels.
d) Contemporary 3-D motion from geodesy (GPS, VLBI, Satellite Laser Ranging SLR).
e) Polar drift, historically from astrometry and now from geodesy.
f) Secular change in the rotation rate of the Earth, or equivalently in the degree 2 zonal spherical harmonic coefficient J_2 (the flattening of the Earth).
g) Gravity change on the surface of the Earth, from pointwise absolute and relative measurements. The Maxwell model predicts a relationship –0.15 μgal/mm between surface gravity change and uplift (Wahr et al., 1995); from this point of view measuring gravity change is another method of measuring vertical motion.
h) Regional gravity change as "seen" from space by the gravity satellite GRACE.

The observables above are "dynamic" in the sense that we need to observe a change to draw conclusions. There are few "static" observables:
i) (Negative) free-air gravity anomalies or equivalently geoid lows in the deglaciated areas.
j) Non-homogeneity in crustal rheology would cause a high-frequency signature in the gravity field, but the problem might be to detect it below other signals (Schotman et al., 2004).

Most observables above depend on the assumed deglaciation history as well, and in inversion there are tradeoffs between the ice history and the rheology. Therefore it is important to try to constrain the ice history with independent data (say end moraines) and with glaciological arguments. Similarly, certain transformed observations are relatively independent of the ice history: the relaxation times derived from sea level curves in the center of the ice sheets (*Mitrovica, 1995*) and the relaxation spectrum (*McConnell, 1968; Wieczerkowski et al., 1999*) determined from shoreline diagrams (*Sauramo, 1958*; *Donner, 1995*).

The results from the standard model can roughly be summarized as follows: The upper-mantle viscosity comes out at around 5×10^{20} Pa s, and the lower-mantle at least one magnitude more (e.g., *Peltier, 2004*; *Mitrovica and Forte, 2004*). These are averaged values; introducing a finer viscosity layering one can simultaneously satisfy also observations related to mantle convection (*Peltier, 1998; Mitrovica and Forte, 2004*). *Peltier (1998)* points out that given that the time-scales of the two processes differ by five orders of magnitude, the ability of the same Maxwell viscosity profiles to explain them is a very strong argument for a Newtonian mantle rheology.

For lithospheric thickness the global inversion, giving an average of different continental and oceanic lithosphere thicknesses is perhaps not as interesting. However, even regional modelling is traditionally done using 1-D stratification. Regional variation can be accommodated using a number of different 1-D models. *Wolf* (1993) and *Martinec and Wolf (2004)* have assembled a number of results from Fennoscandia. They differ considerably, but some kind of average can be seen around 90 km.

For crustal motion, the lithosphere functions as a low-pass filter, suppressing phenomena at short spatial wavelengths (*Fjeldskaar, 1997*). In Fennoscandian solutions using vertical motion as observable, *Wolf* (*1995*) and *Martinec and Wolf (2004)* have found a positive correlation between lithospheric thickness and upper-mantle viscosity: either a thick lithosphere or a low-viscosity asthenosphere is required.

Compared with seismic, thermal, or rheological results, the lithospheric thickness from PGR inversion appears small. *Anderson* (*1994*) points out that these lithospheres all refer to different concepts. He also suggests a rule-of-thumb: the lithosphere in the original sense of the word (the "strong" lithosphere capable of supporting long-term loads) is about half of the thickness of the thermal lithosphere. The thickness of the PGR lithosphere in turn is a kind of scale parameter ("effective elastic thickness") producing the "right" flexural rigidity of the plate given the fixed constant shear modulus. It would be a challenging task to try to relate the PGR thickness to the other definitions. So far, in PGR modelling the aforementioned rule of thumb (1/2) is applied e.g. to the seismic thickness (*Kaufmann et al., 2000*).

The advances in finite-element methods and in computational power has recently made it possible to introduce a 3-D mantle viscosity structure and laterally varying lithosphere thickness, even to detailed global modelling (*Kaufmann et al., 2000*; *Zhong et al., 2003*; *Latychev et al.*, 2005; *Spada et al, 2006*). Compared with 1-D models, forward calculations show a pronounced influence especially in horizontal motion predictions and at the margins of the ice sheets. Obviously, there is a strong trade-off between details of rheology and details of ice history.

References

Anderson, D.L., 1995. Lithosphere, asthenosphere and perisphere. *Rev. Geophysics* 33, 125–149.

Donner, J., 1995. *The Quaternary History of Scandinavia.* Cambridge University Press, Cambridge, 200 p.

Fjeldskaar, W., 1997. Flexural rigidity of Fennoscandia inferred from the postglacial uplift. *Tectonics* 16, 596–608.

Kaufmann, G., Wu, P., Li. G. 2000. Glacial isostatic adjustment in Fennoscandia for a laterally heterogeneous Earth. *Geophys. J. Int.* 143, 262–273.

Lambeck, K., Smither, C., Ekman, M., 1998. Tests of glacial rebound models for Fennoscandia based on instrumented sea- and lake-level records. *Geophys. J. Int.* 135, 375–387.

Latychev, K., Mitrovica, J.X., Tamisiea, M.E., Tromp, J., Moucha1 R., 2005. Influence of lithospheric thickness variations on 3-D crustal velocities due to glacial isostatic adjustment. *Geophys. Res. Letters* 32, L01304, doi:10.1029/2004GL021454.

Martinec Z., Wolf D., 2005. Inverting the Fennoscandian relaxation-time spectrum in terms of an axisymmetric viscosity distribution with a lithospheric root. *J. Geodynamics* 39, 143–163.

Mase, G.E., 1970. *Continuum mechanics.* Schaum's outline series. McGraw-Hill Inc., New York, 221 pp.

McConnell, R.K., 1968. Viscosity of the mantle from relaxation time spectra of isostatic adjustment. *J. Geophys. Res.* 73, 7089–7105.

Milne, G.A., Davis, J.L., Mitrovica, J.X., Scherneck, H.-G., Johansson, J.M., Vermeer, M., Koivula, H., 2001. Space-Geodetic Constraints on Glacial Isostatic Adjustment in Fennoscandia. *Science* 291, 2381–2385.

Mitrovica ,J.X., Forte, A.M. 2004. A new inference of mantle viscosity based upon joint inversion of convection and glacial isostatic adjustment data. *Earth Planetary Sci. Letters* 225, 177–189.

Moisio, K. and Kaikkonen, P., 2004. The present day rheology, stress field and deformation along the DSS profile FENNIA in the central Fennoscandian Shield. *J. Geodynamics* 38, 161–184.

Peltier, W. R., 1974. The implulse response of a Maxwell Earth. *Rev. Geophys. Space Phys*. 12, 649–669.

Peltier, W.R., 1998. Postglacial variations in the level of the sea: Implications for climate dynamics and solid-earth geophysics. *Rev. Geophysics* 36, 603–689.

Peltier W.R., 2004. Global glacial isostasy and the surface of the ice-age Earth: The ICE-5G (VM2) model and GRACE. *Annu. Rev. Earth Planet. Sci.* 32. 111–149 DOI: 10.114/annurev.earth.32.082503.144359.

Ranalli, G., 1994. Nonlinear flexure and equivalent mechanical thickness of the lithosphere. *Tectonophysics* 240, 107–114.

Ranalli, G., 1995. *Rheology of the Earth* (2nd ed.). Chapman & Hall, London, 413 pp.

Sauramo, M., 1958. Die Geschichte der Ostsee. *Ann. Acad. Sci Fenn.* A III:51.

Schotman, H., Visser P., Vermeersen, B., and Koop R., 2004. Recovery of the gravity field signal due to a low viscosity crustal layer in global isostatic adjustment models from simulated GOCE data, in The Second International GOCE User Workshop. *GOCE, The Geoid and Oceanography*, June 2004.

Spada, G., Antonioli, A., Cianetti, S., Giunchi, C. 2006. Glacial isostatic adjustment and relative sea-level changes: the role of lithospheric and upper mantle heterogeneities in a 3-D spherical Erath. *Geophys. J.Int.* 165, 695–702.

Stuwe, K., 2002. *Geodynamics of the lithosphere. An introduction.* Springer-Verlag, Berlin, 449 pp.

Tsenn, M.C. and Carter, N.L., 1987. Upper limits of power law creep of rocks. *Tectonophysics* 136, 1–26.

Turcotte, D.L. and Schubert, G., 2003. *Geodynamics,* Second edition. Cambridge University Press, New York, 456 pp.

Wahr J, Han D, Trupin A (1995): Predictions of vertical uplift caused by changing polar ice volumes on a viscoelastic earth. *Geophys. Res. Letters* **22**, 977–980.

Wieczerkowski, K., Mitrovica, J.X., Wolf, D., 1999. A revised relaxation-time specrum for Fennoscandia. *Geophys. J. Int.* 139, 69–86.

Wolf, D., 1985. Glacio-isostatic adjustment in Fennoscandia revisited. *J. Geophys.* 59, 42–48.

Wolf, D (1993): The changing role of the lithosphere in models of glacial isostasy: a historical review. *Global Planet. Change* 8, 95–106.

Zhong, S., Paulson A., and Wahr, J. 2003. Three-dimensional finite element modeling of Earth's viscoelastic deformation: Effects of lateral variations in lithospheric thickness. *Geophys. J. Int.* 155, 679–695.

Mantle stratigraphy of the Karelian craton: a 620 km long 3-D cross section revealed by mantle-derived xenocryst chemistry

Hugh O´Brien[1], Petri Peltonen[1], Marja Lehtonen[1] and Dmitry Zozulya[2]

[1]Geological Survey of Finland, P.O.Box 96, FI-02151 Espoo, Finland
[2]Geological Institute, Kola Science Centre, Russian Academy of Sciences, Apatity, Russia

Keywords: mantle, stratigraphy, xenocrysts, kimberlites, Karelia, craton, Finland, Russia

1. Introduction

A 620 km cross section of the lithostratrigraphy of the mantle underlying the Karelian craton has been compiled using mantle xenocryst data from 6 localities where the mantle has been sampled by kimberlitic magmatism. Arranged from SW to NE they are: Kuopio kimberlite field, Kaavi kimberlite field, Kuhmo area kimberlites, Lentiira-Kostomuksha area, Kuusamo area, and the Terskii kimberlite field on the southern coast of the Kola Peninsula. Ages and rock types of the kimberlite host rocks vary across this cross section: **1.** The Kuopio and Kaavi fields together contain 20 Group I kimberlites discovered thus far, 4 of which have been dated, giving an age of ca. 600 Ma. **2.** The kimberlitic rocks in the Kuhmo, Lentiira and Kostomuksha area are transitional between olivine lamproites and Group II kimberlites, being very phlogopite rich, but also containing abundant carbonate. Age dates on several Kuhmo and Lentiira dikes fit within a narrow range at 1200 Ma. **3.** The newly discovered field of kimberlites south of Kuusamo are dominantly Group I kimberlites, but also include similar rocks to those in the Kuhmo area. No age dates are yet available, but they are spatially within the boundaries of the Devonian Kola alkaline province, and may represent similar age magmatism. **4.** The Terskii Group I kimberlites and melilitites are located on the southern Kola peninsula coast, 25 km east of the Turiy carbonatite complex, along the northern edge of the NW-SE Kandaluksha graben. Age estimates for Terskii kimberlites range from 360–380 Ma (Kalinkin et al., 1993) to ~ 460 Ma (Delenitzin A.A. et al., 2001.). Xenocrysts used in this study were not taken directly from the kimberlites, but rather collected from sediments of the White Sea and Kola coast south-east from the Terskii kimberlite field.

2. Results

Mantle-derived xenolith and xenocryst studies indicate that the subcontinental lithospheric mantle of the Karelian craton shows considerable variation from margin to core. At the margin, in the **Kuopio and Kaavi area**, the mantle is stratified into at least three distinct layers labeled A, B, and C (Lehtonen et al., 2004). Shallow *layer A* (at ~60–110 km depth) has a knife-sharp lower contact against layer B indicative of a shear zone implying episodic construction of the SCLM. Layer A peridotites have "ultradepleted" arc mantle -type compositions, and have been metasomatised by radiogenic $^{187}Os/^{188}Os$, presumably from slab-derived fluids. Xenoliths derived from the middle *layer B* (at ~110–180 km depth), which is the main source of harzburgitic garnets (G10) in Finnish kimberlites, are characterised by an unradiogenic Os isotopic composition. $^{187}Os/^{188}Os$ shows a good correlation with indices of partial melting implying an age of ~3.3. Ga for melt extraction (Peltonen & Brügmann, 2006). This age corresponds with the oldest formation ages of the overlying crust, suggesting that layer B represents the unmodified SCLM stabilised during

the Paleoarchean. The underlying *layer C* (at 180–250 km depth) is the main source of Ti-rich pyropes of megacrystic composition, which however, lacks G10 pyropes. The osmium isotopic composition of the layer C xenoliths is more radiogenic compared to layer B, yielding only Proterozoic T_{RD} ages. Layer C is interpreted to represent a melt metasomatised equivalent to layer B. This metasomatism most likely occurred at c. 2.0 Ga when the present craton margin formed following break-up of the proto-craton.

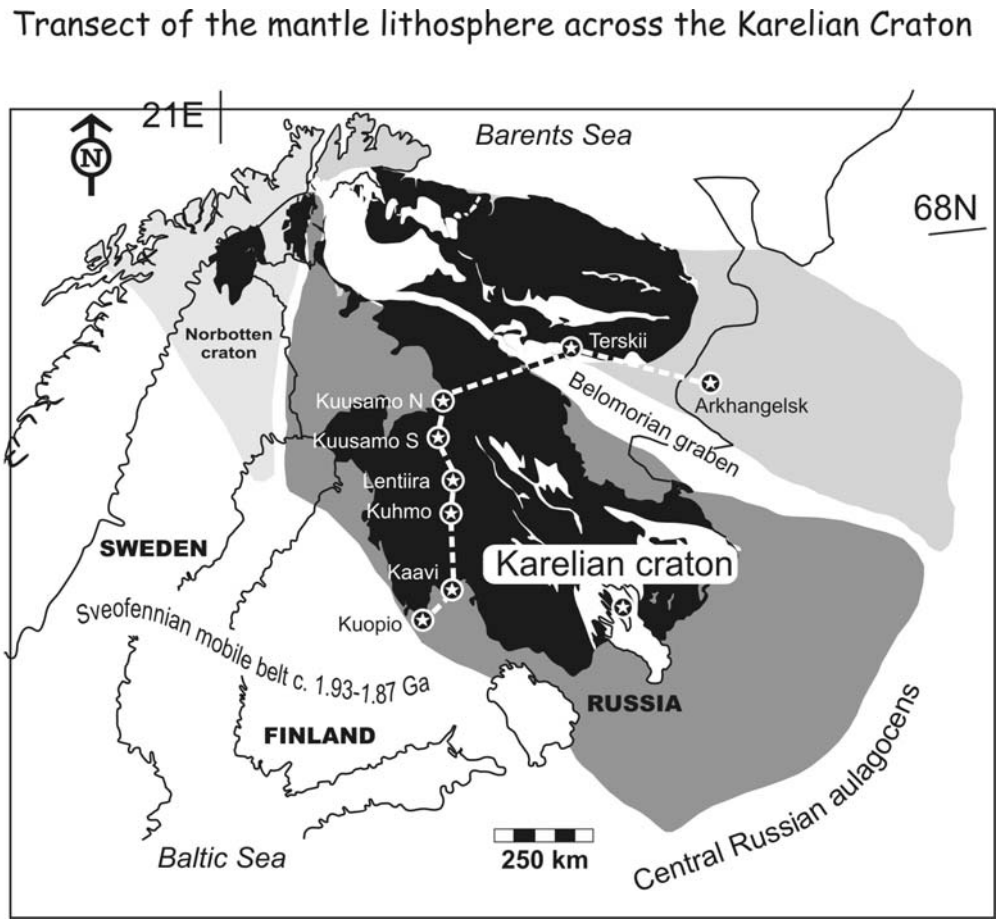

Figure 1. Generalised geological map showing the extent of the three Archean subcratons, Kola, Karelia, and Norbotten, which together make up the Archean of the Fennoscandia. Black shading refers to the exposed Archean crust while grey denotes the Archean crust that is covered by younger supracrustal rocks or that has been reworked during the Proterozoic. Locations of mantle xenocryst-bearing alkaline rocks – used to construct the transect across the craton – are indicated by stars.

The mantle stratigraphy of the craton core, in the **Kuhmo, Lentiira and Kostomuksha** areas, shows less variation (O´Brien et al., 2003). Layer A is absent. Layer B begins with the lowest temperature pyropes at an inferred depth of 70 km and continues to a depth of about 250 km showing a relatively homogenous distribution of harzburgite and lherzolite pyropes throughout. Differences in craton core layer B compared to craton edge layer B include: 1. Wehrlite garnet is very rare, as is chrome diopside. 2. The G10 to G9 ratio in

both exploration samples and hardrock sources is considerably higher implying core layer B is relatively harzburgite-rich. Thus far there is only a weak indication of a G10 pyrope-free Layer C. However, Ti-rich megacryst composition pyropes are very common, so evidence for a deep 250-300 km Layer C may become available with further sampling. 3. The overall magnesium number (*mg*) of the mantle lithosphere in this area is extremely high relative to the worldwide average and to the mantle at Kaavi-Kuopio. Coupled with the rarity of mantle-derived chrome diopside, the implication is that this portion of the mantle underwent unusually high levels of partial melting to produce such a refractory residua.

The position of the **Kuusamo** area well within the Karelian craton would imply it represents craton core and the distribution and composition of mantle xenocrysts derived from this area confirms the existence of depleted, and therefore ancient mantle underlying this area. Xenocryst pyrope chemistry demonstrates that lherzolite and harzburgite are roughly equally distributed down to depths of roughly 180 km. Although the data are relatively sparse, we interpret the existence of harzburgite throughout the mantle section, without any obvious layering, to represent lithospheric mantle similar to that in the Kuhmo region, albeit slightly thinner. The existence of abundant harzburgitic rocks, some with ultra depleted pyrope compositions and extremely high *mg* numbers, implies that the age of this mantle is Archean.

New data from pyrope grains in sediments offshore of the **Terskii** kimberlite field show that the lithospheric mantle underlying this area is also quite thick, similar to that at Kuusamo, with the deepest-derived grains coming from depths of 180 km. As at Kaavi-Kuopio, pyrope compositional distributions show that the Terskii lithospheric mantle is layered, although with quite a different structure. At Terskii a lherzolite-dominated upper mantle exists down to about 110 km, and a harzburgite-dominated middle layer exists from 110 km to about 150 km. Sampling of the mantle deeper than this is extremely sparse, but the few data that exist suggest a roughly equal harzburgite – lherzolite mixture from 150 to 180 km. The existence of abundant harzburgite is taken as evidence that this mantle is Archean in nature. Based on *mg* of the pyropes, the composition of this mantle lies midway between that from the more fertile Kuopio-Kaavi mantle at craton edge and the depleted craton core mantle seen at Kuhmo – Kuusamo.

References:

Kalinkin M.M, Arzamstev A.A. & Polyakov I.V., 1993, Petrology 1, 173-180.

Delenitzin A.A., Gavrilenko B.V., Serov P.N. and Bayanova T.B. Sm-Nd and Rb-Sr age determination of Yermakovskaya-7 kimberlite pipe, Tersky bereg, Kola region. SVEKALAPKO and EUROPROBE project. 6th Workshop.Lammi, Finland, 29.11-2.12.2001. Abstract. University Oulu, Dep. Geophysics, Report №24.2001. P.17.

Lehtonen, M., O`Brien, H., Peltonen, P., Johanson, B. & Pakkanen, L., 2004. Layered mantle at the Karelian Craton margin: P–T of mantle xenocrysts and xenoliths from the Kaavi-Kuopio kimberlites, Finland. Selected papers of the 8th International Kimberlite Conference, Vol. 2 The J. Barry Hawthorne Volume. Lithos 77, 593–608.

O'Brien, H., Lehtonen, M., Spencer, R. & Birnie, A., 2003. Lithospheric mantle in eastern Finland: a 250 km 3D transect. 8th International Kimberlite Conference, Ext. Abst. FLA-0261, 5p.

Peltonen, P. & Brügmann, G., 2006. Origin of layered continental mantle (Karelian craton, Finland): Geochemical and Re-Os isotope constraints. Lithos 89, 405-423.

Tectonic and magmatic evolution of the Svecofennian crust in southern Finland

Matti Pajunen*, Meri-Liisa Airo, Tuija Elminen, Irmeli Mänttäri, Markus Vaarma, Pekka Wasenius and Marit Wennerström

*Geological Survey of Finland, P. O. Box 96, FIN-02151 Espoo, Finland
*E-mail: matti.pajunen@gtk.fi

1. Introduction

J. J. Sederholm, the architect of the modern geological research and mapping in Finland, described with an amazing accuracy the 1.9-1.8 Ga Svecofennian (Achaean at his time) supracrustal sequences and migmatites in the southernmost part of the country. His careful field observations on the Hanko granite, mafic dyke and granitic migmatization relationships (Sederholm 1926) definitely evidenced the cooling stage between the two granitic events, confirming a polyphase tectono-thermal evolution of the crust. Already at 1899 he described a major unconformity between the Svionian and Bothnian sedimentary formations in the Tampere area (Sederholm 1899 and 1931). Even though the present knowledge do not support all his observations, these early interpretations outlined the pathways to construct evolutionary models in the complexly deformed migmatite areas. The studies of Korsman (1977) on progressive metamorphism in the Rantasalmi-Sulkava area and later in the Savo Schist Belt, lead Korsman et al. (1984) to establish the tectono-metamorphic discordance between the tonalitic and granitic migmatite belts. The discordance coincides with a major crustal conductor of central Finland (Korja & Hjelt 1993 and Korsman et al. 1999). These kinds of discordances describe important steps in crustal evolution or refer to geotectonic terrane boundaries, that often are the major shear zones of bedrock.

The collision between the Archaean continent and the Svecofennian domain (e.g. Wegmann 1928 and Koistinen 1981) occurred at ca. 1.9-1.88 Ga ago (e.g. Vaasjoki & Sakko 1988). At 1975 Hietanen represented the first plate tectonic evolution model on the Svecofennian domain. Afterwards several geotectonic compilations have been published (see Lahtinen 1994, Korsman et al. 1999 and Lahtinen et al. 2005 for refs.). The terrane construction of Lahtinen (1994) took comprehensively into consideration the pre-existing geological research data on tectono-thermal discordances, geochemical characteristics and ages of rocks. Nironen (1997) widened the model to constitute the whole Fennoscandian Shield. The Global Geoscience Transect (GGT) (Korsman et al. 1999) was a co-operation project between geologist and geophysicist. The Svecofennian mantle, lower crust and upper crust relationships were interpreted by combining the geological research data with the structure of the crust modeled from the seismic refraction profile SVEKA (Luosto et al. 1984). In their latest approach Lahtinen et al. (2005) concluded the traditional Svecofennian domain was a result of several orogenies. The extensive data collected during the last hundred years and the increasing flow of new information, like the FIRE reflection seismic profiles (Kukkonen et al. 2002) or isotopic ages, help us to fix the tectonic-magmatic events accurately. It must be emphasized that any tectonic model should be fixed with observations on structural, metamorphic and magmatic characteristics of terranes or their boundaries in the field (e.g. Hölttä 1988, Tuisku & Laajoki 1990, Ehlers et al. 1993,

Pietikäinen 1994, Kilpeläinen 1998, Väisänen 2002, Pajunen et al. 2002 and Rutland et al. 2004).

Question arises: What kind of kinematic scheme the tectono-metamorphic and magmatic structures in the southern Svecofennian rocks are implying to? This presentation is based on successions and kinematics of tectonic structures and their relations to magmatic and metamorphic events as they are identified in the field. Wider-scale interpretations of structural patterns were done by using the pre-existing geological maps and databases and processed geophysical data of the Geological Survey of Finland. The events are established by some new age data. Descriptions and interpretations presented are based on the study of Pajunen et al. (in prep.) carried out in the Helsinki area at 1999-2004. Correlations to the northern terranes are based on the studies in the Pori area at 1998-1999 (Pajunen et al. 2001).

2. Tectonic and magmatic evolution of the southern Svecofennian domain

Already Sederholm (1926) established the polyphase tectono-thermal character of the southern Svecofennian domain. The domain can be divided into several geotectonic terranes; the study area is situated in the granite migmatite belt that is separated from the tonalite migmatite belt in the north by the discordance (Korsman et al. 1984). Approximately 100 km wide ENE-trending southern Finland granitoid zone cuts with an oblique angle the granitic migmatite belt; there are substantial variations in compositions and structures of intrusive rocks in the zone. The early volcanic-sedimentary sequences exist in between the intrusive zones or as remnants within the intrusives. Different approaches have been presented to explain the extensive felsic magmatism of the zone. According to Korsman (1977) crustal thickening caused heating that lead to extensive melting of the crust. Väisänen (2002) proposed the magmatism as a product of orogenic collapse. Pajunen et al. (2002) established relations of magmatism and extensional structures. Ehlers et al. (1993) were the first to propose transpressional model for the deformation in the southern Finland granitoid zone. The observations from the study area (Pajunen et al. in prep.) suggest a tectonic succession as following:

Primary associations and the earliest deformation:

The earliest Svecofennian evolution is represented by the primary supracrustal sequences implying different depositional environments of island arc: deep-water pelitic-psammitic metasedimentary rocks; low-water iron formations, sulphide ores, limestones, marbles and calc-silicate rocks; mafic-intermediate-felsic volcanic rocks with co-magmatic intrusives. The earliest deformation structures (D_A) are remnants of isoclinal folds (F_A) with weak penetrative foliation (S_A), mostly consumed by later metamorphic events. The fold axes are ca. E-W-trending coinciding with the S_A/S_B intersection ($L_{A/B}$). According to structural basis two distinct volcanic pulses can be identified. The earlier one was deformed by D_A. Instead, the later volcanic rocks do not show D_A structures but cuts the S_A foliation. The suggestive kinematic indicators of the D_A structures indicate to N-S shortening and the S_A-S_B relations refer to nearly horizontal setting and transport of D_A (thrusting?). As a result crustal slices from different depths and depositional environments were pushed close to each other, often high-strain shear zones in between them. The D_A event occurred at ca. 1.9-1.88 Ga ago (cf. Hopgood et al. 1983).

Early collapse of the island arc:

A penetrative deformation (D_B) under progressive heating produced isoclinal folding (F_B), penetrative foliation (S_B) and migmatization of various extents. It characterizes the supracrustal sequences. The exceptions are the rocks that existed in the upper crustal level during D_B, e.g. the lower-grade rocks of the Orijärvi area, some high-grade rocks showing only one late high-grade event, or the Jokela sedimentary-volcanic association that evolved later. Often the overprint caused by later tectono-thermal events hide the D_B structures. Syn-/late D_B intrusive rocks are predominantly tonalitic in composition; some mafic intrusive rocks also intruded. Generally, the first tectonic structure formed into the tonalites is a compressive foliation S_C; S_B in them is rare. Also the later volcanic sequence shows D_B structures. The kinematic indications, like chocolate-plate D_B boudinage (Koistinen et al. 1996), refer to nearly pure strong flattening strain. Also isoclinal folds are typical for neosome veins that originally formed into inclined position to the main principal stress (σ_1). Such folds only seldom deform the original layers, because of their horizontal position after D_A. According to several studies (see Korsman et al. 1999 for refs.) low-medium-p/high-T peak metamorphism characterizes the Svecofennian domain. The age of D_B in the south, ca. 1.88-1.87 Ga, is based on the age determinations of the later volcanic rocks (Väisänen & Mänttäri 2002) and syn-/late D_B intrusive rocks (Pajunen et al. in prep.). The structural, metamorphic and magmatic evolution proposes an extensional event that can be related to a collapse of the island arc. The later volcanic pulse represents the early, upper crustal phase of the collapse magmatism (intra-arc volcanism) and with continuing extensive evolution and with depth magmatism changed to more intrusive in character. The observations on structure-magma age relations from the northern terranes (cf. Kilpeläinen 1998 and Nironen 1999) indicate that the crust as an entity was under compressional regime during D_B.

From N-S compression to SW-NE transpression:

In the south the extensional deformation was rapidly followed or closely accompanied by N-S shortening D_C. The N-S compression (D_C) pushed the S_B planes to semi-open to tight folds (F_C) with steep axial plane S_C and ca. E-W-trending fold axes (F_C). Due to rotation of principal stress axis into SW-NE trend, transformed deformation soon to transpressional D_D. This transpression can be well exemplified from the Pori area with the clockwise rotational structures of the Pormarkku block. The F_D folds are less tight than F_C folds; F_D fold axes are N-trending and S_D axial plane is steep. The F_C and F_D form the ellipsoidal D_C-D_D dome-and-basin pattern that characterizes the supracrustal belts of southern Svecofennian domain. The D_C and D_D were the major events that constructed the stacked and sliced structures in further north, for example, in the central Finland granitoid area. Rather small mineral growth during the D_C and D_D events refer to decrease in temperature that in the north lead to locking of the deformation at ca. 1.87 Ga ago as dated by intrusions (cf. Mäkitie & Lahti 2001) cutting the D_C -D_D structures. In the southern Finland granitoid zone thermal evolution is different – when the northern terranes were deforming in a zonal way the southern crust still achieved penetrative folding F_D. The age of 1.87 Ga, fixing the fade of the zonal transpressional D_D in the north, establishes the beginning of the complex tectonic and magmatic evolution in the south – this continuing deformation is responsible for the generation of the southern Finland granitoid zone (Pajunen et al. in prep.).

Southern Finland granitoid zone – a product of transpressional/-tensional events:

The southern Finland granitoid zone is composed of intrusives of varying compositions and metamorphic and tectonic characteristics. The present setting of the granitoid terranes are ordered by the simultaneous and later open, map-scale folding patterns. Long-lived shear zones borders often the granitoid terranes. The structural evolution leading to the evolution of the huge amounts on felsic, in a lesser extent also to mafic magmatism, is named here as D_E.

The even though there are in places evidences of some cooling in the south, mostly heat flow remained high after D_D. The earliest magmatic rocks related to D_E phase are garnet-bearing tonalitic rocks and microtonalitic dykes that were set into fractures deforming the D_C -D_D dome-and-basins. Typically, the garnet-bearing tonalites have pegmatite-granitic borders and higher temperature, medium-grained tonalitic internal parts. This kind of zonal structure typifies the D_E magma pulses widely in the southern Svecofennian terrain. The observation suggest progressive opening of the fractures under increasing temperature. The temperature increase was continued as evidenced by metamorphic assemblages and remelting in these dykes. The early garnet tonalites are dated at 1.87-1.86 Ga (Pajunen et al. in prep.); the age closes the major deformation in the north and fixes the onset of southern Finland granitoid zone generation. During the continuing evolution the amount of magmatism increased and the composition turned to tonalites without garnet and granodiorites; also some gabbros intruded. The high-grade evolution in the granulite areas lasted long as indicated by ca. 1.85-1.86 Ga ages of enderbitic intrusives and ca. 1.84-1.83 ages of metamorphic monazites (Pajunen et al. in prep.) and neosome materials (Väisänen et al. 2004). The intrusion of gabbroic magmas at ca. 1.84 Ga (Pajunen et al. in prep.) indicates deep-seated origin for heat flow in the intense stages of D_E. During the latest D_E magmatism was predominantly granitic, as granitic remelting of the earlier magma phases and widespread granite intrusions at ca. 1.82 Ga ago (cf. Kurhila et al. 2005). Still at 1.80 Ga pegmatitic granite magmas were evolved (Pajunen et al. in prep.).

The evolution of magmas in the southern Finland granitoid zone shows a long history and the increased age data had confirmed its continuous character during ca. 70 Ma. The intrusive rocks show varying degree of deformation, depending on stage of their intrusion. The early, ca. 1.87 Ga magmas of D_E are strongly deformed and metamorphosed, whereas the young granites are only openly arched. The kinematic indications, like internal growth structures in the early garnet-bearing tonalite dykes and shearing structures related to their generation, refer to SE dilatation. In gneisses a strong spaced/sheared foliation S_E deforms the early D_A-D_D structures and refers to nearly horizontal upper-side SE movement. The continued extension thinned the crust and caused high-grade and medium-pressure metamorphism in the ca. NE-trending granulite terrane (the West Uusimaa Complex). Kinematically, the SE extension zones fit as transtensional regimes within the crustal-scale, dextral SW-NE transpression between the dextral, N-trending Baltic Sea-Bothnian Bay and Riga-Karelia zones. The generation of the supracrustal Jokela association (quartzites-conglomerates-volcanites-pelites) in Hyvinkää is fixed with structural evidence to these extensional events – the association is interpreted as a pull-apart basin initiated during the early D_E transtension.

Several observations confirm that the main principal axis was rotated into E-W trend at ca. 1.86-1.85 Ga (Pajunen et al. in prep.); in the study area some sinistral NW-trending

faults (e.g. Hiidenvesi) and in eastern Finland zones of N-axial folds generated at that time (Koistinen 1981).

All the granitoids, in spite of the latest granite-pegmatite dykes show compressional open to moderate folding with NE-trending, steep to moderately SE-dipping axial plane. The intensity of this deformation varies and it deforms the horizontal spaced/shear foliation described above. The NE-trending folds turn into E-W trend in the vicinity of the major crustal E-W shear zones. After 1.86-1.85 Ga the main principal stress rotated into SE-NW direction causing the NE folds with some overturning, dextral southwards overthrusting along the E-W-trending major shear zones (Hyvinkää shear zone) and low-angle northwestwards overthrusting in the NE-trending shear zones. The kinematic structures determined from the latest granitoids refer to nearly pure flattening strain; only a weak lineation refers to E-W tension. For example, granite pegmatite dykes, that intruded at 1.83 Ga into brittle fractures of syn-late D_B tonalitic host, show prograde heating and intense flattening deformation (Pajunen et al. in prep.). The flat foliation is openly folded by horizontal NE axis. Correlation of structural characteristics between different areas in the southern Svecofennian domain evidence different grades of late D_E magmatism depending on the distances from the "tensional centers". Simultaneous tension produced predominantly pegmatitic granite dykes far from them, whereas large intrusions formed into the most effective tension areas. Simultaneously in the transpressional areas compressive structures occurred.

The latest Svecofennian events

The Fennoscandian Shield can be divided into N-trending terranes along the major crustal deformation zones: the Transscandinavian Igneous Belt (TIB), the Baltic Sea-Bothnian Bay zone and Riga-Karelia zone. These zones deform the ENE trend of the southern Finland granitoid zone; it bends the compressional D_E folds (NE trend) and the major E-trending shear zones (e.g. Hyvinkää shear zone) into NNE-N trend. The zones deform also the late D_E granitic pegmatite dykes referring to a late evolution of the structure at ca. 1.80 Ga. In the study area ductile N-axial folding with some new granite in the axial plane was generated into the most intense axial zone, especially in the granitoid-dominant areas near the granulites, but the structure is less ductile in areas without intense felsic magmatism. These N-trending zones show a complex history. Evidence from the Pori area establishes that the zone generation began already during D_D. It is difficult to establish how the zones behaved during the E-W compression during the mid-D_E at ca. 1.86-1.85 Ga, but its late reactivation was strong referring to E-W compressional structures with sinistral shear component – the main principal stress in ca. ESE.

The latest intrusive rock is a metamorphosed, N-trending diabase dyke with a presumable age of ca. 1.78-1.80 Ga (Pajunen et al. in prep.). It is weakly NE folded and sinistrally N-sheared, indicating that the SE-NW transpressional event characterizes the late Svecofennian evolution for a long period from ca. 1.85 to ca. 1.80 Ga. The open warps with ca. E-W axial plane refer that ca. southern stress field continued still after the formation of the major N-S deformation zones.

3. Summarizing

The tectonic and kinematic analysis combined with the tectonically fixed age data on magmatic events firms out that the Svecofennian orogeny was a continuous collisional event, which began with the accretion of the Svecofennian island arc components against

the Archaean continent at ca. 1.9-1.88 Ga ago. The southern Svecofennian terranes were already attached together at ca. 1.88-1.87 Ga. The domain was as an entity under compressional state, even though the southernmost Svecofennian domain underwent an intense upper-crustal extension, proposed as a collapse of the island arc, at ca. 1.88-1.87 Ga ago. Stress field transformed rapidly again to N-S compression that was soon followed by rotation into SW-NE transpression. These collisional events are predominantly responsible for the sliced and stacked structures in the northern Svecofennian domain; this kind of stacking and slicing structure is also evident in the Archaean continent along the faults in the craton boundary, the Kainuu schist belt and Kuhmo greenstone belt. The southern Svecofennian domain was under high heat flow at that time and ductile folding patterns were formed. At ca. 1.87 Ga the deformation was locked in the north and the complex evolution of the southern Finland granitoid zone began. The zone was produced in the complex transtensional-transpressional events that reflect several rotations of stress field during its ca. 70 Ma history: the main principal stress was in SW-NE at ca. 1.87-1.86 Ga, in E-W at ca. 1.86-1.85 Ga and in SE-NW at ca.1.85-1.80 Ga. A strong reactivation of the N-S trending major deformation zones occurred at a very late in the Svecofennian evolution.

The characters of structural evolution refer to a single, continuous and long-lasted Svecofennian collisional evolution that exhibits various tectonic characteristics from the early N-S collision to the later transpressional events that caused the generation of the extensive extensional zones of strong magmatism. The rotations of stress field are resulted in the locking effects and "jumps" of the major movements due to the heterogeneity and competency contrasts, like those related to the thermal differences, in the both Archaean and Svecofennian domains.

References

Ehlers, C., Lindroos, A. & Selonen, O. 1993. The late Svecofennian granite-migmatite zone of southern Finland – a belt of transpressive deformation and granite emplacement. Precambrian Research 64, 295-309.

Hietanen, A. 1975. Generation of potassium-poor magmas in the northern Sierra Nevada and the Svecofennian of Finland. J. Res. U.S. Geol. Surv. 3, 631-645.

Hölttä, P. 1988. Metamorphic zones and the evolution of granulite grade metamorphism in the early Proterozoic Pielavesi area, central Finland. Geological Survey of Finland, Bulletin 344. 50 p.

Hopgood, A., Bowes, D., Kouvo, O. & Halliday, A., 1983. U-Pb and Rb-Sr isotopic study of polyphase deformed migmatites in the Svecokarelides, southern Finland. In Atherton, M. & Gribble, C. (eds.) Migmatites, melting and metamorphism. Shiva, Nantwich, 80-92.

Kilpeläinen, T. 1998. Evolution and 3D modelling of structural and metamorphic patterns of the Palaeoproterozoic crust in the Tampere-Vammala area, southern Finland. Geological Survey of Finland, Bulletin 397. 124 p.

Koistinen, T. 1981. Structural evolution of an early Proterozoic stratabound Cu-Co-Zn deposit, Outokumpu, Finland. Transactions of the Royal Society of Edinburgh: Earth Sciences 72, 115-158.

Koistinen, T., Klein, V., Koppelmaa, H., Korsman, K., Lahtinen, R., Nironen, M., Puura, V., Saltykova, T., Tikhomirov, S. & Yanovskiy, A. 1996. Paleoproterozoic Svecofennian orogenic belt in the surroundings of the Gulf of Finland. In: Koistinen, T. J. (ed.) Explanation to the map of Precambrian basement of the Gulf of Finland and surrounding area 1 : 1 mill.. Geological Survey of Finland. Special Paper 21, 21-57.

Korja, T. & Hjelt, S.-E. 1993. Electromagnetic studies in the Fennoscandian Shield - electrical conductivity of Precambrian crust. Physics of the Earth and Planetary Interiors, 81, 107-138.

Korsman, K. 1977. Progressive metamorphism of the metapelites in the Rantasalmi-Sulkava area, southeastern Finland. Geological Survey of Finland, Bulletin 290. 82 p.

Korsman, K., Hölttä, P., Hautala, T. & Wasenius, P. 1984. Metamorphism as an indicator of evolution and structure of the crust in Eastern Finland. Geological Survey of Finland, Bulletin 328. 40 p.

Korsman, K., Korja, T., Pajunen, M. & Virransalo, P. 1999. The GGT/SVEKA transect: structure and evolution of the continental crust in the Paleoproterozoic Svecofennian orogen in Finland. International Geology Review 41, 287-333.

Kukkonen I., Heikkinen, P., Ekdahl, E., Korja, A., Hjelt, S.-E., Yliniemi, J., Berzin, R. & FIRE Working Group 2002. Project FIRE: Deep seismic reflection sounding in Finland 2001-2005. Lithosphere 2002, Second symposium on the structure, composition and evolution of the lithosphere in Finland. Geological Survey of Finland Espoo November 12-13, 2002. Institute of seismology, University of Helsinki, Report S-42, 67-70.

Kurhila, M., Vaasjoki, M., Mänttäri, I., Rämö, T., & Nironen, M. 2005. U-Pb ages and Nd isotope characteristics of the lateorogenic, migmatizing microcline granites in southwestern Finland. Bulletin of the Geological Society of Finland 77 (2), 105-128.

Lahtinen, R. 1994. Crustal evolution of the Svecofennian and Karelian domains during 2.1 - 1.79 Ga, with special emphasis on the geochemistry and origin of 1.93 - 1.91 Ga gneissic tonalites and associated supracrustal rocks in the Rautalampi area, central Finland. Geological Survey of Finland, Bulletin 378. 128 p.

Lahtinen, R., Korja, A. & Nironen, M. 2005. Paleoproterozoic tectonic evolution. In: Lehtinen, M., Nurmi, P.A. & Rämö, O.T. (eds.) Precambrian Geology of Finland. Key to the Evolution of the Fennoscandian Shield. Elsevier Science B.V., Amsterdam, 481-531.

Luosto, U., Tiira, T., Korhonen, H., Azbel, I., Burmin. V., Buyanov, A., Kosminskaya, I., Ionkis, V. & Sharov, V. 1990. Crust and upper mantle structure along the DSS Baltic profile in SE Finland: Gephys. Jour. Int., 101, 89-110.

Mäkitie, H. & Lahti, S. I. 2001. The fayalite-augite quartz monzonite (1.87 Ga) of Luopa, western Finland, and its contact aureole. In: Mäkitie, H. (ed.) Svecofennian granitic pegmatites (1.86-1.79 Ga) and quartz monzonite (1.87 Ga), and their metamorphic environment in the Seinäjoki region, western Finland. Geological Survey of Finland, Special Paper 30, 61-98.

Nironen, M. 1997. The Svecofennian Orogen: a tectonic model. Precambrian Research 86 (1-2), 21-44.

Nironen, M. 1999. Structural and magmatic evolution in the Loimaa area, southwestern Finland. Bulletin of the Geological Society of Finland 71, 57-71.

Pajunen, M., Airo, M.-L., Wennerström, M., Niemelä, R. & Wasenius, P. 2001a. Preliminary report: The "Shear zone research and rock engineering" project, Pori area, south-western Finland. Geological Survey of Finland, Special Paper 31, 7-16.

Pajunen, M., Airo, M-L., Elminen, T., Niemelä, R., J., Vaarma, M., and Wasenius, P. & Wennerström, M. 2002. Kallioperän rakennettavuusmalli taajamiin. Menetelmänkehitys ja ohjeistus. Geologian tutkimuskeskus, Espoo. Julkaisematon raportti K 21.42 / 2002 / 5. 95 s. (in Finnish).

Pajunen, M., Airo, M.-L., Elminen, T., Mänttäri, I., Niemelä, R., Vaarma, M., Wasenius P. & Wennerström, M. 2006. Tectonic evolution of Svecofennian crust in southern Finland. Geological Survey of Finland, Special Paper. in prep.

Pietikäinen, K. 1994. The geology of the Paleoproterozoic Pori shear zone, southwestern Finland, with special reference to the evolution of veined gneisses from tonalitic protoliths. PhD thesis, Michigan Technological University. 130 p.

Rutland, R. W. R., Williams, I. S. & Korsman, K. 2004. Pre-1.91 Ga deformation and metamorphism in the Paleoproterozoic Vammala Migmatite Belt, southern Finland, and implications for Svecofennian tectonics. Bulletin of the Geological Society of Finland 76, 93-140.

Sederholm, J. J. 1899. Űber eine archäische Sedimentfomation im südwestlichen Finnland und ihre Bedeutung für die Erklärung der Entstehungweise des Grundgebirges. Bulletin de la Commission Géologique de Finlande, 6. 257p.

Sederholm, J. J. 1926. On migmatites and associated pre-Cambrian rocks of southwestern Finland. II. The region around the Barösundsfjärd W. of Helsingfors and neighbouring areas. Bulletin de la Commission Géologique de Finlande, 77. 143 p.

Sederholm, J. J. 1931. On the Sub-Bothnian unfonformity and on Archaean rocks formed by secular weathering. Bulletin de la Commission Géologique de Finlande, 95, 81 p.

Tuisku, P. & Laajoki, K. 1990. Metamorphic and structural evolution of the Early Proterozoic Puolankajärvi formation, Finland - II. The pressure-temperature-deformation-composition path. J. Metamorphic Geol. 8, 375-391.

Vaasjoki, M. & Sakko, M. 1988. The evolution of the Raahe-Ladoga zone in Finland: isotopic constraints. In: Korsman, K. (ed.) Tectono-metamorphic evolution of the Raahe-Ladoga zone. Geological Survey of Finland, Bulletin 343, 7-32.

Väisänen, M., 2002. Tectonic evolution of the palaeoproterozoic Svecofennian orogen in Southwestern Finland. Annales Universitatis Turkuensis, A II, 154. 143 p.

Väisänen, M. & Mänttäri, I. 2002. 1.90 – 1.88 Ga arc backarc basin in the Orijärvi area, SW Finland. Bulletin of the Geological Society of Finland 74, 185-214.

Väisänen, M., Andersson, U. B., Huhma, H. & Mouri, H. 2004. Age of late Svecofennian regional metamorphism in southern Finland and south-central Sweden. The 26th Nordic Geological Winter Meeting, 6.-9.1.2004, Uppsala, Sweden, abstract volume. GFF 126, p. 40.

Wegman, C. E. 1928. Über die Tektonik der jungeren Faltung in Ostfinnland. Fennia 50, 1-22.

Gold exploration and the crustal structure of northern Finland as interpreted from FIRE seismic reflection profiles 4, 4A & 4B

N. L. Patison[1]*, V.J. Ojala[2], A. Korja[3], V. Nykänen[4] & the FIRE Working Group[5]

[1]Geological Survey of Finland, PO Box 77, FIN-96101 Rovaniemi, Finland.
[2]Geological Survey of Finland, PO Box 77, FIN-96101 Rovaniemi, Finland. [3]Institute of Seismology, University of Helsinki, P.O. Box 68, FIN-00014, Helsinki, Finland.
[4]Geological Survey of Finland, PO Box 77, FIN-96101 Rovaniemi, Finland. Email:

[5]FIRE Working Group:
Geological Survey of Finland: E. Ekdahl, I. Kukkonen, R. Lahtinen, M. Nironen, A. Kontinen, J. Paavola, H. Lukkarinen, A. Ruotsalainen, J. Lehtimäki, H. Forss, E. Lanne, H. Salmirinne, T. Pernu, P., Turunen, E. Ruokanen
Institute of Seismology, University of Helsinki: P. Heikkinen, A. Korja, T. Tiira, J. Keskinen
Department of Geosciences, University of Oulu: S.-E. Hjelt, J. Tiikkainen
Sodankylä Geophysical Observatory, University of Oulu: J. Yliniemi
Terramecs Ky: E. Jalkanen
Spetsgeofizika S.E.: R. Berzin, A. Suleimanov, N. Zamoshnyaya, I. Moissa, A. Kostyuk, V. Litvinenko

*Email: nicole.patison@gtk.fi

Keywords: lithosphere, FIRE, gold, Central Lapland Greenstone Belt

The Finnish Reflection Experiment (FIRE) seismic reflection profiles 4, 4A and 4B image a 580-kilometre long section of the northern Fennoscandian Shield to a depth of 80 kilometres (Figure 1). The geological units of ages ca. 3.5 Ga to 1.74 Ga covered by the FIRE profiles include greenstone, granulite, and schist belts modified by complex Paleoproterozoic deformation and magmatic events occurring from 2.5 Ga to the end of widespread Paleoproterozoic thermal activity in the area. The imaged Archean areas (Pudasjärvi Complex and Inari Area) include remnants of the cratonic nuclei of the Fennoscandian Shield (Karelian and Kola Cratons) and of amalgamated exotic terranes. The Paleoproterozoic components include autochthonous and allochthonous components (Peräpohja Schist Belt, Central Lapland Granitoid Complex, Central Lapland Area, and the Lapland Granulite Belt).

The FIRE data suggests Paleoproterozoic rocks in northern Finland can be divided into four belts (a southern, central, northern and western), and the structures separating each can be identified (Patison et al., in press; Figure 2). The southern belt coincides with the rifted (cf. Kohonen & Marmo 1992; Vuollo & Huhma 2005, Lahtinen et al. 2005) southern margin of the Karelian Craton. It is a volcano-sedimentary belt including rock from the southern margin of the Peräpohja Schist Belt to the northern margin of the Central Lapland Area. This belt is preserved as layers stacked by thrusting on two major shear zones with apparent southerly dips (Meltaus and Venejoki Shear Zones). The reflectivity of the Central Lapland Granitoid Complex within the southern belt does not suggest an intrusion-dominated belt, and this area may have a composition comparable with the other Paleoproterozoic belts (Peräpohja Schist Belt and the southern parts of the Central Lapland Area).

The northern belt contains the upper and middle crust of the Lapland Granulite Belt. The southernmost Inari Area is also interpreted as belonging to this belt, as is the Tanaelv zone. The appearance of the Lapland Granulite Belt is generally similar to that described by previous research. However, the base of this belt is terminated by the south-dipping Karelian Craton/Kola Craton boundary and does not extend to the crust-mantle boundary. No evidence is recognised in FIRE profile 4A to support earlier models (e.g., Hörman et al. 1980; Barbey et al. 1984; Krill 1985; Daly et al. 2001) involving a Paleoproterozoic subduction zone beneath the Lapland Granulite Belt. The margin between the Lapland Granulite Belt and Inari Area is recognised as the suture zone between the Karelian and Kola Cratons, and this zone dips to the south. Significant post-collisional extension took place beneath the Inari Area, Lapland Granulite Belt and northern Central Lapland Area.

A western Paleoproterozoic belt containing two upper-crustal layers with apparent westerly dips is likely in westernmost Lapland (FIRE 4B). However, much of the geology imaged in FIRE 4B is problematic to correlate with the geology of the Central Lapland Area, and it can be considered unique to western Lapland.

The real value of the FIRE data for gold exploration is that it allows a detailed interpretation of the crustal architecture of the region. The relationship between bedrock elements can be seen, as can significant deformation structures. Such information is critical for understanding the location of known deposits and for predictive modelling of the role of crustal scale structures in determining mineralised sites. These benefits are illustrated in this presentation using as an example the Central Lapland Greenstone Belt (CLGB).

The Proterozoic CLGB is reminiscent of the late Archean greenstone terrains of the Superior and Yilgarn cratons in terms of scale, lithological diversity, structural architecture, alteration history, and metamorphic grade. Historical gold and base metal production is low. However, research and exploration during past two decades has shown that the belt is prospective for structurally controlled orogenic gold and for Fe-oxide-Cu-Au deposits, and that it has the potential to become a significant gold producing region. Discoveries include the Suurikuusikko gold deposit, the largest undeveloped gold deposit in western Europe with 14.2 million tonnes of estimated probable reserves with an average gold grade of 5.16 grams per tonne (Agnico-Eagle Mines Ltd. media release 06.05.2006).

Our knowledge of the CLGB has been advanced significantly following interpretation of the FIRE data. The FIRE data show that, in comparison with existing bedrock maps of the area, the CLGB is very heterogeneous and contains a number of individual blocks with potentially different origins (Figure 3). These blocks belong to a central Paleoprotozoic belt including the Kittilä Group and other components identified in FIRE 4A. These blocks are in unconformable contact with the rift-related southern belt, and may be (partly) allochthonous as previously proposed (Hanski 1997).

The southern margin of this central ‘belt’ is influenced by two significant structures. The first is the south-dipping Venejoki Shear Zone, a thrust structure relating to stacking of the southern belt. Earlier interpretations assumed that the Sirkka ‘Line’/Sirkka Shear Zone structure represented a major thrust structure in this area. However the FIRE data shows the Sirkka structure to be subordinate to the Venejoki Shear Zone. The second structure is a newly identified (north-dipping) structure at the boundary between the CLGB and southern belt (Kittilä Shear Zone). Relatively younger movements can be identified on the Kittilä Shear Zone, but it displays multiple development stages, and the relationship between it and the Venejoki Shear Zone is complex.

The northern boundary of the CLGB is a south-dipping structure that has experienced reverse movements. The central belt and underlying components of the southern belt are

also structurally separated from the western belt, although the orientation of the boundary structure here is not conclusively resolved.

To date interpretations of the FIRE data have significantly changed conceptions on the geometry of the CLGB. Although the proposed structural evolution (orogenic convergence with opposing tectonic transport directions) of the region is supported by the FIRE data, the newly identified structures require interpretation. The next stage is to understand the implications of these geometries for exploration. Questions include how do these structures and lithology block configurations affect crustal scale fluid flow?, what is the age of deformation features seen in the FIRE profiles, what structures were active during mineralisation?

References

Barbey, P., Convert, J., Moreau, B., Capdevila, R. & Hameurt, J. 1984. Petrogenesis and evolution of an early Proterozoic collisional orogenic belt: The granulite belt of Lapland and the Belomorides (Fennoscandia). Geological Survey of Finland, Bulletin 56, 161-168.

Daly, J. S., Balagansky, V. V., Timmerman, M. J., Whitehouse, M. J., Jong, K., de Guise, P., Bogdanova, S., Gorbatschev, R. & Bridgwater, D. 2001. Ion microprobe U-Pb zircon geochronology and isotopic evidence for a trans-crustal suture in the Lapland-Kola Orogen, northern Fennoscandian Shield. Precambrian Res. 105 (2-4), 289-314.

Hanski, E. J. 1997. The Nuttio serpentinite belt, Central Lapland: An example of Paleoproterozoic ophiolitic mantle rocks in Finland. Ofioliti 22, 35-46.

Hörmann, P. K., Raith, M., Raase, P., Ackermand, D. & Seifert, F. 1980. The granulite complex of Finnish Lapland: petrology and metamorphic conditions in the Ivalojoki-Inarijärvi area. Geological Survey of Finland, Bulletin 308, 95.

Kohonen, J. & Marmo, J. 1992. Stratigraphic correlation concepts within multiple rifted Karelian domain: an example from eastern Finland. In: Balagansky, V. V. & Mitrofanov, F. P. (eds.) Correlation of Precambrian formations of the Kola-Karelian region and Finland. Apatity: Russian Academy of Sciences. Kola Science Centre, 54-65.

Korsman, K., Koistinen, T., Kohonen, J., Wennerström, M., Ekdahl, E., Honkamo, M., Idman, H. & Pekkala, Y. (eds.) 1997. 1:1 000 000 Bedrock map of Finland. Geological Survey of Finland, Espoo.

Krill, A.G. 1985. Svecokarelian thrusting with thermal inversion in the Karasjok-Levajok area of the northern Baltic Shield. In: Geology of Finnmark. Norges Geol. Unders. Bulletin 403, 89-101.

Lahtinen, R., Korja A. & Nironen M. 2005. Proterozoic tectonic evolution. In: Lehtinen, M., Nurmi, P.A. & Rämö, O.T. (eds.) Precambrian Geology of Finland: Key to the evolution of the Fennoscandian Shield. Developments in Precambrian Geology 14, 481-531.

Patison, N.L., Korja, A., Lahtinen, R., Ojala, V.J. & the FIRE Working Group, 2006. FIRE seismic reflection profiles 4, 4A and 4B: Insights into the Crustal Structure of Northern Finland from Ranua to Näätämö. Geological Survey of Finland Special Paper, 43, 161-222.

Vuollo, H. & Huhma, H. 2005. Paleoproterozoic mafic dikes in NE Finland. In: Lehtinen, M., Nurmi, P.A., & Rämö, O.T. (eds.) Precambrian Geology of Finland: Key to the evolution of the Fennoscandian Shield. Developments in Precambrian Geology 14, 195-236.

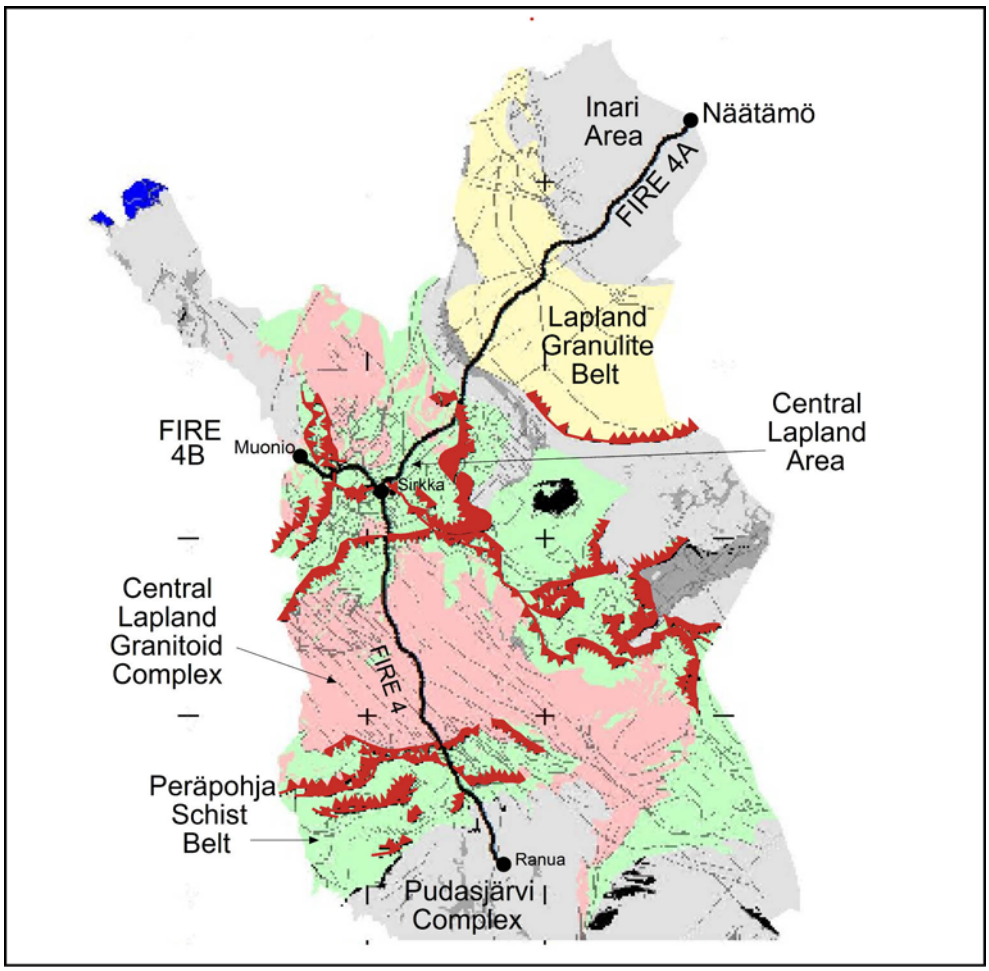

Figure 1. Main geological domains of northern Finland covered by FIRE profiles 4, 4A and 4B (modified after Korsman et al. 1997)

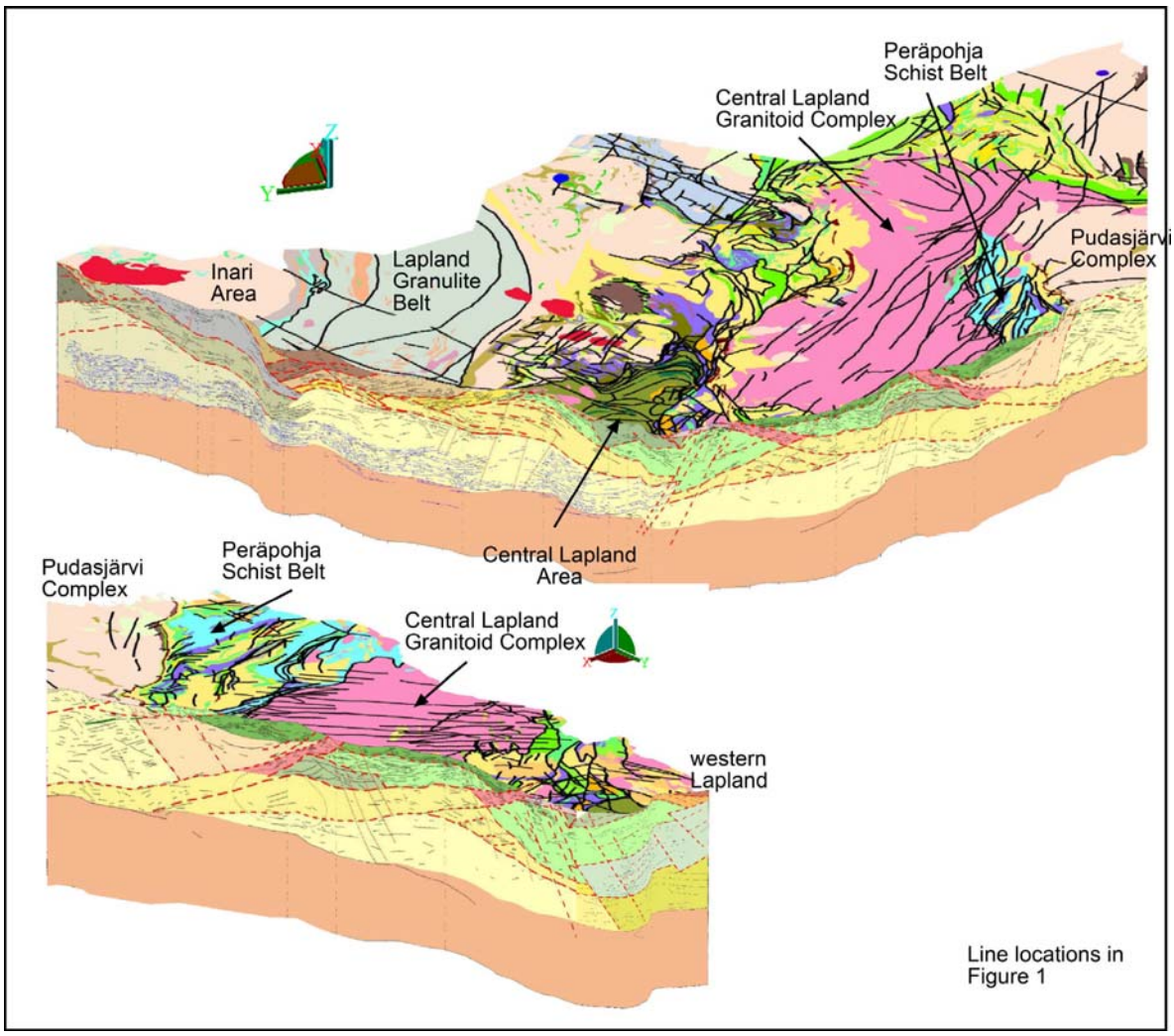

Figure 2. Block diagrams showing the interpretation for FIRE 4 and 4A with a published map (after Korsman et al. 1997) of regional geology. Viewing direction is approximately east. Lower diagram shows the interpretation for FIRE 4 and 4B with a published map (after Korsman et al. 1997) of regional geology. Viewing direction is approximately southwest. Diagrams after Patison et al. (2006)

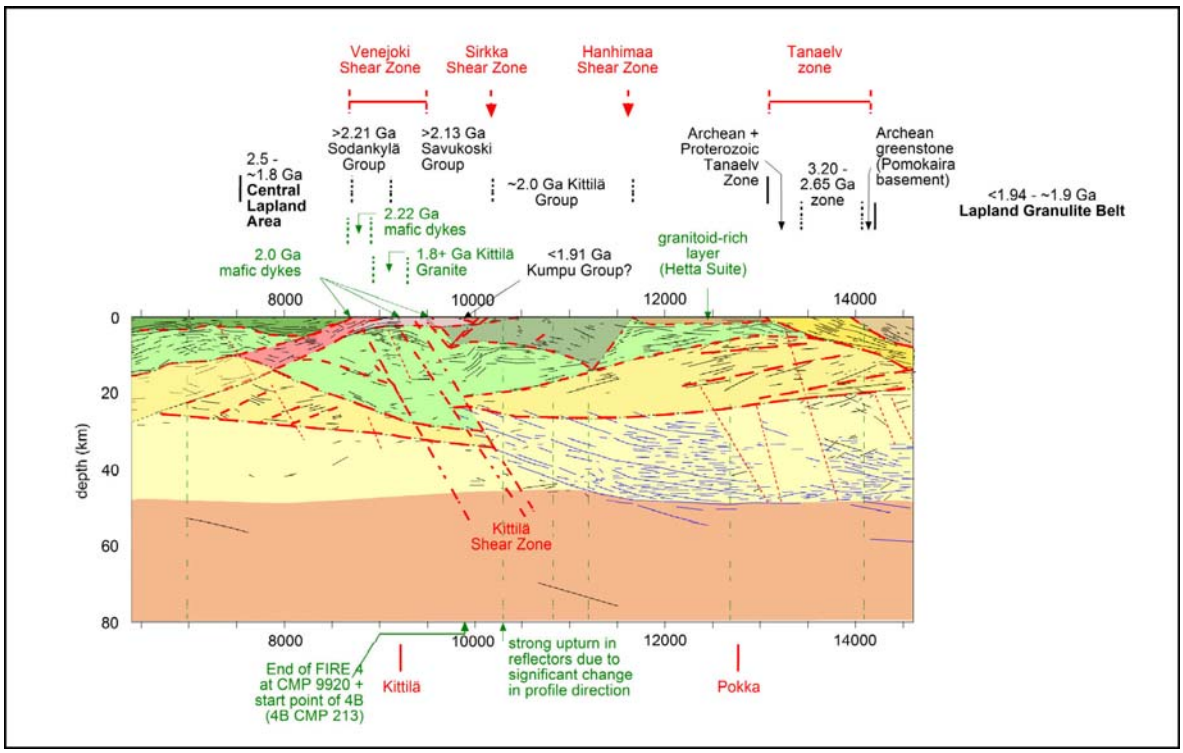

Figure 3. Seismic section interpretation for central Lapland (after Patison et al., 2006)

Upper mantle dynamics and Quaternary climate in cratonic areas: a proposal for an ILP Project

Markku Poutanen[1]* and the National ILP Committee of Finland

[1]Finnish Geodetic Institute, Geodeetinrinne 2, 02430 Masala
*E-mail: Markku.Poutanen@fgi.fi

In Litosphere 2004 meeting in Turku Ilmo Kukkonen raised a question on an interdisciplinary project which would combine several geoscience fields related to the postglacial rebound, upper mantle properties and their causes. This paper gives a short overview and the current status of the proposal.

Keywords: glaciation, Quaternary, post-glacial uplift, climate change, upper mantle, rheology

Aim of the project is to understand the relations between the upper mantle dynamics, mantle composition, physical properties, temperature and rheology, to study the postglacial uplift and ice thickness models, Quaternary climate variations and Weichselian (Laurentian and other) glaciations during the late Quaternary.

Postglacial rebound and the related gravity change in deglaciated areas can be observed with high-resolution geodetic techniques. Geodesy provides accurate measurements of contemporary deformation and gravity change. In Fennoscandian area we have systematic postglacial uplift observations for over than 100 years based on repeated precise levelling, geodetic high-resolution observations of recent movements, and possibilities to monitor postglacial faults in N-Fennoscandia.

In geological and geophysical side we have e.g. kimberlite-hosted mantle xenoliths and thermal and petrological models of the upper mantle. In spite of long and accurate time series and extensive data sets, there exist many open questions in upper mantle dynamics and composition, rebound mechanism and uplift models, ice thickness during the late Quaternary, and Quaternary climate in general. There exist also observational data of ice cover during the Weichselian glaciation and glaciation models, and one can do Palaeoclimatic inversions from deep geothermal data sets.

Questions to be solved include mantle dynamics and mantle composition: are the xenoliths representative, what can infer of mantle fluids from xenoliths, how well can we indicate seismic properties of the mantle from xenoliths and what are the tomographic models of upper mantle. In postglacial rebound one will study the character and mechanism of postglacial uplift, the relation with land uplift and duration of ice cover during the Weichselian, how sensitive is the land uplift for indicated ice free/ice cover periods and response of the gravity field with different ice loads. Finally, there are many open questions on Quaternary climate, like coupling of postglacial uplift models with climatic glaciation models, implications for land uplift and climate and question on new datings of fossils preserved from the last glaciation times.

Proposal is planned to be submitted as an ILP (International Lithosphere Program) program. Project would be linked to ILP project themes:

Theme I: Global change

Theme II: Contemporary dynamics and deep processes.

Project is interdisciplinary (geology, geophysics, geodesy), it has global relevance and potentially wide geographic coverage, it provides new results in basic geosciences, and can

be applied in climate change research. Project is also international. This far there has been announced researchers from Finland, Sweden, Denmark, Germany, UK, and USA. The group is increasing and the preparation phase of the proposal will be late 2006 - early 2007.

Topic has already been accepted as a joint session in the European Geophysical Union (EGU) annual meeting in Vienna, April 2007. The session will be co-organized by Geodesy (G), Geodynamics (GD), Climate: Past, Present, Future (CL), and Geochemistry, Mineralogy, Petrology & Volcanology (GMPV) sections. Deadline of abstracts for the meeting will be in January 2007. Researchers interested in the project are invited to participate the session, and as well take part on the preparation phase of the ILP proposal.

Classification of Finnish bedrock sub-areas using lithogeochemical analysis of Finnish plutonites

Tapio Ruotoistenmäki

Geological Survey of Finland, Betonimiehenkuja 4, P.O. Box 96, FIN-02151 Espoo
Email: tapio.ruotoistenmaki@gtk.fi

Using correlations of geochemical analysis of plutonic rocks of 25 lithological sub-areas of Finland the sub-areas can be classified in groups having characteristic lithogeochemical spectra.

Keywords: Geochemistry, classification, lithological sub-areas, Finland

1. Introduction

In this study 3060 plutonite samples of the lithogeochemical database collected by Lahtinen et al. (2005) are used for grouping and classification of sub-areas of Finnish bedrock. The location of lithological sub-areas (25 in all) and of samples used in this work are shown in Figure 1. The plutonites were chosen, while they are assumed to be less affected by later alteration processes compared to supracrustal rocks and thus better representing the composition of (upper) crust.

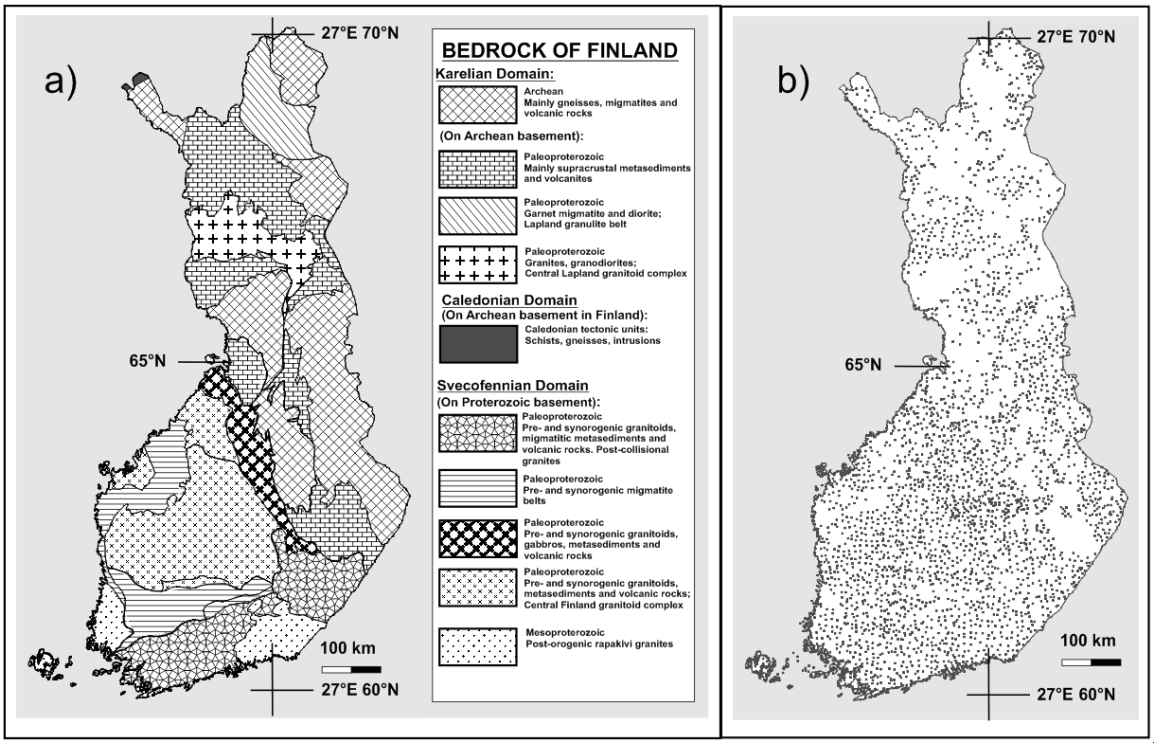

Figure 1. Simplified map of Finnish bedrock (a) (modified from Korsman et al., 1997) and location of plutonite samples used in this work (b).

2. Method and results

The classification of sub-groups was made using the normalized 'in-compatible - compatible' lithogeochemical diagram (termed ‘spectrum’ in the following) suggested by Pearce and Peate (1995). The normalizing was made using the geometric averages of all Finnish plutonites (AFP). Examples of spectra from various sub-areas are given in Figure 2.

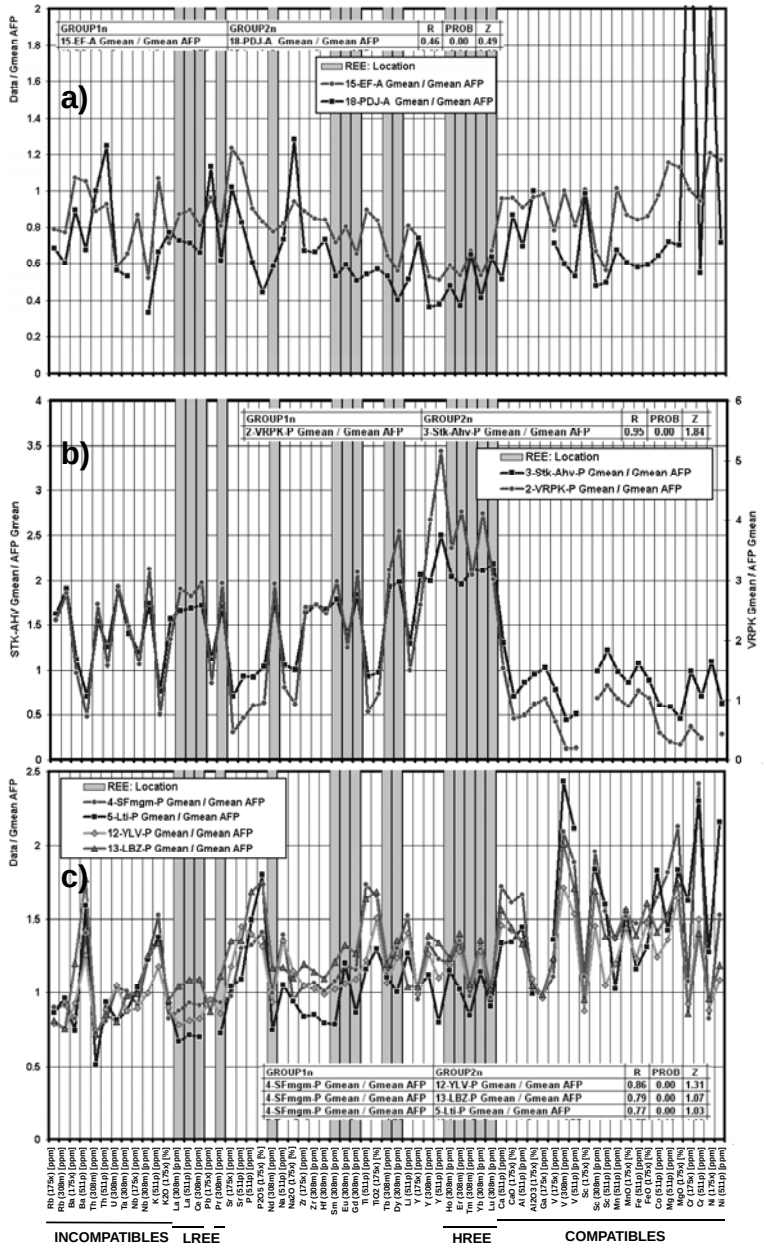

Figure 2. Examples of classification: In (a) is given lithogeochemical spectrum of Archaean Pudasjärvi and East Finland blocks. In (b) is shown characteristics of Proterozoic Viipuri and Satakunta rapakivi and (c) shows the spectra of a group of ore potential Proterozoic central Finland sub-areas having marine affinities. The grey bars show the location of rare earth elements (REE, Light and Heavy).

From Figure 2 it can be seen that Archaean blocks are characterized by relative high LREE (and incompatibles) compared to HREE and increase in compatibles compared to HREE. The spectra of rapakivi samples are complementary to Archaean rocks with increasing LREE - HREE trend and very low compatibles compared to HREE. The spectra of Proterozoic rocks in central Finland are significantly different from both of those above showing relatively constant increase from incompatibles to compatibles.

In this study the lithological sub-areas of Finnish bedrock are grouped by calculating cross-correlations of spectra of all sub-areas. The resulting map of similar lithological sub-groups is shown in Figure 3. In the following is a short summary of the groups:

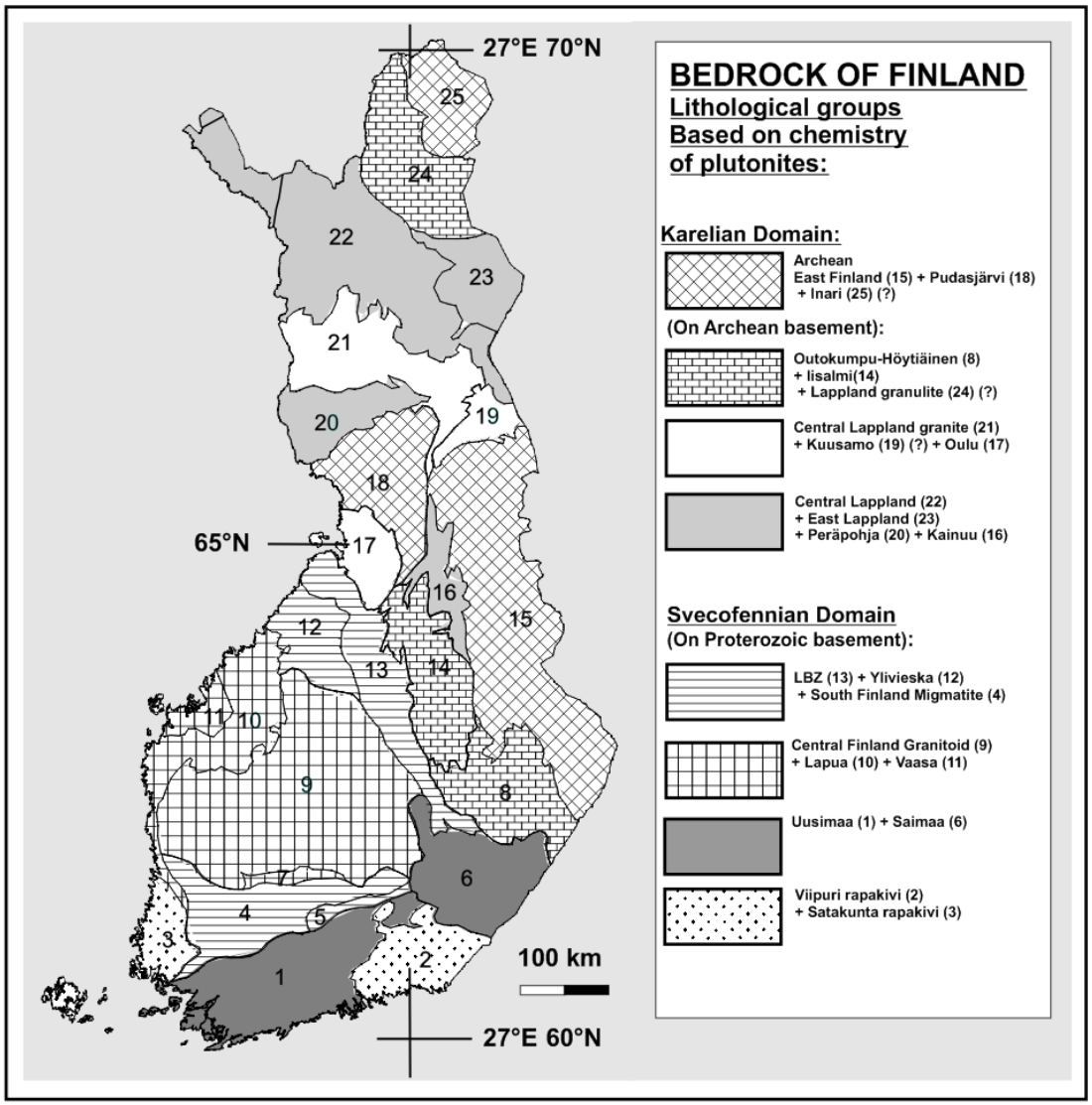

Figure 3. Lithological groups of Finnish bedrock based on chemistry of plutonite samples.

1) Group 1 consist of Proterozoic southern Finland granitoid belt (Uusimaa, #1 in Figure 3) and Saimaa area (#6) close to the Archaean-Proterozoic border. The correlation within these groups is best on the compatible parts of the spectra.

2) Group 2 consists of Proterozoic Viipuri and Satakunta rapakivi sub-areas and their correlation is very good as can be seen from the Figure 2b. Their increasing LREE - HREE trend might refer to their original source of lower crustal garnet-clinopyroxene containing restite while steep Eu and Sr minima refer to upper crust fractionation (above plagioclase stability depth, ca. 40 km) and thus uplift before rapakivi-fractionation.
3) Group 3 consists of Proterozoic ore potential sub-groups whose metasedimentary rocks have marine affinities: Southern Finland migmatite (#4 and #5), Ladoga-Bothnian bay - zone (LBZ, or Pielavesi area, #13) and Ylivieska area (#12). These groups have very coherent chemical spectra, as can be seen from the Figure 2c and their genesis can be assumed to be similar, though not necessarily connected. The Eu and Sr maxima, Y minimum and increasing trend to compatibles refer to more mafic, deeper crustal sources below plagioclase stability field.
4) Group 4 is closely connected with the Proterozoic central Finland granitoid (#9) having island arc affinities. Apparently the Lapua arc (#10) and Vaasa sub-area (#11) are closely genetically connected with this block. Their spectra are relative flat with slight increase from incompatibles to compatibles. The amplitudes vary between the groups, but the locations of the peaks correlate very well. High Rb, Th, U and low Eu, Sr refer to upper crust (above ca. 40 km) fractionation.
5) Group 5 consists of Archaean sub-areas of which the Iisalmi block (#14) and Outokumpu-Höytiäinen sub-area (#8) are on the Archaean-Proterozoic border. They appear to have both Archaean and Proterozoic characteristics. E.g. their LREE-HREE –ratio is close to 1 as that of Proterozoic central Finland granitoid group above. Their high Eu and (partly) Sr refer to deeper crustal fractionation. The Lappland granulite belt (#24) has similar peaks with these areas, though amplitude is different and it is certainly not genetically linked with the southern blocks.
6) The Archaean eastern Finland area (#15) and Pudasjärvi area (#18) have characteristic 'Archaean spectrum' (having also adakitic characteristics) as described earlier and shown in Figure 2a. The northern Finland Inari block (#25) have some similarities with these, but is not genetically linked with them.
7) The groups characterized with Paleoproterozoic supracrustal metasedimentary rocks (Kainuu, #16; Peräpohja, #20; central Lappland, #22 and castern Lappland, #23) correlate relatively well, though also variations exist Thus, their evolution processes might be connected in some degree.
8) The group 8 consist of central Lappland granitoid (#21), and Oulu area granitoids (#17) correlating strikingly well referring to their similar genesis due to remelting and refractionation of pre-existing Archaean crust. The few plutonites in Kuusamo (#19) area have also similarities with them (possibly connected with central Lappland granitoid), though they are too sparse to make any definitive conclusions.

The above study refers that the lithology of Finnish bedrock can further be classified in separate sub-groups using plutonite rock chemistry, which gives possibilities and new ideas for analyzing the connections between the blocks, their genesis and evolution.

References

Korsman, K. (ed.); Koistinen, T. (ed.); Kohonen, J. (ed.); Wennerström, M. (ed.); Ekdahl, E. (ed.); Honkamo, M. (ed.); Idman, H. (ed.); Pekkala, Y. (ed.) 1997. Suomen kallioperäkartta = Berggrundskarta över Finland = Bedrock map of Finland 1:1 000 000. *Geological Survey of Finland. Special maps 37 ISBN 951-690-691-5.*

Lahtinen, R., Lestinen, P., Korkiakoski, e:, Savolainen, H., Kallio, E., Kahelin, H., Hagel-Brunnström, M., Räisänen, M. 2005. Rock geochemistry database: Test version 0.7 (2.6.2005). Guide for the users. Geological Survey of Finland. Unpublished report.

Pearce, J.A., and Peate, D.W., 1995, Tectonic implications of the composition of volcanic arc magmas: Annual Review of Earth and Planetary Sciences, v. 23p. 251-285.

Keurusselkä impact structure – preliminary geophysical investigations

H. E. Ruotsalainen[1], S. Hietala[2], S. Dayioglu[4]*, J. Moilanen[3], L. J. Pesonen[4] and M. Poutanen[1]

[1]Finnish Geodetic Institute, P.O. Box 15, FI-02430 Masala, Finland
[2]Kiveläntie 2 B 13, FI-42700, Keuruu, Finland
[3]Vuolijoentie 2086, FI-91760 Säräisniemi, Finland
[4]Solid Earth Geophysics, Dept. of Physical Sciences, University of Helsinki, P.O. Box 64, FI-00014 Helsinki, Finland
*E-mail: Selen.Dayioglu@helsinki.fi

The Keurusselkä impact structure in Central-West Finland was discovered by Hietala and Moilanen in 2003. They observed shatter cones in situ and boulders in the Keuruselkä lake area. The shatter cone findings locates about 5 km west from the Bouguer anomaly minimum. Four gravity profiles were measured across the impact structure in 2005 to better determine the location of the structure. Inside the 25-26 km gravity low (8-9 mgal) there exits a 2-3 mgal local gravity high, which may indicate the central uplift of fractured, shocked but deep eroded granite target rock.

Keywords: Impact structure, shatter cones, gravity profiles

1. Shatter cones and ancient Precambrian bedrock

The Keurusselkä impact structure (62º09'N, 24º38'E) was discovered by Hietala and Moilanen in 2003 (*Hietala and Moilanen, 2004a*), (*Hietala and Moilanen., 2004b*). They found shatter cones in bedrock and boulders (Fig. 1.). The structure is deeply eroded like the Yarrabubba Granite impact structure in Western Australia (*MacDonald et al. 2003*). There is no clear evidence of circular structure in topography. Preliminary studies related to breccias are going on (*Moilanen, 2006*). This may indicate, that we see only deeply eroded roots of the central uplift of the fractured granite target rock with its boulders.

Figure 1. A rock boulder showing shatter cones, Harmaaniemi Keuruu (Pesonen et.al. 2005). Photo: J. Moilanen

2. Bouguer gravity low – a possible indicator of an ancient Precambrian impact structure

Residual negative gravity anomaly is an indicator of the density decrease (porosity increase) of bedrock. Bouguer anomaly field together with magnetic anomaly may reveal morphological forms of embedded structures (crater diameter, depth, simple/complex crater). By microgravimetry we may find even smaller structures like fracture zones in bedrock.

Bouguer gravity data of the Finnish Geodetic Institute showed suitable gravity low for impact structure (*Pesonen et al. 2005*). The shatter cone area locates appr. 5 km west of the local Bouguer gravity low. The Bouguer gravity data was too sparse to locate the impact structure well enough related to the shatter cones, and therefore we decided to make more gravity measurements across the structure.

3. Gravity profiles across the shatter cone area and Bouguer gravity low

The Finnish Geodetic Institute carried out gravity measurements with Scintrex CG5 Autograph relative gravimeter in 2005. Positioning was made with a Leica SR530 GPS receiver using VRS technique and the Geotrim VRS network (*www.geotrim.fi*). Ellipsoidal heights were converted to orthometric ones by using the Finnish geoid model FIN2000 (*Ollikainen, 2002*). Gravity values were tied to the First Order Gravity Network of Finland (FOGN) (*Kiviniemi, 1964, Kääriäinen and Mäkinen, 1997*). Fig. 2. shows measured gravity stations along profiles across the impact structure (*Ruotsalainen et al., 2006*).

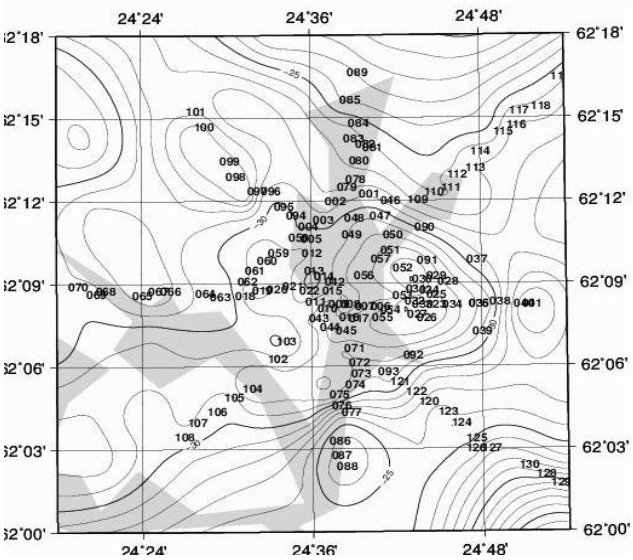

Figure 2. Gravity profiles across Keurusselkä impact structure. Numbering shows the location of the gravity stations. Bouguer anomaly contours are drawn using the gravity data base of the Finnish Geodetic Institute.

The new gravity profile data does not change the location of the Bouguer gravity low. The new data reveals details, which were undetectable in earlier sparse gravity data. There is a Bouguer minimum (right arrow in Fig. 3a) and associated gravity high (left arrow in Fig

3a) within the minimum, which is consistent with impact model. Aeromagnetic anomaly data does not show clear correlation with gravity data and shatter cone findings (Fig 3b.)(Pesonen et al. 2005).

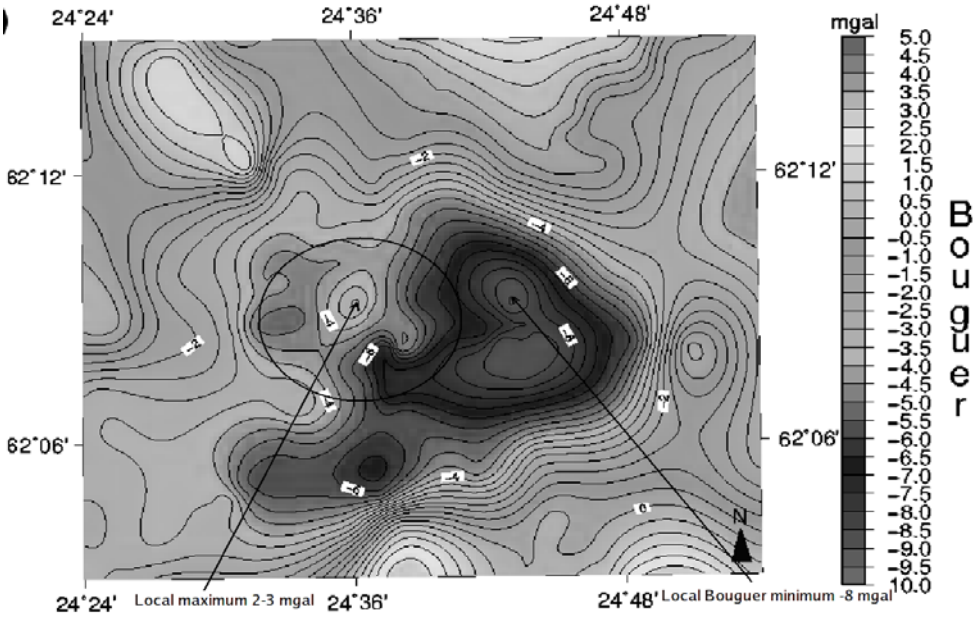

Figure 3 a. Local Bouguer gravity anomaly of the Keurusselkä impact structure (Ruotsalainen, 2006, Dayioglu, 2006). Shatter cones are found mainly inside the ellipsoidal area (Moilanen, 2005).

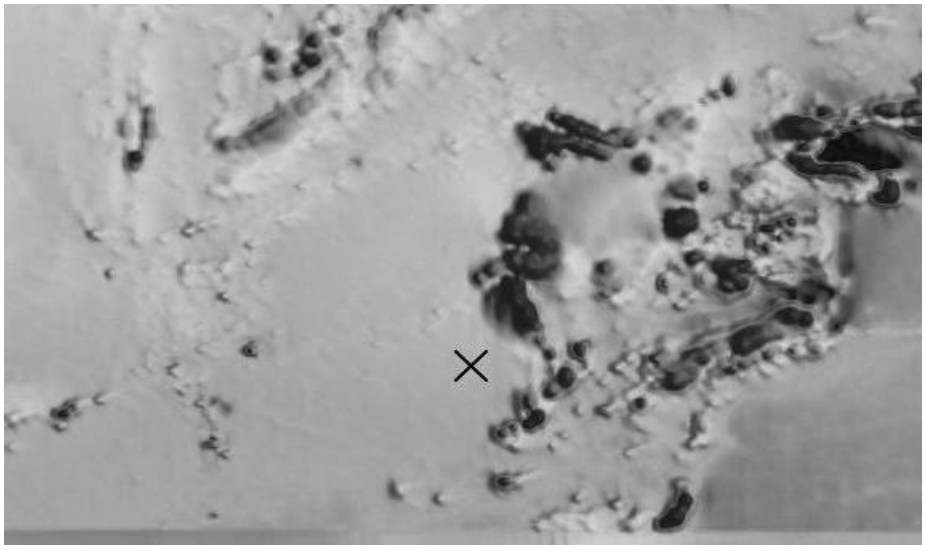

Figure 3 b. Aeromagnetic anomaly from impact structure area. Cross is approximately in the Bouguer anomaly minimum (Aeromagnetic map, courtesy of Hanna Leväniemi, Geological Survey of Finland).

.

4. Plans for new geophysical investigations of the structure

In the global impact data base (http://www.unb.ca/passc/ImpactDatabase/), there are no middle sized impact structures, which are of Precambrian age. The closest one is the Jänisjärvi structure in Russian Karelia (age ca. 600 Ma, D ~22 km; *Salminen et al., 2005*). Keurusselkä structure provides a unique case to study the erosional history of the crust in Central Finland. Three seismic lines (FIRE, SVEKA and FENNIA) which closely passes through the structure will help in interpreting the details of the crust (e.g., *Kukkonen et al., 2002*) (Fig. 4).

The age of the Keurusselkä impact structure is still undefined. Since shatter cones seems to be present in all Palaeoproterozoic (1.88 Ga) rock types of the region, the age of the structure must be younger than ~1.88 Ga (*Pesonen et al. 2005*). Morphological and field studies show that the Keurusselkä structure possibly represent deeply eroded remnants of a large complex impact structure where the erosion level is below the original crater floor . Radiometric and paleomagnetic methods (^{39}Ar- ^{40}Ar) will be used to estimate the age of the impact. The latter method is useful in estimating the amount of uplift of the crust due to impact.

There are also three boreholes south of the shatter cone findings. They can offer more precise data of the shock effect in the bedrock. There is need for more gravity measurements and other geophysical investigations. The project will continue in 2007-2010 partly funded by the Academy of Finland.

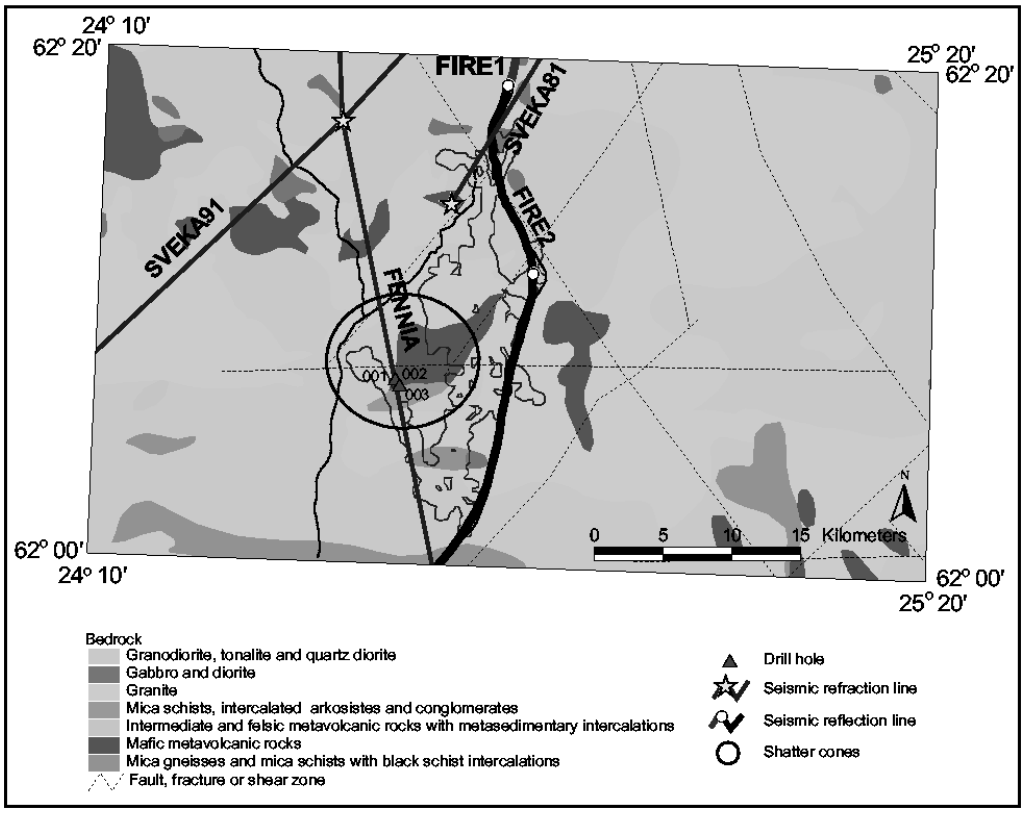

Fig. 4. The three seismic profiles (SVEKA, FENNIA, FIRE) crossing the Keurusselkä area (Geological map by M. Nironen, GSF).

Acknowledgments

We express our sincere thanks to Risto Koho – a member of the amateur geologist club Keuruun Kivipiiri. He helped us by arranging necessary facilities during the gravity measurements in Keurusselkä lake area.

References

Abels, A., Plado J., Pesonen, L.J. Lehtinen M., 2002. The Impact Cratering Record of Fennoscandia. Pp 1-58 in Plado, J., Pesonen, L. J. (Eds.), *Impacts in Precamprian Shields*, *Springer Verlag, Berlin. 336 pp*.

Dayioglu S., 2006. Metsähovin lähiympäristön painovoimakartoitus ja sen tulkinta. Master of Science Thesis, University of Helsinki, (in Finnish).

Grieve, R.A.F and Pesonen, L. J., 1996. Terrestrial impact craters: their spatial and temporal distribution and impacting bodies. In H. Rickman and M. J. Valtonen (eds.) Earth, Moon and Planets, Vol. 72, Nos 1-3, 357-376.

Hietala S. and Moilanen J., 2004a. Keurusselkä – a new impact structure in Central Finland, LPSC XXXV, Houston, Texas, USA (cdrom).

Hietala, S. and J. Moilanen, 2004b. Keurusselkä on muinainen osuma. Tähdet ja Avaruus, 1/2004, 24-29. Magazine of Finnish Amateur Astronomy Society URSA (In Finnish).

MacDonald F.A., Bunting J.A. and Cina S. A., 2003. Yarrabubba, Western Australia: A large, deeply eroded, ancient impact structure in the Yilgarn craton. Lunar and Planetary Science XXXIV.

Kiviniemi A. 1964. The First Order Gravity Net of Finland, Publication of the Finnish Geodetic Institute No 58, Helsinki, Finland

Kukkonen, I., Heikkinen, P., Ekdahl, E., Korja, A., Hjelt, S.-E., Yliniemi, J., Berzin, R. and FIRE Working Group, 2002. Project FIRE: Deep Seismic Reflection Sounding in Finland 2001-2005. In edition: Lahtinen, R., Korja, A., Arhe, K., Eklund, O., Hjelt, S.-E., and Pesonen, L.J. 2002 (Eds.). Lithosphere 2002 - Second Symposium on the Structure, Composition and Evolution of the Lithosphere in Finland. Programme and Extended Abstracts, Espoo, Finland, November 12-13, 2002. Instit. Seismology, Univ. Helsinki, Report S-42, s. 67-70.

Kääriäinen J. and Mäkinen J., 1997. 1979 –1996 gravity survey and results of the gravity survey of Finland 1945 – 1996. Publication of the Finnish Geodetic Institute, No 125. Kirkkonummi, Finland.

Moilanen J., 2005 Personal communication.

Moilanen J., 2006 Personal communication.

Ollikainen M., 2002: The Finnish Geoid model FIN2000. Proc. of the 14th General Assembly of the Nordic Geodetic Commission, Espoo. Report of the Finnish Geodetic Institute, Kirkkonummi, Finland, pp. 111-116

Pesonen L.J., Hietala S., Poutanen M., Moilanen J., Lehtinen M. and Ruotsalainen H., 2005. The Keurusselkä meteorite impact structure, Central Finland: geophysical data. XXII General Assembly of the Finnish Geophysical Society, Helsinki 19.-20.5.2005.

Plado, J., Pesonen, L. J., and V. Puura, 1999. The effect of erosion on gravity and magnetic signatures of complex impact signatures: geophysical modellings and applications. In Dressler, B.O. and Sharpton, V. L. (eds) Large Meteorite Impacts and Planetary Evolution, Geological Society of America, Special Paper 339, 229-239.

Ruotsalainen H. E., S. Hietala, M. Poutanen, J. Moilanen and L. J. Pesonen, 2006. Gravity survey of the Keurusselkä meteorite impact structure. Proc. of the 27. Nordic Geolocigal Winter Meeting. Geological Society of Finland.

Salminen, J., Donadini, F., Pesonen, L.J., Masaitis, V.L., and Naumov, M., 2005. Paleomagnetism and petrophysics of the Jänisjärvi impact structure, Russian Karelia. Meteoritics and Planetary Science, (in print).

Paleomagnetic and petrophysical investigation of the Mesoproterozoic monzodioritic sill, Valaam, Russian Karelia

J. Salminen* and L.J. Pesonen

Division of Geophysics, P.O. Box 64, 00014 University of Helsinki, Finland
*E-mail: johanna.m.salminen@helsinki.fi

A paleomagnetic investigation of the Valaam monzodioritic sill, Russian Karelia (U-Pb ages ~ 1458 Ma, Rämö et al., 2001) was undertaken in an attempt to provide new key pole for Baltica and to test the proposed joint drift history of Baltica and Laurentia in between 1.83 and 1.26 Ga.

Keywords: paleomagnetism, supercontinent Hudsonland

Supercontinents have played a key role in the evolution of the Earth's surface at least since the Archean times. Amalgamation and following break up of supercontinents have had major geological consequences; such as diversification of life, unique climatic conditions including numerous glaciations, global changes in ocean chemistry, and long-lived mantle convection patterns (e.g. *Condie, 2000*; *2004*; *Karlström et al., 2001; Meert, 2002; Pesonen et al., 2003; Rogers and Santosh, 2002; Zhao et al., 2003; 2004* and references therein). There are geological and paleomagnetic evidences that since the Mesoproterozoic three supercontinent assemblies (Rodinia ca. 1050 – 750 Ma, Gondwana ca. 550 – 400 Ma and Pangea ca. 350 – 165 Ma) have existed (*Pesonen et al., 2003* and references therein). Evidences for the pre-Rodinia supercontinents become more controversial as the age of the geological formations increase due to paucity of paleomagnetic data and inherent dating problems. However, most cratonic blocks show evidences of collisional events occurring between 2.1 and 1.8 Ga, which has led many researchers to propose that Mesoproterozoic supercontinents, such as Hudsonland (also known as Columbia), existed in the Early Proterozoic (e.g. *Condie, 2004; Meert, 2002; Pesonen et al., 2003; Rogers and Santosh, 2002; Zhao et al., 2003; 2004* and references therein). Moreover, the temporal and compositional overlap between the interorogenic episodes in W Baltica and the magmatism in E Laurentia supports models of a Mesoproterozoic supercontinent, which included Baltica and Laurentia (e.g. *Åhäll and Connelly, 1998*). The time interval 1.8 – 1.2 Ga is a time period of anorogenic events, rather than major orogenic period. The 1.6 – 1.5 Ga is a period of tectonic stability that reflects cartonization of new lithosphere, maybe due to growth of lithospheric mantle (*Karlstrom et al., 2001*). Periods 1.7-1.6 Ga and 1.55 – 1.35 Ga were the time for intracartonic bimodal A-type magmatism, which involved granites and associated anorthosites and related tectonism (e.g. *Karlstrom et al., 2001; Åhäll and Connelly, 1998*). During the 1.3 – 1.1 Ga period major events were rifting and formation of dykes and sills.

Recently several variations of assemblies of supercontinent Hudsonland have been presented, which differ from Rodinia. For example, *Pesonen et* al (2003) have suggested that Laurentia and Baltica lived together more than 600 Ma (from ca. 1.83 to ca. 1.20 Ga), forming together with Amazonia and perhaps with some other continents, like Australia, the core of this Early Proterozoic supercontinent. Several other authors have suggested a variety of configurations and lifecycles for this supercontinent (e.g. *Karlström et al., 2001; Meert, 2002; Zhao, 2004 and references therein).*

In order to shed light into the question of existence of Mesoproterozoic supercontinent Hudsonland we have carried out paleomagnetic study on Valaam monzodioritic sill in the NW part of the Fennoscandian Shield, in Russian Karelia. The opportunity is excellent since the new U-Pb dating of the Valaam sill yield ages of 1459 ± 3 Ma and 1457 ± 2 Ma (*Rämö et al., 2001*), which are nearly coeval with St Francois Mnt (1476 ± 16 Ma), Michicamau Intrusion (1460 ± 5 Ma), Harp Lake Complex (1450 ± 5 Ma) and other parts of Belt Supergroup formations in Laurentia. This compatibility provides a unique case for testing the proposed long lasting (1.8 - 1.2 Ga) unity of Baltica and Laurentia and this way the existence of supercontinent Hudsonland. The Valaam sill (ca. 1.46 Ga) provides a needed material for a paleomagnetic study since its magnetization is stable and there is a lack of key poles in between 1.5 and 1.3 Ga for Baltica (*Buchan et al., 2000; Pesonen et al., 2003*).

A paleomagnetic investigation of the Valaam monzodioritic sill, Russian Karelia (U-Pb ages ~ 1458 Ma, *Rämö et al., 2001*) was undertaken in an attempt to provide new key pole for Baltica and to test the proposed joint drift history of Baltica and Laurentia in between 1.83 and 1.26 Ga. In total 46 oriented hand samples were collected on the main island for paleomagnetic and rock magnetic studies. Three component of remanent magnetization were obtained. *The first one* is low coercivity component of viscous origin with the direction similar to the direction of the present Earth's field at the sampling site. The *low to intermediate unblocking /coercivity* component **B** (D = 39.3°, I = 25.8°, α_{95} = 7.5°) corresponds to a paleomagnetic pole Plat. = -34.6°, Plong. = 342.0° (A_{95} = 5.9°). The *high unblocking/coercivity* component **A** (D = 43.4°, I = -14.3°, α_{95} = 3.3°) corresponds to a paleomagnetic pole Plat. = 13.8°, Plong. = 166.4° (A_{95} = 2.4°).

Rock magnetic and SEM studies revealed that the main carrier of the magnetization of component A is coarse grained primary titanomagnetite, with varying Ti-content. Component A is interpreted to be of primary origin and it provides a new well dated key pole for Baltica. Whereas, secondary magnetization, component B, is carried by ilmenohematite and with comparison to Baltica's apparent polar wander path (APWP) it yields ages of ca. 290-280 Ma.

References:

Åhäll, K. I., Connelly, J., 1998. Intermittent 1.53 – 1.13 Ga magmatism in western Baltica; age constraints and correlations within a postulated supercontinent. Precambrian Res. 92, 1-20.

Buchan, K. L., Mertanen, S., Park, R. G., Pesonen, L. J., Elming, S.-Å., Abrahamsen, N., Bylund, G., 2000. Comparing the drift of Laurentia and Baltica in the Proterozoic: the importance of key paleomagnetic poles. Tectonophysics 319, 167-198.

Condie, K. C., 2000. Episodic continental growth models: afterthoughts and extensions. Tectonophysics 322, 153-162.

Condie, K. C., 2002. Breakup of a Paleozoic supercontinent. Godwana Res. 5, 41-43.

Condie, K. C., 2004. Supercontinents and superplume events: distinguishing signals in the geologic record. Physics of the Earth and Planetary Science 146, 319-332.

Karlström, K. E., Åhäll, K.-I., Harlan, S., Williams, M. L., McLelland, J., Geissman, J. W., 2001. Long-lived (1.8 – 1.0 Ga) covergent orogen in southern Laurentia, its extensions to Australia and Baltica, and implications for refining Rodinia. Precamb. Res. 111, 5-30.

Koistinen, T., Stephens, M. B., Bogatchev, V., Nordgulen, Ø., Wennerström, M., Korhonen, J., 2001. Geological map of the Fennoscandian Shield, scale 1:2 000 000. Geol. Surv. Finland, Norway and Sweden and the North-West Department of Natural Resources of Russia.

Meert, J. G., 2002. Paleomagnetic evidence for a Paleo-Mesoproterozoic supercontinent Columbia. Gondwana Res. 5, 207-215.

Pesonen, L. J., Elming, S.-Å., Mertanen, S., Pisarevsky, S., D'Agrella-Filho, M. S., Meert, J. G., Schmidt, P.W., Abrahamsen, N., Bylund, G. 2003. Paleomagnetic configuration of continents during the Proterozoic. Tectonophysics 375:289-324.

Rämö, O. T.; Mänttäri, I.; Vaasjoki, M.; Upton, B. G. J.; Sviridenko, L., 2001. Age and significance of Mesoproterozoic CFB magmatism, Lake Ladoga region, NW Russia. In: Boston 2001: a geo-odyssey, November 1-10, 2001: GSA Annual Meeting and Exposition abstracts. Geol. Soc. Am. Abstracts with Programs 33 (6), A-139.

Rogers, J. J. W., and Santosh, M., 2002. Configuration of Columbia, a Mesoproterozoic supercontinent. Gondwana Res. 5, 5-22.

Zhao, G., Sun, M., Wilde, S., Li, S., 2003. Assembly, accretion and breakup of the Paleo-Mesoproterozoic Columbia supercontinent: records in the North China craton. Gondwana Res. 6, 417-434.

Zhao, G., Sun, M., Wilde, S. A., Li, S., 2004. A Paleo-mesoproterozoic supercontinent: assembly, growth and breakup. Earth-Sci. Rev. 67, 91-123.

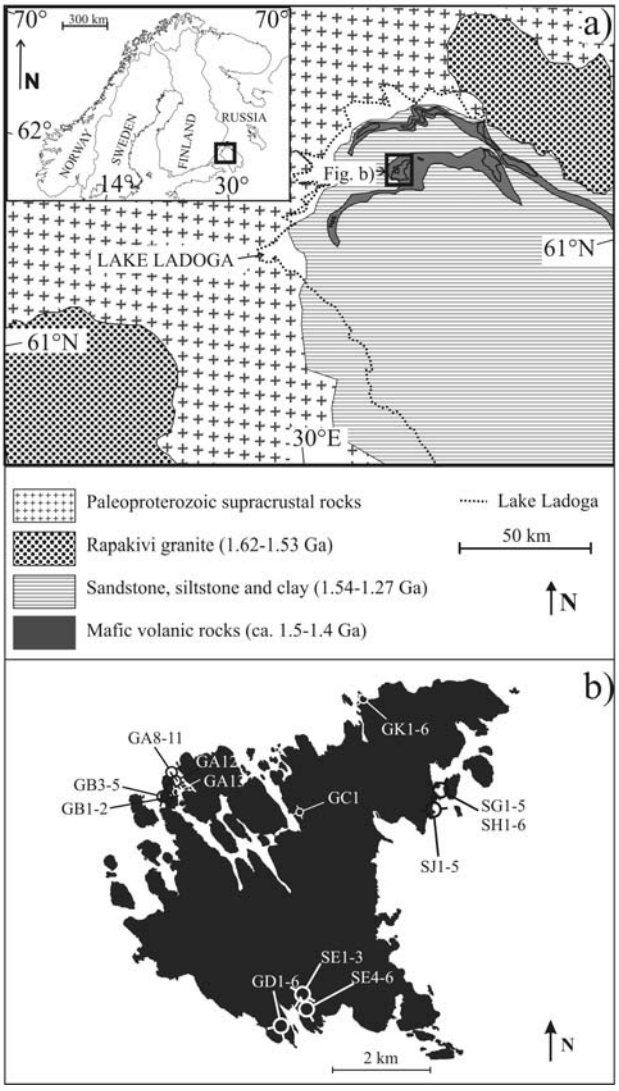

Figure 1. The insert shows the study area (rectangle), Lake Ladoga in Russian Karelia. A) Simplified geological map of the Lake Ladogan area (after *Koistinen et al. 2001*). The Valaam Island is enclosed by a rectangle, B) Sampling sites of the monzodioritic sill of the Valaam Island, where G denotes monzodioritic samples and S syenitic samples.

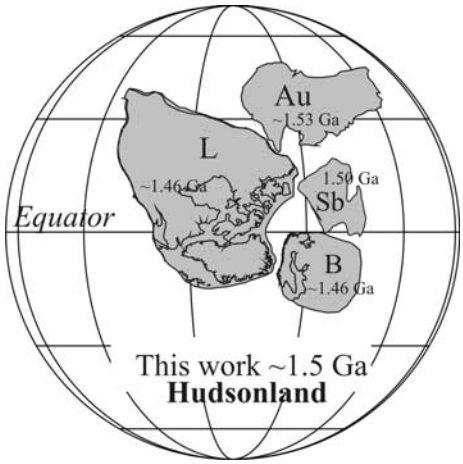

Figure 2. Paleomagnetic reconstruction of Hudsonland based on data from Valaam sill (this work). Data for other continents after *Pesonen et* al. (2003).

3-D structure and physical properties of the Kuhmo Greenstone Belt (eastern Finland): constraints from gravity modelling and seismic data and implications for the tectonic setting

H. Silvennoinen[1]* and E. Kozlovskaya[2]

[1]Department of Physics, Division of Geophysics, POB 3000, FIN-90014, University of Oulu, Finland
[2]Sodankylä Geophysical Observatory/Oulu Unit, POB 3000, FIN-90014, University of Oulu, Finland

*E-mail: hanna.silvennoinen@oulu.fi

The objective of our research was to obtain a 3-D density model of the Kuhmo greenstone belt in the eastern Finland. Although the surface position of the belt is relatively well constrained by geological studies, its 3-D structure is poorly known. The knowledge of the 3-D structure of the belt is essential to understand the formation of the belt. We estimated seismic velocities and density of the main rock types of the belt from modal mineralogy. The result of the modeling suggests that the main rocks types of the belt have low seismic velocities and high densities. We also applied 3-D gravity modeling and inversion in order to obtain the 3-D density structure of the belt. Our result demonstrated that the Kuhmo greenstone belt is a surface structure that is 10 - 12 km wide with depth less than 7 km and average density of $2.84 \cdot 10^3$ kg/m^3.

Keywords: 3-D gravity modeling, Archaean, Fennoscandian Shield, Greenstones, Density

1. Introduction

Archean greenstone belts around the world are of great interest for geologists as they often host gold and other valuable metal deposits. However, the origin and development of these belts is still strongly debated, particularly with regard to the role of plate tectonic (e.g. collision and subduction) processes and magmatic (e.g. diapirism, plume magmatism) processes in evolution of the Archean lithosphere (*Benn et al., 2006; de Wit, 1998; Hamilton, 2003*). As a result, the 3-D structure and physical properties of the greenstone belts may differ significantly from each other. For example, large diapiric batholiths and synclinal greenstone keels may suggest that diapirism was an important tectonic process in the Achaean Slave Province (*Bleeker, 2002*); whereas in the Superior Province the linear distribution of belts suggests that accretion tectonics (i.e. plate tectonics) may have dominated (c.f. *Stott, 1997*). Therefore, studying of the 3-D structure of the greenstone belts is important not only for the purpose of ore exploration, but for understanding the early history of the Earth as well.

2. The data and constraints for modelling

In our research we used the digital map of the Bouguer anomaly compiled by the Geological Survey of Finland from the results of gravity measurements owned by the Finnish Geodetic Institute (*Korhonen et al., 2002*). The average linear spacing of the observations stations is 5 km and the Bouguer anomaly map used in this study is defined on 10 x 10 km^2 regular grid (*Korhonen et al, 2002; Elo, 1997; Kääriäinen and Mäkinen, 1997*). The digital map of the surface bulk density was compiled from results of laboratory measurement of density of rock samples collected all over Finland (*Korhonen et al., 1997*). As the sampling points were not evenly distributed, particularly in the relatively small area considered in this study, the density map was obtained by interpolation of the raw data to a regularly spaced grid of 2 km x 2 km. The density values in the nodes of the grid were obtained as weighted sum of density at points closest to the node and also by taking into

account the boundaries of the geological structures from 1:1 000 000 geological map of Finland (*Pirttijärvi, 2005*).

To constrain the seismic velocities and density of the Kuhmo greenstone belt and to find the explanation of the apparent disagreement between low seismic velocities and the gravity high, we used petrophysical data from the borehole RO-KR1 in Romuvaara area (*Anttila et al., 1990*). The surrounding area is mainly comprised of late Archean banded amphibolites, migmatites, granitoids and the metavolcanic rocks and metasediments of the Kuhmo greenstone belt. The borehole is almost 1 km deep and samples were taken from the drill core with quite even distances between them. To eliminate the influence of random non-lithological factors like porosity and seismic anisotropy, we estimated the physical properties of main types of rocks of the belt from their modal mineralogy using Monte-Carlo simulation. As it was demonstrated by *Kozlovskaya et al.* (*2004b*), such a modelling makes it possible to estimate the influence of certain minerals on density and seismic velocities. The Monte-Carlo method was used to calculate the seismic velocities and densities for the selected rocks. First 10 000 samples of each rock type were calculated with a random number generator. Then the elastic parameters, the seismic P- and S-wave velocities, and the density were calculated for each rock using equations. The density-velocity relations by *Sobolev and Babeyko* (*1994*) for anhydrous magmatic rocks that did not undergo metamorphic reactions can be used as such reference curves. *Kozlovskaya et al.* (*2004b*) demonstrated that rocks with high content of Ca-rich plagioclase have higher values of V_p and lower density than the reference density-velocity relationship, while high content of amphibole results in lower values of V_p and higher density compared to the reference relationship. As can be seen from Fig. 4, all the rocks analysed have lower seismic velocities (in particular, P-wave velocities) and higher densities than the reference curve. This suggests that tonalitic rocks are widely spread within the belt, while other rocks are subordinate. In addition, the rocks of the belt have generally lower P- and S-wave seismic velocities, but higher densities than the velocities and density in the middle crust beneath the belt (6.30-6.65 km/s, 3.68-3.8 km/s and 2.7-2.85 $\cdot$ 10^3 kg/m^3, respectively) (*Kozlovskaya and Yliniemi, 1999*). This indicates their different composition and implies that the belt does not continue to the middle crust.

3. Modelling and inversion

For 3-D gravity modelling and inversion we used an interactive computer program for visualization and editing of large-scale 3-D models (Bloxer) and a gravity modelling and inversion software (Grabox) based on a 3-D block model (*Pirttijärvi et al., 2004*). The starting model was made by selecting about 150 km x 130 km x 16 km rectangular block from the existing regional 3-D density model for central and southern Finland (*Kozlovskaya et al., 2004a*). The regional model does not include such shallow features as the Kuhmo greenstone belt. The regional model was also used to calculate the effect of the densities beside and below the research area. In this way features that affected the research area from outside could be eliminated from the data. The selected part of the regional 3-D model was approximated by 8 km x 8 km x 2 km blocks. To fit the observed Bouguer anomaly, a 4 km deep body with constant density representing the belt was added to the model. The density value of 2.84 $\cdot$ 10^3 kg/m^3 was selected basing on result of 2-D gravity modelling in (*Kozlovskaya and Yliniemi, 1999*). In their work they tested multiple density values and found this value to give best results in their 2-D model along the SVEKA'81 profile. As it was shown in Section 5, this value corresponds to the average density of

tonalities. It is also in agreement with the data about the density of rocks of the belt obtained from laboratory measurements (*Elo et al., 1978, Elo, 1997*). The shape and position of the body were defined from the geological map. The final model was made by trial and error method using Grablox program to compute the Bouguer anomaly of the model and to compare it to the observed Bouguer anomaly.

After the model was made by trial-and-error as good as possible, inversion was tried in order to improve the fit to the observed Bouguer anomaly. However, inversion of the gravity data is generally non-unique; therefore, we applied different methods of gravity data inversion in order to evaluate the stability and uniqueness of the solutions obtained. The program Grablox uses two major inversion methods, namely, singular value decomposition (SVD) and Occam inversion (*Hjelt, 1992*). In each method three possible ways to parameterise the model (height, density and height + density inversions) are available. The parameters regulate the maximal change of density of the blocks and define whether the inversion should give more importance to minimizing the data error or to the model roughness. The strength of the smoothing is controlled by so called F-option (factor), that may take values between 0 and 1.

4. Conclusions

Petrophysical modelling demonstrates that the main rocks types of the Kuhmo greenstone belt have lower seismic velocities (in particular, P-wave velocities) and higher densities than the density-velocity relationship by *Sobolev and Babeyko* (*1994*) selected as a reference curve. This can be explained by high content of amphibole, biotite and muscovite. This specific modal mineralogy explains the gravity high and relatively low seismic velocities in the area of the Kuhmo greenstone belt.

The rocks of the belt have generally lower P- and S-wave seismic velocities, but higher densities than the velocities and density in the middle crust beneath the belt. This indicates their different composition and implies that the belt does not continue to the middle crust.

The average density of the surrounding rock west of the belt differs only slightly from the density east of the belt ($2.69 \cdot 10^3$ kg/m^3 and $2.72 \cdot 10^3$ kg/m^3, respectively). Therefore, the difference in regional Bouguer anomaly west and east of the belt is explained by the trend produced by the Moho uplift. This verifies the previous results by *Kozlovskaya and Yliniemi* (*1999*).

Based on both forward modelling and inversion, the Kuhmo Greenstone Belt is a surface structure that is 10-12 km wide with depth less than 7 km and average density of $2.84 \cdot 10^3$ kg/m^3. The belt has no deep "root" in the middle crust and lower crust. Values of the depth to the lower boundary of the belt obtained in various inversion trials did not vary significantly.

References

Anttila, P. (ed.), Ahokas, H., Front, K., Hinkkanen, H., Johansson, E., Paulamäki, S., Riekkola, R., Saari, J., Saksa, P., Snellman, M., Wikström, L., Öhberg, A., 1990. Final disposal of spent nuclear fuel in Finnish bedrock – Romuvaara site report. *Posiva 99-11*. Posiva Oy, Finland.

Benn, K., Mareschal, J.-C., Condie, K. (Ed.), 2006. Archean geodynamics and environments. Geophysical monograph 164. American Geophysical Union. United States of America. 320 pp.

Bleeker, W., 2002, Archean tectonics: a review, with illustrations from the Slave craton. Geological Society of London, Special Paper 199, 151-181.

de Wit, M.J., 1998. On Archean granites, greenstones, cratons and tectonics—does the evidence demand a verdict? Precambrian Research, 91, 181-226.

Elo, S., Puranen, R., Airo, M., 1978. Geological and areal variation of rock densities, and their relation to some gravity anomalies in Finland. GeoScrifter, 10, 123-164.

Elo, S., 1997. Interpretation of the gravity map of Finland. Geophysica 33(1), 51-80.

Hamilton, W.B., 2003, An alternative Earth. GSA Today, 13, 4-12.

Hjelt, S.-E., 1992. Pragmatic inversion of geophysical data. Springer –Verlag. Germany. 262 pp.

Korhonen, J., Säävuori, H., Kivekäs, L., 1997. Petrophysics in the crustal model program of Finland. In: Autio, S. (Ed.), Geological Survey of Finland, Current Research 1995-1996, GSF, Special Paper 23, 157-173.

Korhonen, J.V., Aaro, S., All, T., Elo, S., Haller, L.Å., Kääriäinen, J., Kulinich, A. Skilbrei, J.R., Solheim, D., Säävuori, H.,Vaher, R., Zhdanova, L. and Koistinen, T. 2002. Bouguer Anomaly Map of the Fennoscandian Shield 1 : 2 000 000. Geological Surveys of Finland, Norway and Sweden and Ministry of Natural Resources of Russian Federation.

Kozlovskaya, E., Yliniemi, J., 1999. Deep structure of the Earth's crust along the SVEKA profile and its extention to the north-east. Geophysica, 1-2, 111-123.

Kozlovskaya, E., Elo, S., Hjelt, S.-E., Yliniemi, J., Pirttijärvi, M., SVEKALAPKO STWG, 2004a. 3D density model of the crust of southern and central Finland obtained from joint interpretation of SVEKALAPKO crustal P-wave velocity model and gravity data. Geoph . J. Int., 158, 827-848.

Kozlovskaya, E., Janik, T., Yliniemi, J., Karatayev, G., Grad, M. 2004b. Density-velocity relationship in the upper lithosphere obtained from P- and S-wave velocity models along the EUROBRIDGE'97 wide-angle reflection and refraction profile and gravity data. Acta Geophysica Polonia, 52,4, 397-424.

Kääriäinen, J. and Mäkinen, J., 1997. The 1979-1996 gravity survey and results of the gravity survey of Finland. Publications of the Finnish Geodetic Institute, 125, 24 p.

Pirttijärvi M., 2005. Petrock - Lithologically weighted interpolation of petrophysical data. User's Guide. Report: Q16.2/2005/1. Geological Survey of Finland.

Silvennoinen, H. and Kozlovskaya, E., 2006. 3-D structure and physical properties of the Kuhmo Greenstone Belt (eastern Finland): constraints from gravity modelling and seismic data and implications for the tectonic setting. Journal of Geodynamics. (In print.)

Sobolev, S.V. and Babeyko, A.Y., 1994. Modeling of mineralogical composition, density and elastic wave velocities in anhydrous magmatic rocks. Surveys in Geophysics, 15, 515-544.

Stott, G.M., 1997. The Superior Province, Canada. In: M. DeWit and L.D. Ashwol (ed.). Greenstone Belts. Oxford Monographs on Geology and Geophysics, no. 35, p. 480–507.

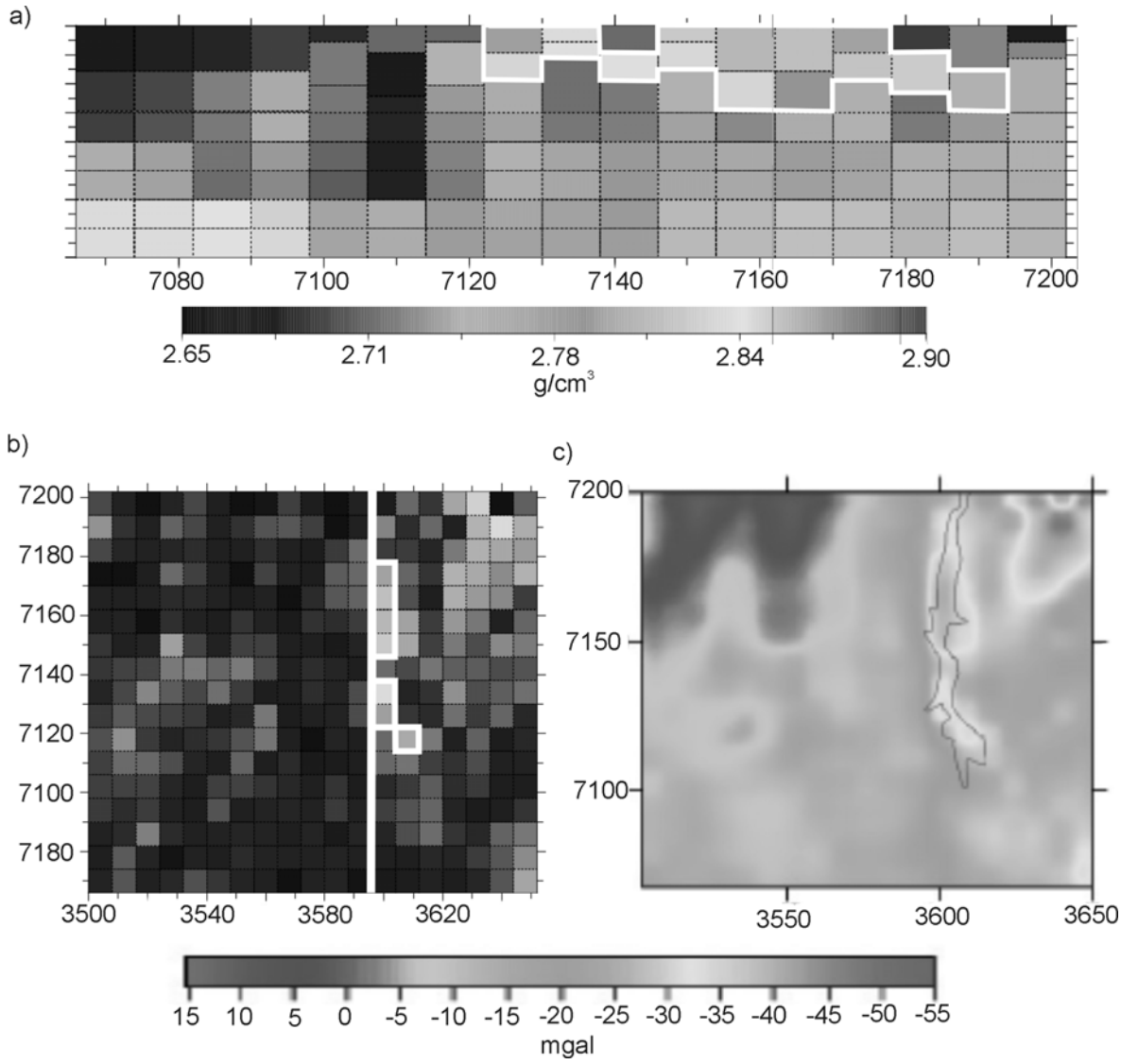

Figure 1. One example of the density models obtained with inversion. Subplot (a) is the surface density map and Subplot (b) a vertical section in north-south direction marked in Subplot (a) with white line. Also borders of the modelled greenstone belt have been marked with the white line in Subplots (a) and (b). Subplot (c) is the Bouguer-anomaly calculated from the model. The borders of the Kuhmo greenstone belt from 1:10 000 000 geological map of Finland have been marked in Subplot (c) with black line.

Three-dimensional visualization of FIRE seismic reflection sections

Topias Siren[1]* and Ilmo Kukkonen[1]

[1]Geological Survey of Finland, P.O Box 96, FI-02151 Espoo, Finland
*E-mail: topias.siren@gtk.fi

We are developing easy-to-use three-dimensional models of the FIRE (Finnish Reflection Experiment) seismic reflection data to be used in GTK web pages. The objective in the present project is to build models, which are accessible in as many interfaces as possible. Important interfaces are the standard web browsers, and currently the models are accessible with Internet Explorer using an ActiveX Surpac Minex 3D Stream Control plug-in. The visualization is done using the Surpac Vision program from Surpac Minex Group.

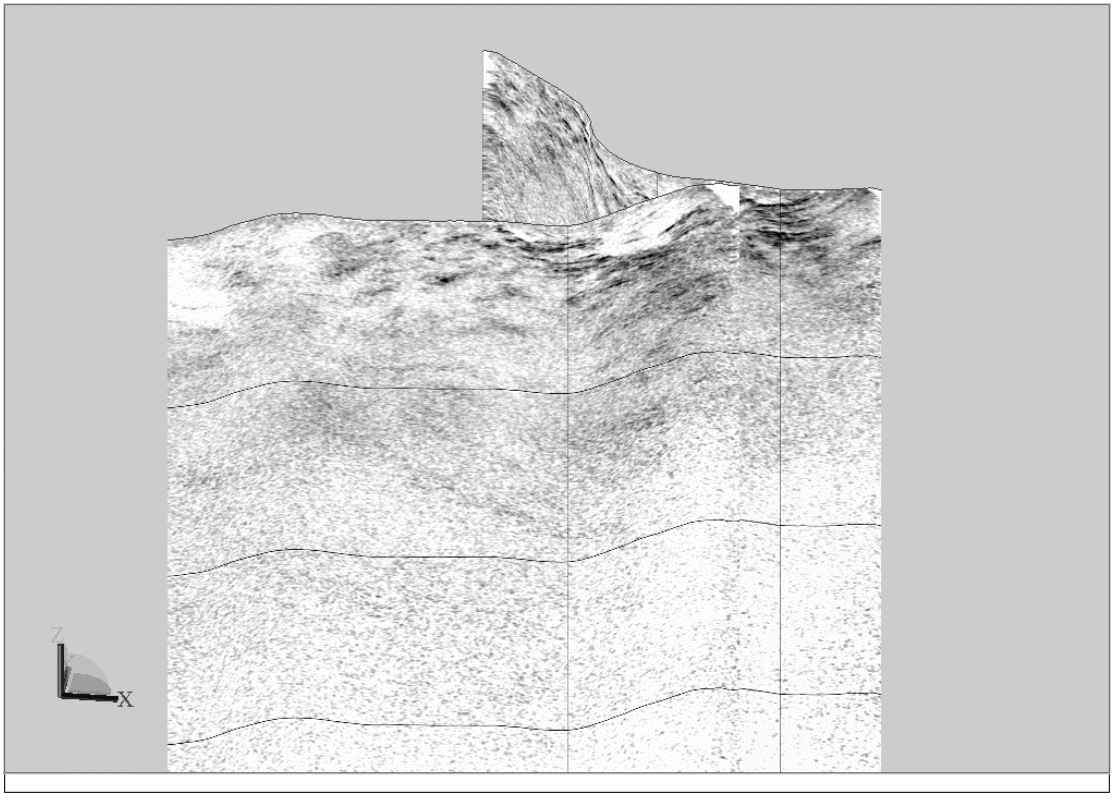

Figure 1. 3D image of the crossing between FIRE 3 and FIRE 3A in eastern Finland. The depth of the section is about 60 km. Ratio between vertical and horizontal is 1:1. (for FIRE data description and first interpretations, see Kukkonen and Lahtinen, 2006).

This kind of an interface design allows the users to examine seismic reflection data easily without complicated programs and tedious procedures. A sser examining the data is easily able to zoom in and out, as well as rotate the image and move within the model freely in real-time. Easy accessibility of the 3D model also narrows the gap between scientists,

students and public as everyone is able to access the content without expensive programs and extensive knowledge.

Two-dimensional surface maps can also be attached to the model to illustrate the relationships between subsurface features and, for instance, aeromagnetic data or geological maps. This helps to perceive the three-dimensional relationships and shapes fast and creates a new usage to the acquired data.

In the Lithosphere 2006 meeting, we will demonstrate 3D FIRE images in the GTK web pages.

Reference

Kukkonen, I.T. and Lahtinen, R. (eds.), 2006. Finnish Reflection Experiment FIRE 2001-2005. Geological Survey of Finland, Special Paper 43, 247 p.

Orogenic processes and mineralization through time – some general concepts and comparisons with FIRE 3 and 3A reflection seismic interpretation

Peter Sorjonen-Ward

Geological Survey of Finland, PO Box 70211, Kuopio, Finland
Peter.Sorjonen-Ward@gtk.fi

Likely similarities and differences between Archean and younger mineralizing processes, and orogenic architecture of some mineralized terrains are briefly reviewed, with emphasis on the Yilgarn craton. Comparisons are then made with respect to crustal scale interpretations of the FIRE 3 and FIRE 3A

Keywords: Finland, Yilgarn, Archean, Paleoproterozoic, seismic, architecture, mineral systems evolution, gold mineralization.

1. Were Archean geologic processes and mineral systems inherently different from younger those of the younger Earth?

When studying geodynamic controls on mineralization, we need both empirical data on the distribution and magnitude of ore deposits throughout Earth history, and theoretical considerations of potential variations in fundamental earth processes in space and time. Expressed in another way, if we define an ore deposit as the result of a highly efficient metal enrichment process driven by a hydrothermal or magmatic event, then have boundary conditions controlling such events changed over time? Answers to this question depend largely on the scale of the system under consideration, and the relative importance of the mantle to crustal mineralising processes. For example, has the role of the mantle been relatively passive, in terms of simply regulating heat flux, and hence thermal regime, rheology and fluid flux in intracrustal mineral systems? Or is the mantle lithosphere more actively involved in mineralizing processes in the crust, through transfer of metals or fluids?

There are three principal sources of information from which we may infer that Archean lithosphere is compositionally distinct and formed under a different thermal regime. Firstly, statistical studies of garnets from kimberlite xenoliths have been used to infer a subtle but potentially significant difference in the composition and hence buoyancy of Archean subcontinental lithospheric mantle compared to Proterozoic and Phanerozoic mantle lithosphere (Poudjom-Doumani et al., 2001). Secondly, the abundance of komatiitic magmatism, with its implications for a distinctive Archean style of nickel mineralization, is interpreted as evidence for somewhat – though not radically – higher ambient temperatures for the Archean asthenosphere (Arndt, 2001.) Thirdly, depending on preferred models for the rate of growth of continental lithosphere, the preferential transfer of incompatible elements, notably K, Th and U from mantle to crust must have a significant impact on partitioning of radiogenic heat production between mantle and crust, and hence crustal rheology as well (Sandiford and Maclaren, 2002; Riegenauer-Lieb et al., 2006). A complex, if not causal feedback between these three phenomena is likely. For example, conductive thermal modeling of the decay of an anomaly due to plume impingement at the base of the crust at 2700 Ma would be consistent with the generation of widespread

anatexis in the lower and middle crust at 2650-2630 Ma (Hobbs et al., 1998), which agrees well with available geological constraints in the two most extensively mineralized Archean terranes – the Norseman-Wiluna belt of the Yilgarn Craton and the Abitibi belt of the Superior Craton. Therefore, potential contrasts between the composition and behaviour of modern and Archean lithosphere should be evaluated within the context of ambient thermal regime. Moreover, there are examples where Archean lithosphere has been modified by melt infiltration and metasomatism during lithospheric extension, as testified by the Mesozoic to Cenozoic history of the North China craton. This is incidentally the only example – perhaps except for the contemporary Wyoming craton and western North America – where significant post-Archean gold mineralization is found within an Archean terrrain.

It is implicit from the above observations that at least gold mineralization in Archean terrains shows a spatial association with areas subjected to anomalous lithospheric heat flux. Global analysis of the distribution and setting of gold deposits through time moreover reinforces the correlation with convergent margin subduction zones and particularly with terrains involving rapid lithospheric growth and accretion (Goldfarb et al.,, 2001; Groves et al., 2005; Leahy et al., 2005). The crucial role of water and the hydrosphere in initiating and sustaining plate tectonics, through hydration of oceanic lithosphere (Fyfe, 1990) and the distinctive chemical signatures of late Archean sanukitoid plutonic complexes (Martin, Halla) further suggests that we ought to consider similarities between late Archean and modern processes, instead of emphasizing differences. While the rheology and strength of the deep crust may have been very sensitive to an enhanced mantle heat flux and radiogenic heat production in late Archean time (cf. Ridley 1992), metamorphic and mineral deposit studies indicate that upper crustal geotherm was indistinguishable from those of modern terrains (Bickle, 1978). The existence of crustal scale strike-slip shear zones (Sleep, 1982), and deposition and deformation of the Witwatersrand sequence as a foreland basin also testify to the stability and strength of at least some cratonic domains during late Archean time.

2. Mineral systems in relation to orogenic architecture and evolution

We may conclude from the above discussion that - except for processes sensitive to atmospheric and oceanic redox state - the mineral endowment of any given orogenic terrain is not primarily a function of age. Instead, we may expect mineralization to be the result of dynamic interaction between external boundary conditions – thermal and far-field stress regime, including rate, direction and duration of plate convergence – and the inherited or evolving internal thermal and material properties of the orogen, such as presence or absence of an inherited basement structure, the architecture of passive margin sequences, and the distribution of fertile material for fluid release and partial melting. Optimal conditions for the formation of regional scale and pluton-centered hydrothermal systems, as well as stratiform basin-hosted deposits, occur when thermal and chemical gradients are initiated and maintained within a structural framework that promotes metal extraction, efficient transport and focussing of fluids and magmas and ultimately, ensures deposit preservation.

The increasing availability of deep crustal seismic surveys for many orogenic terrains of different age, combined with an understanding of kinematic and thermal evolution, provides us with new opportunities for comparing mineral endowment and prospectivity in relation to large scale lithospheric processes (Drummond et al., 2000b). Although it may

not be possible to extract an unambiguous geological event history from seismic data, can we use results from known mineralized terrains to nevertheless define favourable structural architectures which are inherently more favourable for the formation and preservation of mineral deposits?

We may define two fundamental collisional orogenic architectures, in terms of whether the polarity of subduction is away from the orogen, or beneath the orogen (Cook and Varsek, 1994). Depending on degree of coupling and decoupling within the crust or between crust and mantle, we may further distinguish two general types of fold belt profiles: (1) asymmetric, foreland migrating wedges with various combinations of imbricates, duplexes and antiformal stacks, and (2) doubly vergent profiles, with either tectonic wedges, backthrusts and triangle zones, or conversely, divergent thrusts leading to pop-up wedges. Another important variable is obliquity of convergence, or more probably, changes in convergence vector, which may have a significant effect on thermal regime and fluid production (cf. Goldfarb et al., 2001). A critical feature in all of these architectures is, by analogy with traps in petroleum systems, the potential exists for creating fault-bounded domains of differential uplift and overpressuring beneath relatively impermeable units that act as seals to contain hydrothermal systems.

Foreland-propagating fold and thrust belt architecture is evidently favourable for fluid migration and formation of relatively low temperature zinc mineralization in deforming sedimentary basins but may be less favourable for formation and long-term preservation of orogenic deposits, if associated with rapid uplift and exhumation. On the other hand, the architecture of doubly vergent deformation (Koons 1990) and tectonic wedging (Jamison 1993) has the potential to provide uplift in combination with efficient fluid transfer, including deep penetration of meteoric fluids (Craw et al. 2001), at the same time maintaining effective impermeable seals and promoting focussing, circulation and retention of fluids within a middle crustal environment during orogenic deformation (Sorjonen-Ward et al., 2002).

The Yilgarn craton of Western Australia provides useful insights into the relationship between orogenic gold mineralization and crustal architecture, with both asymmetric imbrications and excellent examples of doubly vergent tectonic wedging and crustal decoupling (*Drummond et al. 2000a; Sorjonen-Ward et al., 2002*). For example, beneath the highly mineralized Kalgoorlie region, there is a prominent subhorizontal reflective zone that appears to represent an effective mechanical decoupling between the upper crust, perhaps corresponding to the late orogenic brittle-ductile transition. Above this level, the upper crust deformed in a very heterogeneous manner, accompanied by uplift and erosion, while below it, the middle and lower crust, which displays a distinctly different asymmetric tectonic imbrication. A corollary of this interpretation is that middle crustal deformation zones facilitated melt transfer from the lower crust to higher levels, giving rise to sheeted granitic complexes at the base of the greenstone sequences, at conditions approximating the brittle-ductile transition, at the same time providing an appropriate source for late orogenic mineralising fluids.

3. Comparisons with Archean and Paleoproterozoic structures in seismic reflection profiles FIRE 3 and FIRE 3A

The FIRE 3 and FIRE 3A deep seismic profiles form a combined traverse across the transition zone from the Archean Karelian craton to Paleoproterozoic Svecofennian lithosphere. Apart from several steep discrete features which may represent episodic brittle

reactivation of older structures, the overall seismic fabric is considered to record the original Archean and Paleoproterozoic crustal architecture. Several crustal domains can be delineated, based on a combination of known geological constraints and patterns of seismic reflectivity, representing four principal geodynamic zones.

Geodynamic zone 1. Archean rocks at the eastern end of Profile FIRE 3 have been thermally overprinted by Svecofennian orogeny but there is no penetrative Paleoproterozoic deformation. Accordingly, seismic fabric may be interpreted as a record of Neoarchean orogenic processes. The two greenstone belts in the profile do not correlate with strong reflectivity contrasts, either at surface or depth, but the distribution and orientation of some reflectors and an extensive transparent zone in the upper ten kilometres is consistent with field evidence for late orogenic E-NE vergent deformation associated with emplacement of potassic migmatites and monzogranite plutons. Below this level, seismic fabric is more homogeneous, with a Moho discernible at around 40 km and is in this respect appears typical for undisturbed Archean lithosphere and correlates well with other sections through the Karelian craton;

Geodynamic zone 2. Paleoproterozoic rifting and basin subsidence may be inferred in the Höytiäinen Domain from a moderately W-dipping discordance in reflectivity that projects to the surface at the Archean –Proterozoic unconformity. There is however some ambiguity as to whether an asymmetric extensional fault system would have dipped eastwards, beneath the craton, instead of westwards, as favoured by earlier models. Eastwards dipping reflectors can be identified, although some at least appear to be relatively late orogenic features. An eastwards dipping system is plausible, and would be appropriate for extensional exhumation of the Jormua and Outokumpu subcontinental mantle lithosphere during eventual continental breakup. On the other hand, reactivation of westwards dipping extensional faults is in accordance with inversion of the rift sequence, including an inferred antiformal stack to a depth of nearly 10 km is consistent with inversion of the rift basin and emplacement over the Archean foreland;

Geodynamic zone 3. A broad zone, across the Outokumpu, Suvasvesi, Kuopio and Unnukka domains, within which the FIRE 3A profile is oblique to structural trends is characterized at the surface by allochthonous Paleoproterozoic and Archean basement, disrupted by NW-SE strike-slip shear systems and bivergent thrusting, accompanying emplacement of granitoids, some of which were derived from Archean crust. Discrete granitoid plutons are clearly imaged as transparent zones, and down-plunge projections from areas to the north of the profile imply the presence of thoroughly reworked Archean crust beneath the Outokumpu region. The seismic fabric in this area is thus attributed to complex interaction between thrusting and strike-slip shear systems, with maximum compressive direction subparallel to the buried craton margin;

Geodynamic zone 4. The Svecofennian section of the FIRE 3+3A traverse, within the Unnukka, Äänekoski-Perho, Kaustinen and Kokkola domains is characterized by a series of prominent reflective bands that have a gentle to moderate southerly dip gently southwards to Moho depths in the plane of section. These could be interpreted as accretion of metasediments beneath a W-facing magmatic arc, in which case many of the features would have originated at 1.89-1.87 Ga. Alternatively the structure could represent post-magmatic crustal scale imbrication, with a NNW vergence being appropriate for late orogenic deformation, and potentially correlated with events between 1.84-1.80 Ga in southern Finland. This interpretation would also imply that this whole region was already a rigid plate capable of transmitting and sustaining collision stresses by 1.85 Ga.

If we attempt to compare these crustal scale geodynamic zones with examples from other mineralized terrains in other cratons, we can at least make some simple first order statements. The seismic character of the Archean terrain in eastern Finland along the FIRE 3 profile is more reminiscent of a deeper crustal level or more intense thermal reworking than the architecture inferred beneath the most highly mineralized terrain in the Yilgarn craton. Indeed the seismic patterning and geological constraints are more appropriate for the Southern Cross Province rather than Eastern Goldfields Province. By way of contrast, the geological diversity and structural framework of the Lapland greenstone belt, including doubly vergent deformation represents a closer analog for the latter terrain.

The architecture and kinematic history of the craton margin (Geodynamic zones 2 and 3) is in principal similar to mineralized terrains such as the NE Pacific during the Mesozoic, in terms of a change in kinematic framework oblique to the former craton margin, with the emplacement of late orogenic plutons. At present however, there is little evidence of widespread pluton-related or shear-hosted mineralization in this region, although this may depend on how we view the transition to the Central Finland Granitoid Complex and Bothnia (Geodynamic zone 4 above), including the adjacent Skellefte district in Sweden. Though transecting a Paleoproterozoic terrain, the FIRE 3A profile shows a distinct subhorizontal reflective zone, separating crustal layers with different seismic patterning, just as in the case of the Yilgarn seismic surveys. However, in the case of the FIRE 3a profile, the upper and lower crustal layers share a distinctly uniform N-NW vergent structural asymmetry. We may therefore combine these structural constraints, together with characteristics of known mineral deposits in the region and results of other crustal scale geophysical studies (eg. Korja et al., 1993), to develop more refined exploration strategies.

References

Arndt, N. T., 2001. How hot was the Archaean mantle? *In: Cassidy, K. F., Dunphy, J. M. & VanKranendonk, M. J. (Eds.), 4th International Archaean Symposium, 24-28 September 2001, Perth, Western Australia, Extended Abstracts. AGSO – Geoscience Australia, Record 2001/37, 5.*

Bickle, M. J., 1978. Heat loss from the Earth: a constraint on Archaean tectonics from the relationships between geothermal gradients and the rate of plate production. Earth and Planetary Science Letters, 40, 301-315.

Cook F. A. & Varsek J. L.1994. Orogen-scale decollements. Reviews of Geophysics 32, 37-60.

Craw D., Koons P. O., Horton T. & Chamberlain C. P. 2002. Tectonically driven fluid flow and gold mineralisation in active collisional orogenic belts: comparison between New Zealand and western Himalaya. Tectonophysics 348, 135-153.

Fyfe, W. S., 1990. Plate tectonics and the hydrosphere. Chapter 8 in B. E. Nesbitt (Ed.) Short Course on Fluids in Tectonically Active Regimes of the Continental Crust, Mineralogical Association of Canada, Short Course Handbook 18, May 1990, Vancouver, B. C., 299-312.

Drummond, B. J., Goleby B. R. & Swager, C. P., 2000a. Crustal signature of Late Archaean tectonic episodes in the Yilgarn craton, Western Australia: evidence from deep seismic sounding. Tectonophysics, 329, 193-221.

Drummond B. J., Goleby B. R., Owen A. J., Yeates A. N., Swager C., Zhang Y. &

Goldfarb, R. J., Groves, D. !. and Gardoll, S., 2001. Orogenic gold and geologic time: A global synthesis. Ore Geology Reviews 18, 1-75.

Groves, D. !., Vielreicher, R. M., Goldfarb, R. J. and Condie, K. C., 2005. Controls on the heterogeneous distribution of mineral dposits through time. In McDonald, I., Boyce, A. J., Butler, I. B., Herrington, R. J. and Polya, D. A., (Eds.), 2005. Mineral Deposits and Earth Evolution. Geological Society London, Special Publications 248, 71-101.

Hobbs B. E., Ord A. & Walshe, J. L., 1998. The concept of coupled geodynamic modelling with special reference to the Yilgarn. In: Wood, S., (ed.), Geodynamics and Gold Exploration in the Yilgarn.

Australian Geodynamics Cooperative Research Centre Workshop, Perth, 6th August 1998, Extended Abstracts Volume, 36-39.

Jackson J. K., 2000b. Seismic reflection imaging of mineral systems: Three case histories. Geophysics 65: 1852-1861.

Jamison W R, 1993. Mechanical stability of the triangle zone: the backthrust wedge. Journal of Geophysical Research 98B: 20015-20032.

Koons P. O. 1990. The two-sided orogen: Collision and erosion from the sandbox to the Southern Alps, New Zealand. Geology 18: 679-682.

Korja A, Korja T, Luosto U and Heikkinen P, 1993. Seismic and geoelectric evidence for collisional and extensional events in the Fennoscandian Shield – implications for Precambrian crustal evolution. Tectonophysics 219: 129-152.

Leahy, K., Barnicoat, A. C., Foster, R. P., Lawrence, S. R. and Napier, R. w., 2005. Geodynamic processes that control the global distribution of giant gold deposits. In McDonald, I., Boyce, A. J., Butler, I. B., Herrington, R. J. and Polya, D. A., (Eds.), 2005. Mineral Deposits and Earth Evolution. Geological Society London, Special Publications 248, 119-132.

Poudjom-Domani, Y. H., O'Reilly, S. Y., Griffin, W. L. & Morgan, P., 2001. The density structure of subcontinental lithosphere through geological time. Earth and Planetary Science Letters, 184, 604-621.

Regenauer-Lieb, K., Weinberg, R. F. and Rosenbaum, G., 2006. The effect of energy feedbacks on continental strength. Nature 442, 67-70.

Ridley, J. R., 1992. The thermal causes and effects of voluminous late Archaean monzogranite plutonism. In: Glover, J. E. & Ho, S. E., (eds.) The Archaean, Terrains, Processes and Metallogeny. University of Western Australia, Geology Department (Key Centre) and University Extension, Publication 22, 275-285.

Sandiford, M. and MacLaren, S., 2002. Tectonic feedback and the ordering of heat-producing elements within the continental lithosphere. Earth and Planetary Science Letters 204, 133-150.

Sleep, N. H., 1992. Archean plate tectonics; what can be learned from continental geology? Canadian Journal of Earth Sciences, 29, 2066-2071.

Sorjonen-Ward P., Zhang Y. & Zhao C., 2002. Numerical modelling of orogenic processes and gold mineralisation in the southeastern part of the Yilgarn Craton, Western Australia. Australian Journal of Earth Sciences 49: 935-964.

Numerical simulations of geological processes relating to the Outokumpu mineral system

P. Sorjonen-Ward[1,2]*, A. Ord[1], Y. Zhang[1], P. Alt-Epping[1,3], T. Cudahy[1], A. Kontinen[2] and U. Kuronen[4]

[1]CSIRO Exploration and Mining, PO Box 1130, Bentley, WA 6102, Australia
[2]Geological Survey of Finland, PO Box 1237, FIN-70211, Kuopio, Finland,
[3]Institute of Geological Sciences, University of Bern, Baltzerstrasse 1-3, CH-3012 Bern, Switzerland,
[4]Polar Mining Oy, P.O. Box 15, FIN-83501 Outokumpu, Finland
*E-mail: Peter.Sorjonen-Ward@gtk.fi

Numerical models are used to simulate a range of geological processes related to the Outokumpu mineral system, including testing of submarine hydrothermal systems and the revised conceptual model developed during the GEOMEX project. Conductive and convective thermal numerical models are used to demonstrate the potential effect of sedimentary sequences on the formation and containment of hydrothermal systems in underlying oceanic lithosphere. Reactive transport models evaluate interaction between serpentinite and marine or metamorphic fluids. Deformation and fluid flow models are designed to illustrate processes ranging from regional tectonic framework to local scale remobilization.

Keywords: Numerical modelling, hydrothermal processes, submarine alteration, deformation, fluid flow, Outokumpu

1. The Outokumpu mineral system and the GEOMEX project.

The Paleoproterozoic Outokumpu Cu-Co-Ni-Zn-Au deposits occupy an important place in the history of mining and metals processing in Finland. Between discovery in 1910 and closure in 1988, the main Outokumpu deposit produced 28.54 Mt or ore grading 3.8% Cu, 0.24% Co, 0.12% Ni, 1.1 % Zn, 8.9 ppm Ag and 0.8 ppm Au. The Vuonos deposit contained 5.82 Mt at lower grades and was mined from 1972-1984. Current mining operations are restricted to extraction of significant talc deposits in the eastern part of the district, where metamorphic grade is lower (Kontinen et al., 2004; Säntti et al.,2006). The blind Kylylahti deposit, which was discovered in 1979 at depth along strike from the mined deposits, has yet to be exploited, but is currently under further evaluation by Vulcan Resources. The rather unusual metal association of the Outokumpu deposits occurs within an equally distinctive host rock assemblage, comprising (metamorphosed) serpentinites, metalliferous black shales and banded quartz rocks and Cr-diopside skarns, all enclosed within an isoclinally folded and monotonous sequence of turbidites. While the highly strained and allochthonous nature of the Outokumpu assemblage, and tectonic remobilization of the ore have long been recognized (Koistinen, 1981), the prevailing interpretation has been that the Outokumpu deposits originally formed as massive sulfide accumulations associated with seafloor exhalative processes (Koistinen, 1981; Park, 1988).

Research undertaken during the GEOMEX collaborative joint venture between Outokumpu Mining and the Geological Survey of Finland, was aimed at an enhanced understanding of the mineral system and refinement of exploration strategies, leading to a reappraisal of the origin of mineralization and relationships between hydrothermal alteration, deformation and metamorphism (Kontinen et al., 2004, 2005, 2006). Textural and structural studies affirm the importance of structural remobilization of the ore deposits during prograde metamorphism, and highlight the difficulty or inferring primary processes (Säntti et al., 2006).

GEOMEX geochemical studies, and comparisons with the Jormua ophiolite (Kontinen, 1987; Peltonen et al., 1998) also indicate that the Outokumpu host rocks are dominated by serpentinized depleted mantle harzburgites. If the original metal enrichment is related to submarine hydrothermal processes, the relative lack of evidence for magmatic activity, apart from remnant mafic dykes, and gabbroic intrusions within the serpentinites, and sporadic low-Ti and rhyolitic volcanics, suggest convection at relatively deep levels within oceanic lithosphere, which was subsequently buried beneath a turbidite sequence. Furthermore, revaluation of the quartz-rocks of the Outokumpu assemblage during GEOMEX research demonstrates that they represent extreme hydrothermal leaching of serpentinites, rather than silica exhalites. By analogy with similar, less metamorphosed Paleozoic deposits in Quebec (Auclair et al., 1993), this was apparently a relatively low-temperature (70-150°C) process, consistent with textural evidence that this silicification and carbonate formation at Outokumpu predated metamorphism and significant deformation. The primitive Pb isotopic composition of the Outokumpu ores apparently precludes this silica-carbonate alteration from being related to Cu mineralization via fluid and metal exchange between serpentinite, black shale and turbidites, since the latter have more evolved crustal radiogenic Pb signatures.

While the serpentinites are an unlikely source for copper, mass balance studies indicate that adequate amounts of nickel could have been supplied by breakdown of silicate minerals such as olivine and pyroxene during serpentinization, provided that sulfur was also available. Indeed, this may explain why the distribution patterns of Cu and Ni differ, as well as account for the distinctive Ni enrichment at Outokumpu, compared to typical oceanic seafloor hydrothermal systems. The same isotopic arguments can be used to refute the concept of introduction of copper during structural focussing and trapping of metalliferous fluids within a regional scale synmetamorphic hydrothermal regime. The regional structural architecture is in principle appropriate for a metamorphic hydrothermal model – the structural geometry of the main lode at Outokumpu for example, is readily interpreted as mobilization, if not introduction of ore by duplexing of ore during late stage folding under peak metamorphic conditions. However, there is an evident lack of hydrothermal alteration in regional scale thrust systems and shear zones, so that synmetamorphic mobilization, rather than introduction of sulfides is favoured.

2. Numerical modelling of the Outokumpu mineral system

A further collaborative project between GEOMEX partners and CSIRO Exploration and Mining (Australia) was designed to investigate aspects of the GEOMEX genetic model, as well as simulate and test earlier conceptual models for Outokumpu earlier hypotheses, using a range of numerical process modelling techniques. Here we present the some results from this project, to illustrate how numerical modelling can be applied specific case studies, as well as generic insights into mineralising processes.

A range of numerical models have been designed to simulate the alternative processes outlined above, with the following issues being considered most relevant to understanding the Outokumpu system:

(1) Thermal regimes appropriate for hydrothermal processes in ultramafic oceanic lithosphere;

(2) Fluid interaction with ultramafic oceanic lithosphere, in order to determine conditions favourable for copper enrichment and appropriate fluid compositions for low-T silica alteration of serpentinite;

(3) Simulating the kinematics of regional deformation and mobilization of ore as constrained by field observations, including the possibility of synmetamorphic structural controlled fluid flow.

3. Conductive and convective thermal models of oceanic lithosphere

We have simulated the conductive thermal evolution of lithospheric scale models using the finite difference code, FLAC (Fast Lagrangian Analysis of Continua; Cundall and Board, 1988; Itasca, 1998), based on a Mohr-Coulomb crustal rheology overlying a viscous mantle lithosphere and asthenosphere. A tapering turbidite wedge extends half way across the upper surface of the models. A range of static and extensional deformational scenarios were modelled, with systematic variations in strain rate, radiogenic heat production and distribution of thermal anomalies, in order to simulate the effects of gabbroic intrusions at different emplacement depths (Fig. 1). Results indicate that thermal anomalies appropriate for hydrothermal metal leaching and transport are restricted to close proximity to intrusions and decay rapidly. The relatively small volume of gabbroic bodies, and erratic spatial distribution with respect to known mineralization further suggests that geophysical targeting of gabbroic bodies is probably not a useful exploration strategy.

Thermal convective modelling has been done with the reactive transport code OS3D (Steefel and Yabusaki 1996). The 2-D model represents a simplified section simulating the permeability structure of oceanic lithosphere, with a fixed mantle heat flux maintaining a thermal gradient sufficient to drive convective flow. As in the thermal conductive models a tapering wedge of sediment, with low permeability is modelled across one half of the model. It is clear from the solution for steady state Darcy flow and the temperature distribution that the sediments have a critical influence on the formation and efficiency of convective flow cells in the underlying basement (Ord et al., 2003; Sorjonen-Ward et al., 2005). One of the more significant generic outcomes from both conductive and convective thermal modelling was the significance of a low permeability seal to the system, whether due to blanketing by sediments or disruption to permeability structure by vertical sheeted dyke complexes. The presence of such seals showed a clear correlation with efficiency and sustainability of underlying convective flow cells. At a general level this implies that the presence or absence for a rapidly prograding sediment wedge over a volcanic complex could be a useful exploration criterion for subseafloor replacement VHMS deposits (cf. Allen et al., 1996; Binns et al., 2002; Brauhart et al., 1998; Cathles, 1983).

4. Reactive transport models involving serpentinites and fluids

Hydrothermal fluid-rock interaction was modeled with the reactive transport code OS3D, firstly to demonstrate thermal regimes and permeability structures for efficient hydrothermal convection, followed by 1-dimensional flowpath simulations. Because of the symmetric zonation of the Outokumpu deposits, such simplifications were considered both realistic and computationally efficient. Various scenarios were then tested, varying length of flow path and relative proportions of rock units (peridotite, carbonaceous shale, turbidite) and initial composition of infiltrating fluid (seawater, H2O-CO2), and systematically changing thermal gradients, both in terms of maximum temperature and up-temperature (influx) and down-temperature (discharge) regimes. As well as being of generic value for simulating fluid interaction with ultramafic rocks, the results obtained were consistent with the proposition that the initial copper enrichment at Outokumpu was separate from the silica-carbonate alteration serpentinites. Because of the inherently low Cu

abundances in the depleted harzburgitic serpentinites, infiltrating seawater requires an a priori enrichment in Cu; as discussed above, this may be feasible if the serpentinites were once buried beneath a basaltic gabbroic crustal carapace, subsequently removed by extensional processes, prior to turbidite deposition. Even so, seawater influx alone could not precipitate chalcopyrite in serpentinite, due to the effect of anhydrite stability. At lower temperatures, anhydrite precipitation is less efficient, so that sulfate-rich fluids can circulate deeper into the system, maintaining higher oxygen fugacity, and favouring prolonged metal leaching and transport. Precipitation of Cu (and Ni) sulfides then depends upon the capacity of ultramafic rocks for sulfate reduction. For example, the serpentinization of peridotite can produce methane where olivine breakdown produces serpentine and magnetite (Frost 1985, O'Hanley, 1996). It is therefore critical, though difficult in metamorphosed terrain, (Gole et al., 1987) to establish whether serpentinization of the harzburgites occurred during this process, or at an earlier stage. Higher temperature fluid-rock reaction tends to promote precipitation, including silica at the interface between leached peridotite and sediments. This may be more relevant to prograde metamorphic modification to the mineralization, although we were unable to simulate temperatures above 400°C, nor did we simulate fluid absent diffusive processes.

5. Regional to local scale numerical modelling of deformation in relation to the Outokumpu mineral system

Based on previous studies (e.g. Koistinen, 1981), it is geometrically and kinematically reasonable to infer that the present structural setting of the Outokumpu ore zone is a result of later orogenic deformation superimposed on early thrust tectonics. Thus the main Outokumpu ore zone can be seen as lying within a structurally duplexed lense of serpentinite, as a result of mechanical contrasts between the Outokumpu assemblage and country rocks (Sorjonen-Ward, 2003). Therefore, deformation and fluid flow modeling with FLAC was designed to illustrate a scale transition, beginning with the kinematics and geometry of strain partitioning between regional scale shear zones and folding, which controls the structural architecture of the Outokumpu district (Ord et al., 2003; Zhang, 2003). Successive models focused on smaller scales, addressing the effects of rheological contrasts within the Outokumpu assemblage. Results were particularly successful in demonstrating how sections through the main Outokumpu ore body can be explained by structural duplexing of serpentinite and mobilization of ore on the limb of a regional synform. Additional models simulated the expected flow patterns if synmetamorphic and granite-related fluid flow are invoked.

References

Allen, R. L., Weihed, P. And Svenson, S.-Å., 1996. Setting of Zn-Cu-Au-Ag massive sulfide deposits in the evolution and facies architecture of a 1.9 Ga marine volcanic arc, Skellefte district, Sweden. *Economic Geology 91, 1022-1053*.

Auclair M., Gauthier M., Trottier J., Jébrak M. & Chatrrand, F., 1993, Mineralogy, geochemistry, and paragenesis of the Eastern Metal serpentinite-associated Ni-Cu-Zn deposit, Quebec Appalachians, Economic Geology, 88, 123-138.

Binns, R. A., Barriga, F. J. A. S., Miller, D. J., et al., 2002. Proceedings of the Ocean Drilling Program, Initial reports, Volume 193.

Brauhart, C. W, Groves, D. I. & Morant, P., 1998. Regional alteration system associated volcanogenic massive sulfide mineralization at Panorama, Pilbara, Western Australia. Economic Geology 93, 292-302.

Cathles L. M. 1983. An analysis of the hydrothermal system responsible for massive sulfide deposition in the Hokuroku Basin of Japan. In: Ohmoto H. & Skinner B. J. eds. The Kuroko and Related Volcanogenic Massive Sulfide Deposits, pp. 439-487. Economic Geology Monograph 5.

Cudahy, T., 2004 Mapping alteration zonation associated with massive sulphide mineralisation using airborne hyperspectral data. In McConachy T. F. & McInnes B. I. A. (eds.) Copper-zinc massive sulphide deposits in Western Australia. CSIRO Explores 2, 113-120.

Cundall, P. A., and M. Board, M. (1988). A microcomputer program for modelling large-strain plasticity problems. In: Swoboda, G. (Ed.), Proceedings of the Sixth International Conference on Numerical Methods in Geomechanics. Numerical Methods in Geomechanics 6, 2101-2108.

Frost B. R., 1985, On the stability of sulfides, oxides and native metals in serpentinites, Journal of Petrology, 26, 31-63.

Gole M.J, Barnes S.J & Hill R.E.T, 1987. The role of fluids in the metamorphism of komatiites, Agnew nickel belt, Western Australia, Contributions to Mineralogy and Petrology, 96, 151-162.

Itasca (1998). FLAC: Fast Lagrangian Analysis of Continua, User Manual, Version 3.4. Itasca Consulting Group, Inc., Minneapolis.

Koistinen T.J., 1981, Structural evolution of an early Proterozoic stratabound Cu-Co-Zn deposit, Outokumpu, Finland, Transactions of the Royal Society of Edinburgh: Earth Sciences, 72, 115-158.

Kontinen A., 1987, An early Proterozoic ophiolite – the Jormua mafic-ultramafic complex, northern Finland, Precambrian Research, 35, 313-341.

Kontinen, A., Sorjonen-Ward, P., Santti, J., Peltonen, P. & Kuronen, U., 2004: Superimposed fluid-rock reaction during prograde and retrograde metamorphism of serpentinites and controls on the formation of talc deposits in the Outokumpu Cu-Co-Ni-Zn-Au ore province. In: M. Radvanec, W. Prochaska, A. C. Gondim & Z. Nemeth (eds.): Magnesite and talc - from their origin to the environmental impacts of exploitation and dressing (IGCP 443; Workshop DWO 14). 32nd International Geological Congress, Florence - Italy, August 20-28, 2004, Abstracts book Part 2, 1522-1523.

Kontinen, A., Sorjonen-Ward, P., Peltonen P and Kuronen, U., 2005. Some new constraints on hydrothermal alteration and deformation of the Paleoproterozoic serpentinite-hosted Outokumpu Cu-Co-Ni-Zn-Au deposits, Finland. Pp. 639-641 in Mao, J. and Bierlein, F. P. (eds.), Mineral Deposit Research: Meeting the Global Challenge, Proceedings of the 8th Biennial SGA Meeting, Beijing, China, 18-21 August, 2005, Springer Verlag.

Kontinen, A., Peltonen, P., and Huhma, H., 2006. GEOMEX Outokumpu Modeling Project final report.

Loukola-Ruskeeniemi K., 1999, Origin of black shales and serpentinite-associated Cu-Zn-Co ores at Outokumpu, Finland, Economic Geology, 94, 1007-1028.

O'Hanley D.S., 1996, Serpentinites: records of tectonic and petrological history, Oxford Monographs on Geology and Geophysics 34, Oxford University Press, 277p..

Park A.F., 1988, Nature of the Early Proterozoic Outokumpu assemblage, eastern Finland, Precambrian Research 38, 131-146.

Ord, A., Sorjonen-Ward, P., Zhang, Y. & Alt-Epping, P. A., 2003. Outokumpu Mineralising System: Executive Summary. CSIRO Exploration and Mining Report 1133C, 46p.

Peltonen P., Kontinen, A. & Huhma H., 1998, Petrogenesis of the mantle sequence of the Jormua Ophiolite (Finland): Melt migration in the upper mantle during Palaeoproterozoic continental break-up, Journal of Petrology, 39, 297-329.

Säntti, J., Kontinen, A., Sorjonen-Ward, P., Johanson, B. & Pakkanen, L., 2006. Metamorphism and Chromite in Serpentinized and Carbonate-Silica-Altered Peridotites in the Paleoproterozoic Outokumpu–Jormua Ophiolite Belt, Eastern Finland. International Geological Review 48, 494-546.

Sorjonen-Ward, P., 2003. Outokumpu Mineralising System: Geological Interpretation. CSIRO Exploration and Mining Report 1143C, 215p.

Sorjonen-Ward P, Zhang, Y., Alt-Epping, P., Ord, A., Cudahy, T. & Kuronen, U., 2005. The effect of sedimentary cover on submarine hydrothermal processes – some simple numerical simulations and applications. Pp. 1497-1499 in Mao, J. and Bierlein, F. P. (eds.), Mineral Deposit Research: Meeting the Global Challenge, Proceedings of the 8th Biennial SGA Meeting, Beijing, China, 18-21 August, 2005, Springer Verlag.

Steefel, C. I, & Yabusaki, S. B., 1996. OS3D/GIMRT, software for multicomponent-multidimensional reactive transport, user manual and programmer's guide PNL-111666, Pacific Northwest National Laboratory, Richland, WA.

Zhang, Y., 2003. Outokumpu Mineralizing System: Deformation and fluid flow models. CSIRO Exploration and Mining Report 1144C, 49p.

The granite-migmatite zone of southern Finland – A history of structural control and intrusions

Tom Stålfors*, Carl Ehlers and Anna Johnson

Åbo Akademi University, Department of Geology and Mineralogy, FIN-20500 Turku, Finland
*E-mail: tom.stalfors@abo.fi

Late-orogenic (1.83 Ga) migmatites and granites in southern Finland form a 100×500 km long zone which is connected to a major shear zone system. In the Nagu synform in SW Finland, a couple of kilometres of deformed and banded granite sheets are exposed underneath an 18 kilometres long amphibolite synform. Occasional layers of undeformed gabbros of apparently the same late-tectonic age occur interlayered with the granite sheets. Whether these gabbros and the temperature rise caused by them was sufficient or not to produce the granites is still an ongoing debate.

Keywords: Granites, gabbro, emplacement mechanisms, structural control

1. Introduction

The Palaeoproterozoic crust in southern Finland was formed during the Svecofennian orogeny about 1.89-1.87 Ga ago. It is comprised of I-type tonalites, granodiorites and gabbros (Nurmi and Haapala (1986). The late-Svecofennian granite-migmatite zone (LSGM-zone, Ehlers et al. 1993) in southern Finland is a large crustal section composed mainly of S-type granites and migmatites (Figure 1). This regional belt of migmatites and granites that discordantly transected the earlier Svecofennian crust around 1.83 Ga ago, is related to a tectonic event in the early crust involving shearing and elevated temperatures along a c. 500 kilometre long zone. Partial melts that moved upward through the crust along syn-intrusive shears formed either granitic massifs in the middle and upper crust or froze as migmatites. In SW Finland these potassium granites form large sub-horizontal sheets. The granites are of porphyry type with large microcline phenocrysts that are tiled and deformed both during and after the emplacement (Ehlers et. al. 1993, Selonen et. al. 1996, Stålfors and Ehlers 2006).

The Nagu synform in SW Finland is a perfect area to study these tectonically banded and fractionated late-orogenic granites. A couple of kilometres of deformed and banded granite sheets are exposed underneath an 18 kilometres long amphibolite synform. Stålfors and Ehlers showed earlier that these granites are geochemically inhomogeneous and apparently emplaced as a succession of small individual melt batches (Stålfors and Ehlers 2000, 2006). The granitic plutons are thus composed of individual sheets of granites with varying chemical compositions. Occasional layers of undeformed gabbros of apparently the same late-tectonic age occur interlayered with the granite sheets. They differ chemically from the early-Svecofennian calc-alkaline gabbros in the area as well as from post-collisional monzodiorites in south Finland (Väisänen et al. 2000). The Nagu gabbros were first described by Edelman (1973, 1985) and recently by Rikberg et al. in 2006. They occur as layer-parallel sills within the granite sheets (Figure 2), as larger bodies (in the western part of the area) or as local small intrusion fingers in the surrounding granites (Figure 3).

The gabbros were also emplaced in pulses (see Figure 4), which resulted in complex patterns in the area. Some gabbros are discordant against the banding in sheared granites, while granitic back veining along cracks in the gabbro sills can be seen at other localities.

2. Tectonic setting

Three regional deformational episodes are identified in the Svecofennian rocks in southern Finland: D_1 D_2 and D_3 (e.g. Väisänen and Hölttä 1999). Due to the high metamorphic grade, the oldest deformational structures are very sparse, even if some isoclinal F_1 folds can be observed. Most recorded F_1 folds are intrafolial small folds, while F_2 folds occur at all scales and dominate among the early structures. The tight F_2 folds are overturned towards W or NW with north-westerly vergences, while the F_3 folds are upright and transpose earlier structural features parallel to the steep E-W trending F_3 axial planes.

The late Svecofennian granites were emplaced and locally deformed during D_3. They have recorded only the D_3 structures, defining the "late-tectonic" timing of the emplacement and the culmination of the high-grade metamorphism.

The F_3 folds are mostly open in areas dominated by early Svecofennian granitoids, whilst areas dominated by supracrustal layers usually shows tighter F_3 folds.

Tiling (imbrication) of microcline phenocrysts in horizontal granite sheets indicates syn-magmatic shear during D_3 (Selonen et. al. 1996, Stålfors and Ehlers 2006) and indicates a top to the W or NW movement. Both the granites and the gabbros intruded along sub-vertical ductile D_3 shear zones, which define a major system of transpressive shear zones, and were emplaced along sub-horizontal surfaces parallel to the previously overturned D_2 axial planes. Continuing deformation after the emplacement resulted in the strongly sheared fabric in the granites, squeezing out the last melt fractions. The gabbro sills are, however, mostly undeformed due to their faster crystallisation rate and are therefore petrologically better preserved in outcrops even if boudinaged or brittly broken during the synchronous deformation.

3. Intrusion relations between gabbro sills and surrounding granite

There are three types of interaction found between the felsic and mafic magmas in the Nagu area. The different types of interaction is probably a result of the successive emplacement of small batches of granites over time in relation to the intrusion of mafic sills (which also have intruded as smaller batches). This resulted in complex patterns where gabbros show both post- and syn-intrusive behaviour in relation to the surrounding granite sheets. The large volumes of slowly crystallising granite generally show traces of overprinting ductile deformation whereas the smaller gabbro bodies quenched instantly and principally resisted the simultaneous D_3 deformation or was accommodated by boudinage or breccia formation. In places, these two magmas are co-existing. The coevality of these contrasted magmas is seen as net veining where the mafic rock shows a pillowed form with a decreasing grain-size towards the margins against the granite. This is illustrated in Figure 5, where the host granite appears as an intrusive vein.

4. Conclusions

Structural observations indicate that the gabbroic layers are intruded simultaneously with the banded and sheared granites. Because the late-orogenic granites, migmatites and gabbros in the Nagu area were transported and emplaced as small batches over an extended time interval, the internal relationships between these two types of melts produced, in places, complex patterns. Some gabbros are discordant against the banding in sheared granites, while sometime granitic back veining along cracks in the gabbro sills can be seen. Due to the temperature difference between granite and gabbro, the small gabbroic bodies

quenched fast against the granites and were therefore better preserved during the synchronous deformation.

The large quantities of ductilly deforming granites forced smaller pulses of gabbro to intrude along the E-W trending layer-parallel shear zones of the synform, thus creating sill-like bodies, whereas larger bodies collected to form small local intrusion-fingers.

We propose the following model of emplacement for granites of the LSGM zone. The microcline granites occurred as sub-horizontal sheets surrounded by more intensely deformed and sheared zones. The sheets were gently folded and stretched during the D_3 episode, while the steep dykes of the granite occurring along the margins of the sheets were strongly deformed and drawn out into boudins during the final D_3 deformation.
The melt batches were transported through repeatedly activated vertical shear zones created during D_3 and were emplaced at a structural level in the crust, perhaps corresponding to the brittle-to-ductile transition zone or some other horizontal discontinuity. In the Nagu area, the melt was trapped and spread out under a roof of overturned amphibolites that collected the melt batches by cutting off the escape route.

It has been suggested that mafic intrusives caused the temperature anomaly needed to produce the high-grade metamorphism and the late-orogenic granites in southern Finland. Whether the amounts of gabbros and the temperature rise was sufficient or not is still an ongoing debate.

References

Edelman, N. (1973) Geological map of Finland 1:100 000. Pre-Quaternary rocks. Sheet 1034 Nagu. Geological Survey of Finland. Helsinki.

Edelman, N. (1985) Explanations to the maps of pre-Quaternary rocks. Sheet 1034 Nagu. Geological Survey of Finland. Helsinki.

Ehlers, C., Lindroos, A. and Selonen, O. (1993) The late Svecofennian granite-migmatite zone of southern Finland – a belt of transpressive deformation and granite emplacement. Precambrian Res. 64, p. 295-309.

Nurmi, P. A., Haapala, I. (1986) The Proterozoic granitoids of Finland: granite types, metallogeny and relation to crustal evolution. Bull. Geol. Soc. Finland 58(1), pp. 203-233.

Rikberg, A., Stålfors, T. and Ehlers, C. (2006) Intrusive gabbros interlayered with late-orogenic 1.83 Ga granitic sheets in South-western Finland. Bull. Geol. Soc. Finl. Spec. Issue 1 (The 27th Nordic Geological Winter Meeting, Abstract volume). p. 131.

Selonen, O., Ehlers, C., Lindroos, A. (1996) Structural features and emplacement of the late Svecofennian Perniö granite sheet in southern Finland. Bull. Geol. Soc. Finland 68, part 2, 5-17.

Stålfors, T. and Ehlers, C. (2000) Granite emplacement during the 1.83 Ga late-orogenic stages in southern Finland. In Pesonen, L. J., Korja, A. and Hjelt, S-E. (eds) Lithosphere 2000 A symposium on the structure, composition and evolution of the lithosphere in Finland. Institute of Seismology, Univ. of Helsinki, Report S-41, pp. 91-96.

Stålfors, T. and Ehlers, C. (2006) Emplacement mechanisms of late-orogenic granites – structural and geochemical evidence from southern Finland. International Journal of Earth Sciences 95(4), 557-568.

Väisänen, M. and Hölttä, P. (1999). Structural and metamorphic evolution of the Turku migmatite complex, southwestern Finland. Bulletin of the Geological Society of Finland 71 (1), 177-218

Väisänen, M., Mänttäri, I., Kriegsman, L. M. and Hölttä, P. (2000) Tectonic setting of post-collisional magmatism in the Palaeoproterozoic Svecofennian Orogen, SW Finland. Lithos 54, pp. 63-81.

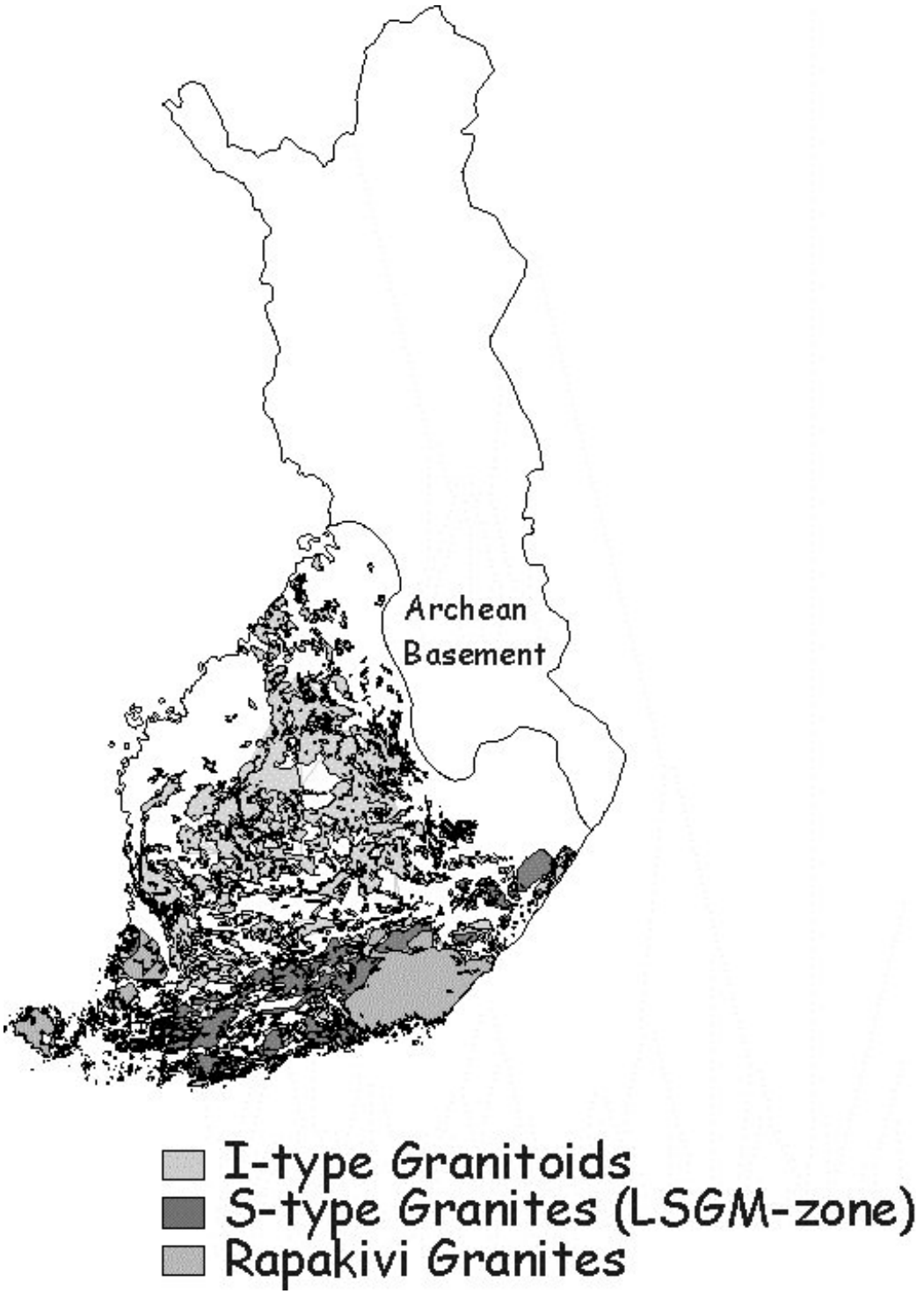

Figure 1. Geological overview of southern Finland. The Svecofennian domain consists mainly of granodiorites, gneisses and gabbros. The LSGM-zone is characterised by late-orogenic migmatites and granites, which are intruded by later rapakivi granites.

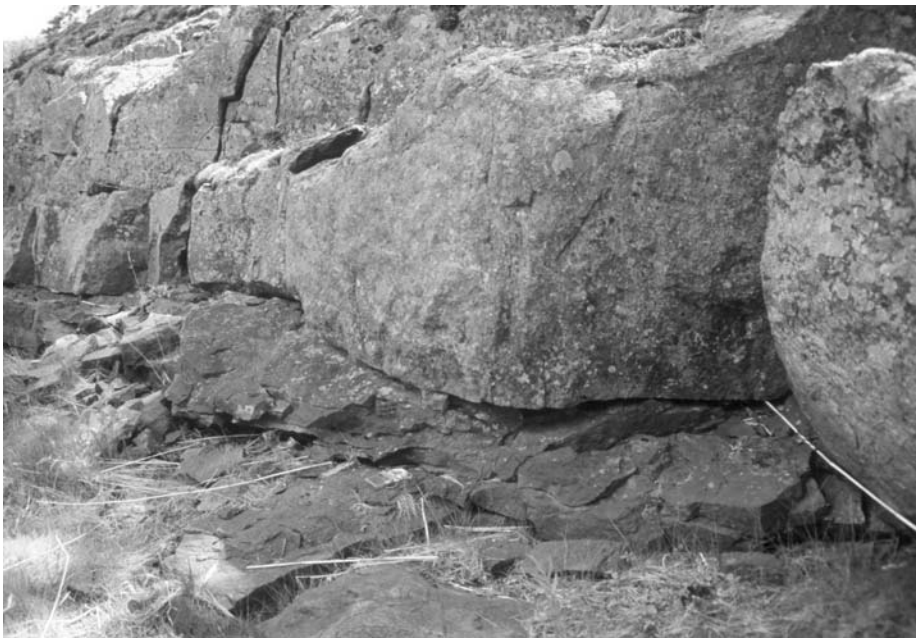

Figure 2. Layer-parallel gabbro sill within sub-horizontal granite sheets in the Nagu area, SW Finland.

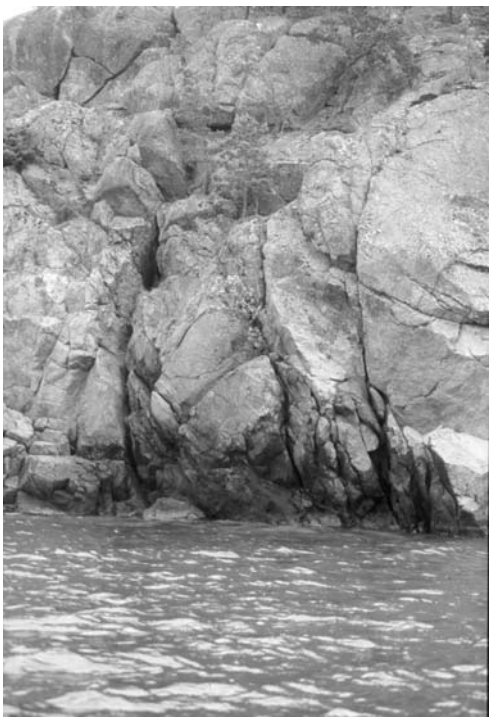

Figure 3. Larger concentrations of gabbro formed local intrusion fingers in the surrounding granite sheets.

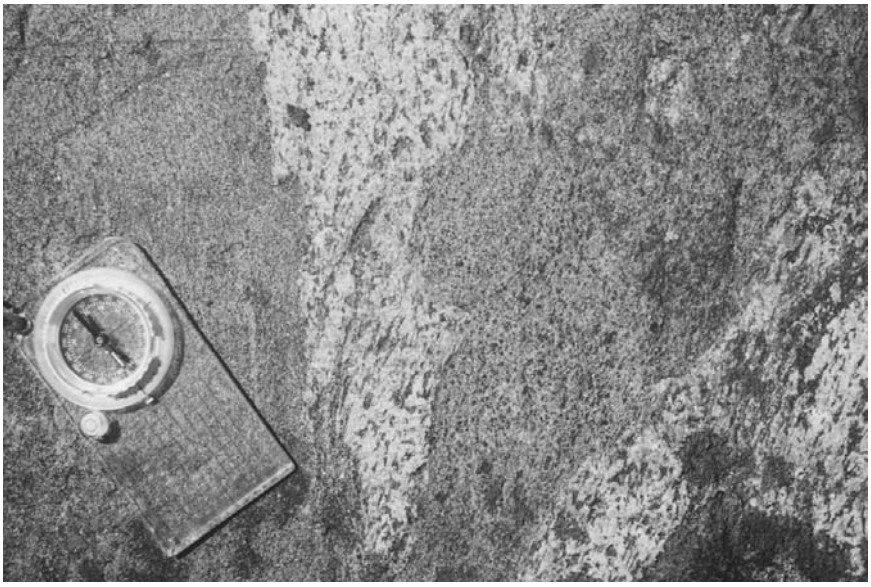

Figure 4. Fragments of a coarse-grained gabbro surrounded by a later pulse of fine-grained gabbro, Nagu SW Finland.

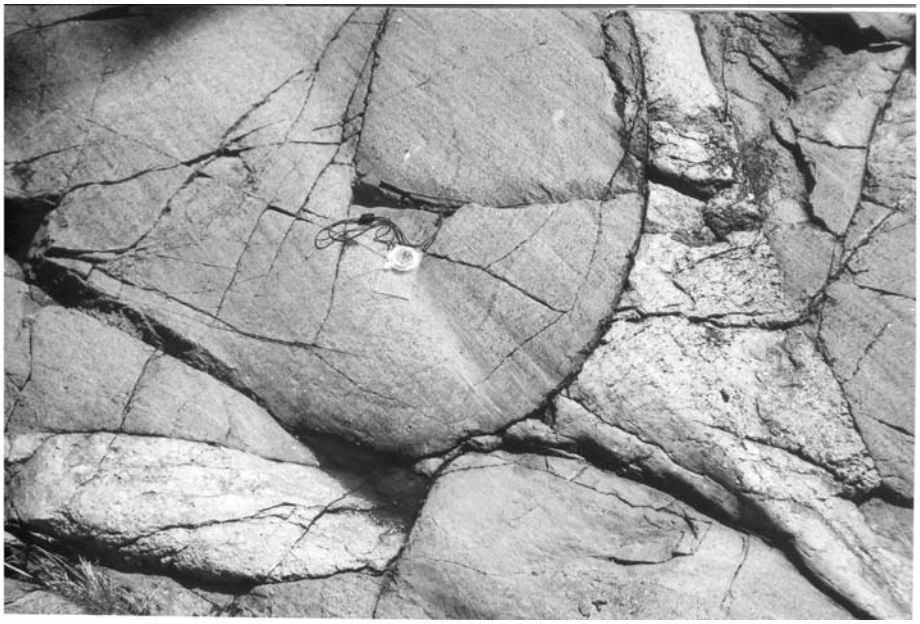

Figure 5. Mingling between granite and gabbro in the Nagu area. The coevality of these contrasted magmas is seen as net veining where the mafic rock shows a typical pillowed form.

Palaeozoic metallogeny of Røros (Norway); a tool for improving Palaeoproterozoic crustal models in Karelia

K. Sundblad[1]*, M. Beckholmen[2], O. Nilsen[3] ja T. Andersen[3]

[1]Department of Geology, University of Turku, Finland,
[2]Backbo, Bälinge, Sweden
[3]Department of Geology, Oslo University, Norway
*E-mail: krisun@utu.fi

Keywords: Metallogenesis, crustal models, Caledonian, Precambrian.

The Köli units of the Scandinavian Caledonides represent a complex of ore-bearing outboard terranes that were formed in the Iapetus Ocean during the Ordovician to Early Silurian. As a result of the closing of the Iapetus Ocean, these terranes were thrust on top of Seve units (interpreted as the outermost remnants of the continental margin of Baltica) during the Late Silurian to Early Devonian. Furthermore, the Köli units (and underlying Seve units) were tectonically emplaced on top of even lower nappes as well as the passive continental basement of Baltica. The Köli units were tectonostratigraphically divided into Lower, Middle and Upper Köli (Stephens, 1982).

Numerous ore deposits have been found in the Köli units, both in Norway and Sweden and significant metal production has taken place in several mining districts. The Røros district was for more than 300 years one of the most important metal produceres in Norway, with a leading role in the domestic production of copper, zinc and chromium. Geological facts and models for the Røros ore types are, however, poorly documented, although recent work has revealed that several ore types can be distinguished, each representing specific geological environments and distinct types of crustal evolution. Three environments are reviewed here.

1. Gabbro-intruded turbidites; host for the main Røros ore type (Middle Köli)

The most common ore type in the Røros district is Zn-Cu-bearing massive sulphides, hosted by a metamorphosed Ordovician gabbro-intruded turbidite sequence. This unit belongs to the Middle Köli and is stratigraphically underlain by submarine volcanics and Tremadocian U-Mo-V-rich black schists. The ore-bearing and gabbro-intruded turbidite sequence can be followed through the entire Røros district into the Blåsjön region (including Ankarvattnet; Sundblad, 1981) as well as through Usmeten and Sulitjelma to Ruonasvagge (Sundblad, 1991), thus constituting a tectonostratigraphic key unit for more than 600 km along the orogen.

It has been suggested (Sundblad et al., 2006) that this ore type represents an ancient analogue to the Escanaba type of sulphide ores, documented by Morton et al. (1994) in the present Pacific. The recognition of an ancient analogue to Escanaba type VMS deposits in the Scandinavian Caledonides implies that the ore-bearing turbidite environment in Røros not can have been dramatically distant from a continent prior to nappe transport. Furthermore, a close link, both with respect to age and geochemistry, between the underlying Tremadocian black schists and Dictyonema-bearing “alum” shales (which constitute a wide-spread platform unit in Norway, Sweden, Estonia and Poland) suggests that this continent was Baltica (Sundblad & Gee 1984).

2. Lower Köli turbidites

Another turbidite unit, with only occasional expressions of magmatic activity (trondhjemitic dykes) and without any metalliferous concentration, is located southeast of the ore-bearing gabbro-intruded turbidite sequence. From work carried out in Sweden (e.g.

in the Lövfjäll formation), this ore-barren unit is considered to belong to the Lower Köli, with a tectonic break to the ore-bearing, gabbro-intruded turbidites (Lasterfjäll formation) of the Middle Köli (Stephens, 1982).

3. The Harsjøen tectonic lens (Lowermost Köli)

The presence of ultramafic pods, along the contact between the Lower Köli and Seve units, is well-documented throughout the entire Caledonian orogen in Scandinavia (Stigh, 1979). These units are particularly abundant in the Røros region, from where serpentine- and talc-altered dunites and peridodites can be followed for 150 km kilometres along strike towards the Vågåmo ophiolite in the southwest (Nilsson et al., 1997). Corresponding ophiolite fragments have also been recognized at the same tectonostratigraphic position at Handöl (Bergman (1993), 80 km northeast of Røros, suggesting that all these solitary ultramafic units represent disfragmented ophiolites in the lowermost parts of the Köli tectonostratigraphy.

The Harsjøen lens is a previously unrecognized tectonic unit, located only a couple of kilometres to the southeast and east of Røros town. This lens has a maximum thickness of 5 km, can be followed along strike for 35 km and is tectonically squeezeed between the overlying Lower Köli turbidites and the underlying Seve units. The upper tectonic border of the Harsjøen lens is marked by a quartzite mylonite running along the northern limit of the ultramafic bodies. Other units in the Harsjøen lens consist of tholeiitic metabasalts, graphitic schists and grey phyllites. Three types of ores can be distinguished in the Harsjøen lens:

a. Podiform chromite ores

A number of podiform chromium ores, with Cr/Cr+Al ratios from 0.74 to 0.86, were mined in several serpentine- and talc-altered dunite bodies from 1820 to 1940 (Nilsson et al., 1997). Feragen is the largest body consisting of Cr-rich dunite, cpx-bearing harzburgite and cpx-poor lherzolite (Nilsson et al., 1997).

b. Cyprus type VMS deposit

Fine-grained, banded, pyritic Cu-Zn-bearing ores have been recognized south of lake Harsjøen in meta-basalts, close to the stratigraphically overlying graphitic schists and grey phyllites. The meta-basalts have locally a relatively unaltered chemistry but are strongly hydrothermally altered in the stratigraphic foot wall to the sulphide ores. This mineralization type is interpreted to have formed on the sea floor as a Cyprus-type VMS deposit. Neverthesless, when moving along strike to the west (towards the Lossius and Sara Cu mines) the ore type changes gradually in character.

c. Lossius and Sara Cu-Pb-Ni-bearing sulphide deposits

In spite of being the earliest ores recognized at Røros, the Cu-Pb-Ni-bearing deposits at Lossius and Sara are poorly documented. They are hosted by the same volcanic unit as the Harsjøen VMS deposit but are more coarse-grained and lack banding. Irregular high contents of Ni and Pb, the latter with radiogenic isotopic ratios are interpreted as a result of late-orogenic/metamorphogenic remobilization.

4. Comparisons between the Røros region and the Precambrian of Karelia

The Archaean basement in Karelia is overlain by Palaeoproterozoic autochthonous sedimentary units which are tectonically overlain by a number of exotic Palaeo-proterozoic terranes. These allochthonous units comprise ophiolites (Jormua) with associated Cu-Zn deposits (Outokumpu) as well as a turbidite sequences.

Ore-bearing gabbro-intruded turbidites are the hall mark of the Scandinavian Caledonides and have recently been discovered in modern environments outside the North American Pacific cost. If such a unit also would be recognized in the Precambrian successions in Finland, it would not only represent an economic value, it would reveal a unique interaction between endogenic (oceanic rift) and exogenic (continental margin sedimentation) forces. Until such a key unit is found in the Precambrian of Fennoscandia, it may indicate that such an endogenic/exogenic interaction was *not* active in the ancient sea outside the Archaean continent.

The Kalevian turbiditic schists, that can be followed from Kajaani to Ladoga, appear to be unrelated to any metal accumulation. This kind of monotonous sedimentary units are as such very similar to the Lower Köli turbidites.

A number of genetic models have been proposed for the Outokumpu deposit (Cyprus-type VMS deposition, black shale related deposition under anoxic conditions and orogenic remobilization associated with metamorphogenic Ni enrichment). Regardless which genetic model is preferred, the close relations between Cu-Zn ores, black schists and Cr-bearing ultramafics are evident features, both in Karelia and in the Harsjøen lens. Further studies of the Harsjøen lens may thus help us to understand the crustal processes that led to the formation of the Outokumpu environment. In any case, studies of the ore-bearing units in Karelia have certainly helped our understanding of the Røros district.

5. Conclusions

Comparisons between Precambrian and Lower Palaeozoic orogens in Fennoscandia are very useful when crustal models are created, particularly if metal concentrations, with or without economic potential, are considered as a scientific instrument.

Acknowledgement

This contribution was inspired by discussions with Asko Kontinen during a field trip to Jormua in late September 2006.

References

Bergman, S., 1993. Geology and geochemistry of mafic-ultramafic rocks (Köli) in the Handöl area, central Scandinavian Caledonides. Norsk Geologisk Tidsskrift 73, 21.42.

Morton, J.L., Zierenberg, R.A. & Reiss, C., 1994. Geologic, hydrothermal, and biologic studies at Escanaba Trough, Gorda Ridge, offshore northern California. USGS Bull. 2022, 359 pp.

Nilsson, L.P., Sturt, B.A. & Ramsay, D.M., 1997. Ophiolitic ultramafites in the Folldal-Røros tract, and their Cr-(PGE) mineralisation. NGU Bulletin 433, 10-11.

Stephens, M.B., 1982. Field relationships, petrochemistry and petrogenesis of the Stekenjokk volcanites, central Swedish Caledonides. Sveriges Geologiska Undersökning C786, 111 pp.

Stigh, J., 1979. Ultramafites and detrital serpentinites in the central and southern parts of the Caledonian Allochthon in Scandinavia. PhD thesis A27, Geologiska Institutionen, Chalmers Tekniska Högskola och Göteborgs Universitet, 222 pp.

Sundblad, K., 1981. Chemical evidence for, and implications of, a primary FeS phase in the Ankarvattnet Zn-Cu-Pb massive sulphide deposit, central Swedish Caledonides. Mineralium Deposita 16, 129-146.

Sundblad, K., 1991. The Ruonasvagge massive sulphide deposit in the Norrbotten Caledonides, Sweden. Geol. Fören. Stockholm Förh. 113, 65-67.

Sundblad, K. & Gee, D.G., 1984. Occurrence of a uraniferous – vanadiniferous graphitic phyllite in the Köli nappes of the Stekenjokk area, central Swedish Caledonides. Geol. Fören. Stockholm Förh. 106, 269-274.

Sundblad, K., Andersen, T., Beckholmen, M. & Nilsen, O., 2006. Ordovician Escanaba type VMS deposits in the Scandinavian Caledonides. 27th Nordic Geological Winter Meeting, Oulu, p. 156.

Deformation history of a ductile, crustal-scale shear zone in SW Finland – reactivation and deformation partitioning

Taija Torvela

Åbo Akademi, Dept. of Geology and Mineralogy, Tuomiokirkontori 1, FI-20500 Turku, Finland
E-mail: taija.torvela@abo.fi

A crustal-scale deformation zone, 'South Finland shear zone' (SFSZ) defines a major discontinuity between 1.88 Ga, unmigmatitised igneous rock to the S and SW and the 1.88 Ga supracrustals, extensively migmatitized at ca. 1.83 Ga, to the N and NE. The SFSZ has been repeatedly reactivated during the main and late stages of the Palaeoproterozoic Svecofennian orogeny. After the intrusion of the ca. 1.88 Ga granitoid rocks, at least three separate deformation phases affected the shear zone within the ductile regime, producing striped granodioritic and tonalitic gneisses without extensive migmatitization. Also mylonites and ultramylonites were formed, especially, but not exclusively, during the last ductile deformation phase. The latest reactivation of the shear zone occurred within the semi-brittle to brittle regime, producing pseudotachylytes.

Keywords: shear zone, ductile, brittle, reactivation, Palaeoproterozoic, Svecofennian, deformation, partitioning, age determination, geothermobaromtery

Within this Ph.D. project, the deformation history and structural development of a part of a major ductile shear zone, 'the South Finland shear zone' (SFSZ; *Ehlers et al., 2004*) was studied. The SFSZ extends for almost 200 km through the Åland archipelago and along the southern and southwestern coast of Finland (fig. 1). The transpressive shear zone defines a major discontinuity between 1.88 Ga, steeply dipping, igneous rocks to the S and SW and the 1.88 Ga, structurally overturned supracrustals, extensively migmatitized at ca. 1.83 Ga, to the N and NE (e.g. *Ehlers et al., 2004, Ehlers et al. 1993*).

The area of this study comprises large parts of the parishes of Kökar and Sottunga in Åland archipelago. The approximately NW-SE striking, more than a kilometre wide SFSZ is well exposed within the study area along the shores of the small islets and skerries. The deformation along the shear zone within the study area initiated shortly after the juvenile, mainly granitoid rocks were formed, and recommenced within the ductile regime during at least two additional, separate deformation phases. The regional, ductile dextral shearing phases produced striped granodioritic and tonalitic gneisses with no or very limited migmatitization. Also some mylonites were formed, especially during and/or after the last ductile deformation phase. The ductilely deformed synorogenic rocks are locally overprinted or cut by late- to post-orogenic ductile to semi-ductile ultramylonite zones of variable width. The latest stage of activity along the shear zone is recorded by brittle pseudotachylytes, which, contrary to the ductile gneisses and mylonites, show sinistral kinematics.

During this study, approaches involving e.g. structural geology, geochronology and metamorphic petrology (geothermobarometry) were utilised in order to reconstruct the overall deformation history of the SFSZ. The structural features of the study area were mapped during field work, the P-T conditions of deformation were calculated based on the results from electron microprobe analysis, and the different deformation phases were dated with SIMS U-Pb (zircon), ID-TIMS (titanite) and Ar-Ar (pseudotachylyte whole-rock) methods. The microprobe results indicate a peak metamorphism around 7 kbar and 680ºC (*Torvela and Annersten, 2005*). The obtained pressure estimation is higher than usually

reported for SW Finland (migmatites), possibly reflecting tectonic pressure during shearing and/or local thickening of the crust. Age determinations reveal repeated deformation along the shear zone with at least three, possibly four separate deformation phases occurring within the ductile regime (ca. 1.85 Ga, 1.83 Ga and 1.79 Ga), one possible deformation phase within the semi-ductile regime (<1.78 Ga), and at least one reactivation of the shear zone within or close to brittle crustal conditions (between 1.78 - 1.58 Ga). The results suggest that the crustal-scale shearing along the South Finland shear zone, and possibly also along other Palaeoproterozoic shear zones in southern Finland, was not restricted to the late-orogenic deformation phases. In fact, the SFSZ accommodated much of the strain not only from the very beginning of the Svecofennian orogeny to the late-orogenic period, but was reactivated at least once during a post-orogenic deformational event. Furthermore, the results indicate that the crust in the area of present SW Finland cooled rapidly around and soon after 1.79 Ga, probably due to uplift and exhumation, bringing the rocks into increasingly semi-ductile and, subsequently, brittle regimes.

Structural studies reveal that the partitioning of the deformation was more complex than a simple division into simple shear structures and flattening structures. Instead, the simple shear component of the deformation is, in addition to the main dextral shear zone, partly distributed into conjugate (SW-NE), sinistral, less intensive deformation zones SW of the main shear zone, and partly manifested as conical and sheath folds within the deformation zones. Moreover, while the simple shear component of deformation is responsible for the lateral movements along the deformation zones, the compressive component of the partitioned deformation produced flattening structures within the shear zone, as well as large-scale folds with SE-NW axes along the southwestern margin of the shear zone (fig. 2).

References

Ehlers, C., Lindroos, A. and Selonen, O., 1993. The late Svecofennian granite-migmatite zone of southern Finland – a belt of transpressive deformation and granite emplacement. Precambrian Research 64, 295-309.

Ehlers, C., Skiöld, T. and Vaasjoki, M., 2004: Timing of Svecofennian crustal growth and collisional tectonics in Åland, SW Finland. Bull. of the Geol. Soc. of Finland, 76, 63-91.

Korsman, K., Koistinen, T., Kohonen, J., Wennerström, M., Ekdahl, E., Honkamo, M., Idman, H. and Pekkala, Y., 1997 (Eds.). Bedrock Map of Finland 1:1000000. Geological Survey of Finland.

Torvela, T. and Annersten, H., 2005. PT-conditions of deformation within the Palaeoproterozoic South Finland shear zone: some geothermobarometric results. Bull. of the Geol. Soc. of Finland, 77, 151-164.

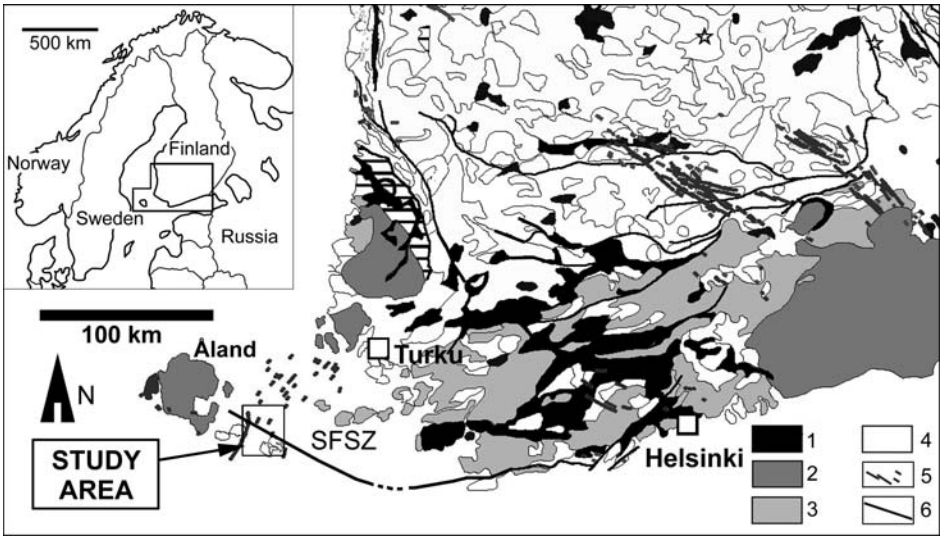

Figure 1. Generalised geological map of southern Finland (modified from Korsman et al. 1997). Key: SFSZ = South Finland shear zone, (1) Metavolcanic rocks ca. 1.92-1.88 Ga, (2) Rapakivi granites ca. 1.6 Ga, (3) Late-orogenic granites and migmatites of the LSGM ca. 1.85-1.80 Ga, (4) Granitoids and/or mica schists ca. 1.89-1.88 Ga, (5) Diabase dykes ca. 1.65-1.57 Ga, (6) Major faults and shear zones.

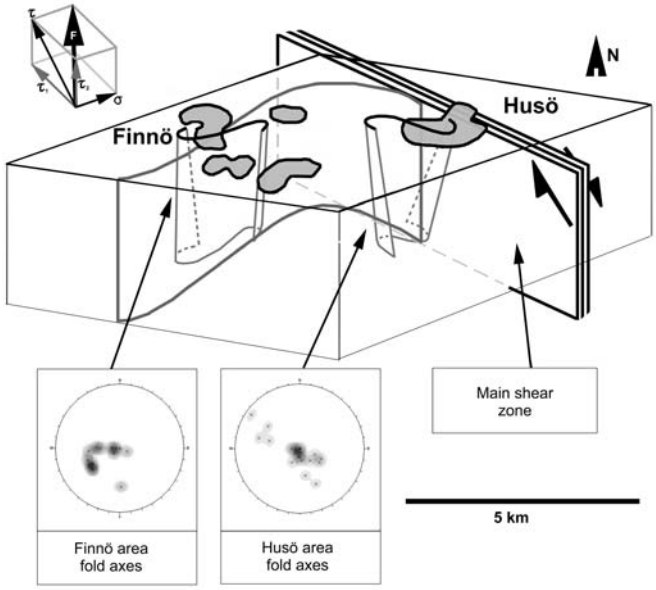

Figure 2. A schematic drawing with a structural interpretation of a part of the study area. The stereographic projections of the measured fold axes define conical folds, especially in Finnö area, formed as a response to the vertical component (τ_2) to the overall shear stress. The field mapping further reveals that the conical folds are refolded into large-scale folds along NW-SE fold axes as a result of the compressional (normal) component (σ) of the overall, regional force field affecting the area. The same overall structures area repeated over the entire study area.

Geology and correlation of the Lapland Granulite Belt

Pekka Tuisku[1]*, Hannu Huhma[2] , Perttu Mikkola[3] and Martin Whitehouse[4]

[1]Department of Geosciences, University of Oulu, P.O. Box 3000, FIN-90014 University of Oulu, Finland
[2]Geological Survey of Finland, P.O. Box 96, FIN-02151 Espoo, Finland
[3]Geological Survey of Finland, P.O. BOX 1237, FIN-70211 Kuopio, Finland
[4]Laboratory for Isotope Geology, Swedish Museum of Natural History, P.O. Box 50007, 10405 Stockholm, Sweden
*E-mail: pekka.tuisku@oulu.fi

This paper summarizes the geological, metamorphic and geochronological evolution of the approx. 1.9 Ga Lapland Granulite Belt (LGB) and discusses its correlation with the other ~ 1.9 Ga orogenic belts of the world. The provenance of the metasediments of the belt is mostly from a ~ 2 Ga silicic source. There is no such a silicic rock complex, large enough to have provided the sediment supply of the LGB, in the Fennoscansian Shield, Greenland or eastern part of the Canadian shield. Orogenic belts having an approx. age of 2 Ga seem to be abundant in some other continents like South America, Africa and Sinokorean craton. The igneous, moustly enderbitic rocks of the belt could be correlated with similar ~ 1.9 Ga rocks in Greenland and Canadian shield. On the other hand, metamorphism, deformation and exhumation of the Lapland granulite belt took place considerably earlier (30 – 50 Ma) than in those high-grade belts of Greenland and Canada that have earlier been correlated with the LGB.

Keywords: Lapland, granulite, petrology, migmatite, enderbite, high-grade metamorphism, zircon, U-Pb-dating, SIMS

1. Introduction and geological setting

The migmatitic metapelites of the Lapland granulite belt (LGB) in the NE part of the Fennoscandian Shield represent an arc-related greywacke basin metamorphosed in the granulite facies. The belt is bordered in the northeast by the Archaean and Proterozoic Inari and Kola gneiss complexes and in the southwest by the Archaean Karelian gneiss complex and the Proterozoic Central Lapland schist and greenstone belts. The granulite belt was juxtaposed between Archaean and Proterozoic terrains in the NE part of the Fennoscandian Shield concurrently with the accretion of Svecofennian arc complexes at ~1.9 Ga. The belt consists mainly of aluminous migmatitic metagreywackes. Abundant noritic to enderbitic magmas were intruded concordantly into the metasediments and were probably an important heat source for metamorphism, which took place during the crystallization of the magmas. This is supported by structural and contact relations of metasediments and igneous rocks, and by the lack progressive metamorphic reaction textures in the igneous rock series.

2. Regional metamorphism

The peak of metamorphism took place above the dehydration melting temperature of the biotite-sillimanite-plagioclase-quartz assemblage at 750–850 °C and 5–8.5 kbar which lead to formation of a restitic palaeosome and peraluminous granitic melt in metapelites. Subsequently, the rocks were decompressed and cooled below the wet melting temperature of pelitic rocks (650 °C) under the stability field of andalusite coexisting with potassium feldspar (2–3 kbar). Cooling was accompanied by the crystallization of the neosomes, often carrying aluminium-rich phases (*Tuisku et al., 2006*). Postmetamorphic duplexing of the LGB is clearly seen in the distribution of calculated PT conditions (*Korja et al., 1996*).

3. Isotopic dating

Detrital zircons from migmatitic metapelites are derived from 1.94–2.9 Ga old acid source rocks (U-Pb SIMS ages). The clustering of detrital zircon ages between 1.97 and 2.2 Ga is problematic, because abundant felsic crust of this age is rare in the shield. The metasediments are characterized by Sm-Nd model ages of ca. 2.3 Ga. A younger, 1905–1880 Ma population of homogeneous zircons was formed during regional metamorphism. The peak high-grade metamorphism took place at ~1900 Ma and the latest chronological record from subsequent decompression and cooling phase is from ca. 1880 Ma (*Tuisku and Huhma, 2006*).

Monazite U-Pb ages of migmatitic metasediments in the range 1906–1910±3 Ma overlap the late stage of enderbite intrusion and growth of early metamorphic zircons. Garnet-whole rock Sm-Nd ages from leucosomes in the range 1880–1886±7 Ma are concurrent with the growth of the youngest metamorphic zircons and probably indicate the crystallization of leucosomes or the influence of a fluid liberated from them. Isotopic and petrologic data reveal that the evolution of Lapland Granulite belt from the erosion of source rocks to the generation of a sedimentary basin, its burial, metamorphism and exhumation took place within ca. 60 Ma (*Tuisku and Huhma, 2006*).

The norite-enderbite series of the LGB represents arc-magmas, which were intruded into the metasediments at ~1920 –1905 Ma ago according to ID-TIMS zircon U-Pb ages and were probably an important heat source for metamorphism (*Tuisku and Huhma, 2006*). Zircon SIMS U-Pb dating and BE-imaging reveal that the zircons in these intrusions usually have igneous ~ 1.90 – 1.92 Ga old cores, which are often surrounded by slightly younger rims (*Tuisku and Huhma, 2005*). Older, zoned zircon grains in a quartz norite vein, initial ε_{Nd} values of 0 to +1 and the continuous spectrum of LILE enrichment in the enderbite-series probably reflect assimilation of metasediments by magmas (*Tuisku and Huhma, 2006*). Similar zoned, inherited, older grains are are also abundant in Myössäjävi biotite-garnet granodiorite body, although the trace element pattern of this intrusion is similar to the intrusion with lesser amount of inherited grains (*Tuisku and Huhma, 2005*).

4. Correlation

The orogenic evolution of the LGB may be considered part of the Svecofennian orogeny, which had its most active phase between 1.93 and 1.87 Ga in Finland. The ca. 1.92–1.91 Ga norite-enderbite series of the LGB has the same age as the pre- or syntectonic tonalites of the primitive arc complex of Central Finland, dated at 1.93–1.91 Ga (*Vaasjoki et al., 2003*). The supracrustal sequences of the primitive arc are considered 1.92–1.88 Ga old and the active arc-continent collision phase 1.89–1.87 Ga old, which is similar to the exhumation stage of the LGB, obtained in the present study. The difference between the Svecofennian orogen and the LGB is that the LGB evolved within a relatively short period of time around 1.9 Ga. Its evolution was terminated in an oblique continent-continent collision between the Karelian terrain and Kola Peninsula terrain at the NE edge of Karelian terrain (*Korja et al., 1996*), while the Svecofennian orogen evidently was built up over a longer interval by accretion of separate arc complexes at the SW edge of the cratonic nucleus.

The age of the norite-enderbite series of the LGB is similar to 1.92 Ga Arfersiorfik quartz diorite and Sisimiut charnockites of the Nagssugtoqidian belt in Greenland. Correlation of the igneous event of the LGB to Greenland is thus justified on a geochronological basis. However, later tectonic and thermal events evident in the

Nagssugtoqidian belt are lacking in the high-grade rocks of the LGB. The assembling of Nagssugtoqidian took place at ca. 1850 to 1820 Ma and was considerably later than the 1910–1880 Ma assembling event in the LGB. The Greenland events are thus not correlated to the thrusting and exhumation event of the LGB, even if diachronous assembling were to be considered, and it is evident that *Hoffman's (1989)* construction needs refining in this respect.

If we go further west to North America, and the Canadian Shield (i.e. Torngat Orogen), it may be stated that in relation to the LGB, the same applies as with Greenland. Ca. 1.9 Ga arc magmatism is widespread in the Torngat Orogen and may be chronologically correlated to the LGB, but again, the orogenic deformation is much younger in the Torngat than in the LGB. Even arc magmatism is considerably younger, i.e. 1865–1800 Ma, in other orogens of the eastern North America *(Wardle et al., 2002)*.

However, arc magmatism and deformation of about the same age or slightly older as in the LGB are found in the Taltson-Thelon magmatic zone in the Western part of the Canadian Shield *(Bostock and van Breemen, 1994)* and in the Aldan Shield *(Frost et al., 1998)*. In the western Canadian Shield, 2.3–2.0 Ga juvenile crust is present in the Wopmay orogen, which could be a potential provenance for the sedimentary protoliths of the LGB metapelites (*Hoffman, 1988*). Also, the first two arc episodes of the Wopmay orogen overlap the arc and granulite-facies evolution of the LGB (*Bowring & Podosek, 1989*). As proposed by *Frost et al. (1998)*, the Aldan and western Canadian Shields could be linked, but, according to our data, the LGB could possibly be added to that linkage. It is quite evident that the intercontinental correlation of terranes having different protoliths, different metamorphic and accretion history is often possible only after their final juxtaposition during crustal assembly. *Friend and Kinny (2001)* actually showed this for the Lewisian Complex of Scotland. It is also evident that even if we have terranes of approximately the same protolith or metamorphic age side by side in this kind of late assembly, the age criteria alone does not prove their past close relationship.

References

Bostock, H.H., & van Breemen, O., 1994. Ages of detrital and metamorphic zircons and monazites from a pre-Taltson magmatic zone basin at the western margin of Rae Province. *Canadian Journal of Earth Sciences* 31, 1353–1364.

Bowring, S.A. & Podosek, F.A., 1989. Nd isotopic evidence from Wopmay Orogen for 2.0-2.4 Ga crust in western North America. Earth and Planetary Science Letters 94, 217–230.

Friend, C.R.L. & Kinny, P.D., 2001. A reappraisal of the Lewisian gneiss complex: geochronological evidence for its tectonic assembly from disparate terranes in the Proterozoic. Contributions to Mineralogy and Petrology 142, 198–218.

Frost, B.R., Avchenco, O.V., Chamberlain, K.R. & Frost, C.D., 1998. Evidence for extensive Proterozoic remobilization of the Aldan shield and implications for Proterozoic plate tectonic reconstruction of Siberia and Laurentia. Precambrian Research 89,1–23.

Hoffman, P.F., 1988. United plates of America, the birth of a craton: Early Proterozoic assembly and growth of Laurentia. Annual Reviews of Earth and Planetary Sciences 16, 543–603.

Hoffman, P.F., 1989. Precambrian geology and tectonic history of North America. In: Bally, A.W. & Palmer, A.R. (eds) The Geology of North America-An Overview. Geological Society of America, Boulder, Colorado, 447–512.

Korja, T., Tuisku, P., Pernu, T. & Karhu, J., 1996. Field, petrophysical and carbon isotope studies on the Lapland Granulite Belt: implications for deep continental crust. Terra Nova 8, 48–58.

Tuisku, P., & Huhma, H., 2006, in print. Evolution of Migmatitic Granulite Complexes: Implications from Lapland Granulite Belt, Part II: Isotopic dating. Bulletin of the Geological Society of Finland 78, xxx-xxx.

Tuisku, P. & Huhma, H., 2005. Generation of the norite-enderbite series of the Lapland Granulite Belt: implications from SIMS U-Pb-dating of zircons. EGU General Assembly, Vienna, Austria, 24 – 29 April 2005, Geophysical Research Abstracts, Vol. 7, 08022, 2005

Tuisku, P., Mikkola, P. & Huhma, H., 2006. Evolution of Migmatitic Granulite Complexes: Implications from Lapland Granulite Belt, Part I: Metamorphic geology. Bulletin of the Geological Society of Finland 78, 71–105.

Vaasjoki, M., Huhma, H., Lahtinen, R., Vestin, J,. 2003. Sources of Svecofennian granitoids in the light of ion probe U-Pb measurements on their zircons. Precambrian Research 121, 251-262.

Wardle, R.J., Gower, C.F., James, D.T., St-Onge, M., Scott, D.J., Garde, A.A., Culshaw, N.G., van Gool, J.A.M., Connelly, J.A., Perreault, S. & Hall, J., 2002b. Correlation Chart of the Proterozoic assembly of the northeastern Canadian – Greenland Shield. Canadian Journal of Earth Sciences 39, Chart 1.

Modeling the source of the Svecofennian late orogenic granites: a case study from West Uusimaa, Finland

Mari Tuusjärvi[1]* and Laura S. Lauri[1]
[1]Department of Geology, P.O. Box 64, FI-00014 University of Helsinki, Finland
*E-mail: mari.tuusjarvi@helsinki.fi

In this study we have described the host rocks of the 1.85–1.79 Ga late orogenic granites in the West Uusimaa area and modeled partial melting of local felsic volcanic rocks and mica gneisses to see if Ba, Rb, and Sr evolve towards the values observed in the late orogenic Tynnärlampi granite pluton. The models used were modal and non-modal batch melting and muscovite dehydration melting. Muscovite dehydration melting of mica gneiss and fractionation of K-feldspar and plagioclase from the partial melt produce Rb, Ba, and Sr concentrations close to those of the Tynnärlampi pluton.

Keywords: S-type granite, partial melting, West Uusimaa, Finland

1. Introduction

Peraluminous S-type granites are thought to originate by melting of crustal sources (e.g., *Chappell and White, 1974*). In this study we are trying to find the most probable source for the late orogenic, peraluminous granites in the West Uusimaa area in south-western Finland. Based on earlier studies related on the genesis of peraluminous granites (e.g., *Jung et al., 2000; Solar and Brown, 2001; Milord et al., 2001; Johannes et al., 2003*) we have focused our modeling on acidic gneisses, formerly felsic volcanic rocks, and mica bearing gneisses that are both abundant in the West Uusimaa area. To model partial melting of these rocks we have used modal and non-modal batch melting models (e.g., *Allègre and Minster, 1978*) for felsic volcanic rocks and muscovite dehydration melting model (e.g., *Patiño Douce and Harris, 1998*; *Zou and Reid, 2000*) for mica gneisses.

2. Geology of the West Uusimaa area

The study area is located in the central part of the Uusimaa belt, within the Kemiö–Järvenpää field (see e.g., *Kähkönen, 2005*). It is delimited by the ~1.83 Ga late orogenic granites of Perniö (*Selonen et al., 1996*), Veikkola, and Tenhola (*Kurhila et al., 2005*) on three sides and the Somero shear (*Skyttä et al., 2006*) in the north. The area consists of ca. 1.90–1.87 Ga old volcano-sedimentary rocks, granodiorites and mafic rocks of the Arc complex of southern Finland (e.g., *Huhma, 1986; Korsman et al., 1997; Väisänen and Mänttäri, 2002; Väisänen et al., 2002*). The area was metamorphosed in low-P, high-T (amphibolite and granulite facies) conditions at 1.83–1.81 Ga (*Schreurs and Westra, 1986; Mouri et al., 2005*). The 1.85–1.79 Ga late orogenic granites are present throughout the area in small volumes, occurring as dikes and small patches that migmatize and intrude the metamorphic rocks. Some larger granite masses (a few km^2), such as the Tynnärlampi and Kovela plutons, are also found in the area.

Late orogenic granites within the West Uusimaa area are mostly coarse-grained or pegmatitic and quite leucocratic. Biotite is the most common mafic mineral and garnet (up to a few cm in diameter) is also abundant. Some pyroxenes or amphiboles were also observed in granites within the granulite facies metamorphic block, but these may be due to partly digested xenoliths within the granites.

In the West Uusimaa area the synorogenic Svecofennian rocks types such as acidic gneisses, mica schist, and mica gneisses form a potential source of the peraluminous,

microcline-rich granites (see e.g., *Jung et al., 2000; Solar and Brown, 2001; Milord et al., 2001; Johannes et al., 2003*). Based on field observations, acidic gneisses can be divided into three groups: (1) Fine to medium-grained, texturally homogenous or slightly schistose rocks which are mainly composed of quartz and biotite. Feldspars and garnet are present in some samples; (2) Porphyritic, matrix-supported rocks, which are mainly composed of quartz, K-feldspar and biotite. Matrix is fine-grained. Round porphyroclasts or porphyroblasts, mainly composed of quartz, are 0.5-1 cm in diameter; (3) Medium-grained, schistose, light brown rocks composed mostly of quartz, K-feldspar and biotite. Some samples were pyroxene-bearing. These rocks were found within the granulite facies metamorphic block and resemble the metamorphic charnockites that *Helenius et al. (2004)* have described in the Turku granulite area further west. Mica schists and gneisses are also abundant in the West Uusimaa area. They are usually grey, medium-grained rocks which are schistose and/or strained and consist mostly of quartz, biotite±muscovite±garnet±cordierite. In some places these rocks are strongly schistose and/or strained, folded and migmatized. Strongly migmatitic, garnet-bearing rocks are mostly located within the granulite facies metamorphic block, and biotite is the main mafic mineral in them. Other rock types in the study area comprise limestones, amphibolites, ultramafic rocks, and granodiorites.

3. Geochemical modeling

For modeling purposes, a sample set was chosen from samples collected for the "Granite Petrology and Uranium Metallogenesis in Southern Finland" –project of the Department of Geology, University of Helsinki and from the Lithogeochemistry Database of the Geological Survey of Finland (GTK). The samples include three late orogenic granite analyses from the Tynnärlampi and Kovela plutons and 89 analyses from the host rocks in the West Uusimaa area.

The Tynnärlampi and Kovela granites are both peraluminous. The Kovela granite is higher in CaO, Na_2O, and Sr and lower in K_2O, SiO_2, Ba, and Rb than the Tynnärlampi granite. The low SiO_2 content of the Kovela granite suggests that the pluton has suffered from episyenitization (i.e., leaching of silica during hydrothermal alteration). REE patterns of the two granites are similar in shape and seem to be controlled by monazite which is an abundant accessory mineral in both plutons.

The modeling was focused on the Tynnärlampi granite as the pluton seems to have suffered less from hydrothermal alteration than the Kovela granite. In addition, the host rocks of the Tynnärlampi pluton include both felsic volcanic rocks and mica gneisses. Felsic volcanic rock sample 92008769 and mica gneiss sample 92008782 from the Lithogeochemistry Database of the GTK were used as the source compositions and granite sample LSL-05-29.1 from the Tynnärlampi pluton was used as the modeling target. Models were based on evolution of Rb, Ba, and Sr in the partial melt as the distribution of these elements is controlled by major rock forming minerals such as feldspars and micas.

The models used in the study were (1) modal and non-modal batch melting models (e.g., *Allègre and Minster, 1978*) for congruent melting of sample 92008769 and (2) muscovite dehydration melting model using the incongruent dynamic melting equation of *Zou and Reid (2000)* for sample 92008782.

The mass-proportional reaction

22Ms + 7Pl + 8Qtz -> 25Melt + 5Kfs + 5Sil + 2Bt *(Patiño Douce and Harris, 1998)*

was used to describe the muscovite dehydration reaction in model (2). K_D-values used were from *Ewart and Griffin (1994)*.

Neither congruent melting of felsic volcanic rock nor muscovite dehydration melting of mica gneiss could produce Rb and Ba contents comparable to those in the Tynnärlampi granite (Figs. 1 and 2). However, Rb values comparable to the Tynnärlampi sample were obtained with 50% fractionation of K-feldspar from melt generated by 20% partial melting of mica gneiss (Fig. 3). Minor plagioclase fractionation would be needed to generate Ba and Sr values observed in the Tynnärlampi pluton. Our modeling result is consistent with the leucosome–granite model of *Johannes et al. (2003)* based on the migmatites of the Turku area.

References

Chappell, B.W., White, A.J.R., 1974. Two contrasting granite types. *Pacific Geol. 8, 173–174*.

Ewart, A. and Griffin, W.L., 1994. Application of Proton-Microprobe Data to Trace-Element Partitioning in Volcanic-Rocks. Chem. Geol. 117, 251-284.

Helenius, E-M., Eklund, O., Väisänen, M., Hölttä, P., 2004. Petrogenesis of charnockites in the Turku granulite area. In: Ehlers, C., Eklund, O., Korja, A., Kruuna, A., Lahtinen, R. and Pesonen, L. J. (Eds.). Lithosphere 2004 – Third Symposium on the Structure, Composition and Evolution of the Lithosphere in Finland. Programme and Extended Abstracts, Turku, Finland, November 10–11, 2004. Institute of Seismology, University of Helsinki, Report S-45, 17–20.

Huhma, H., 1986. Sm-Nd, U-Pb and Pb-Pb isotopic evidence for the origin of early Proterozoic Svecokarelian crust in Finland. Geol. Surv. Finland, Bull. 337.

Johannes, W., Ehlers, C., Kriegsman, L.M., Mengel, K., 2003. The link between migmatites and S-type granites in the Turku area, southern Finland. Lithos 68, 69-90.

Jung, S., Hoernes, S. and Mezger, K., 2000. Geochronology and Petrolgenesis of Pan-African, syn-tectonic, S-type and post-tectonic A-type granite (Namibia): products of melting of crustal sources, fractional crystallization and wall rock entrainment. Lithos 50, 259-287.

Korsman, K., Koistinen, T., Kohonen, J., Wennerström, M., Ekdahl, E., Honkamo, M., Idman, H., Pekkala, Y. (Eds.), 1997. Suomen kallioperäkartta – Bedrock map of Finland 1:1 000 000. Espoo: Geol. Surv. Finland.

Kurhila, M.I., Vaasjoki, M., Mänttäri, I., Rämö, O.T., Nironen, M., 2005. U-Pb ages and Nd isotope charasteristics of the lateorogenic, migmatizing microline granites in southwestern Finland. Bull. Geol. Soc. Finland 77, 105–128.

Kähkönen, Y., 2005. Svecofennian supracrustal rocks. In: Lehtinen, M., Nurmi P.A., Rämö, O.T (Eds.), Precambrian Geology of Finland – Key to the Evolution of the Fennoscandian Shield. Developments in Precambrian Geology 14, Elsevier Science B.V., Amsterdam, 343–406.

Milord, I., Sawyer, E.W., Brown, M., 2001. Formation of Diatexite Migmatite and Granite during Anatexis of Semi-pelitic Metasedimentary Rocks: an example from St. Malo, France. J. Petrol. 42, 3, 487–505.

Mouri, H., Väisänen, M., Huhma, H. and Korsman, K., 2005. Sm-Nd garnet and U-Pb monazite dating of high-grade metamorphism and crustal melting in the West Uusimaa area, southern Finland. GFF 127, 123-128.

Patiño Douce, A., Harris, N., 1998. Experimental Constraints on Himalayan Anatexis. J. Petrol. 39, 4, 689-710.

Schreurs, J., Westra L., 1986. The thermotectonic evolution of a Proterozoic, low pressure, granulite dome, West Uusimaa, SW Finland. Contrib. Mineral. Petrol. 93, 236–250.

Selonen, O., Ehlers, C., Lindroos, A., 1996. Structural features and emplacement of the late Svecofennian Perniö granite sheet in southern Finland. Bull. Geol. Soc. Finland 68, 5–17.

Skyttä, P., Väisänen, M., Mänttäri, I., 2006. Preservation of Palaeoproterozoic early Svecofennian structures in the orijärvi area, SW Finland—Evidence for polyphase strain partitioning. Precambrian Res. (in press).

Solar, G.S. and Brown, M. 2001. Petrogenesis of Migmatites in Maine, USA: Possible Source of Peraluminous Leucogranite in Plutons? J. Petrol. 42, 4, 789-823.

Väisänen, M., Mänttäri, I., 2002. 1.90–1.88 Ga arc and back-arc Basin in the Orijärvi area, SW Finland. Bull. Geol. Soc. Finland 74, 185–214.

Väisänen, M., Mänttäri, I., Hölttä, P., 2002. Svecofennian magmatic and metamorphic evolution in southwestern Finland as revealed by U–Pb zircon SIMS geochronology. Precambrian Res. 116, 111–127.
Zou, H. and Reid, M., 2000. Quantitative modelling of trace element fractionation during incongruent dynamic melting. Geochim. Cosmochim. Acta 65, 153–162.

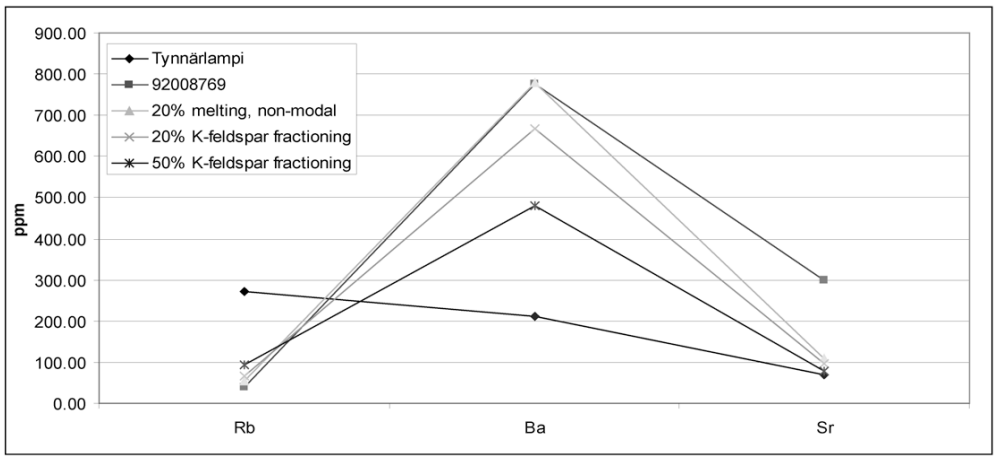

Figure1. Congruent, non-modal melting (F = 20%) of sample 92008769 (felsic volcanic rock) and fractionation of K-feldspar from the partial melt.

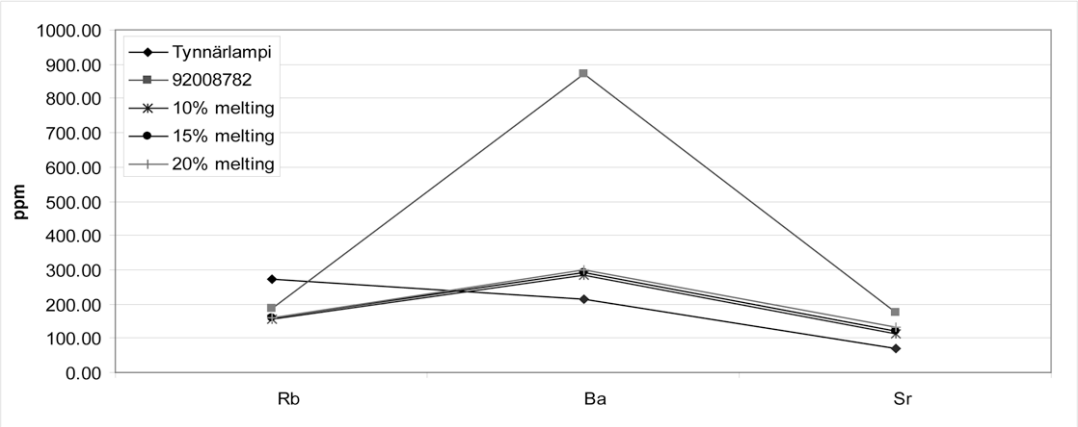

Figure 2. Incongruent muscovite dehydration melting of sample 92008782 (mica gneiss).

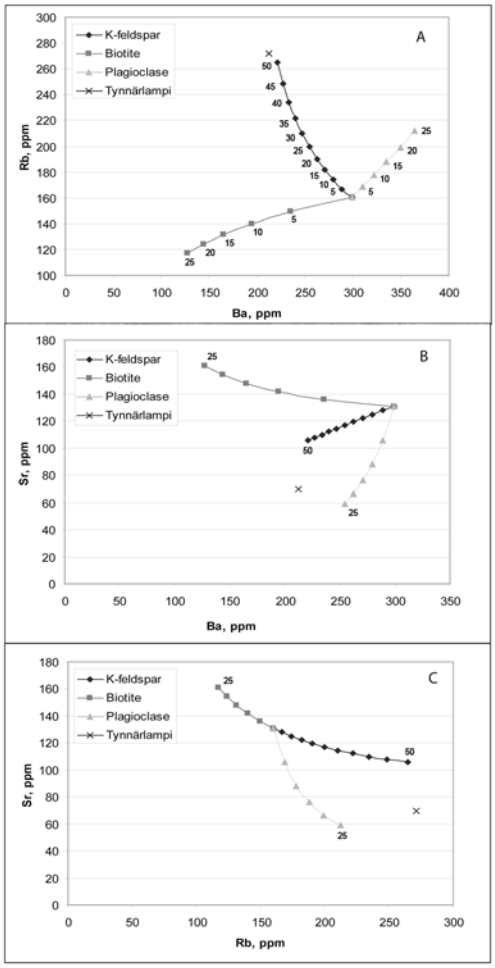

Figure 3. The effect of fractionation of K-feldspar, plagioclase and biotite from partial melt acquired by 20% melting of sample 92008782, (A) Ba vs. Rb, (B) Ba vs. Sr and (C) Rb vs. Sr.

Crustal conductivity of the central Fennoscandian Shield revealed by 2D inversion of GGT/SVEKA and MT-FIRE datasets

K. Vaittinen[1*], I. Lahti[2], T. Korja[1] and P. Kaikkonen[1]

[1]University of Oulu, Department of Physical Sciences, Geophysics
[2]Geological Survey of Finland, Rovaniemi
*E-mail: katri.vaittinen@oulu.fi

By 2D inversion we have acquired new crustal conductivity models for the central Fennoscandian Shield along the GGT/SVEKA transect and across the Archaean - Proterozoic border zone. The original magnetotelluric dataset was collected during several projects in 1985-1998. The latest addition to this data is the broadband sites measured during years 2003-2005 in the frame of MT-FIRE project.

Keywords: Magnetotellurics, 2D inversion, crustal conductivity, Fennoscandian Shield

1. Introduction

Magnetotelluric studies of the Fennoscandian Shield have a history of more than 20 years. In early studies the models were obtained by forward trial and error search (e.g. Kaikkonen & Pajunpää, 1984; Korja & Koivukoski, 1994). Only recently the 2D inversion techniques and tools have developed enough to provide geologically meaningful models routinely. Using these new tools on older data previously modeled with forward techniques helps us to verify the results. Recently Lahti et al. (2002, 2006) have inverted the GGT/SVEKA data which consists of old SVEKA sites and previously unmodeled data from the southwestern and northeastern parts of the GGT/SVEKA profile (Fig 1). The latest acquired and inverted dataset is the MT-FIRE (Vaittinen et al., 2005) which aims to complement the reflection seismic data of the FIRE project. This dataset coincides partially with GGT/SVEKA but also provides information from areas where no previous magnetotelluric work has been done (Fig 1). Also the vertical component of magnetic field is measured and used in the inversion of the new data. In this presentation we combine the crustal conductivity models and results of these two studies.

2. Datasets and inversion

The two profiles of lengths 710 km and 255 km along the GGT/SVEKA transect cross the main tectonic units in the central part of the Fennoscandian Shield (Fig. 1). These units are the Archaean Karelian Province in the northeastern part of the profile 1 and several Paleoproterozoic arc complexes in the Svecofennian Domain to the southwest from the Karelian Province (e.g. Korsman et al., 1999). In MT-FIRE we have several shorter profiles crossing the same borders at different areas, which give us better possibility to model the essentially three dimensional environment. Due to the development in instrumentation, in the latter field campaign we were able to gain data at much shorter periods than before. Thus the new data has penetration depth range from about one kilometer to upper mantle whereas the older data in average misses the uppermost ten kilometers. Description of the data acquisition and processing of the GGT/SVEKA and MT-FIRE dataset can be found in Korja and Koivukoski (1994) and Vaittinen et al. (2005), respectively.

In the traditional 2D inversion of magnetotelluric data the geoelectrical strike of the area must be known in order to rotate the impedance tensor so that only the principal (=off-diagonal) components remain. These components correspond to two perpendicular directions known as the TE (electrical field along the strike) and TM (electrical field perpendicular to the strike) modes for which the apparent resistivity and phase are fit in inversion. In the areas where the determination of a stable regional strike is difficult (e.g. due to three-dimensionality), it is possible to invert the determinant apparent resistivity and phase since they are independent of the selected strike. This is the case in most of our profiles, and thus the inversion was carried out using the REBOCC code (Siripunvaraporn & Egbert, 2000) modified for determinant inversion by Pedersen & Engels (2005). For more specific details on data dimensionality analysis and inversion see Lahti et al (2002) for GGT/SVEKA profiles and Vaittinen et al (2005) for MT-FIRE.

3. Models and discussion

As examples of our work we show in this abstract 2D inversion models of the GGT/SVEKA profile 1 and the MT-FIRE profile C (Fig. 2a and 2b, respectively). These models are chosen because they are partly collocated and illustrate very well the difference of the datasets and how the shorter site distance and wider period range of the new data affect the resolution of the model. In the collocated part of these profiles the conductor associated with the Kainuu Belt is dipping under the resistive Iisalmi Complex to the approximate depth of 20 km. The Kainuu Belt conductor can be traced very close to surface using the high-density MT-FIRE data. The MT-FIRE data shows also clearly that the southwestward dipping Kainuu Belt conductor and the eastward dipping conductor beneath the Iisalmi complex are two separate conductors.

Main results from all of our models are: (1) resistive Archaean lower crust as opposed to generally conductive Palaeoproterozoic lower crust, (2) conductivity structure of the Tampere Belt and Pirkkala Belt supporting a theory of two subductions, (3) subsurface discontinuity of the conductive metasediments of the Kainuu and North Karelia Belts as well as the Kainuu and Savo Belts.

Note that the very thick conductors in the models are more likely a result of the Occam inversion procedure that is looking for a smooth transition between structures instead of sharp boundaries. It is shown by 2D forward modeling (Lahti et al. 2006) that, for instance in the case of the Kainuu Belt, a model with a 10 km thick conductor having resistivities from 0.4 Ωm to 40 Ωm and the inversion model with smooth structures (Fig. 2a) have equal fit to measured data. Also due to the very high electrical conductivity the resolution beneath good conductors is very limited or the data may provide no information beneath the conductors.

References

Kaikkonen, P. and Pajunpää, K., 1984. Audiomagnetotelluric measurements across the Lake Ladoga - Bothnian Bay Zone in Central Finland.Geophys. J. R. Astron. Soc., 78: 439 - 452.

Koistinen, T., Stephens, M.B., Bogatchev, V., Nordgulen, O., Wennerström, M. & Korhonen, J. 2001. Geological map of the Fennoscandian Shield, scale 1:2 000 000. Geological Surveys of Finland, Norway and Sweden and the North-West Department of Natural Resources of Russia.

Korja, T. ja Koivukoski, K., 1994. Crustal conductors of the SVEKA Profile in the Fennoscandian (Baltic) Shield, Finland, Geophys. J. Int., 116, 173-197.

Korsman, K., Korja, T., Pajunen, M., Virransalo, P. & the GGT/SVEKA Working Group 1999. The GGT/SVEKA transect: structure and evolution of the continental crust in the Paleoproterozoic Svecofennian Orogen in Finland, International Geological Review, 41, 287–333.

Lahti, I., Korja, T., Pedersen, L. B. and the BEAR Working Group 2002. Lithospheric conductivity along GGT/SVEKA Transect: implications form the 2-D inversion of magnetotelluric data. Pp. 75 - 78 in Lahtinen, R. et al (eds), 2002. Lithosphere 2002, Second Symposium on the Structure, Composition and Evolution of the Lithosphere in Finland. Institute of Seismology, University of Helsinki, Report S- 42.

Lahti, I., Korja, T., Pedersen, L. and BEAR working group, 2006. Lithospheric conductivity along the GGT/SVEKA transect in the central Fennoscandian Shield. Geophysical Journal International (in rev).

Pedersen, L. and Engels, M., 2005. Routine 2D inversion of magnetotelluric data using the determinant of the impedance tensor. Geophysics, 70, 33-41.

Siripunvaraporn W. and Egbert G., 2000. An efficient data-subspace inversion method for 2-D magnetotelluric data. Geophysics, 65(3), 791-803.

Vaittinen, K., Korja T., Kaikkonen, P., Lahti, I., Smirnov M. ja Pedersen L.P., 2005. MT-FIRE –hankkeen alustavia tuloksia kuoren sähkönjohtavuudesta Kainuun liuskejakson ja Iisalmen lohkon alueella. Teoksessa: Viljanen, A. ja Mäntyniemi, P. (toim.): XXII Geofysiikan päivät Helsingissä 19.-20.5.2005. Geofysiikan seura ry, Helsinki, 241 – 245.

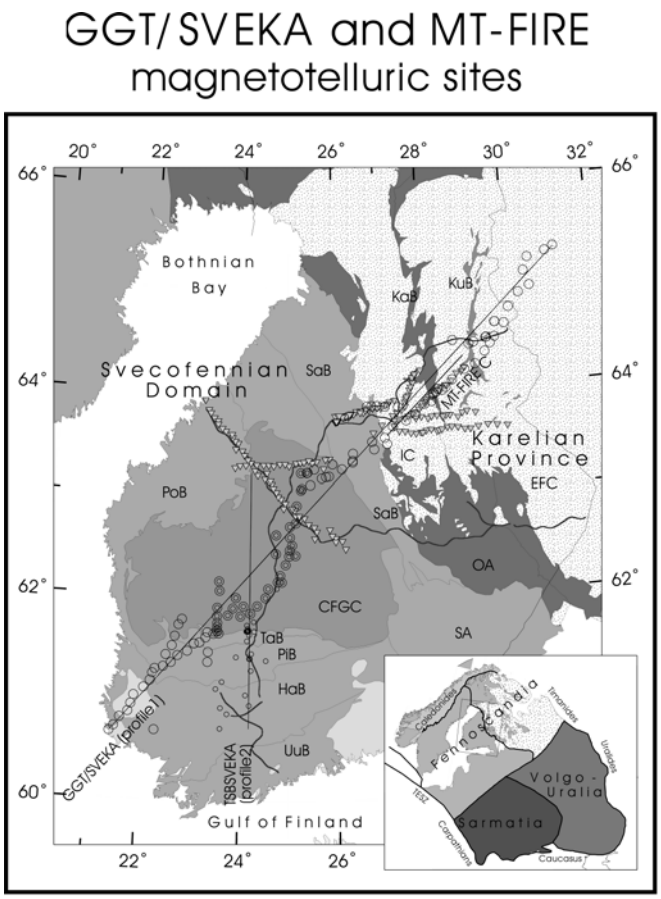

Figure1. Location of magnetotelluric sites used in this study. Geological map is simplified from Koistinen et al., 2001. Circles indicate magnetotelluric sites that were used in the inversion by Lahti et al (2006), large circles and small circles belong to profile 1 and profile 2, respectively. Black thin lines indicate the location of the 2D models of the profiles 1 and 2. Note that only the model from profile 1 is shown in Fig. 2. Inverted triangles show MT-FIRE sites. Profile C (model shown in Fig. 2b) is part of the profile 1 and is shown by a parallel thin line. Thick lines show the FIRE reflection seismic lines. Abbreviations: EFC = Eastern Finland Complex, IC = Iisalmi Complex, KaB = Kainuu Belt, SA = Saimaa Area, PiB = Pirkkala Belt, TaB = Tampere Belt, CFGC = Central Finland Granitoid Complex, PoB = Pohjanmaa Belt, OA = Outokumpu Area, SaB = Savo Belt, UuB = Uusimaa Belt, HaB = Hämeenlinna Belt, KuB = Kuhmo Belt

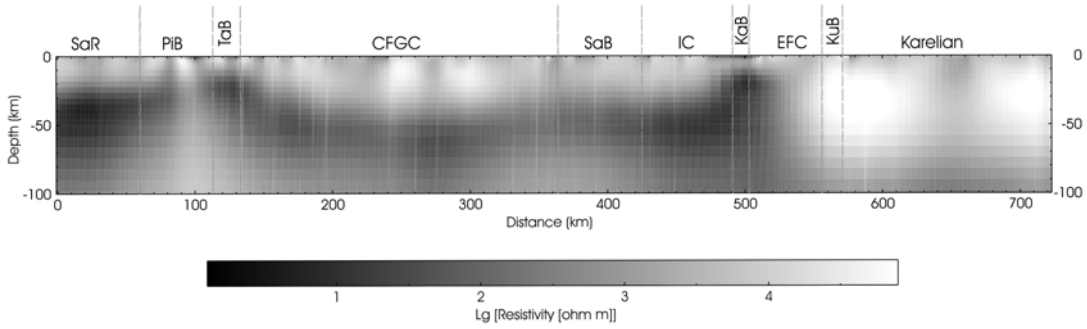

a)

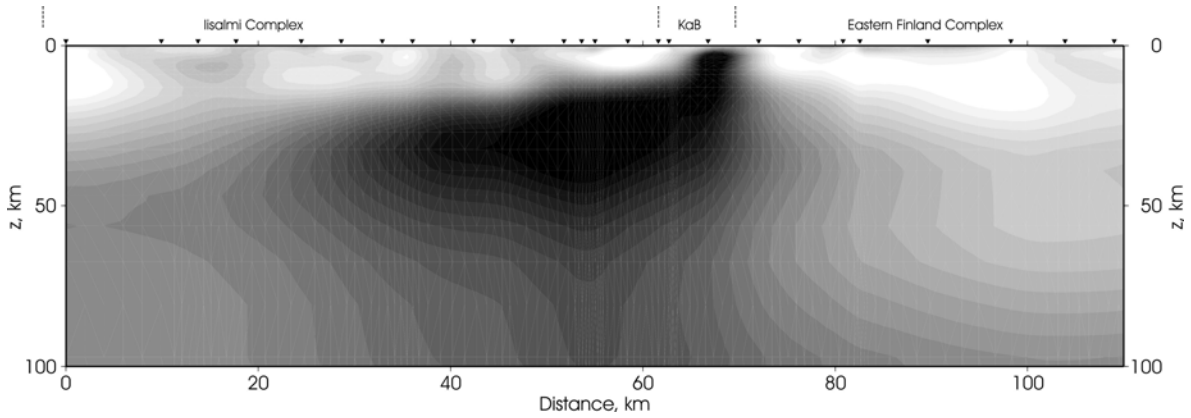

b)

Figure 2. The two laterally collocated electrical resistivity models obtained by 2D inversion of magnetotelluric data. Panel (a) is the smooth (Occam) inversion model along the profile 1 (RMS = 2.6%) *(Lahti et al., 2006)*. Panel (b) is similar inversion model of MT-FIRE profile C (RMS = 3.0%). Gray scale refers to model resistivities in Ωm. Abbreviations used to mark geological units for models: EFC = Eastern Finland Complex, IC = Iisalmi Complex, KaB = Kainuu Belt, PiB = Pirkkala Belt, TaB = Tampere Belt, CFGC = Central Finland Granitoid Complex, SaB = Savo Belt, SaR = Satakunta Rapakivi area, KuB = Kuhmo Belt.

Dyke swarms and plate movements

Jouni Vuollo[1]* and Satu Mertanen[2]

[1]Geological Survey of Finland, P.O. Box 77, FI-96101 Rovaniemi, Finland
[2]Geological Survey of Finland, P.O. Box 96, FI-02151 Espoo, Finland
*E-mail: jouni.vuollo@gtk.fi

Dyke swarms of the Fennoscandian shield reflect the rifting of the litosphere in several episodes during Archean – Early Paleoproterozoic. 2.6-2.45 Ga dykes are geochemically similar between each other, but diverse from 2.32-1.98 Ga dykes. Considerable plate movement from high to low paleolatitudes took place at 2.6-2.45 Ga.

Keywords: mafic dyke swarms, geochemistry, paleomagnetism, Archean, Paleoproterozoic, Fennoscandian shield

1. Introduction

The eastern and northern Fennoscandian shield is transected by a number of dyke swarms that were injected in different episodes of crustal rifting during Archean - Paleoproterozoic. Dyke swarms provide invaluable material for studies on crustal evolution and are essential for understanding of the tectonic evolution of rift-related environments and mantle plumes and for defining plate tectonic processes and plate movements (see *Hanski et al., 2006)*. Recently, *Bleeker and Ernst (2006)* have stressed the importance of dykes in a model of a long-lasting, ca. 2.7-2.0 Ga supercontinent that is constructed according to the occurrence of dyke swarms on presently dispersed cratons. The Precambrian dyke swarms of the Fennoscandian Shield provide excellent material for such studies due to their extensive spatial and temporal coverage. The present paper shows the latest knowledge on the dyking events and plate movements of the Fennoscandian shield during Archean – Paleoproterozoic.

2. Dyke swarms

A map of the areal distribution of mafic dyke swarms in the eastern Fennoscandian Shield is shown in Figure 1. Together with previous zircon ages (*Vuollo 1994*), the present results (Table 1) indicate that there were several dyke emplacement events especially between 2.5 and 1.98 Ga *(Vuollo and Huhma, 2005)*.

2.1. Achaean dykes/intrusions

At present, there are only few geochronological evidences of older Archean dyke swarms in the Fennoscandian Shield. *Bayanova and Yegorov (1999)* have obtained an age of 2740±10 Ma from two gabbronorite dykes (Fig 1.) in Kola Province. A new age determination from the Shalskiy gabbronorite dyke near the Burakovka layered intrusion (Fig. 1) gives a Sm-Nd age of 2608±56 Ma *(Mertanen et al. 2006b)*. Furthermore, new preliminary unpublished age dating from the Tervonkangas dyke at Pudasjärvi block shows nearly the same age - 2623±34 Ma *(*pers. comm., *Mutanen and Huhma, 2006)*. A typical feature of the Archean dykes/intrusions is their so called gabbro-noritic geochemical signature. Dykes from the Kola Peninsula *(Fedotov 2005)* and Shalskiy do not principally differ geochemically from those of the 2.45 Ga gabbronorite - norites in the Karelian

Province (Karelian block, Kuhmo-Paajarvi area). All the dykes are quite similar showing slight calc-alkaline affinity and low TiO_2 and high SiO_2 with moderate MgO and low Cr and Ni (see Fig. 2).

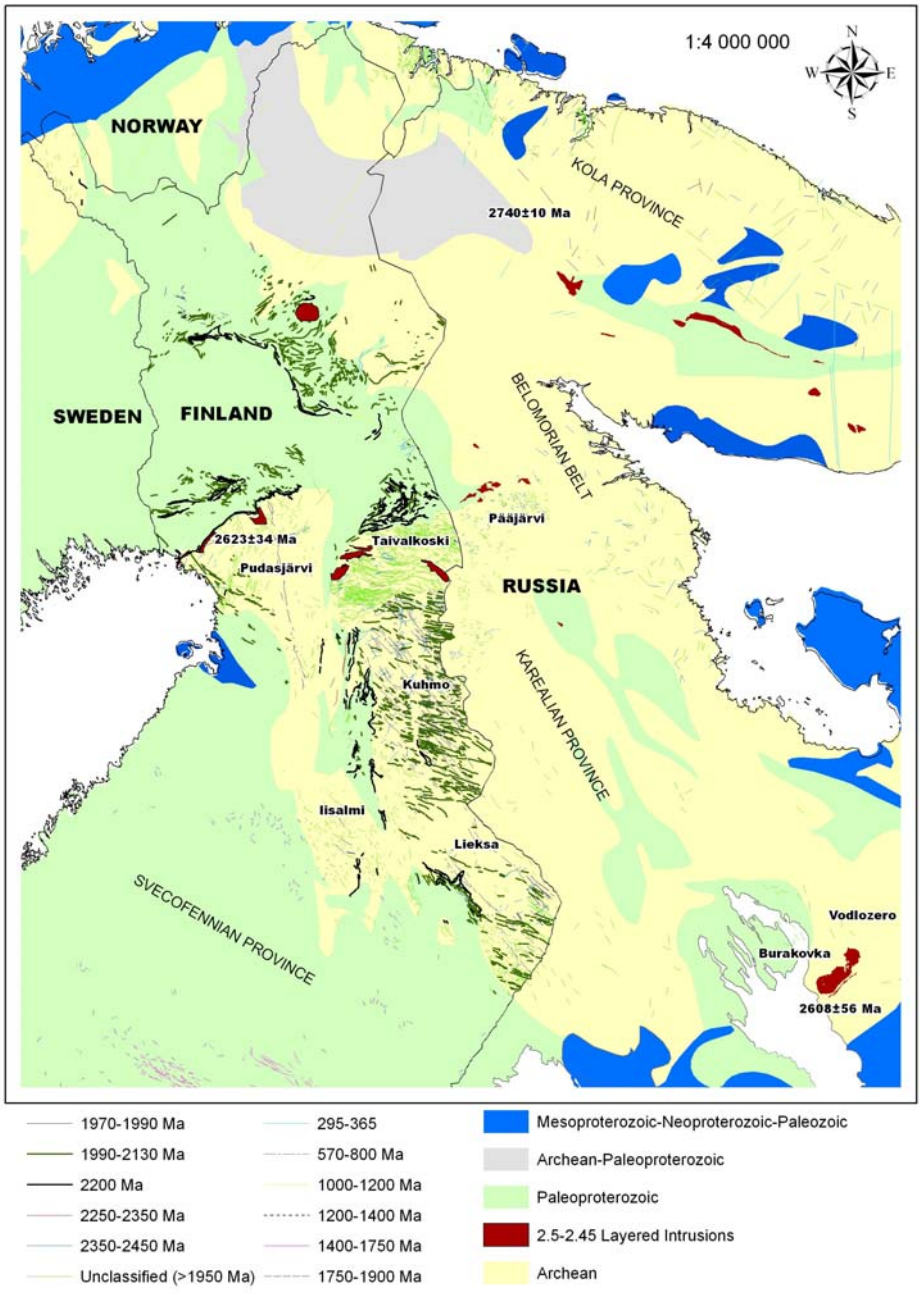

Figure 1. Areal distribution of 2.7-1.98 Ga dyke swarms in the eastern and northern Fennoscandian shield.

2.2. Paleoproterozoic dyke swarms

The first Paleoproterozoic continental rifting phase of the cratonized Archean basement involved emplacement of layered intrusions of the ages of ~2.5 Ga (Kola Province) and ~2.45 Ga (Kola and Karelian Provinces; Tornio-Näränkävaara area, Central Lapland and

Burakovka) and associated boninitic–noritic–gabbronoritic–tholeiitic to Fe-tholeiitic dykes in the northeastern part of the Fennoscandian Shield. Moreover, gabbronorite and gabbroic dykes at Troms area in Norway show an age of 2403±3 Ma (U-Pb, zircon and baddeleyite) (*Kullerud et al. 2006*). The next rifting phase occurred at ~2.32 Ga, and was represented by small intrusions and dykes (Taivalkoski and Iisalmi blocks).

Table 1. Classification of Archean-Paleoproterozoic dyke swarms in the eastern Fennoscandian shield.

Eastern Fennoscandian Shield	
1.98 Ga Fe-tholeiitic-tholeiitic dyke swarm	**2.32 Ga Fe-tholeiitic dyke swarm/ intrusions**
– predate 1.95 Ga ophiolites	–f ew dykes and intrusions identified
– NW trend (Kuhmo), continental thol. to IAT type	– E trend?
– mainly unaltered (plagioclase and pyroxenes)	**2.45 Ga dyke swarms**
~2.1 – 2.05 Ga Fe-tholeiitic dyke swarm	– connected with layered intrusions; two magma types
–includes several pulses between 2.13 to 2.05 Ga	(1) boninite-norite dykes (high MgO, SiO_2, Cr, Ni and LREE, low TiO_2 and Zr), NE trend
– continental tholeiitic type	(2) gabbronorite dykes (low TiO_2, Cr and Zr), NW trend
– mainly E trend (Kuhmo) and minor NW trend	(3) low-Ti tholeiitic (NW trend) and (4) Fe-tholeiitic dykes (E trend), continental type
2.2 Ga low-Al thol. (karjalitic) layered sills	(5) orthopyroxene-plagioclase phyric dykes (high SiO_2, LREE; calc- alkaline aff.), E trend
– layered intrusions/sills (max. length 150km) and minor dykes	**2.6 – 2.7 Ga dyke swarms and intrusions**
– wehrlite–clinopyroxenite–gabbro–granophyre	- gabbronorite dykes (low TiO_2, Cr and Zr), Kola Peninsula – Burakovka and Pudasjärvi
– widespread in eastern and northern Finland	

Low-Al tholeiitic or karjalitic magmas intruded through the basement at 2.2 Ga. Most of the karjalites (gabbro-wehrlite association of *Hanski, 1984*) occur as layered sills. The extensive E-W trending set of dyke swarms cutting through the whole Archean crust and the Jatulian Group in Kuhmo is Fe-tholeiitic and points to a pronounced extensional development at ~2.1 Ga.

A significant sign of the break-up event, which predates the formation of the 1.95 Ga Outokumpu and Jormua ophiolites (*Kontinen 1987, Peltonen et al. 1996*) and the ophiolite in Central Lapland *(Hanski 1997*), is the existence of the 1.98 Ga tholeiitic and Fe-tholeiitic dyke swarm.

The 2.32–1.98 Ga dyke swarms form a homogeneous group in terms of their geochemical composition (Fig 2.), resembling that of continental tholeiitic basalts. This means that subclassification of the younger Paleoproterozoic dykes according to their chemistry is virtually impossible. Nevertheless, it has been possible to classify the dykes with ages of ~2.1 Ga and 1.98 Ga in the Kuhmo block by reference to their geochemistry, age, and orientation.

3. Plate movements

Dyke swarms are used extensively in studies on plate movements and global paleogeographic reconstructions. This is mainly because of voluminous precise isotopic age datings, the occurrence of dykes as tectonically controlled formations and the suitability of dykes for carrying out paleomagnetic field tests that can link the age of magnetization to the isotopic age of the dyke magma. In the following, plate movement of the Fennoscandian Shield during Archean and Paleoproterozoic is presented based on paleomagnetic data (Figure 3).

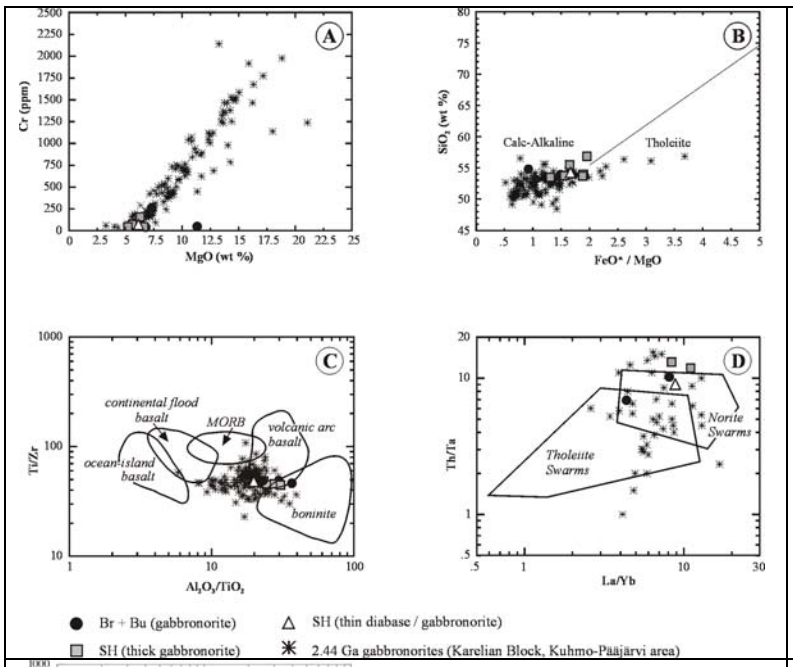

Figure 2.1. Geochemical analyses of the Avdeev dyke (Br and Bu, circles) related to the 2.45 Ga Burakovka layered intrusion and the Shalskiy dykes (SH, square; gabbronorite and triangle; diabase dyke). Analyses from other 2.45 Ga dykes from the Karelian Province are shown for comparison.

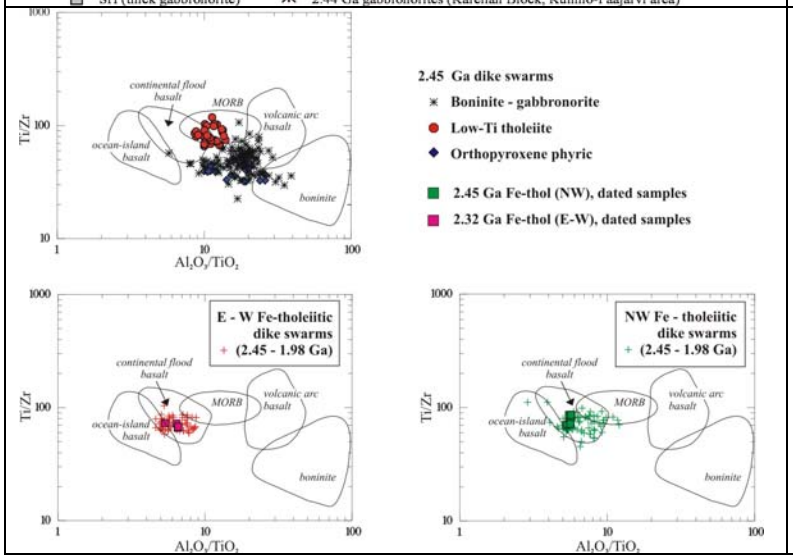

Figure 2.2. Geochemical analyses (320 samples) of the Paleoproterozoic dyke swarms (~2.45 Ga, 2.32 Ga, 2.1 Ga, and 1.98 Ga) from the Kuhmo block and Russian Karelia plotted on Al_2O_3/ TiO_2 – Ti/Zr (Wilson and Versfeld, 1994) diagram.

Figure 2. Geochemical analyses of dyke swarms.

3.1. Archean

The oldest paleomagnetic data of the Fennoscandian shield are obtained from the high grade granulitic intrusions in the Lieksa and Varpaisjärvi areas (Iisalmi block) in central Finland (Fig. 1). In the Lieksa area the granulites are dated at 2.72 Ga (U-Pb on zircon, P. Hölttä, pers. comm., 2006), but the near-by Kutsu granite gives a U-Pb zircon age of 2.62 Ma which may reflect the age of metamorphism of the area (P. Hölttä, pers comm., 2006). In the Varpaisjärvi area Sm-Nd garnet-whole rock ages of granulites have given ages of 2.48-2.59 Ga (*Hölttä et al., 2000*, *Mänttäri and Hölttä, 2002*) which likely correspond to the magnetization age of the formation. Both formations give a very stable steep inclination remanence direction which in the Lieksa granulites is pointing upwards (*Mertanen, 2000*) and in the Varpaisjärvi granulites downwards (*Neuvonen et al., 1997, Mertanen et al., 2006a*). Based on these directions, the Karelian craton was located at high paleolatitudes at ca. 2.6-2.5 Ga (Fig. 3a).

On the contrary, the 2608±56 Ma Shalskiy gabbronorite dyke in the Vodlozero block (Fig. 1) shows a low inclination magnetization (*Mertanen et al., 2006b*) which places the Fennoscandian shield at the equator (Fig. 3). Two alternatives for the difference in paleopositions are suggested. First, the Fennoscandian Shield formed a single craton and the shield drifted as a unity from high paleolatitudes to the equator during Neoarchean (Fig. 3). Second, the Karelian Province and the Vodlozero block were separated during Neoarchean when the blocks were in close connection, but still capable of mutual rotations and block movements, until their amalgamation at Early Paleoproterozoic, before the emplacement of the 2.45 Ga formations.

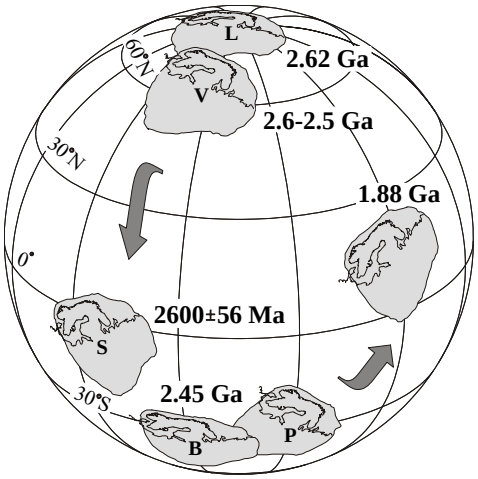

Figure 3. Plate movement of the Fennoscandian shield based on data from Lieksa (L), Varpaisjärvi (V), Shalskiy (S), Burakovka (B) and Pääjärvi (P) formations. 1.88 Ga position is from *Pesonen et al. (2003*). The shield is shown in its present form.

3.2. Paleoproterozoic

The 2.45 Ga position of the Fennoscandian shield (Fig. 3) is based on data from the gabbro-norite dykes at Lake Paajarvi (*Mertanen et al., 1999*) and on data from the Shalskiy diabase dyke which is related to the 2.45 Ga Burakovka intrusion in the Vodlozero block (*Mertanen et al., 2006b*). Based on a positive baked contact test, the remanent magnetization of the Shalskiy diabase dyke has been proven to be primary. The data are in close agreement and place the Fennoscandian shield at the paleolatitude of about 30°. Reliable paleomagnetic data for the 2.2 –2.0 Ga dykes and sills are still lacking. Based on data from the 1.88 Ga gabbroic intrusions in central Finland (see *Pesonen et al., 2003*), the shield had drifted about 50° across the equator between 2.45-1.88 Ga.

References

Bayanova T.B., Yegorov D.G., 1999. U-Pb age of the banded iron formation on the Kola Peninsula. Geology and minerals of the NW and central Russia. – Apatity, 19-24 (in Russian).

Bleeker, W. and Ernst, R., 2006. Short-lived mantle generated magmatic events and their dyke swarms: the key unlocking Earth's palaeogeographic record back to 2.6 Ga. In: E. Hanski, S. Mertanen, O.T. Rämö and J. Vuollo (eds.), Dyke Swarms - Time Markers of Crustal Evolution. Proceedings of the Fifth International Dyke Conference 2005 Rovaniemi, Finland, 31 July- 3 Aug. 2005 & Fourth International Dyke Conference, Kwazulu-Natal, South Africa 26-29 June 2001. A.A. Balkema.

Fedotov, Zh. A., 2005. Mafic dykes of the Kola region. In: Vuollo, J. I. and Fedotov, Zh. A. (eds.), Fifth International Dyke Conference : "Dyke swarms - time markers of crustal evolution", Rovaniemi, Finland, 31 June - 3 August 2005 : post-conference field trip B guidebook : eastern and northern Finland - Belomoride mobile belt and Kola Peninsula. Geological Survey of Finland, Rovaniemi, 84 p. + 1 app. map.

Hanski, E., 1997. The Nuttio serpentinite belt, Central Lapland: An example of Paleoproterozoic ophiolitic mantle rocks in Finland. Ofioliti 22, 35–46.

Hanski, E., 1984. Geology of the gabbro–wehrlite association in the eastern part of the Baltic Shield. Unversity of Oulu, Arkeeisten alueiden malmiprojekti, Report 20, 1–78.

Hanski, E., Mertanen, S., Rämö, O.T. and Vuollo, J. (eds.), 2006. Dyke Swarms - Time Markers of Crustal Evolution. Proceedings of the Fifth International Dyke Conference 2005 Rovaniemi, Finland, 31 July- 3 Aug. 2005 & Fourth International Dyke Conference, Kwazulu-Natal, South Africa 26-29 June 2001. A.A. Balkema.

Hölttä, P., Huhma, H., Mänttäri, I., Paavola, J., 2000. P-T-t development of Archaean granulites in Varpaisjärvi, Central Finland, II: Dating of high-grade metamorphism with the U-Pb and Sm-Nd methods. Lithos 50, 121-136.

Kontinen, A., 1987. An early Proterozoic ophiolite – the Jormua mafic–ultramafic complex, northeastern Finland. Precambrian Research 35, 313–341.

Kullerud, K., Skjerlie, K.P., Corfu, F. and de la Rosac, J.D., 2006. The 2.40 Ga Ringvassøy mafic dykes, West Troms Basement Complex, Norway: The concluding act of early Palaeoproterozoic continental breakup. Precambrian Research doi:10.1016/ j.precamres.2006.08.003

Mertanen, S., 2000. Paleomagnetism of Archean rocks in the Karelian Province (Baltica) - comparison of data from Superior, Pilbara and Kaapvaal cratons. 25th General Assembly, EGS Symposium, CD-ROM Geophysical Research Abstracts 2.

Mertanen, S., Halls, H.C., Vuollo, J., Pesonen, L.J., & Stepanov, V.S. 1999. Paleomagnetism of 2.44 Ga mafic dykes in Russian Karelia, eastern Fennoscandian Shield - implications for continental reconstructions. Precambrian Research 98, 197-221.

Mertanen, S., Pesonen, L.J., Hölttä, P., Paavola, J., 2006a. Palaeomagnetism of Palaeoproterozoic dolerite dykes in central Finland. In: E. Hanski, S. Mertanen, O.T. Rämö and J. Vuollo (eds.), Dyke Swarms - Time Markers of Crustal Evolution. Proceedings of the Fifth International Dyke Conference 2005 Rovaniemi, Finland, 31 July- 3 Aug. 2005 & Fourth International Dyke Conference, Kwazulu-Natal, South Africa 26-29 June 2001. A.A. Balkema.

Mertanen, S., Vuollo, J.I., Huhma, H., Arestova, N.A., Kovalenko, A., 2006b. Early Paleoproterozoic-Archean dykes and gneisses in Russian Karelia of the Fennoscandian Shield – new paleomagnetic, isotope age and geochemical investigations. Precambrian Research 144, 239-260.

Mutanen, T. and Huhma, H., 2001. U–Pb geochronology of the Koitelainen, Akanvaara and Keivitsa layered intrusions and related rocks. In: Vaasjoki, M. (ed.), Radiometric age determinations from Finnish Lapland and their bearing on the timing of Precambrian volcano–sedimentary sequences. Geological Survey of Finland. Special Paper 33, 229–246.

Mänttäri, I. and Hölttä, P., 2002. U–Pb dating of zircons and monazites from Archean granulites in Varpaisjärvi, Central Finland: Evidence for multiple metamorphism and Neoarchean terrane accretion. Precambrian Research 118, 101-131.

Neuvonen, K.J., Pesonen, L.J., Pietarinen, H., 1997. Remanent Magnetization in the Archaean Basement and Cutting Diabase Dykes in Finland, Fennoscandian Shield. Geophysica 33(1), 111-146.

Peltonen, P., Kontinen, A. and Huhma, H., 1996. Petrology and geochemistry of metabasalts from the 1.95 Ga Jormua Ophiolite, northeastern Finland. Journal of Petrology 37, 1359–1383.

Pesonen, L.J., Elming, S.Å., Mertanen, S., Pisarevsky, S., D´Agrella-Filho, M.S., Meert, J.G., Schmidt, P.W., Abrahamsen, N., Bylund, G., 2003. Paleomagnetic configuration of continents during the Proterozoic. Tectonophysics 375, 289-324.

Vuollo, J.I., 1994. Palaeoproterozoic basic igneous events in Eastern Fennoscandian Shield between 2.45 Ga and 1.97 Ga, studied by means of mafic dyke swarms and ophiolites in Finland. Acta Universitatis Ouluensis Ser. A 250, 1–47.

Vuollo, J. and Huhma, H., 2005. Paleoproterozoic mafic dikes in NE Finland. In: Lehtinen, M., Nurmi, P. A. & Rämö, O. T. (eds.) Precambrian geology of Finland: key to the evolution of the Fennoscandian Shield. Developments in Precambrian geology 14, 195-236.

Wilson, A.H and Versfeld, J.A., 1994. The early Archaean Nondweni greenstone belt, southern Kaapvaal Craton, South Africa; Part II, Characteristics of the volcanic rocks and constraints on magma genesis. Precambrian Research 67, 227-320.

The composition of fluorapatite and monazite from the Naantali Carbonatite, southwest Finland: implications for timing and conditions of carbonatite emplacement

Jeremy Woodard[1]*and Callum J. Hetherington[2]

[1]Department of Geology, University of Turku, FIN-20014 Turku, Finland
[2]Department of Geosciences, University of Massachusetts, 611 N Pleasant St., Amherst, MA 01003-9297, USA
*E-mails: jdwood@utu.fi, callum@geo.umass.edu

Fluorapatite from the Naantali Carbonatite in southwest Finland have been investigated for trace element chemistry using electron microprobe analysis (EMPA). Monazite inclusions within the apatite grains were also analysed for the purposes of EMPA monazite geochronology. The aim of this study is to determine the conditions of crystallisation and the timing of the carbonatite emplacement.

Keywords: carbonatite, alvikite, apatite, trace elements, REE, monazite geochronology, Naantali, Finland

1. Introduction

The Naantali Carbonatite is 20 west of Turku in southwest Finland. It is comprised of 20-30 fine-grained calciocarbonatite (alvikite) dykes, which strike roughly parallel concurrent with a NW-SE trending shear zone. The dykes contain 90-90% calcite, 5-8% fluorapatite, and 1% allanite. Other minor accessory minerals include quartz and titanite.

Fluorapatite appears as dark red, euhedral or partially rounded subhedral phenocrysts. Crystals show complex zoning patterns in BSE images and have abundant inclusions of calcite, quartz, monazite, bastnäsite, and magnetite. Other minerals such as celestine and thorite have also been identified.

Based on field relations and trace element geochemistry, Woodard (2005) proposed an association with post-orogenic shoshonitic magmatism, particularly the 1.76-1.77 Ga (Eklund & Shebanov 2005) bimodal Åva ring complex, 40 km west of Naantali. A Sm-Nd model age of 1.8 Ga obtained from ID-TIMS analysis of whole-rock samples of the Naantali dykes (Woodard et al. 2006) supports this hypothesis.

2. Samples and Methods

Three samples from the Naantali dykes swarm were selected for this study. JW06-001C is from the centre area of a dyke and therefore exhibits relatively little interaction with the wall rock. JW06-002A is from the contact area of the same dyke, and JW06-004B is from the contact area of a second dyke. The samples from the contact areas also contain chlorite, epidote, and prehnite in addition to the minerals listed above, reflecting the infiltration of elements (Si, Al, Fe, Mg) from the wall rocks during fenitisation.

Several polished thin sections (50µm thick) were prepared from each of the samples in order to select the best possible apatite grains for analysis. Samples were mapped using SEM, and selected grains analysed using the Cameca SX-50 and SX-100 Ultrachron electron microprobes housed at the Department of Geosciences, University of Massachusetts, Amherst.

3. Results

Fluorapatite chemistry

BSE images of two of the analysed apatite grains are shown in Figure 1. The variable backscatter intensity, resulting in brighter and darker areas, is a function of the Th+LREE concentrations. As the darker zones in the Naantali apatites commonly surround inclusions of LREE-rich minerals (monazite, bastnäsite), they are interpreted as having been depleted in Th+LREE during dissolution-reprecipitation. It should be noted that HREE concentrations remain constant throughout the grains. Experimental data by Ito (1968) show that most divalent cations, including Sr^{2+}, can readily substitute for Ca^{2+} in the apatite structure. Monovalent Li^{+} and Na^{+} also substitute for Ca^{2+} via charge-coupled substitution, however incorporation of K^{+} is limited. REE+Y (hereafter referred to only as REE) are incorporated into the apatite structure via two main charge-coupled substitution reactions (e.g. Ito 1968, Rønsbo 1989):

$$REE^{3+} + Si^{4+} \leftrightarrow Ca^{2+} + P^{5+} \quad (1)$$

$$Na^{+} + REE^{3+} \leftrightarrow 2Ca^{2+} \quad (2)$$

Na is below detection limits in all analysed points. There is a positive correlation between Si and REE in all samples (Figure 2), suggesting reaction (1) was the controlling charge-coupled substitution reaction in this system. Apatite in JW06-001C is particularly rich in REE, containing up to 11.8 wt-% ΣREE_2O_3. Apatite in samples JW06-002A and JW06-004B have lower concentrations, with ΣREE_2O_3 at a maximum of 5.3 wt-%. Sr concentrations, however, are uniformly around 1 wt-% regardless of the distance from the contact.

Monazite Geochronology

Eight points on a monazite inclusion in apatite from sample JW06-002A were analysed (Table 1) using the methodology described by Jercinovic & Williams (2005). A total U-Th-Pb age of 1776 ± 18 Ma (2σ) for the formation of the inclusion was calculated in accordance with Williams et al. (2006).

4. Discussion and conclusion

Partition coefficients given by Watson & Green (1981) for fluorapatite vs. basaltic melt are 2.6-4.7-4.2-1.8 (D_{La}-D_{Sm}-D_{Dy}-D_{Lu}) at 1080ºC and 8 kbar. Their experiments showed a strong positive correlation between the partition coefficients and the silica activity of the melt, as well as a negative correlation with temperature. Klemme & Dalpé (2003) report partition coefficients between fluorapatite and carbonatite melt of 0.37-0.44-0.34 (D_{La}-D_{Sm}-D_{Lu}) at 1250ºC and 10 kbar, demonstrating that the positive correlation continued even as silica activity was reduced to zero. Interpolation of these data shows that partition coefficients at 1250ºC approach unity at 25 wt-% SiO_2, which would shift towards lower silica concentrations with decreasing temperature.

The partition coefficient data show that fluorapatite is commonly more enriched in MREE compared to both the light and heavy REE's. A consequence of this is that REE patterns for apatites normalised to whole rocks have a bell shaped profile. However, plots of the Naantali apatite versus whole rock have a slightly positive slope, which increases with increasing alteration (Figure 3). The Naantali dykes have high chondrite normalised La/Lu ratios (average $La:Lu_N > 235.5$, Woodard 2005), which is a characteristic feature of

carbonatite (Woolley & Kempe 1989). The most likely explanation for the deviation from the expected bell curve shape of the REE profile is the low HREE concentrations in the whole rock samples.

The near constant composition of unaltered domains across individual apatite crystals in the Naantali dykes indicates that they crystallised as homogenous phenocrysts. The growth of quartz, monazite and bastnäsite inclusions, coupled to the depletion in Si, Th and LREE content in altered apatite suggests that the development of the inclusion assemblage resulted from an in situ, intra-crystalline reaction, similar to the following:

(Th,Si,LREE)-Apatite + CO_2 → Apatite + Monazite + Quartz + Bastnäsite

Similar reaction textures, which require the addition of a fluid, have recently been discussed within the framework of dissolution-reprecipitation (Putnis, 2002). This reaction, coupled with the variable diffusion rates in apatite for the REE (Cherniak 2000), could account for the different slopes in Figure 3.

Near the contact, the availability of Si, Al, Fe, and Mg from the wall rock alteration also resulted in the growth of allanite mantles around apatite (Woodard 2005). The alteration of apatite, requiring fenitisation of the host-rock to promote allanite growth, and the presence of CO_2 to facilitate the dissolution-reprecipitation reaction in apatite grains, suggests that the alteration textures developed in response to auto-metasomatism of apatite during carbonatite dyke emplacement.

Subsequently, the calculated monazite age of 1776 ± 18 Ma places an age, not only on the timing of apatite alteration, but also the timing of carbonatite emplacement, which is within error limits equivalent to the timing of emplacement of the Åva ring complex (Eklund & Shebanov 2005). This conclusion supports the findings of Woodard (2005), who postulated an igneous association between these two intrusions.

References

Cherniak, D.J., 2000. Rare earth element diffusion in apatite. Geochemica et Cosmichemica Acta 64, 3871-3885.

Eklund, O., & Shebanov, A., 2005. Prolonged postcollisional magmatism in the southern Svecofennian domain - a case study of the Åva granite-lamprophyre ring complex. Lithos 80, 229-247.

Ito, J., 1968. Silicate apatites and oxyapatites. American Mineralogist 53, 890-907.

Jercinovic M.J. and Williams M.L., 2005. Analytical perils (and progress) in electron microprobe trace element analysis applied to geochronology: Background acquisition, interferences, and beam irradiation effects. American Mineralogist 90, 526-546.

Klemme, S., & Dalpé, C., 2003. Trace-element partitioning between apatite and carbonatite melt. American Mineralogist 88, 639-646.

Putnis, A., 2002 Mineral replacement reactions: from macroscopic observations to microscopic mechanisms. Mineralogical Magazine 66, 689-708

Puustinen, K., & Karhu, J.A., 1999. Halpanen calcite carbonatite dike, southeastern Finland. Geological Survey of Finland, Special Paper 27, 39-41.

Rønsbo, J.G., 1989. Coupled substitutions involving REEs and Na and Si in apatites in alkaline rocks from the Ilimasussaq intrusion, South Greenland, and the petrological implications. American Mineralogist 74, 896-901.

Watson, E.B., & Green, T.H., 1981. Apatite/liquid partition coefficients for the rare earth elements and strontium. Earth and Planetary Science Letters 56, 405-421.

Williams M. L., Jercinovic M. J., Goncalves P., and Mahan K. 2006. Format and philosophy for collecting, compiling, and reporting microprobe monazite ages. Chemical Geology 225, 1-15.

Woodard, J., Mänttäri, I., & Huhma, H., 2006. Radiogenic isotope systematics and the age of the Naantali Carbonatite. In: Peltonen, P., & Pasanen, A., (eds.) The 27th Nordic Geological Winter Meetings, 9-12 January, 2006, Oulu, Finland, Abstract Volume. Bulletin of the Geological Society of Finland, Special Issue 1, p.174.

Woodard, J. D., 2005. Recognition and classification of a carbonatite dyke swarm at Naantali, southwest Finland. Unpublished Master's Thesis, University of Turku. 79p.

Woolley, A.R. & Kempe, D.R.C., 1989. Carbonatites: nomenclature, average chemical compositions, and element distribution. In: Bell, K. (ed.) Carbonatites: Genesis and Evolution. London: Unwin Hyman. 1-14.

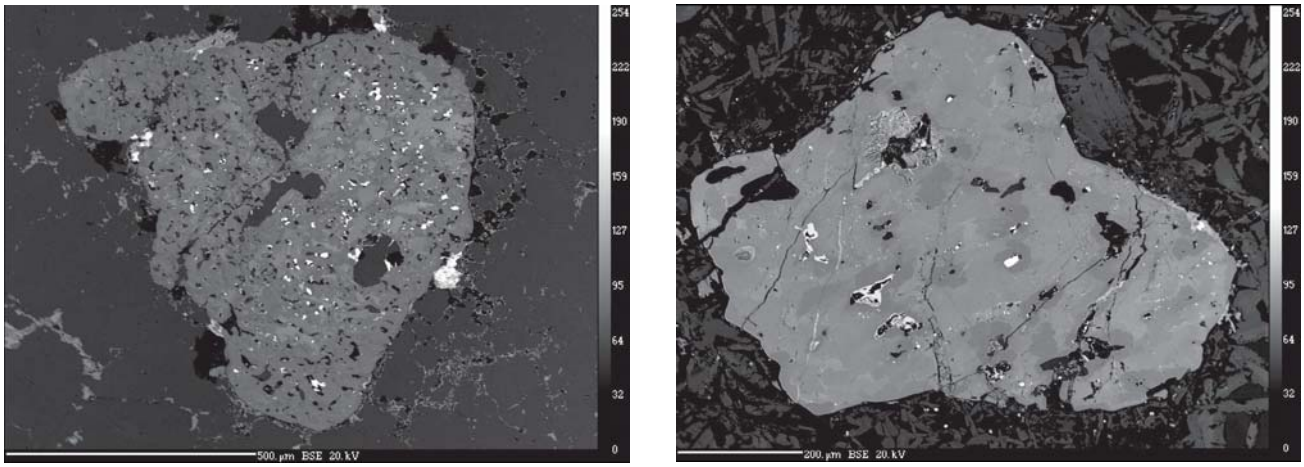

Figure 1. BSE images of apatite grains analysed in this study, a) JW06-001C, b) JW06-002A.

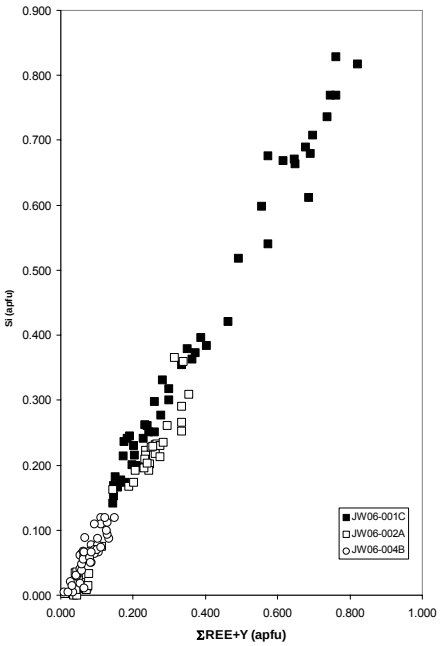

Figure 2. Plot of Si (apfu) versus □REE+Y (apfu) for all analyses in this study.

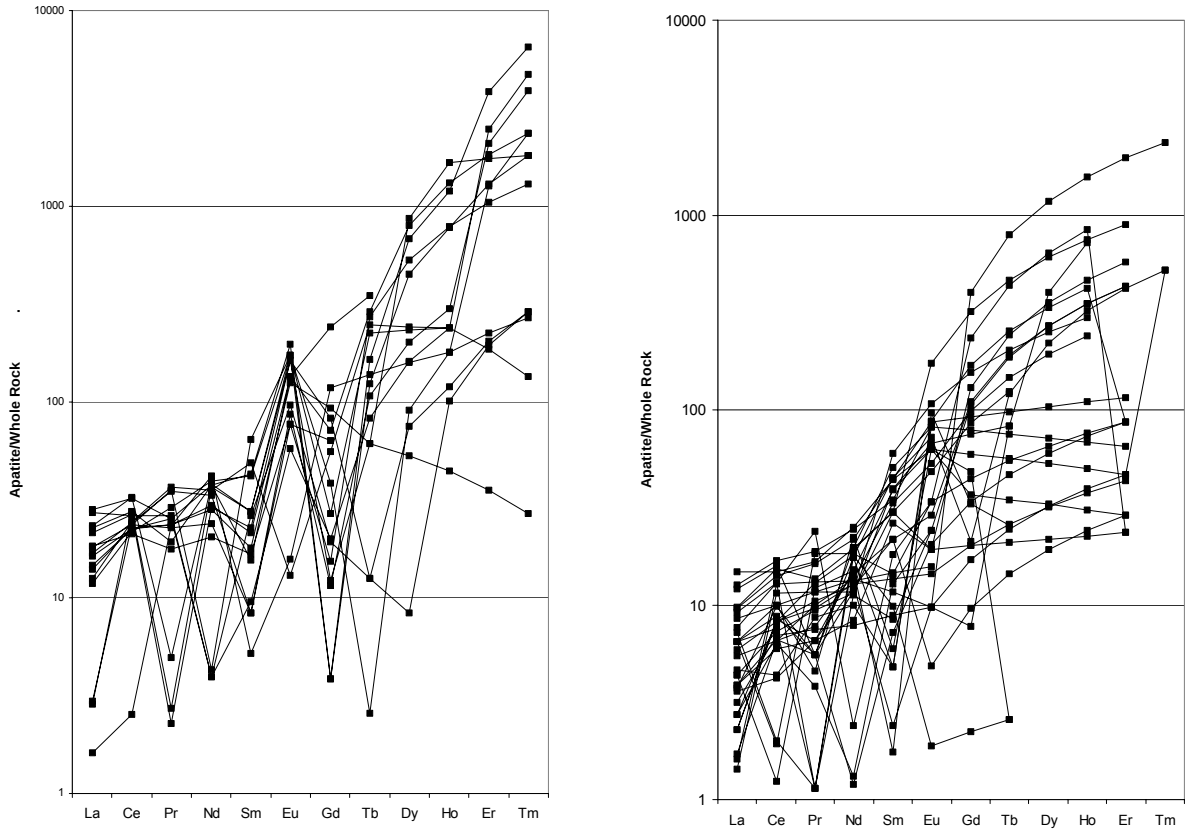

Figure 3. REE patterns for selected apatite analyses normalised to average whole-rock compositions of the Naantali carbonatite dykes, a) Unaltered zones, JW06-001C, b) Altered zones in proximity to inclusions, JW06-001C.

Table 1. Measured concentrations (ppm) and calculated ages for monazite in JW06-002A.

Pt	Th	Y	Pb	U	age
1	10047	472	856	82	1782
2	9643	469	836	125	1783
3	11692	773	994	87	1783
4	13338	707	1170	220	1782
5	10394	532	840	21	1731
6	10627	423	888	70	1759
7	13304	618	1154	130	1803
8	12932	645	1136	198	1792
avg.	11497	579	984	116	1776
st.dev.	1523	124	149	66	22
1s	539	44	53	23	8